Universidad de Navarra

Facultad de Ciencias

Chemical composition and sources of particulate matter across urban and rural sites in the Caribbean region of Cienfuegos (Cuba)

Yasser Morera Gómez

Universidad de Navarra

Facultad de Ciencias

Chemical composition and sources of particulate matter across urban and rural sites in the Caribbean region of Cienfuegos (Cuba)

Memoria presentada por D. Yasser Morera Gómez para aspirar al grado de Doctor por la Universidad de Navarra

El presente trabajo ha sido realizado bajo mi dirección en el Departamento de Química y autorizo su presentación ante el Tribunal que lo ha de juzgar.

Pamplona, 18 de mayo de 2018

Dr. Jesús Miguel Santamaría Ulecia Dr. David Elustondo Valencia

Dr. Carlos Manuel Alonso Hernández

Look deep into nature, and then you will understand everything better.

Albert Einstein

A mis abuelos

Agradecimientos

Deseo expresar mi más sincero agradecimiento a todas las personas e instituciones que me han ayudado de una manera u otra a llevar a buen puerto este trabajo.

En primer lugar, quiero agradecer a mi familia por el apoyo incondicional desde que comencé este viaje. A mis padres Omar y Mari Nieves, mi hermana Rosi, mis tíos y tías, mis primas y muy especialmente a mis abuelos; ellos me dieron todo el cariño del mundo y todas las fuerzas necesarias para vencer cada obstáculo.

A mi compañera en la vida, Yudexi, no solo por su implicación en la realización experimental de este trabajo, sino también por su infinito amor, toda su compresión, su paciencia y su apoyo en todo momento. Tú has sido y eres mi estrella polar.

Mi eterno agradecimiento a los directores de esta tesis, los profesores Dr. Jesús Miguel Santamaría Ulecia y Dr. David Elustondo Valencia y el Dr. Carlos Manuel Alonso Hernández, quienes me brindaron la oportunidad de aprender a su lado y cuyo apoyo y guía ha sido fundamental para la consecución de este trabajo. Quiero decir que durante este tiempo me he sentido como en casa trabajando con ellos.

A la Universidad de Navarra por el apoyo técnico, económico y humano. Mi agradecimiento, además, a la Asociación de Amigos y a la fundación 'Obra social La Caixa' por la concesión de la beca y la ayuda de movilidad que apoyaron el desarrollar de este proyecto de investigación. Quiero agradecer especialmente a Carmen Janet de la Asociación de Amigos por su ayuda antes y durante estos cuatro años de estudio.

Agradecer al centro de investigación GEOTOP en la UQAM (Montreal, Canadá) y, especialmente, al profesor Dr. David Widory, por la exitosa estancia de investigación desarrollada en esas instalaciones bajo su supervisión. Agradecer también, a Agnieszka y Jean François por su ayuda en el laboratorio durante la estancia.

A las profesoras Carolina Santamaría y Esther Lasheras, gracias por toda la ayuda en el LICA y también por los momentos compartidos fuera del laboratorio. Un agradecimiento especial a Josemi, mucho en esta tesis se debe a ti y a todo tu apoyo en el laboratorio.

A la dirección del Centro de Estudios Ambientales de Cienfuegos (CEAC), por la confianza depositada en mí y por el soporte técnico e investigativo. A todos mis

compañeros y amigos del CEAC que estuvieron implicados en los muestreos de campo y en el trabajo en el laboratorio: Alejandro, Orlando, Evelio, Yanadín, Dismey, Héctor, Osmel y Aniel. A Tania, por toda su ayuda con la documentación. A Laura, por su gran ayuda con los mapas. Y a todos los que no nombro pero que han contribuido también a este trabajo, mi profundo agradecimiento.

A Raúl Cruz, su esposa Carmen y su familia, por su amistad y por haberme acogido tan cariñosamente en Pamplona.

A Esther Rodríguez, quien me enseñó cada rincón de esta bella ciudad y me acogió con tanto amor y cariño en su casa. Ella ha sido como una madre para mí aquí en Pamplona. Gracias Cubana. Agradecer también a Yantai y Pepe, por la linda amistad y por los excelentes momentos compartidos.

A todos mis compañeros del departamento de Química y un poquito más allá con los que he navegado este inmenso mar, el de las ciencias, pero también el de los buenos momentos. A Sheila, María, David, Marcos, Fidel, Bea, María Pérez, Joan, Max, Marta, Mikel y Luisfer. A Marisa por estar disponible siempre, su ayuda ha sido esencial. A Raúl Bermejo. Y a todos los profesores con los que he tenido la suerte de compartir la actividad de docencia, en especial a las profesoras Cristina Martínez y Cristina Sola, todos ellos han sido verdaderos maestros para mí.

Todos ustedes han sido imprescindibles para lograr este sueño, ¡MUCHAS GRACIAS!

Abstract

Particulate matter (PM) is a complex mixture of small particles and liquid droplets suspended in the atmosphere originated from a wide range of natural and anthropogenic sources that has been related with many adverse effects on human health, ecosystems and climate. Consequently, the deterioration of air quality caused by the release of PM is one of the main environmental concerns in the world and has resulted in many resources being invested in monitoring and controlling air pollution.

In Cuba, the study of atmospheric PM pollution constitutes one of the most challenging issues in environmental research because there are still technical and analytical limitations that prevent its correct monitoring. Therefore, conducting studies on PM are of paramount importance to fill the existing gap, providing useful information to develop effective strategies to improve air quality in this region.

The general objective of this thesis is to investigate the levels and chemical composition of atmospheric particulate material present in rural and urban areas of Cuba. More specifically, the work aims to identify the main sources of emission of PM, evaluating its possible effects on air quality and the environment. For this purpose, during a period of one year (January 2015 to January 2016) samples of PM_{10} were simultaneously collected in a rural and an urban site of Cienfuegos by means of high-volume samplers. Likewise, in the rural site monthly samples of bulk depositions were collected between March 2014 and November 2016. In order to improve the process of identification of sources, several samples from aerosol emitters were also collected during 2015 and 2016 in the region studied. The samples thus collected were later analyzed by applying various analytical techniques, determining a high number of chemical elements and the stable carbon and nitrogen isotope signatures.

The different research works carried out in this thesis have been presented in five chapters. In the first one it is shown that concentrations of PM_{10} reached annual averages of 35.4 and 24.8 $\mu g\ m^{-3}$ in the rural and urban sites respectively. The highest concentrations of PM were observed between March and August, coinciding with a strong advection of Saharan dust clouds. The PM_{10} daily limit (50 $\mu g\ m^{-3}$) established in the Cuban legislation for air quality was exceeded 3 and 8 times in the rural and urban sites, respectively. Chemical characterization of PM_{10} showed important contributions of mineral matter, total carbon and secondary inorganic compounds in the region,

detecting higher concentrations in the urban site. A source apportionment analysis using Positive Matrix Factorization (PMF) model identified 5 main sources in the studied sites (Saharan intrusions, marine aerosol, combustion, road traffic and cement plant). Saharan dust contribution was quantified for the first time in Cuba, proving to be one of the most important pollution sources in the region.

In the second chapter the content, pattern and sources of lanthanoid elements (La to Lu) in PM_{10} are investigated. Lanthanoid elements concentrations were distributed unevenly throughout the year, showing higher values in the period between April and August when Saharan dust intrusions are more frequent. According to the results, most lanthanoid elements exhibited a dominant crustal origin, but the influence of anthropogenic emissions was also demonstrated by the strong fractionation of lanthanoid ratios as well as the higher enrichment factors of heavier lanthanoids. By using different approaches, including the application of the conditional bivariate probability function (CBPF) and the concentration-weighted trajectory (CWT), four pollution sources were identified: crustal matter (driven by Saharan dust and local soils), oil combustion (power plant and shipping emissions), petroleum-coke combustion (cement plant) and urban road traffic.

Chapter 3 reports on the study of the stable isotope compositions ($\delta^{13}C$ and $\delta^{15}N$) of total carbon (TC) and nitrogen (TN) in both PM_{10} and emissions from potential sources of contamination. $\delta^{13}C$ isotope signatures revealed that air quality was degraded by the mixed contributions from two main emitters: combustion of fossil fuel and cement plant and quarries, with this last source impacting more air quality at the urban site. In addition, TN and $\delta^{15}N$ values from the urban site demonstrated that nitrogen in PM_{10} was generated by secondary processes through the formation of $(NH_4)_2SO_4$ and that the corresponding ^{15}N enrichment is controlled by exchange between gaseous NH_3 and particle NH_4^+ in the $(NH_4)_2SO_4$ molecule under stoichiometric equilibrium. By comparing $\delta^{15}N$ values in PM_{10} at lower nitrogen concentrations with those measured in samples from potential sources of pollution it was concluded that emissions from diesel cars and the power plant may represent the major vectors of primary nitrogen.

The fourth research study carried out in this thesis describes exhaustively the major and trace elements analyzed in monthly bulk depositions. Bulk depositions and fluxes of the elements studied showed a high variability, without exhibiting any evident pattern between dry and wet periods, result that was attributed to fluctuations in emissions from their main sources. However, stronger correlations were found between typical crustal elements, which showed a marked seasonality related to the presence of Saharan clouds dust in the Caribbean. Most of the analyzed elements were found in the variation range of those reported in rural environments around the world but the elements V, Ni, As and Sb presented higher levels, typically founded in urban and industrial areas. The elements Zn, Sb, Pb, W, Sn, S, Cu, Mo, Nb and P were significantly enriched, revealing their anthropogenic origin. Finally, the application of Principal Components, Multilinear Regression and Cluster statistical analyses led the identification of 5 main sources contributing to bulk deposition: crustal matter (39.5%), marine aerosol (38.2%), combustion processes (6.7%), industries (8.7%) and road traffic (1.4%).

In the last chapter, the implications of the results obtained in the air quality and the environment of the studied area are evaluated. It should be noted that the results obtained in this work can contribute to significantly improve the understanding of the properties of aerosols in the atmosphere and the potential impacts of air pollutants on terrestrial and aquatic ecosystems. Moreover, this thesis is a valuable source of information to expand the existing datasets in Cuba, thus providing a very useful information to environmental managers and policy makers to take sound decisions that contribute to improving air quality in Cuba.

Table of Contents

Table of Contents

Chapter 1

General introduction

1. Atmospheric particulate matter

Atmospheric particulate matter (PM), also known as particle pollution, is defined as a mixture of solid particles and liquid droplets found in the air (U.S. EPA, 2016a). This term encompasses both the particles in suspension and those with an aerodynamic diameter greater than 20 µm, called sedimentary particles and characterized by having a short lifetime in the atmosphere. In the literature, the terms MPA and atmospheric aerosol are used as synonyms; however, the term aerosol encompasses both the particulate material in suspension and the mass of air in which it is contained (Putaud et al., 2004). Atmospheric PM levels are defined as mass concentration or number of particles per unit volume of air and is expressed in µg m^{-3} and N cm^{-3}, respectively. Atmospheric PM can be emitted by a wide variety of sources that influence its physical properties (size, surface area, density, chemical composition and size distribution).

Atmospheric PM is a common constituent of the Earth's atmosphere from a natural or anthropogenic origin and considered, in both cases, as an atmospheric pollutant due to the alteration of the original composition of the atmosphere. On a global scale, natural emissions, such as resuspended crustal matter, marine aerosol or particles from volcanic activity and biogenic emissions, are much higher than the anthropogenic emissions (Smithson, 2002). Some of the main anthropogenic sources are the emissions coming from industries, road traffic, biomass burning, oil combustion, agriculture and construction activities. Nowadays, air pollution due to release of PM from these anthropogenic and natural sources is one of the major issues of global concern. The exposure to high levels of PM has negative implications on human health (Pope and Dockery, 2006; WHO, 2016), visibility (Kanakidou et al., 2005), climate (Pöschl, 2005) and ecosystems (Grantz et al., 2003). Comprehensive studies on daily time series of PM levels and chemical composition are, therefore, necessary to evaluate the air quality and to develop effective air quality management strategies.

1.1. Classification of the atmospheric particulate matter

Atmospheric PM can be classified according to different criteria such as its origin (natural or anthropogenic), formation process (primary or secondary), size or chemical composition.

1.1.1. Sources origin of particulate matter

Sources of particulate matter can be natural or anthropogenic (Pöschl, 2005; U.S. EPA, 2009). Particles of natural origin are called to those that come from emissions not caused, directly or indirectly, by human activities. Naturally occurring particles are produced by volcanoes, sea spray, grassland fires, desert dust and by a variety of biological sources (pollen, bacteria, fungal spores, fragments of vegetable organisms and of animals).

Anthropogenic particles are derived from human activities, and include those related to the burning of fossil fuels in vehicles, domestic heating, power plants and industrial processes (Adamiec et al., 2016; Alastuey et al., 2006; Gualtieri et al., 2015; Lawrence et al., 2016). It is also included in this group the mineral material associated with demolition and erosion processes of the road pavement and brakes and tires in vehicles (Amato et al., 2009; Grigoratos and Martini, 2015; Johansson et al., 2009). There are a wide variety of emissions of industrial origin, highlighting the metallurgical activities and the production of cement and bricks, among others (Alastuey et al., 2006; Querol et al., 2001; Sanchez-Soberon et al., 2015; Taiwo et al., 2014). Another large group consists of those particles formed in the atmosphere from gaseous precursors emitted by these and other anthropogenic sources. Averaged over the globe, anthropogenic PM accounts for about 10% of the total aerosol amount.

1.1.2. Primary and secondary particulate matter

PM may be classified as primary or secondary in accordance with its formation mechanism: primary particles are directly emitted into the atmosphere while secondary particles are formed after chemical transformation of their gaseous precursors.

The main primary particles are derived from natural arid regions, oceans, vegetation and volcanoes; while the primary anthropogenic particles are mainly linked to the emissions of road traffic and industrial activities (U.S. EPA, 2009).

Secondary particles can form at locations distant from the sources that release the precursor gases. Examples include sulfates formed from sulfur dioxide emissions from power plants and industrial facilities and nitrates formed from nitrogen oxides released from power plants, mobile sources, and other combustion sources (U.S. EPA, 2014). The transformation of gas to particle can occur through nucleation, condensation and growth processes.

1.1.3. Particles size distribution

Size is the most important parameter for understanding the behavior of aerosols. The size of particles gives information on their sources, determines their transport scale, residence times, removal mechanisms and their environmental and human effects.

Atmospheric particles often are not spherical. Therefore, the size of particles is defined by the equivalent diameter rather than the geometric diameter. The most common is the aerodynamic diameter, which refers to the diameter of a unit density sphere of the same settling velocity as the particle in question. The notation PM_X refers to particulate matter comprising particles less than X μm in aerodynamic diameter.

The diameters of atmospheric particles range from 0.001 to 100 micrometers (μm) and have a modal size distribution. The modal character of the atmospheric PM size distribution results from continuous processes leading to particle formation, and processes leading to removal of particles from the atmosphere. Often, in the literature, particles with diameter greater than 2.5 μm and less than 10 μm are referred as coarse particles ($PM_{2.5-10}$), and particles with diameter less than 2.5 μm are referred as fine particles ($PM_{2.5}$). Traditionally, ultrafine particles (UP, diameters less than 0.1 μm) and nanoparticles (Nano, diameters less than 0.01 μm) are also differentiated. However, the size ranges of particles are handled differently in literature, adding the term “mode” to emphasize references to the fine or coarse mode particles (Wilson and Suh, 1997). This terminology will be used throughout the thesis.

Figure 1.1. illustrates an updated understanding of ambient particle size distributions with multiple modes (Cao et al., 2013), elaborated from the original bimodal distribution from Whitby et al., (1972). Total suspended particles (TSP) are defined as those measured by a high-volume sampler in the particle size range from 0 to ~30 – 50 µm. Nucleation and ultrafine modes denote particles less than 0.01 and 0.1 µm, respectively. The accumulation mode contains most of the fine particles from ~0.1 to ~2 µm. The ~0.2 µm condensation mode results from gas phase reaction products while the ~0.7 µm droplet mode results from gas absorption and reactions in water droplets. The coarse mode extends from ~2 or 3 µm to 100 µm.

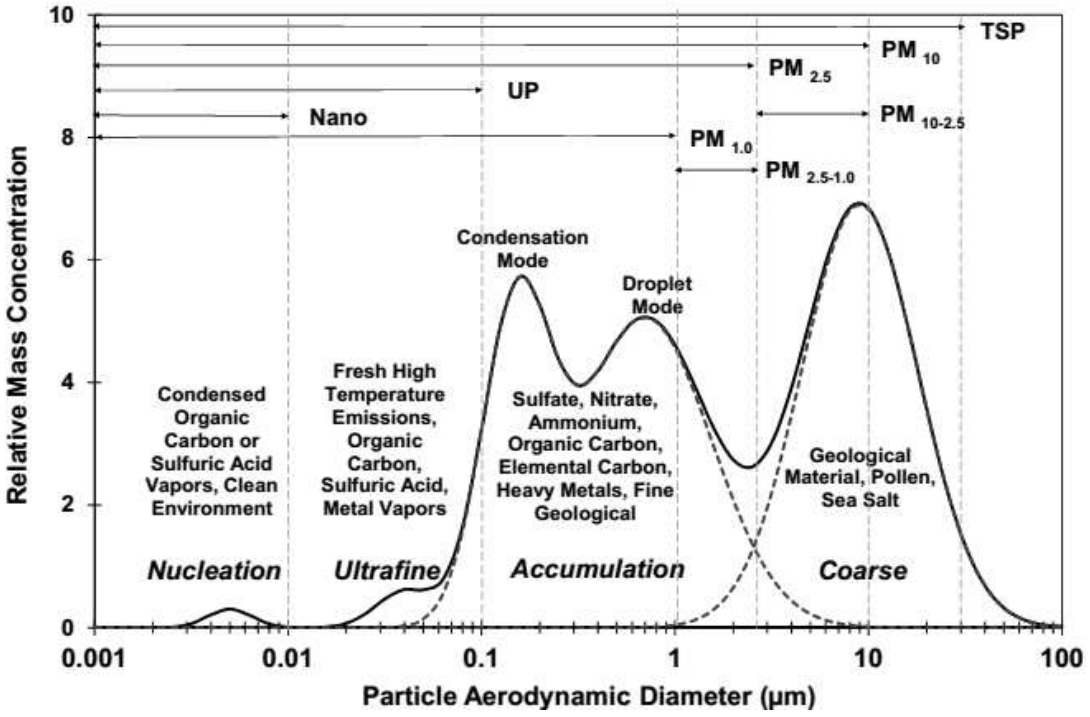

Figure 1.1. Different modes in an idealized example of atmospheric particle size distribution (Cao et al., 2013).

Coarse mode particles are usually produced by mechanical disruption of large particles, by crushing or grinding, the bursting bubbles in the ocean (sea spray) or dust resuspension. The aerosol mass is mainly found in coarse mode. Although most of the coarse particles are primary, some secondary particles may also be found in this fraction. Nitrate formed from the reaction of nitric acid with sodium chloride, and sulfate formed from the reaction of sulfur dioxide with basic particles from a crustal or marine origin,

are examples of secondary particles in the coarse mode (Alastuey et al., 2005; Mariani and de Mello, 2007). In addition, fly ash from uncontrolled combustion of coal, oil and wood, as well as oxides of crustal elements (Si, Al, Ti, Fe), pollen, fungal spores or animal and plant fragments are also found in the coarse mode (Wilson and Suh, 1997). Coarse particles can settle out rapidly from the atmosphere with lifetimes ranging from minutes to hours. The largest coarse particles do not travel long distances as a consequence of their removal by gravitational settling close to the emission source or the impaction on surfaces (Watson and Chow, 1994). In contrast, the smallest coarse particles have longer lifetimes and can be transported across larger regions.

The accumulation mode is comprised of direct PM emissions from combustion sources, such as gasoline- and diesel-fueled engines, and the conversion of oxides of nitrogen (NO_x), sulfur dioxide (SO_2), ammonia (NH_3), and some reactive organic gases (ROG) to PM through atmospheric chemical processes (Watson et al., 2010). The condensation portion of the accumulation mode is formed mostly under dry gas-to-particle conversion conditions. The droplet mode is consistent with aqueous-phase reactions in fogs and clouds; more material accumulates within the water droplet that leaves larger particles when the water evaporates. Another interpretation of these modes for relative humidity > 80% is that the water-absorbing sulfate and nitrate compounds grow into the droplet mode while the water repellent soot and some organic carbon retain their original sizes (Cao et al., 2013). Particles in accumulation mode have long residence times in the atmosphere, ranging from days to weeks (Meszaros, 1993). As a result, they can be transported over long distances until they are removed by wet or dry deposition mechanisms.

Ultrafine particles are both directly emitted by combustion sources and can form by nucleation and growth in the atmosphere (Watson et al., 2010). Fossil fuels often include trace amounts of sulfur that can oxidize to sulfuric acid, and ROG that can oxidize to condensable compounds. As these gases are cooled by dilution with ambient air, they may condense onto larger particles or nucleate into UP. Black carbon soot is produced during oxygen-starved combustion. Some of this soot is UP, but these particles increase in size with time owing to condensation and adsorption of vapors, and by coagulation with other small particles. UP number concentrations decrease and particle sizes

increase rapidly with distance from the source. These particles have relatively short lifetimes of minutes to a few hours after emission or formation similar to the smaller coarse particles ($PM_{2.5-10}$) (Cao et al., 2013).

1.1.4. Chemical composition

During the last decades, substantial improvements have been carried out in the chemical characterization and identification of the main atmospheric aerosol components (Alastuey et al., 2006; Aldabe et al., 2011; Cesari et al., 2016; Kim et al., 2007; Mukherjee and Agrawal, 2017; Viana et al., 2008). Nowadays, most of the individual inorganic species that typically represent more than 1% of the total PM mass, can be easily determined and their main sources identified. Thus, inorganic atmospheric PM can be divided into several major categories, such as crustal material (Si, Al, Fe, Ca, CO_3^{2-}), sea-salt aerosol (Na, Cl), inorganic secondary species (nitrate, sulphate, ammonium), carbonaceous aerosol (elemental carbon) and trace elements.

Much more complex is the case of organic compounds, as this class constitutes a relevant fraction of PM mass (20 – 60%) but includes a wide variety of individual species, each one at very low concentration level (U.S. EPA, 2014). Organic matter can be measured as a whole, but only a small part of the species that constitute this group can be determined individually (Aldabe et al., 2012; Gorka et al., 2014; Parra et al., 2006; Seinfeld and Pankow, 2003). This is the reason why the monitoring of organic species in PM is generally addressed only to harmful (toxic and carcinogenic) compounds or to species that can be considered as tracers of specific PM emission sources (Bonvalot et al., 2016; McDonald et al., 2018 and references therein). Table 1.1 shows an overview of the chemical constituents of atmospheric particles and their major sources.

Table 1.1. Chemical constituents of atmospheric particles and their major sources (U.S. EPA, 2009).

	Primary (PM<2.5 µm)		Primary (PM>2.5 µm)		Secondary PM Precursors (PM<2.5µm)	
Aerosol species	Natural	Anthropogenic	Natural	Anthropogenic	Natural	Anthropogenic
Sulfate (SO_4^{2-})	Sea spray	Fossil fuel combustion	Sea spray	–	Oxidation of reduced sulfur gases emitted by the oceans and wetlands and SO_2 and H_2S emitted by volcanism and forest fires	Oxidation of SO_2 emitted from fossil fuel combustion
Nitrate (NO_3^-)	–	Mobile source exhaust	–	–	Oxidation of NOx produced by soils, forest fires, and lightning	Oxidation of NOx emitted from fossil fuel combustion and in motor vehicle exhaust
Minerals	Erosion and reentrainment	Fugitive dust from paved and unpaved roads, agriculture, forestry, construction, and demolition	Erosion and reentrainment	Fugitive dust, paved and unpaved road dust, agriculture, forestry, construction, and demolition	–	–
Ammonium (NH_4^+)	–	Mobile source exhaust	–	–	Emissions of NH_3 from wild animals, and undisturbed soil	Emissions of NH_3 from motor vehicles, animal husbandry, sewage, and fertilized land
Organic carbon (OC)	Wildfires	Prescribed burning, wood burning, mobile source exhaust, cooking, tire wear and industrial processes	Soil humic matter	Tire and asphalt wear, paved and unpaved road dust	Oxidation of hydrocarbons emitted by vegetation (terpenes, waxes) and wild fires	Oxidation of hydrocarbons emitted by motor vehicles, prescribed burning, wood burning, solvent use and industrial processes
EC	Wildfires	Mobile source exhaust (mainly diesel), wood biomass burning, and cooking	–	Tire and asphalt wear, paved and unpaved road dust	–	–
Metals	Volcanic activity	Fossil fuel combustion, smelting and other metallurgical processes, and brake wear	Erosion, reentrainment, and organic debris	–	–	–
Bioaerosols	Viruses and bacteria	–	Plant and insect fragments, pollen, fungal spores, and bacterial agglomerates	–	–	–

Dash (—) indicates either very minor source or no known source of component.

The chemical and mineralogical composition of the crustal material vary from one region to another depending on the characteristics and composition of soils, being generally constituted by calcite ($CaCO_3$), quartz (SiO_2), dolomite [$CaMg(CO_3)_2$], clays [especially kaolinite, $Al_2Si_2O_5(OH)_4$, and illite, $K(Al,Mg)_3SiAl_{10}(OH)$], feldspars [$KAlSi_3O_8$ and $(Na,Ca)(AlSi)_4O_8$] and lower amounts of calcium sulfate ($CaSO_4\ 2H_2O$) and iron oxides (Fe_2O_3) among others (Sanchez de la Campa et al., 2007). These are mostly primary particles, except some sulfates and nitrates, which can be generated in the atmosphere by reaction with carbonated particles. In particular, the composition of the mineral particulate material transported from arid regions usually includes clays, aluminium oxide (Al_2O_3), iron oxide (Fe_2O_3), magnesium oxide (MgO) and calcium oxide (CaO) (Moreno et al., 2006; Viana et al., 2002). Although most of the mineral material emissions are of natural origin, some are also derived from anthropogenic activities such as the construction, mining, wear of pavement and wheels of cars and the resuspension by the road traffic, especially in urban areas (Castillo et al., 2013; Mazzei et al., 2008; Querol et al., 2004). On a global scale, the emissions of crustal material represent the major mass fraction, reaching up to 44% of the global emissions (Smithson, 2002).

Marine aerosol particles are mainly composed of NaCl, although other species such as $MgCl_2$, Na_2SO_4 and $MgSO_4$ may also be found. Similar to the crustal material, the marine aerosol particles are mostly primary and from an abiotic origin, but there are also secondary sulphate particles derived from the oxidation of natural compounds. Overall, this group represent 38% of the total emissions (Smithson, 2002), being considered the second most important after crustal material.

Sulphate, nitrate and ammonium are mainly generated as result of the oxidation of gaseous precursors in the atmosphere and are generally found in the ultrafine particle fraction. About 90% of the sulphate present in the atmosphere is originated from the oxidation of the SO_2 in the liquid phase in the clouds. This gas is mainly emitted by anthropogenic sources during the fossil fuel combustion in industries (Bove et al., 2016; Mazzei et al., 2008); nevertheless, it can also be emitted by oceans, volcanoes and biogenic activities (Friedrich, 2009). Nitrogen oxides (NO_x), on the other hand, constitute the most important gaseous precursor of nitrate in the atmosphere. Fossil fuel combustion, motor vehicle exhaust, biomass burning and agricultural and livestock

activities are the most relevant anthropogenic contributors of NO_x. Natural nitrogen compounds are produced by soils (N_2O), forest fires (NO_2, NO), lighting (NO) and biogenic activities (NH_3) (Librando and Tringali, 2005).

Oxidation of NO_x and NH_3 results in the formation of HNO_3 and NH_4^+. Nitric acid reacts with the ammonium generating ammonium nitrate (NH_4NO_3). However, the thermodynamic instability of this compound, a consequence of the high vapor pressure of NH_3 and HNO_3, makes it volatile at temperatures above 20-25 ^oC and transforms it into gaseous nitric acid. As a result of this thermal effect, the ammonium nitrate usually shows a marked seasonality (Aldabe et al., 2011; Querol et al., 2001). Relative humidity is another factor that influences the stability of these compounds so that the higher the relative humidity, the more favored is the formation of NH_4NO_3 (Park et al., 2005). The presence of sulfates in the atmosphere also influences the formation of ammonium nitrate. Thus, NH_4^+ has a greater tendency to react with H_2SO_4 and SO_4^{2-} than with NO_3 so in order for NH_4NO_3 to form, there must be excess of ammonium with respect to the sulphate (Bove et al., 2016; Seinfeld and Pandis, 2012).

The carbonaceous material encompasses a wide variety of natural and anthropogenic species with different composition and chemical structures and represents between 2 and 5% of the global emissions (Smithson, 2002). The carbonaceous particles are traditionally divided into an organic carbon (OC), elemental carbon (EC), and a carbonate carbon fraction, being the latter almost exclusively derived from soil dust in the form of K_2CO_3, Na_2CO_3, $MgCO_3$, and $CaCO_3$. By contrast, EC is considered to exclusively derive from primary emissions, which makes it a useful tracer for the primary component of atmospheric particles (Seinfeld and Pankow, 2003). The OC fraction are primary and secondary pollutants (from a natural and anthropogenic origin) formed by condensation of organic volatile compounds (Richter and Howard, 2000; Seinfeld and Pankow, 2003). The primary OC particles of natural origin are mainly constituted by vegetal and edaphic compounds, such as spores, pollen, humic and fulvic acids, microorganisms and fungi. Primary anthropogenic OC emissions, on the other hand, are mainly due to the incomplete combustion processes of organic material and traffic (Gorka et al., 2014; Jones and Harrison, 2005). The three types of carbonaceous

material are traditionally summarized as total carbon (TC) content of the atmospheric PM.

Finally, trace elements, generally found in the fine and UP particles fraction, are released to the atmosphere by natural and, mainly, anthropogenic sources (Birmili et al., 2006; Utsunomiya et al., 2004). Natural sources include volcanism, wind erosion, forest fires and organic debris, whereas anthropogenic sources include combustion of fossil fuels and wood, high temperature industrial activities and waste incineration (Taiwo et al., 2014; U.S. EPA, 2009). Specifically, combustion of fossil fuels is one of the main anthropogenic sources for Be, Co, Hg, Mo, Ni, Sb, Se, Sn and V, and also represents an important contribution to the release of As, Cr, Cu, Mn and Zn (Lin et al., 2005; Moreno et al., 2010). Traffic play also a key role in the emission of trace metals as variable quantities of Cu, Zn, Pb, Fe, Cd, Sn, Sb, V, Ni and Ba are derived from exhaust and non-exhaust traffic emissions (Adamiec et al., 2016; Grigoratos and Martini, 2015; Johansson et al., 2009). Lastly, industrial metallurgical processes emit the largest percentage of As, Cd, Cu, Mn, Cr, Ni and Zn (Querol et al., 2002; Taiwo et al., 2014).

1.2. Dispersion and deposition of atmospheric particulate matter

1.2.1. Factors controlling the dispersion of atmospheric PM

The local meteorological conditions play an important role in the dispersion of atmospheric PM. The degree of dispersion or, in other words, the concentration of the atmospheric particles, will strongly depend on wind speed and atmospheric stability. Wind speed and pollutant concentration (including PM) are reciprocally correlated, i.e. low wind speeds will result in high pollutant concentrations and vice versa. This becomes very clear when considering a chimney that emits smoke at a constant rate. The volume of air into which the smoke is blown will increase with increasing wind speed. Thus, the pollutant concentration will be directly proportional to the rate of emission but inversely proportional to the wind speed. It is important to consider the prevailing wind directions, as the pollution condition is worse down-wind of the sources. However, the concentration of pollutants in urban areas usually does not drop as quickly as predicted by wind speed.

In addition to the direction and velocity of the wind, the vertical mixing of air in the boundary layer of the troposphere [lowest 1 – 2 km of the atmosphere, (Smithson, 2002)] also affect the concentration of the pollutants (Gramsch et al., 2014). The larger the surface roughness the stronger the resulting turbulence when wind blows across it and, as a result, the larger the vertical mixing of air. The roughness coefficient indicates the degree of surface roughness and increases with an increase in obstacles in the pathway of the wind. Large-scale vertical mixing is dominated by the stability of the atmosphere, which in turn is largely controlled by the thermal buoyancy. An air package that is warmed at ground level will rise due to buoyancy, i.e. the surrounding air is colder and heavier. It will then ascend at a rate and to a degree given by the stability of the atmosphere. The rate at which it will cool and expand is called the adiabatic lapse rate, which is about 1 °C over 100 m for dry air and approximately 0.6 °C/100 m for moist air. This effect occurs because the pressure in the atmosphere decreases exponentially with height, and as the air cools, it expands. In the real atmosphere the lapse rate can be smaller, almost equal to, or larger than the adiabatic lapse rate. This has consequences on the extent of vertical mixing. There are various stability categories of the atmosphere. It shall suffice to mention only the ground level and aloft inversion condition (also called thermal inversions), as these will inhibit the dispersion of the pollutants (Harrison, 1999; Miao et al., 2017; Tomaz et al., 2017).

Ground-level inversion (also called surface thermal inversion) most often occurs when the lowest layer of air is cooled by the underneath ground, which frequently takes place during ground's overnight radiative cooling in cloudless nights. This condition usually does not last longer than next midmorning when the warming effect of the sun removes that low-lying layer. Furthermore, the ground level inversion layer is not very thick (often 100 – 200m) and factories with very high chimneys will emit into the well-mixed higher altitude layer above. The increase in the concentration of pollutants during the inversion is facilitated by the decrease in wind speed, since fast moving air above the inversion layer does not mix with the low-level air. Consequently, there will be no exchange in downward momentum and the air in the inversion layer will become stagnant.

The situation is different in the case of the aloft inversion (also called subsidence inversion), which occurs during a certain meteorological condition termed anticyclone. Under these conditions, the pressure gradient becomes progressively weaker so that winds become light. These light winds greatly reduce the horizontal transport and dispersion of pollutants. At the same time, the subsidence inversion aloft continuously descends, acting as a barrier to the vertical dispersion of the pollutants. These pollutants can persist for several days, and the resulting accumulation of pollutants can cause serious health hazards (Liu and Liptak, 1999). In a recent study in a megacity (the metropolitan area of Lima-Callao, Peru) the seasonal fluctuations in the PM were explained by subsidence thermal inversion (Silva et al., 2017). Nevertheless, the local pollution situation is generally worse during episodes of ground-level inversion (Harrison, 1999). Today, when such events occur in big cities (Viard and Fu, 2015), there are restrictions to human activities mainly traffic-related.

The local geography also has a considerable impact on the potential of pollutants to accumulate. Cities located in valleys are especially susceptible to increased pollution levels, as cool air tends to flow down the valley triggering low-level inversions. A quite similar situation occurs in coastal cities. The sea breeze blowing from the cooler sea towards the warmer land during the day will result in cooler air from the sea being forced underneath warmer air on land.

Chimney emission from factories is often a major contributor to air pollution. However, the dispersion of pollutants from chimneys strongly depends on the stability of the atmosphere, the wind speed, chimney (stack) height, and the temperature and exit velocity of the flue gasses. While the ground-level concentration of pollutants is zero close to the chimney, as some time is necessary for vertical mixing to transport pollutants to the ground, it will reach a maximum at some distance downwind that will be larger with increasing stack height and atmospheric stability. As a rule of thumb, the maximum ground-level concentration is inversely proportional to the square of the chimney height. Thus very high chimneys tend to shift a local problem to a regional and/or transboundary one (Harrison, 1999).

Finally, atmospheric lifetime of particles, which is dependent on their size, also influence the dispersion of PM in the atmosphere. The nucleation-mode particles will rather quickly coagulate and, hence, grow into the accumulation mode, where no further growth into the coarse mode takes place. The fine particles from the accumulation mode remain in the atmosphere for a number of days and can travel over thousands of kilometers before being deposited onto surfaces. On the other hand, coarse-mode particles do not remain suspended in the atmosphere for more than minutes to a few hours. As a consequence, the possible range they can travel is considerably shorter. The only exception arises during extreme weather events, such as strong dust storms, when the smallest coarse-mode particles can reach higher altitudes and be transported over longer distances (U.S. EPA, 2009).

1.2.2. Wet and dry deposition of PM

Atmospheric deposition is the transfer of atmospheric pollutants (dust, particulate matter containing heavy metals, polycyclic aromatic hydrocarbons, dioxins, furans, sulphates, nitrates, etc.) to terrestrial and aquatic ecosystems. Nowadays, it is receiving growing attention from the scientific community, becoming the subject of a specific research area in the environmental sciences (Amodio et al., 2014). The research in atmospheric deposition has increased a great deal over the past years, because of its increasing significant contribution to the explanation of pollution phenomena in many environmental compartments. In addition, it enable evaluating the impacts of pollution sources at long and short distances (as in fugitive emissions) and the possibility to carry out long term studies aimed at performing health impact assessment on exposed population (Anatolaki and Tsitouridou, 2007; Bari et al., 2014). The atmosphere is the carrier on which some natural and anthropogenic organic and inorganic chemicals are transported, and deposition events are the most important processes that remove these chemicals, depositing it on soil and water surfaces.

Wet and dry deposition are important processes for removing PM and other pollutants from the atmosphere on urban, regional, and global scales (U.S. EPA, 2009). Wet deposition results from the incorporation of atmospheric particles and gases into cloud droplets and their subsequent precipitation as rain or snow, or from the

scavenging of particles and gases by raindrops or snowflakes as they fall. Wet deposition depends on precipitation amount and ambient pollutant concentrations. Vegetation surface properties have little effect on wet deposition, although leaves can retain liquid and solubilized PM. Wet deposition is most efficient at scavenging the 2 – 10 μm size fraction.

Dry particulate deposition, especially of heavy metals, base cations, and organic contaminants, is a complex and poorly characterized process. It appears to be controlled primarily by such variables as atmospheric stability, macro- and micro-surface roughness, particle diameter, and surface characteristics (Aas et al., 2009). The range of particle sizes, the diversity of canopy surfaces, and the variety of chemical constituents in airborne particles have made it difficult to predict and to estimate dry particulate deposition (Dämmgen et al., 2005; U.S. EPA, 2009). Larger particles >5 μm diameter are dry-deposited mainly by gravitational sedimentation and inertial impaction. Smaller particles, especially those with diameters between 0.2 and 2.0 μm, are not readily dry-deposited and may travel long distances in the atmosphere until their eventual deposition, most often via precipitation. Plant parts of all types, along with exposed soil and water surfaces, receive steady deposits of dry dusts, EC, and heterogeneous secondary particles formed from gaseous precursors.

In arid and semi-arid regions, dry deposition is the major pollutant pathway contributing 90-99% to the total deposition flux due to the limited precipitation (Sabin et al., 2006). Although dry deposition is a slow process, it is continually occurring unlike wet deposition; therefore, it can be of greater importance for net pollutant deposition. Dry deposition will dominate the total deposition flux particularly in areas of low rainfall.

Particles in the atmosphere are also removed via clouds, mist or fog (also called occult deposition) (Amodio et al., 2014). The occurrence of cloud and fog deposition tends to be geographically restricted to coastal and high mountain areas. Several factors make it particularly effective for the delivery of dissolved and suspended particles to vegetation. Concentrations of particulate-derived materials are often many times higher in cloud or fog water than in precipitation or ambient air due to orographic effects and

gas-liquid partitioning. Table 1.2 summarizes the characteristics of ambient PM discussed both in the current and previous sections.

Table 1.2. Characteristics of ambient fine (ultrafine plus accumulation-mode) and coarse particles (U.S. EPA, 2009).

	Fine		**Coarse**
	Ultrafine	**Accumulation mode**	
Formation Processes	Combustion, high-temperature processes, and atmospheric reactions		Break-up of large solids/droplets
Formed by	Nucleation of atmospheric gases including H_2SO_4, NH_3 and some organic compounds Condensation of gases	Condensation of gases Coagulation of smaller particles Reactions of gases in or on particles Evaporation of fog and cloud droplets in which gases have dissolved and reacted	Mechanical disruption (crushing, grinding, abrasion of surfaces) Evaporation of sprays Suspension of dusts Reactions of gases in or on particles
Composed of	Sulfate EC Metal compounds Organic compounds with very low saturation vapor pressure at ambient temperature	Sulfate, nitrate, ammonium, and hydrogen ions EC Large variety of organic compounds Metals: compounds of Pb, Cd, V, Ni, Cu, Zn, Mn, Fe, etc. Particle-bound water Bacteria, viruses	Nitrates/chlorides/sulfates from HNO_3/HCl/SO_2 reactions with coarse particles Oxides of crustal elements (Si, Al, Ti, Fe) $CaCO_3$, $CaSO_4$, NaCl, sea salt Bacteria, pollen, mold, fungal spores, plant and animal debris
Solubility	Not well characterized	Largely soluble, hygroscopic, and deliquescent	Largely insoluble and nonhygroscopic
Sources	High temperature combustion Atmospheric reactions of primary, gaseous compounds.	Combustion of fossil and biomass fuels, and high temperature industrial processes, smelters, refineries, steel mills etc. Atmospheric oxidation of NO_2, SO_2, and organic compounds, including biogenic organic species (e.g., terpenes)	Resuspension of particles deposited onto roads Tire, brake pad, and road wear debris Suspension from disturbed soil (e.g., farming, mining, unpaved roads) Construction and demolition Fly ash from uncontrolled combustion of coal, oil, and wood Ocean spray
Atmospheric half-life	Minutes to hours	Days to weeks	Minutes to hours
Removal processes	Grows into accumulation mode Diffuses to raindrops and other surfaces	Forms cloud droplets and rains out Dry deposition	Dry deposition by fallout Scavenging by falling rain drops
Travel distance	<1 to 10s of km	100s to 1000s of km	<1 to 10s of km (100s to 1000s of km in dust storms for the small size tail)

1.3. Effects of atmospheric particulate matter

1.3.1. Health effects

The impact of PM on human health is clearly connected with the different capacities of the particles to penetrate into the breathing apparatus, with smaller ones reaching more easily the deeper parts of the lungs and being therefore more dangerous. Particles with aerodynamic diameter greater than 10 μm are trapped in the outermost tracts of the respiratory system and are then easily expelled. Particles with aerodynamic diameter between about 10 and 2.5 μm tend to be inhaled and trapped in the nose, throat, and upper bronchial tract. The removal from the body is generally by swallowing. Particles smaller than about 2.5 μm enter the deep lung and are retained in the alveoli; removal tends to be through the blood stream, which is generally more hazardous than through the respiratory system (Cao et al., 2013). The physical and chemical properties (particle size, structure, number, mass concentration, solubility, chemical composition, and individual components, etc.) determine the adverse health effects of particles deposited in different parts of the human body.

Numerous epidemiological studies show that atmospheric PM, especially those particles smaller than 2.5 μm and traffic-related air pollution, are correlated with severe health effects, including elevated mortality and cardiovascular, respiratory, and allergic diseases (Batterman et al., 2014; Hopke et al., 2006; Le Tertre et al., 2002; Pope and Dockery, 2006). The effects of exposure to atmospheric particulate matter are observed in both chronic and acute contamination episodes (U.S. EPA, 2009). Both types of episodes involve increases in hospital admissions for respiratory and cardiovascular diseases, being these the main causes of the increase in mortality (Tie et al., 2009).

A recent review has highlighted many studies in which the relationship between short-term and long-term exposure to PM_{10} concentrations and mortality has been reported (Mukherjee and Agrawal, 2017). Time-series analysis of mortality effects from particulate matter size fractions in Beijing, China, found significant associations of daily mortality with PM_{10} (Li et al., 2013). In Shenyang, China, an increase in adverse health effects with reduction in particle size was found (Meng et al., 2013). Short-term effects

of ambient particles on cardiovascular and respiratory mortality study in 29 European cities found that an increase of 10 μg m^{-3} PM_{10} was associated with increases of 0.76% in cardiovascular deaths and 0.58% in respiratory deaths. A study in 20 US about fine particulate air pollution and mortality showed that death from cardiovascular and respiratory causes had higher association with PM_{10} than the rate of death from all causes (Samet et al., 2000).

In a recent report by the World Health Organization (WHO) on air pollution exposure and health impact it was estimated that some 3 million deaths a year are linked to exposure to outdoor air pollution, and an estimated 6.5 million deaths (11.6% of all global deaths) were associated with indoor and outdoor air pollution together in 2012 (WHO, 2016). In this report is also provided a new WHO air quality model that highlight (via interactive maps) areas within countries that exceed WHO limits and show countries where the air pollution ($PM_{2.5}$) danger spots are. It also represented the most detailed outdoor (or ambient) air pollution-related health data by country, ever reported by WHO.

1.3.2. Effects on climate

Aerosol particles scatter and absorb solar and terrestrial radiation (influencing the global radiative balance) and they are involved in the formation of clouds and precipitation as cloud condensation and ice nuclei (CCN and IN) (Meszaros, 1993; Wurzler et al., 2000).

Aerosol effects on climate are generally classified as direct or indirect with respect to radiative forcing (W m^{-2}) of the climate system. Radiative forcings are changes in the energy fluxes of solar radiation (maximum intensity in the spectral range of visible light) and terrestrial radiation (maximum intensity in the infrared spectral range) in the atmosphere, induced by anthropogenic or natural changes in atmospheric composition, Earth surface properties, or solar activity. Negative forcings such as the scattering and reflection of solar radiation by aerosols and clouds tend to cool the Earth's surface, whereas positive forcings such as the absorption of terrestrial radiation by greenhouse gases and clouds tend to warm it (greenhouse effect) (Smithson, 2002).

Sulphates and mineral materials are extremely effective in the dispersion of the incident radiation, producing a negative radiative forcing. On the other hand, EC is characterized by its ability to absorb the radiation emitted by the earth's surface, so it produces a positive radiative forcing. The global mean direct radiative forcing effect from individual components of aerosols had been estimated for sulfate (-0.4 ± 0.2 W m^{-2}), for fossil fuel-derived organic carbon (-0.05 ± 0.05), for fossil fuel-derived black carbon (+0.2 ± 0.15), for biomass burning (+0.03 ± 0.12), for nitrates (-0.1 ± 0.1), and for mineral dust (-0.1 ± 0.2) (U.S. EPA, 2009).

Direct effects result from the scattering and absorption of radiation by aerosol particles, whereas indirect effects result from their CCN and IN activity (influence on clouds and precipitation), or from their chemical and biological activity (influence on aerosol and trace gas emissions and transformation) (Pöschl, 2005). Taken together, direct and indirect effects from aerosols increase Earth's shortwave albedo or reflectance thereby reducing the radiative flux reaching the surface from the Sun. This produces net climate cooling from aerosols. However, while the overall global average effect of aerosols at the top of the atmosphere and at the surface is negative, absorption and scattering by aerosols within the atmospheric column warms the atmosphere between the Earth's surface and top of the atmosphere (U.S. EPA, 2009).

1.3.3. Environmental effects

On ecosystems

Ecological effects of PM include direct effects to metabolic processes of plant foliage; contribution to total metal loading resulting in alteration of soil biogeochemistry and microbiology, plant growth and animal growth and reproduction; and contribution to total organics loading resulting in bioaccumulation and biomagnification across trophic levels (Grantz et al., 2003; U.S. EPA, 2009). Exposure to a given concentration of PM may, depending on the mix of deposited particles, lead to a variety of phytotoxic responses and ecosystem effects (Okin et al., 2011). Moreover, many of the ecological effects of PM are due to the chemical constituents (e.g., metals, organics, and ions) and their contribution to total loading within an ecosystem. The ecosystem response to pollutant deposition is a direct function of the level of sensitivity of the ecosystem and

its ability to ameliorate the resulting change. Many of the most important ecosystem effects of PM deposition occur in the soil. Upon entering the soil environment, PM pollutants can alter ecological processes of energy flow and nutrient cycling, inhibit nutrient uptake, change ecosystem structure, and affect ecosystem biodiversity. Likewise, the deposit of atmospheric particulate material can contribute to the acidification and eutrophication of soils and surface waters, which in turn can have an impact on the composition of groundwater.

On material

PM can stain and damage stone and other materials, including culturally important objects such as statues and monuments. Some of these effects are related to acid rain effects on materials (Xie et al., 2004). The stones most susceptible to deterioration are calcareous stones, such as limestone, marble and carbonated cement. The damage occurs when salts are formed in the stone (specially by the interaction with sulfate particles) which are subsequently washed away and will leave the surface of the stone more susceptible to the effects of pollution (Ausset et al., 1999). Other damage is related to the corrosion. Metals form a protective film of oxidized metal that slows environmentally induced corrosion. However, the natural process of metal corrosion is enhanced by exposure to anthropogenic pollutants. For example, formation of hygroscopic salts increases the duration of surface wetness and enhances corrosion (U.S. EPA, 2009).

On visibility

The reduction in visibility is primarily due to the scattering and absorption of light by suspended fine particles and gases in the atmosphere. Particles and gases in the atmosphere attenuate light on its way from an object to the observer (Sisler and Malm, 2000). The fractional attenuation of light per unit distance is termed light extinction coefficient, and it is composed by the sum of four components (i.e., absorption and scattering by gases and particles). Although a larger particle scatters more light than a similarly shaped smaller particle of the same composition, the light scattered per unit of mass is greatest for particles with diameters from ~0.3-1.0 μm (U.S. EPA, 2009). The light scattering of gases only dominate the light extinction under pristine atmospheric

conditions. Otherwise, it is the particles that have the greatest effect on visibility. The single most important factor determining the amount of light scattered by a particle is its size and the maximum single-particle scattering efficiency (i.e. scattering per cross-sectional area of a particle) is achieved by particles with diameters of about the wavelength of visible light, centered at around 0.53 μm. Therefore, the effects of relative humidity on particle size will significantly affect the amount of particle light scattering.

1.4. Source identification and source apportionment of atmospheric particulate matter

1.4.1. Receptor models

The identification and apportionment of pollutants to their sources is an important step in air quality management. Source apportionment is the practice of deriving information about pollution sources and the amount they contribute to ambient air pollution levels. In the last two decades receptor models have been widely used to apportion sources of PM (Belis et al., 2011; Contini et al., 2016; Kim et al., 2003; Singh et al., 2017). They are used to evaluate the contamination and pollutant sources contributions in different kind of samples, starting from the information carried out by the samples (registered at monitoring site) and hence at the point of impact, or receptor (Comero et al., 2009). Particulate matter emissions from specific sources often have unique elemental profiles by which the contribution of these sources to the total PM at the receptor can be recognized. Figure 1.2 shows typical identified sources of PM_{10} around the world (Mukherjee and Agrawal, 2017).

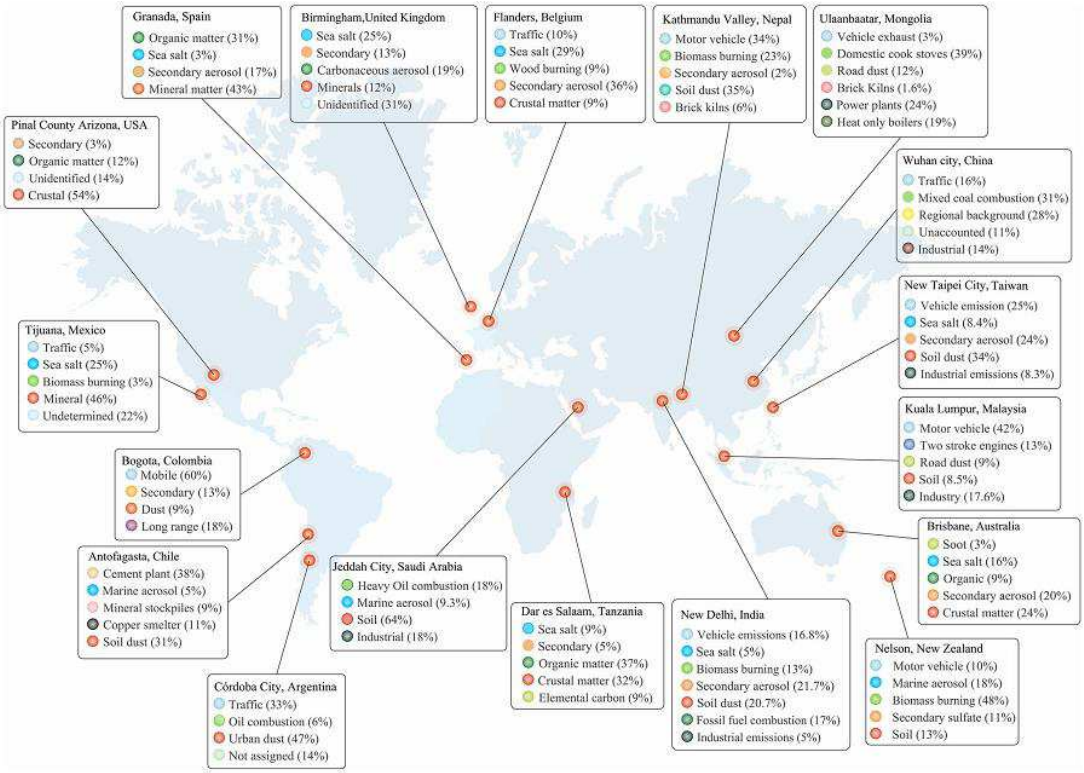

Figure 1.2. Sources of PM_{10} in selected cities of the world. Source profiles are given in percentage with respect to different sources (Mukherjee and Agrawal, 2017).

Receptor models are based on the Chemical Mass Balance (CMB) equations that considered a single sample taken at a single location and time period, and can be expressed as:

$$c_{ij} = \sum_{i} f_{ik} g_{kj} + e_{ij} \qquad (1.1)$$

where c_{ij} is the amount of the i^{th} variable (e.g. a chemical element or compound concentration, or a physical property amount) measured at the location (sample) j; f_{ik} is the fractional abundance of the i^{th} variable in the k^{th} source type and g_{kj} is the contribution of the k^{th} source at the location j. Parameter e_{ij} represents the residuals that is the difference between the measured and calculated amounts.

Receptor models are categorized in two principal classes, based on the CMB (equation 1.1): chemical mass balance models and multivariate models. In addition to chemical measurements at a receptor, CMB models requires the additional inputs of the source emission profiles. Sources profiles are customary known from preceding studies

or extracted from existing data sets. The most useful model in this class is the Chemical Mass Balance (CMB). However, in many cases, the main sources are not well-known and/or inappropriate source profiles from other locations are used, making the model usually very inaccurate. In contrast to CMB, multivariate receptor models do not require source profiles as an input, as this is part of the solution. In other words, these models estimate the number, composition and contribution of the sources starting from observations (e.g. element concentrations data set) at the receptor site. The most widely applied multivariate receptor models are principal component analysis (PCA), factor analysis (FA), multiple linear regression analysis (MLRA), positive matrix factorization (PMF) and combinations of the above.

PCA-MLRA

PCA and its variants attempt to reduce the initial set of variables into a new set of casual factors with reduced dimension, by means of correlations between the measured variables (Comero et al., 2009). This technique is based on the idea that the time dependence of a chemical species at the receptor site will be similar to that of other species from the same source (Chueinta et al., 2000). Correlations of the measured chemical and other species are analyzed and groups of underlying 'factors' (typically called *principal components*) that depict the common variability in the analyzed dataset are extracted. Since the originally extracted factors are often difficult to interpret, the factors are usually transformed by a specific procedure called factor rotation. The most commonly used method is known as VARIMAX rotation, which results in orthogonal factors that are virtually uncorrelated with each other and often easier to interpret than the original factors (Vallius, 2005). The rotated factors are assumed to correspond to specific sources, or source categories. Since PCA as such does not yield quantitative source contributions, the apportionment of particulate matter among the identified source categories has to be done separately. This is usually done by regressing the measured PM either directly on the source tracer elements or on factor scores obtained from PCA (Oravisjärvi et al., 2003; Thurston and Spengler, 1985). This technique is known as multiple linear regression analysis (MLRA).

Since the scores of the factors extracted from the PCA are traditionally normalized, the application of MLRA on factor scores obtained from PCA begin with the introduction of an "absolute zero" for the principal component (PC) score, which it estimated for each PC by separately scoring an extra "sample" wherein all the elemental concentrations are zero (Thurston and Spengler, 1985):

$$(Z_0)_i = \frac{0 - \overline{C_i}}{\sigma_i} \qquad (1.2)$$

Here $\overline{C_i}$ and σ_i are the average concentration and the standard deviation for the ith variable, respectively.

Then the rotated absolute zero PC scores P_{0_i} for each of p components are calculated:

$$P_{0_i} = \sum_i B_{pi}(Z_0)_i \qquad (1.3)$$

where B_{pi} is the rotated matrix of coefficients for the calculation of the PC scores derived from the PCA (e.g. after the VARIMAX rotation).

These estimates of the PC scores for each component at absolute zero are then used to estimate the Absolute PC Scores (APCS) for each component on each sample as follows:

$$APCS_{pj} = P_{pj} - P_{0_{pj}} \qquad (1.4)$$

where P_{pj} are the rotated PC scores given after the PCA and the j columns of $P_{0_{pj}}$ are all identically equal to the values calculated in (1.3).

Now, regressing the total PM mass data on these APCS gives estimates of the coefficients which convert the APCS into pollutant source mass contributions for each sample, as follows:

$$C_k = a_0 + \sum_{j=1}^{p} a_j APCS_{jk} \qquad (1.5)$$

where C_k, is the PM mass recorded during observation k; $APCS_{jk}$ is the rotated absolute component score for component j on observation k; $a_j APCS_{jk}$ is the particle mass contribution on observation k made by the pollution source identified with component j; and a_0 the particle mass contribution made by sources unaccounted for in the PCA.

PCA followed by MLRA has been extensively used in different kinds of studies related to the atmosphere, such as: atmospheric PM (Alastuey et al., 2007; Guo et al., 2016; Tai et al., 2010) and atmospheric deposition (Castillo et al., 2013; Latif et al., 2015).

PMF

Positive Matrix Factorization (PMF) is a multivariate factor analysis tool for quantifying the contribution of sources to samples based on the detailed composition of the samples collected in one or more sites (Paatero, 1997; Paatero and Tapper, 1994). PMF solves the CMB equation, by decomposing a matrix of known speciated sample data (X), into the product of two new matrices: the factor profile (F) and the factor contribution (G) plus a residual matrix (E). This formulation can be respectively written in matrix and index notation as follows,

$$X = GF + E \qquad (1.6)$$

$$x_{ij} = \sum_{k=1}^{p} g_{ik} f_{kj} \; + \; e_{ij}, \qquad i \in [1, n];\; j \in [1, m] \qquad (1.7)$$

where n and m are the number of samples and species, respectively; and p is the calculated number of factors. The coefficients of F and G are constrained to be non-negative and they are calculated by the PMF model minimizing the objective function Q, which uses both sample concentration and user-provided uncertainty (s_{ij}) associated with the sample.

$$Q = \sum_{i=1}^{n} \sum_{j=1}^{m} \left[\frac{x_{ij} - \sum_{k=1}^{p} g_{ik} f_{kj}}{s_{ij}} \right]^2 \qquad (1.8)$$

Two main algorithms are used to solve this problem: PMF2 and ME-2 (Multilinear Engine). The lattes is used to solve the PMF problem in the latest version (5.0) of EPA

PMF, a freely available program and graphical user interface (GUI) developed by the U.S. Environmental Protection Agency (EPA) (Brown et al., 2015). ME-2 performs iterations via the conjugate gradient algorithm until convergence to a minimum Q value is obtained. The minimum Q may be global or local; users can attempt to determine whether Q values are global or local by using different starting points for the iterative process and comparing the minimum Q values reached. To maximize the chance of reaching the global minimum, the model should be run 20 times developing a solution and 100 times for a final solution, each time with a different starting point (Norris et al., 2014).

One of the main potentialities included in the latest version of EPA PMF is the estimation of the variability in the PMF solution by two new error estimation methods (Brown et al., 2015; Paatero et al., 2014). Variability due to chemical transformations or process changes can cause significant differences in factor profiles among PMF runs. These variabilities can be now estimated using three complementary methods, which allow to understand the uncertainty of a PMF solution (Norris et al., 2014):

1. Bootstrap (BS) analysis is used to identify whether there are a small set of observations that can disproportionately influence the solution. BS error intervals include effects from random errors and partially include effects of rotational ambiguity. Rotational ambiguity is caused by the existence of infinite solutions that are similar in many ways to the solution generated by PMF. BS errors are generally robust and are not influenced by the user-specified sample uncertainties.
2. Displacement (DISP) is an analysis method that helps the user understand the selected solution in finer detail, including its sensitivity to small changes. DISP error intervals include effects of rotational ambiguity but do not include effects of random errors in the data. Data uncertainty can directly impact DISP error estimates. Hence, intervals for downweighted species are likely to be large.
3. BS-DISP error intervals include effects of random errors and rotational ambiguity. BS-DISP results are more robust than DISP results since the DISP phase of BS-DISP does not displace as strongly as DISP by itself.

Resolving PMF algorithms is slower than PCA and, in addition, PCA is simpler to use because of less parameters to control. In contrast, PMF is generally more powerful than the best possible PCA or at least equivalent to PCA (Belis et al., 2015a, 2015b; Comero et al., 2009). Nevertheless, both methods can be complementary. If very little information is available on the study area or if skilled staff are not available for running the standard applications, exploratory and simpler methods can be used to obtain a preliminary picture of the most relevant sources (Belis et al., 2013). Moreover, different receptor models can be used in combination with independent methodologies (e.g. emission inventories and chemical transport models) to achieve more robust estimations by mutual validation of the outputs.

1.4.2. Stable C and N isotopic composition of atmospheric PM

The ratio between the rare (or heavy) to common (or light) stable C and N isotopes varies in the biosphere as a result of isotope fractionation in physical, chemical and biological processes (Heaton et al., 1997; Hoefs, 2015; West et al., 2006). This isotopic fractionation is produced because the rates of reaction and transport, in which they are involving, depend on nuclidic mass, and isotopic substitutions subtly affect the partitioning of energy within molecules. As a result, the molecules containing ^{13}C and ^{15}N are discriminated against ^{12}C and ^{14}N in a number of processes associated with chemical equilibriums and kinetics. It is precisely this characteristic that makes these isotopes useful in atmospheric aerosols studies.

Carbon and nitrogen isotopic ratios in the atmosphere are usually studied by measuring the natural abundances of the rare stable isotopes (^{13}C and ^{15}N), relative to those of the most abundant (^{14}N and ^{12}C) (Agnihotri et al., 2011; Widory, 2006). Because the interesting isotopic differences between natural samples usually occur at and beyond the third significant figure of the isotope ratio, it has become conventional to express isotopic abundances relative to an international accepted standard using a delta notation (δ). Commonly, the standard used for carbon is a particular calcareous fossil, the Pee Dee Belemnite (PDB) and for nitrogen it is atmospheric air (AIR). Then, ^{13}C and ^{15}N relative abundances ($\delta^{13}C$ and $\delta^{15}N$) are expressed as:

$$\delta^{13}C\ (‰\ \text{vs. PDB}) = \left[\left(R_{sample}/R_{standard} - 1\right)\right] x\ 1000 \qquad (1.9)$$

$$\delta^{15}N\ (‰\ \text{vs. AIR}) = \left[\left(R_{sample}/R_{standard} - 1\right)\right] x\ 1000 \qquad (1.10)$$

where $R = {}^{13}C/{}^{12}C$ or ${}^{15}N/{}^{14}N$.

Several works have used stable carbon and nitrogen isotopes to establish the source and reaction processes in gases, aerosols and atmospheric particles. Pioneering studies differentiated anthropogenic from natural (marine and continental) particulate carbon emissions (Cachier et al., 1985; Chesselet et al., 1981). δ^{15}N in aerosols had been used to investigate atmospheric N cycling and to help elucidating the sources of primary and possibly of secondary nitrogen (Moore, 1977; Pavuluri et al., 2010; Widory, 2007; Yeatman et al., 2001). Coupled δ^{13}C and δ^{15}N have been studied to discern between C-3 and C-4 vegetation type (Kelly et al., 2005; Martinelli et al., 2002). More recently, these isotope systematics also have been used to trace the sources of atmospheric particles in urban environments by comparing the isotopic composition (δ^{13}C and δ^{15}N) of ambient samples with those characteristic of potential sources (Chen et al., 2017; Gorka et al., 2012; Guo et al., 2016; Lopez-Veneroni, 2009; Sudheer et al., 2016; Widory et al., 2004).

Unlike receptor models, isotopic analysis is a non-statistical fingerprinting technique and is mostly used for source identification purposes (Mari et al., 2016). However, isotope mixing equations (or isotope mass balance equation) have been used to calculate relative contributions from different aerosol sources (Ceburnis et al., 2011; Garbariene et al., 2016; Masalaite et al., 2015; Turekian et al., 2003). When n isotope systems are used to determine the proportional contributions of n+1 sources to a mixture, standard linear mixing models can be used to mathematically solve for the unique combination of source proportions that conserves mass balance for all n isotopes (Phillips and Gregg, 2003). For example, with two isotope systems (denoted by 1 and 2) and three sources, the following system of mass balance equations can be solved to determine the proportions (f_A, f_B and f_C) of source isotopic signatures (δ_A^1, δ_B^1, δ_C^1 and δ_A^2, δ_B^2, δ_C^2) which coincide with the observed signature for the mixture (δ_M^1, and δ_M^2):

$$\delta_M^1 = f_A\delta_A^1 + f_B\delta_B^1 + f_C\delta_C^1 \qquad (1.11)$$

$$\delta_M^2 = f_A\delta_A^2 + f_B\delta_B^2 + f_C\delta_C^2 \qquad (1.12)$$

$$1 = f_A + f_B + f_C \qquad (1.13)$$

It should be noted that Equations 1.11 to 1.13 can be solved explicitly only if individual source isotopic signatures are fixed. Distinct isotopic signatures generally persist for only one or two elements per system, so relative source contribution determinations are often limited to estimates for two or three sources. Although resolution of the contribution of relatively few sources can be useful for specific applications, the inherent complexity of natural systems often requires the inclusion of a larger number of sources. Nevertheless, a procedure to calculate the range of all possible source contributions for systems where the number of potential sources is greater than n+1 has also been developed (Phillips and Gregg, 2003).

1.5. Air quality regulations

1.5.1. International regulations

Due to the effects of atmospheric PM on health, climate and ecosystems, the estimate of the particulate matter content in the atmosphere along with the determination of some of their chemical constituents are classic parameters in the control of air quality. In most countries and regions of the world, air quality regulations have been established with the objective of controlling and reducing the levels of these pollutants in the air.

In the United States, EPA has set National Ambient Air Quality Standards (NAAQS) for six common air pollutants (also known as "criteria air pollutants"), which are periodically reviewed and revised when necessary (U.S. EPA, 2016b). These pollutants include particulate matter ($PM_{2.5}$ and PM_{10}), ground-level ozone (O_3), carbon monoxide (CO), lead (Pb), sulfur dioxide (SO_2) and nitrogen dioxide (NO_2). The current standard for the concentration of PM_{10} in air is 150 μg m^{-3} measured over an average time of 24 hours. In the European Union (EU), Directive 2008/50/EC (Directive 2008/50/EC, 2008) establishes air quality objectives for the same pollutants, including ambitious, cost-

effective targets for improving human health and environmental quality by 2020 throughout the European Union. This Directive sets a PM_{10} daily limit of 50 μgm^{-3}, that should not be exceeded more than 35 times per year, although also states that the exceedances attributable to natural sources, shall not be considered as such for the purpose of compliance with the limits established.

In general, air quality standards vary between countries and regions depending on many factors and conditions. In an effort to protect world public health from the effects of air pollution and eliminate or minimize exposure to hazardous pollutants, WHO published Air Quality Guidelines for classical air pollutants: PM, O_3, NO_2 and SO_2 (WHO, 2005). These guidelines were also formulated to assist Governmental Agencies in the preparation of their Air Quality Standards, thereby guiding the authorities and environmental health professionals who are responsible for protecting the population from the harmful effects of Air Pollution. Table 1.3 provides the guideline values for classical pollutants and for different average times.

Table 1.3. WHO Air quality guidelines for particulate matter, ozone, nitrogen dioxide and sulfur dioxide (WHO, 2005).

Pollutant	Concentration ($\mu g\ m^{-3}$)	Averaging Time
PM_{10}	50	24 hours
	20	1 year
$PM_{2.5}$	25	24 hours
	10	1 year
Ozone	100	8 hours
Nitrogen dioxide	200	1 hour
	40	1 year
Sulfur dioxide	500	10 minutes
	20	1 year

Even today, in many countries and states, including those of greater economic development, the number of pollutants subject to air quality standards is almost exclusively limited to the so-called “criteria air pollutants” because of the precise knowledge of its adverse effects. Some countries also regulate some additional pollutants at national or regional level, but the vast majority of the hazardous pollutants present in the air are not directly regulated, but their management is based on reducing

and limiting the quantity and conditions of emissions (Directive 2010/75/EU, 2010; Regulation (EU) 2016/2286, 2016).

1.5.2. Cuban regulations

By 2014, the Cuban Air Quality standard (NC 39: 1999 Air quality – Health and Sanitary Requirements), already included 115 pollutants (NC 39, 1999). However, PM_{10} and $PM_{2.5}$ were not considered in this standard. In fact, the control of atmospheric PM levels continued to be carried out by measuring total suspended particles (TSP) and soot. By the same token, the rest of pollutants followed standards that had not been modified since 1984. In 2014, a new legislation (NC 1020: 2014 Air quality — Pollutants — Maximum admissible concentrations and guidelines at inhabitable zones), that includes concentration limits for $PM_{2.5}$, PM_{10} and other pollutants, was additionally adopted (NC 1020, 2014). Table 1.4 provide the maximum admissible concentrations (MAC) for the classical and other selected pollutants included in the new legislation. This also includes guide values for several pollutants for which there is no possibility to establish a MAC because of the lack of toxicological and epidemiological information. These guide values are based on the WHO guidelines and, while not mandatory, are important references for the proposal of future air quality standards.

Table 1.4. Maximum admissible concentrations (MAC) of air pollutants at inhabitable zones in Cuba (NC 1020, 2014).

Pollutant	MAC ($\mu g\ m^{-3}$)	Average Time	Form
PM_{10}	50	24 hours	Not to be exceeded
	30	1 year	
$PM_{2.5}$	25	24 hours	Not to be exceeded
	15	1 year	
Ozone	150	1 hour	95th percentile of the year determinations not to be exceeded
	100	8 hours	98th percentile of the year determinations not to be exceeded
Nitrogen dioxide	40	24 hours	95th percentile of the year determinations not to be exceeded
	35	1 year	98th percentile of the year determinations not to be exceeded
Sulfur dioxide	45	24 hours	98th percentile of the year determinations not to be exceeded
	40	1 year	Not to be exceeded
Lead	1	24 hours	Not to be exceeded
	0.5	1 year	
Mercury	2	24 hours	Not to be exceeded
	1	1 year	
Arsenic	0.02	24 hours	Not to be exceeded
	0.01	1 year	
Cadmium	0.02	24 hours	Not to be exceeded
	0.01	1 year	
Nickel	0.1	24 hours	Not to be exceeded
	0.02	1 year	
Vanadium	1	24 hours	Guide value
Chlorine	10	24 hours	Not to be exceeded
Cobalt	1	24 hours	Not to be exceeded
Chromium	1	24 hours	Not to be exceeded
Manganese	10	24 hours	98th percentile of the year determinations not to be exceeded
Benzene	5	24 hours	Not to be exceeded
	3	1 year	

Other important air quality regulations in Cuba are included in the legislation NC 111: 2004 (Air Quality — Rules for the observation of air quality in human establishments) (NC 111, 2004). This legislation establishes, among others important aspects, the characteristics to be considered when choosing the sampling points, the types of environmental monitoring plans (systematic and special) and the establishment of an Air Quality Index (ICA, Spanish acronyms) to assess the degree of air pollution in

human settlements. The ICA is calculated for each pollutant according to the following equation:

$$ICA_x = \frac{C_x}{MAC_x} x100 \qquad (1.14)$$

where C_x is the measured average concentration of the pollutant x and MAC_x is the maximum admissible concentrations of the same pollutant x for the resolution period according to the NC 39: 1999 or NC 1020: 2014 . Based on the results of this calculation, the ICA include a scale of six categories:

1) Buena (“good”): 0 – 79
2) Aceptable (“acceptable”): 80 – 99
3) Deficiente (“deficient”): 100 – 199
4) Mala (“poor”): 200 – 299
5) Pésima (“very poor”): 300 – 499
6) Crítica (“critical”): ≥500

Although the ICA is calculated for daily and hourly periods, in order to allow the adoption of appropriate control measures, its retrospective analysis is also valid for longer periods of time (monthly and annual). It allows evaluating different aspects such as the trend of air quality over time or the effectiveness of the control measures adopted. Moreover, it also makes it possible to relate the air quality to the epidemiological patterns of diseases linked to environmental pollution or to meteorological or climatic modifications. The evolution of the ICA is also an interesting tool to compare the situation in the region with the existing situation in other territories or countries or to assess the perspectives of economic and social development of the area. Lastly, the standard also includes general actions that must be carried out according to the category of the ICA.

In addition, since 2010 Cuba has a specific legislation to control the emission of pollutants into the air at fixed point sources, especially focused on large combustion power plants (NC-TS 803: 2010 Air quality — Admissible maximum emissions of

pollutants atmosphere in punctual fixed sources of generating facilities of electricity and steam) (NC-TS 803, 2004).

1.6. Status of studies on atmospheric PM in Cuba

Atmospheric PM in the Gulf of Mexico, southern and eastern United States and some region of the Caribbean have been largely studied (Boman and Gaita, 2015; Bozlaker et al., 2013a; Gichuki and Mason, 2014; Gioda et al., 2007; Golomb et al., 1997; Harris et al., 2012; Jusino-Atresino et al., 2016; Prospero et al., 2001; Strayer et al., 2007). Many studies have been not only focused on the input amount of several pollutants, such as heavy metals from anthropogenic and natural local sources, but also on long-range contributions, mainly due to the African transported dust that affect these regions every year (Bozlaker et al., 2013b; Lenes et al., 2012; Prospero, 1999; Prospero et al., 2014; Prospero and Mayol-Bracero, 2013; Rodriguez et al., 2015; Trapp et al., 2010). However, in many regions of the Caribbean basin, and especially in Cuba, atmospheric PM has been poorly investigated.

To date, experimental studies in Cuba have been restricted to some urban locations, mainly in the capital of the country (Havana city). This situation has been a consequence of the technical difficulties associated to the instrumentation maintenance and availability (Barja et al., 2013). Most of the studies carried out in Havana were performed near industrial and traffic sources, in a station located in the *Instituto Nacional de Higiene, Epidemiología y Microbiología (INHEM).* These studies included reports on TSP, $PM_{2.5}$, PM_{10}, gaseous pollutants (NO_2, SO_2 and NH_3) and chemical constituents (Cuesta-Santos et al., 2002; Martínez Varona et al., 2015a, 2015b, 2013, 2011, 2008; Molina Esquivel et al., 2011; Pérez et al., 2010, 2009). The results of these studies suggested a dominant influence from marine aerosol and local anthropogenic sources. The unique PM source apportionment study found in Cuba was carried out in Havana (Piñera et al., 2010). In this work, it identified the main sources of $PM_{2.5}$ using to that end a PCA-MLRA model. Finally, 5 main sources were identified in this study: waste incineration, fossil fuel combustion, resuspended soil, industrial emissions and marine aerosol. Other studies also carried out in Havana showed the close relationship among the concentration of PM_{10} levels and other pollutants and respiratory diseases (Romero-

Placeres et al., 2004; Suárez Tamayo et al., 2010). Additionally, a recent work determined the atmospheric fungal spore concentration in Havana (Almaguer et al., 2014).

Very few studies have been conducted in the rest of the country. In one of them, a work carried out in the region of Camagüey (Barja et al., 2013), the chemical composition and the optical absorbing properties of PM_{10} and PM_1 were determined, showing a remarkable influence of the marine aerosols and Saharan dust intrusions in the PM composition. In other works, daily PM_{10} and gaseous pollutants have been measured in some areas of Pinar del Rio city during 2011 (Cuesta Santos et al., 2014), atmospheric O_3, NO_2 and SO_2 have been monitored in the region of Santa Clara city using passive samplers (Alejo et al., 2013, 2011) and nitrogen compounds in the air (NO_2^-, NH_4^+ and NO_3^-) have been measured in some meteorological stations of the island (Cuesta Santos et al., 1998). However, as far as the author knowledge, there are no reports of PM content or composition in other regions of Cuba. Tables 1.5 and 1.6 summarize the atmospheric PM levels ($PM_{2.5}$ and PM_{10}) recorded in Cuba and the range of variation of their chemical composition, respectively.

Table 1.5. Atmospheric PM levels ($PM_{2.5}$ and PM_{10} expressed in μg m^{-3}) recorded in Cuba.

Location	Period	$PM_{2.5}$		PM_{10}		Reference
		Mean	Range (Min-Max)	Mean	Range (Min-Max)	
Havana	1996 - 1998			59.2	7.6 - 201.9	(Romero-Placeres et al., 2004)
Havana	2001 - 2003			63.2	1.7 - 438.7	(Suárez Tamayo et al., 2010)
Havana	2006 - 2007	10.1	4.17 - 22.4	32.2	18.40 - 59.80	(Molina Esquivel et al., 2011)
Havana	2012			36.0	9.5 - 85.1	(Martínez Varona et al., 2013)
Havana	2013 - 2014			30.7	1.80 - 82.80	(Martínez Varona et al., 2015a)
Camagüey	2008			27.9	13.15 - 73.35	(Barja et al., 2013)
Pinar del Río	2011				13.3 - 52.3	(Cuesta Santos et al., 2014)

Table 1.6. Concentration of chemical elements (μg m^{-3}) measured in $PM_{2.5}$ and PM_{10} fraction in Cuba.

	$PM_{2.5}$		PM_{10}				
	Havana 2006 – 2007 (Pérez et al., 2009)		Havana 2006 - 2007* (Pérez et al., 2009)		Havana 2013 – 2014 (Martínez Varona et al., 2015a)		Camagüey 2008** (Barja et al., 2013)
Element	Mean	Range (Min - Max)	Mean	Range (Min - Max)	Mean	Range (Min - Max)	Mean
NH_4^+							1.88
Cl^-	0.066	0.012 - 0.315	1.901				2.69
NO_3^-							1.5
SO_4^{2-}							2.45
Na							1.87
Mg							0.23
S	0.659	0.122 - 1.711	1.088				
K	0.043	0.006 - 0.210	0.160				0.8
Ca	0.111	0.037 - 0.515	2.140				0.98
Fe	0.061	0.016 - 0.656	0.296				
V	0.022	0.002 - 0.115	0.036				
Cr	0.003	0.001 - 0.012	0.006				
Mn	0.010	0.001 - 0.132	0.021				
Ni	0.005	0.001 - 0.022	0.008		0.029	0.002 - 0.806	
Cu	0.002	0.001 - 0.010	0.006				
Zn	0.019	0.001 - 0.293	0.037				
As					0.002	0.001 - 0.003	
Cd					0.005	0.001 - 0.026	
Pb	0.011	0.005 - 0.056	0.021		0.039	0.001 - 0.249	
Ti	0.005	0.002 - 0.026	0.027				

* Mean values obtained as the sum of mean concentration in $PM_{2.5}$ and $PM_{2.5-10}$ fractions.

** Mean values obtained as the sum of mean concentration in PM_1 and PM_{1-10} fractions.

There is also a limited literature focused on the presence of African dust clouds in Cuba and it is merely based on the information obtained from different satellites and sensors. In this regard, Mojena López et al., (2015) reported the presence and characteristics of Sahara dust clouds in all the Cuban provinces. They noted that their presence was especially remarkable between March and September with the highest peaks in June and July. However, neither they nor other researchers have yet addressed the study of the impact of African dust on human health and ecosystems in Cuba (Venero-Fernández, 2016).

The lack of information is even more striking for studies of atmospheric deposition, in such a way that the current understanding of its chemical composition in the island is quite limited. Even so, several studies have provided some valuable information on the deposition of nitrogen compounds (NO_3^- and NH_4^+) in rainfall (Cuesta Santos et al., 1998; Cuesta-Santos et al., 2001; González-De Zayas et al., 2012), heavy metals in bulk depositions (Jomolca-Parra et al., 2014) and rain (Montero Alvarez et al., 2007; Préndez et al., 2014) and radionuclides in bulk depositions (Alonso-Hernández et al., 2014, 2006). Moreover, others studies have been indirectly carried out using dated marine sediment cores (Diaz-Asencio et al., 2014, 2009). Beyond these works, no more experimental studies have been performed on the sources of atmospheric pollutants or the factors controlling the atmospheric dispersion and deposition processes.

On the other hand, air dispersion models have been used in Cuba to assess air quality. The studies have been mainly oriented to the local implementation of modeling systems like AERMOD (American Meteorological Society–AMS/Environmental Protection Agency–EPA Regulatory MODel) and the meteorological pre–processor Weather Research and Forecasting model (WRF) when local data is incomplete and is not in the format required by the model, which is a typical situation in many countries, particularly in developing ones (Turtos Carbonell et al., 2013, 2010b). These models have proved to be valuable tools to evaluate the dispersion of air pollutants emitted from stationary industrial sources and Turtos Carbonel et al., (2007) used them to model the dispersion of the atmospheric pollutants emitted by power plants in the vicinity of Havana both at local and regional scales. Turtos Carbonell (2010a) also reported Cuba's contribution to global greenhouse gases emissions from modelling estimations. However, the reality is that the scarcity of systematic measurements in Cuba makes it difficult to verify the modeling validity. Nonetheless, modeling works are not an effective management tools in many countries because of the lack of regulations. Thus, in developing countries like Cuba, the regulatory framework is based on screening models, which are many years behind the state-of-the-art dispersion models and generally yield inaccurate predictions. However, the implementation in the last years of high–resolution models such as AERMOD, have largely improved the accuracy of predictions in this country (Turtos Carbonell et al., 2010b).

2. Objectives and outline

In recent years, both the scientific community and the public opinion are paying increasing attention to the protection of the environment. Nowadays, problems associated with global warming, climate change, greenhouse gases or the increase of pollution in big and industrialized cities, as well as the damage they cause on human health and aquatic and terrestrial ecosystems, have led to the investment of a large amount of resources in the monitoring and control of pollutant emissions into the atmosphere.

Monitoring studies of air pollution are, therefore, of paramount importance for the selection and implementation of measures that allow an adequate harmony between the various socio-economic activities that are carried out in a territory, so that the environment is not damaged.

Air pollution is one of the main environmental concerns worldwide, both in developed and developing countries. In the Caribbean, air pollution has become a major issue because of the accelerated urban development, the increase of traffic-related emissions and growing industrialization. In Cuba, air pollution is caused by deficiencies in some aspects related to the territorial planning of human settlements, industry, use of obsolete technologies in productive activities and other sources such as an ageing fleet of vehicles (Romero-Placeres et al., 2004; Turtos Carbonell et al., 2010a, 2007).

As previously discussed, Cuban legislation controls a large number of pollutants when compared to other countries. However, studies carried out so far are mainly focused on assessing compliance with current regulations in very few locations in the country, limiting the national and regional evaluations. As a result, there is scarce information about the background levels of air pollutants throughout the national territory and about the nature of the factors that control atmospheric dispersion and deposition processes of most of these pollutants. Therefore, studies focused on the estimation of the content, chemical composition and main sources of atmospheric particulate matter are necessary to develop effective air quality and environmental management strategies in the country.

In this framework, the general objective of the present thesis is to investigate the levels and chemical composition of atmospheric particulate material present in rural and urban areas of Cienfuegos (Cuba) through the use of different monitoring and statistical approaches, paying special attention to their sources and effects on air quality and the environment.

More specifically, the work aims to:

1. Simultaneously quantify the levels of PM_{10} for the first time in two sites located in Cienfuegos (Cuba), characterized by exhibiting a different degree of anthropogenic influence (rural and urban sites).
2. Determine the atmospheric bulk deposition fluxes in a coastal site in Cienfuegos.
3. Exhaustively characterize the chemical composition of atmospheric particulate matter (PM_{10} and bulk deposition).
4. Investigate the spatial and temporal variability of the content/flux and chemical composition of atmospheric particulate matter and evaluate the compliance with current regulations.
5. Identify and quantify the main sources of the atmospheric particulate matter through the application of different statistical approaches and modeling tools.
6. Study the suitability of stable isotope signatures ($\delta^{15}N$ and $\delta^{13}C$) and lanthanoid elements as tracers of potential sources of air pollution.
7. Provide new insights into the atmospheric pollution to support policy decision making, which demands scientific knowledge on relevant environmental issues.

The thesis has been structured in six chapters. The first one, '*General Introduction*' (Chapter 1), gives state-of-the-art information on atmospheric particulate matter, gathering a summary background review on their origin, chemical composition, size distribution, dispersion and deposition, effects on human health, climate and the environment, as well as current regulations and approaches for the identification and apportionment of their main sources. Ultimately, this chapter summarizes the status of studies on atmospheric PM in Cuba and presents the main objectives of the present work.

In Chapter 2 '*Chemical characterization of PM_{10} samples collected simultaneously at a rural and an urban site in the Caribbean coast: local and long-range source apportionment*' it is assessed the air quality in Cienfuegos through the simultaneous characterization of PM_{10} samples in rural and urban sites. The study exhaustively characterizes samples of PM_{10} collected simultaneously in a rural and an urban site in Cuba in order to identify and quantify their main sources of contribution. To that end, we couple the PMF source apportionment results with the conditional bivariate probability function (CBPF) and concentration weighted trajectory (CWT).

Chapter 3 '*Lanthanoid elements as geochemical tracers of atmospheric aerosol in a Caribbean region*' relies on the study of the pattern and sources of lanthanoid elements in PM_{10} in order to gain insight into their role in the atmospheric pollution dynamics in Cienfuegos. Different approaches, including the analysis of lanthanoid fractionation, the estimation of enrichment factors and the application of the conditional bivariate probability function (CBPF) and the concentration-weighted trajectory (CWT) are used to identifying potential sources of pollution.

Chapter 4 '*Carbon and nitrogen isotopes unravels sources of aerosol contamination at Caribbean rural and urban coastal sites*' investigates the stable isotope compositions ($\delta^{13}C$ and $\delta^{15}N$) of total carbon (TC) and nitrogen (TN) in both PM_{10} and emissions from potential sources for the first time in a rural and an urban Caribbean costal sites in Cuba to better understand the origin of the contamination.

In Chapter 5 '*Determination and source apportionment of major and trace elements in bulk atmospheric deposition in a Caribbean rural area*' the monthly bulk deposition samples, their levels, temporal variation, chemical composition and main sources are studied. In this work a source apportionment study using PCA-MLRA in order to quantify the contributions of the main sources of pollutants to the bulk depositions is conducted.

Chapter 6 '*General discussion*' provides a discussion about the implications for air quality and the environment of the findings discussed in Chapters 2 to 5.

Finally, I present a summary of the main conclusions obtained in Chapters 2 to 6 and, in the Annex I section, it is briefly described the IAEA TC Project CUB/7/008 and National Program PNUOLU /4-1/ 2 No. /2014, which supported a large part of the activities developed in this thesis. In this section a brief explanation of other research activities related to this thesis developed in the framework of these projects, and also with the support of *Laboratorio Integrado de Calidad Ambiental (LICA)* is included. In Annex II a summary of the published papers related to this PhD can be found.

Note:

The four central chapters of this thesis (Chapters 2 to 5) are presented in scientific paper format, which have been sent to journals and subjected to peer review. This might result in some redundancy in the introduction and methods information of the different chapters. In addition, the datasets not included as supplementary materials in each chapter, are provided in a CD attached to this thesis.

References

Aas, W., Alleman, L.Y., Bieber, E., Gladtke, D., Houdret, J.-L., Karlsson, V., Monies, C., 2009. Comparison of methods for measuring atmospheric deposition of arsenic, cadmium, nickel and lead. J. Environ. Monit. JEM 11, 1276–1283. https://doi.org/10.1039/b822330k

Adamiec, E., Jarosz-Krzemińska, E., Wieszała, R., 2016. Heavy metals from non-exhaust vehicle emissions in urban and motorway road dusts. Environ. Monit. Assess. 188. https://doi.org/10.1007/s10661-016-5377-1

Agnihotri, R., Mandal, T.K., Karapurkar, S.G., Naja, M., Gadi, R., Ahammmed, Y.N., Kumar, A., Saud, T., Saxena, M., 2011. Stable carbon and nitrogen isotopic composition of bulk aerosols over India and northern Indian Ocean. Atmos. Environ. 45, 2828–2835. https://doi.org/10.1016/j.atmosenv.2011.03.003

Alastuey, A., Moreno, N., Querol, X., Viana, M., Artíñano, B., Luaces, J.A., Basora, J., Guerra, A., 2007. Contribution of harbour activities to levels of particulate matter in a harbour area: Hada Project-Tarragona Spain. Atmos. Environ., Harbours and Air Quality 41, 6366–6378. https://doi.org/10.1016/j.atmosenv.2007.03.015

Alastuey, A., Querol, X., Castillo, S., Escudero, M., Avila, A., Cuevas, E., Torres, C., Romero, P.M., Exposito, F., Garcia, O., Diaz, J.P., Van Dingenen, R., Putaud, J.P., 2005. Characterisation of TSP and PM2.5 at Izana and Sta. Cruz de Tenerife (Canary Islands, Spain) during a Saharan Dust Episode (July 2002). Atmos. Environ. 39, 4715–4728. https://doi.org/10.1016/j.atmosenv.2005.04.018

Alastuey, A., Querol, X., Plana, F., Viana, M., Ruiz, C.R., Sánchez de la Campa, A., de la Rosa, J., Mantilla, E., García dos Santos, S., 2006. Identification and chemical characterization of industrial particulate matter sources in southwest Spain. J. Air Waste Manag. Assoc. 1995 56, 993–1006. https://doi.org/10.1080/10473289.2006.10464502

Aldabe, J., Elustondo, D., Santamaria, C., Lasheras, E., Pandolfi, M., Alastuey, A., Querol, X., Santamaria, J.M., 2011. Chemical characterisation and source apportionment of PM2.5 and PM10 at rural, urban and traffic sites in Navarra (North of Spain). Atmospheric Res. 102, 191–205. https://doi.org/10.1016/j.atmosres.2011.07.003

Aldabe, J., Santamaría, C., Elustondo, D., Parra, A., Foan, L., Simon, V., Santamaría, J.M., 2012. Polycyclic aromatic hydrocarbons (PAHs) sampled in aerosol phase at different sites of the western pyrenees in Navarra (Spain). Environ. Eng. Manag. J. 11, 1049–1058.

Alejo, D., Morales, M., de la Torre, J., Grau, R., Bencs, L., Van Grieken, R., Van Espen, P., Sosa, D., Nuñez, V., 2013. Seasonal trends of atmospheric nitrogen dioxide and sulfur dioxide over North Santa Clara, Cuba. Environ. Monit. Assess. 185, 6023–6033. https://doi.org/10.1007/s10661-012-3003-4

Alejo, D., Morales, M.C., Nuñez, V., Bencs, L., Van Grieken, R., Van Espen, P., 2011. Monitoring of tropospheric ozone in the ambient air with passive samplers. Microchem. J. 99, 383–387. https://doi.org/10.1016/j.microc.2011.06.010

Almaguer, M., Aira, M.-J., Rodríguez-Rajo, F.J., Rojas, T.I., 2014. Temporal dynamics of airborne fungi in Havana (Cuba) during dry and rainy seasons: influence of meteorological parameters. Int. J. Biometeorol. 58, 1459–1470. https://doi.org/10.1007/s00484-013-0748-6

Alonso-Hernández, C.M., Cartas Águila, H., Diaz-Asencio, M., Muños-Caravaca, A., Martín-Pérez, J., Sibello-Hernández, R., 2006. Atmospheric deposition of 137Cs between 1994 and 2002 at Cienfuegos, Cuba. J. Environ. Radioact. 88, 199–204.

Alonso-Hernández, C.M., Morera-Gómez, Y., Cartas-Águila, H., Guillén-Arruebarrena, A., 2014. Atmospheric deposition patterns of 210Pb and 7Be in Cienfuegos, Cuba. J. Environ. Radioact. 138, 149–155. https://doi.org/10.1016/j.jenvrad.2014.08.023

Amato, F., Pandolfi, M., Viana, M., Querol, X., Alastuey, A., Moreno, T., 2009. Spatial and chemical patterns of PM10 in road dust deposited in urban environment. Atmos. Environ. 43, 1650–1659. https://doi.org/10.1016/j.atmosenv.2008.12.009

Amodio, M., Catino, S., Dambruoso, P.R., de Gennaro, G., Di Gilio, A., Giungato, P., Laiola, E., Marzocca, A., Mazzone, A., Sardaro, A., Tutino, M., 2014. Atmospheric Deposition: Sampling Procedures, Analytical Methods, and Main Recent Findings from the Scientific Literature. Adv. Meteorol. 161730. https://doi.org/10.1155/2014/161730

Anatolaki, C., Tsitouridou, R., 2007. Atmospheric deposition of nitrogen, sulfur and chloride in Thessaloniki, Greece. Atmospheric Res. 85, 413–428. https://doi.org/10.1016/j.atmosres.2007.02.010

Ausset, P., Del Monte, M., Lefèvre, R.A., 1999. Embryonic sulphated black crusts on carbonate rocks in atmospheric simulation chamber and in the field: role of carbonaceous fly-ash. Atmos. Environ. 33, 1525–1534. https://doi.org/10.1016/S1352-2310(98)00399-9

Bari, M.A., Kindzierski, W.B., Cho, S., 2014. A wintertime investigation of atmospheric deposition of metals and polycyclic aromatic hydrocarbons in the Athabasca Oil Sands Region, Canada. Sci. Total Environ. 485, 180–192 https://doi.org/10.1016/j.scitotenv.2014.03.088

Barja, B., Mogo, S., Cachorro, V.E., Carlos Antuna, J., Estevan, R., Rodrigues, A., de Frutos, A., 2013. Atmospheric particulate matter levels, chemical composition and optical absorbing properties in Camaguey, Cuba. Environ. Sci.-Process. Impacts 15, 440–453. https://doi.org/10.1039/c2em30854a

Batterman, S., Ganguly, R., Isakov, V., Burke, J., Arunachalam, S., Snyder, M., Robins, T., Lewis, T., 2014. Dispersion Modeling of Traffic-Related Air Pollutant Exposures

and Health Effects Among Children with Asthma in Detroit, Michigan. Transp. Res. Rec. 105–113. https://doi.org/10.3141/2452-13

Belis, C., Larsen, B., Amato, F., El Haddad, I., Favez, O., Harrison, R., Hopke, P., Nava, S., Paatero, P., Prevot, A. s. h., Quass, U., Vecchi, R., Viana, M., 2013. European guide on air pollution source apportionment with receptor models (JRC Reference Reports No. EUR 26080 EN). Publications Office of the European Union.

Belis, C.A., Cancelinha, J., Duane, M., Forcina, V., Pedroni, V., Passarella, R., Tanet, G., Douglas, K., Piazzalunga, A., Bolzacchini, E., Sangiorgi, G., Perrone, M.-G., Ferrero, L., Fermo, P., Larsen, B.R., 2011. Sources for PM air pollution in the Po Plain, Italy: I. Critical comparison of methods for estimating biomass burning contributions to benzo(a)pyrene. Atmos. Environ. 45, 7266–7275. https://doi.org/10.1016/j.atmosenv.2011.08.061

Belis, C.A., Karagulian, F., Amato, F., Almeida, M., Artaxo, P., Beddows, D.C.S., Bernardoni, V., Bove, M.C., Carbone, S., Cesari, D., Contini, D., Cuccia, E., Diapouli, E., Eleftheriadis, K., Favez, O., El Haddad, I., Harrison, R.M., Hellebust, S., Hovorka, J., Jang, E., Jorquera, H., Kammermeier, T., Karl, M., Lucarelli, F., Mooibroek, D., Nava, S., Nojgaard, J.K., Paatero, P., Pandolfi, M., Perrone, M.G., Petit, J.E., Pietrodangelo, A., Pokorna, P., Prati, P., Prevot, A.S.H., Quass, U., Querol, X., Saraga, D., Sciare, J., Sfetsos, A., Valli, G., Vecchi, R., Vestenius, M., Yubero, E., Hopke, P.K., 2015a. A new methodology to assess the performance and uncertainty of source apportionment models II: The results of two European intercomparison exercises. Atmos. Environ. 123, 240–250. https://doi.org/10.1016/j.atmosenv.2015.10.068

Belis, C.A., Pernigotti, D., Karagulian, F., Pirovano, G., Larsen, B.R., Gerboles, M., Hopke, P.K., 2015b. A new methodology to assess the performance and uncertainty of source apportionment models in intercomparison exercises. Atmos. Environ. 119, 35–44. https://doi.org/10.1016/j.atmosenv.2015.08.002

Birmili, W., Allen, A.G., Bary, F., Harrison, R.M., 2006. Trace metal concentrations and water solubility in size-fractionated atmospheric particles and influence of road traffic. Environ. Sci. Technol. 40, 1144–1153. https://doi.org/10.1021/es0486925

Boman, J., Gaita, S.M., 2015. Mass, black carbon and elemental composition of PM2.5 at an industrial site in Kingston, Jamaica. Nucl. Instrum. Methods Phys. Res. Sect. B-Beam Interact. Mater. At. 363, 131–134. https://doi.org/10.1016/j.nimb.2015.08.068

Bonvalot, L., Tuna, T., Fagault, Y., Jaffrezo, J.-L., Jacob, V., Chevrier, F., Bard, E., 2016. Estimating contributions from biomass burning, fossil fuel combustion, and biogenic carbon to carbonaceous aerosols in the Valley of Chamonix: a dual approach based on radiocarbon and levoglucosan. Atmospheric Chem. Phys. 16, 13753–13772. https://doi.org/10.5194/acp-16-13753-2016

Bove, M.C., Brotto, P., Calzolai, G., Cassola, F., Cavalli, F., Fermo, P., Hjorth, J., Massabò, D., Nava, S., Piazzalunga, A., Schembari, C., Prati, P., 2016. PM10 source apportionment applying PMF and chemical tracer analysis to ship-borne measurements in the Western Mediterranean. Atmos. Environ. 125, 140–151. https://doi.org/10.1016/j.atmosenv.2015.11.009

Bozlaker, A., Buzcu-Güven, B., Fraser, M.P., Chellam, S., 2013a. Insights into PM10 sources in Houston, Texas: Role of petroleum refineries in enriching lanthanoid metals during episodic emission events. Atmos. Environ. 69, 109–117. https://doi.org/10.1016/j.atmosenv.2012.11.068

Bozlaker, A., Prospero, J.M., Fraser, M.P., Chellam, S., 2013b. Quantifying the Contribution of Long-Range Saharan Dust Transport on Particulate Matter Concentrations in Houston, Texas, Using Detailed Elemental Analysis. Environ. Sci. Technol. 47, 10179–10187. https://doi.org/10.1021/es4015663

Brown, S.G., Eberly, S., Paatero, P., Norris, G.A., 2015. Methods for estimating uncertainty in PMF solutions: Examples with ambient air and water quality data and guidance on reporting PMF results. Sci. Total Environ. 518, 626–635. https://doi.org/10.1016/j.scitotenv.2015.01.022

Cachier, H., Buat-Menard, P., Fontugne, M., Rancher, J., 1985. Source terms and source strengths of the carbonaceous aerosol in the tropics. J. Atmospheric Chem. 3, 469–489. https://doi.org/10.1007/BF00053872

Cao, J.J., Chow, J.C., Lee, F.S.C., Watson, J.G., 2013. Evolution of PM2.5 measurements and standards in the U.S. and future perspectives for China.

Castillo, S., de la Rosa, J.D., Sanchez de la Campa, A.M., Gonzalez-Castanedo, Y., Fernandez-Caliani, J.C., Gonzalez, I., Romero, A., 2013. Contribution of mine wastes to atmospheric metal deposition in the surrounding area of an abandoned heavily polluted mining district (Rio Tinto mines, Spain). Sci. Total Environ. 449, 363–372. https://doi.org/10.1016/j.scitotenv.2013.01.076

Ceburnis, D., Garbaras, A., Szidat, S., Rinaldi, M., Fahrni, S., Perron, N., Wacker, L., Leinert, S., Remeikis, V., Facchini, M.C., Prevot, A.S.H., Jennings, S.G., Ramonet, M., O'Dowd, C.D., 2011. Quantification of the carbonaceous matter origin in submicron marine aerosol by 13C and 14C isotope analysis. Atmos Chem Phys 11, 8593–8606. https://doi.org/10.5194/acp-11-8593-2011

Cesari, D., Donateo, A., Conte, M., Merico, E., Giangreco, A., Giangreco, F., Contini, D., 2016. An inter-comparison of PM2.5 at urban and urban background sites: Chemical characterization and source apportionment. Atmospheric Res. 174, 106–119. https://doi.org/10.1016/j.atmosres.2016.02.004

Chen, Y., Du, W., Chen, J., Hong, Y., Zhao, J., Xu, L., Xiao, H., 2017. Chemical composition, structural properties, and source apportionment of organic macromolecules in atmospheric PM10 in a coastal city of Southeast China. Environ. Sci. Pollut. Res. 24, 5877–5887. https://doi.org/10.1007/s11356-016-8314-5

Chesselet, R., Fontugne, M., Buat-Ménard, P., Ezat, U., Lambert, C.E., 1981. The origin of particulate organic carbon in the marine atmosphere as indicated by its stable carbon isotopic composition. Geophys. Res. Lett. 8, 345–348. https://doi.org/10.1029/GL008i004p00345

Chueinta, W., Hopke, P.K., Paatero, P., 2000. Investigation of sources of atmospheric aerosol at urban and suburban residential areas in Thailand by positive matrix factorization. Atmos. Environ. 34, 3319–3329. https://doi.org/10.1016/S1352-2310(99)00433-1

Comero, S., Capitani, L., Gawlik, B., 2009. Positive Matrix Factorisation (PMF) - An Introduction to the Chemometric Evaluation of Environmental Monitoring Data Using PMF (EUR - Scientific and Technical Research Reports). OP. https://doi.org/10.2788/2497

Contini, D., Cesari, D., Conte, M., Donateo, A., 2016. Application of PMF and CMB receptor models for the evaluation of the contribution of a large coal-fired power plant to PM10 concentrations. Sci. Total Environ. 560, 131–140. https://doi.org/10.1016/j.scitotenv.2016.04.031

Cuesta Santos, O., Collazo Aranda, A., Sánchez Navarro, P., Manrique Suárez, R., Fonseca Hernández, M., Rodríguez Valdés, D., Sánchez Díaz, A., Miló López, M.V., Díaz Díaz, J.M., Victorero Hernández, A., González Jaime, Y., Sosa Pérez, C., 2014. Air quality of Pinar del Rio city. Experimental values. Rev. Cuabana Meteorol. 20, 98–113.

Cuesta Santos, O., Ortiz Bulto, P., Gonzalez Gonzalez, M., 1998. Deposition and Atmospheric Nitrogen Concentrations Trends in Cuba. Water. Air. Soil Pollut. 106, 163–169. https://doi.org/10.1023/A:1004980612612

Cuesta-Santos, O., Collazo, A., Wallo, A., Labrador, R., Gonzalez, M., Ortiz, P., 2001. Deposition of atmospheric nitrogen compounds in humid tropical Cuba. Sci. World J. 1, 238–244.

Cuesta-Santos, O., Wallo Vázquez, A., Collazo Aranda, A., Sánchez Navarro, P., González González, M., Labrador Montero, R., 2002. Aspectos de la composicion quimica del aire en la zona de la ribera este de la bahia de la Habana. Rev. Cuabana Meteorol. 9, 90–99.

Dämmgen, U., Erisman, J.W., Cape, J.N., Grünhage, L., Fowler, D., 2005. Practical considerations for addressing uncertainties in monitoring bulk deposition. Environ. Pollut. 134, 535–548. https://doi.org/10.1016/j.envpol.2004.08.013

Diaz-Asencio, M., Alonso-Hernández, C.M., Bolaños-Álvarez, Y., Gómez-Batista, M., Pinto, V., Morabito, R., Hernández-Albernas, J.I., Eriksson, M., Sanchez-Cabeza, J.A., 2009. One century sedimentary record of Hg and Pb pollution in the Sagua estuary (Cuba) derived from 210 Pb and 137 Cs chronology. Mar. Pollut. Bull. 59, 108–115.

Diaz-Asencio, M., Sanchez-Cabeza, J.-A., Bolanos-Alvarez, Y., Carolina Ruiz-Fernandez, A., Gomez-Batista, M., Morabito, R., Alonso-Hernandez, C., 2014. One century of sedimentation and Hg pollution at the mouth of the Sagua la Grande River (Cuba). Cienc. Mar. 40, 321–337. https://doi.org/10.7773/cm.v40i4.2472

Directive 2008/50/EC, 2008. Directive 2008/50/EC of the European Parliament and of the Council of 21 May 2008 on ambient air quality and cleaner air for Europe. [WWW Document]. URL http://eur-lex.europa.eu/legal-content/ES/TXT/?uri=uriserv:ev0002 (accessed 10.30.15).

Directive 2010/75/EU, 2010. Directive 2010/75/EU of the European Parliament and of the Council of 24 November 2010 on industrial emissions (integrated pollution prevention and control) Text with EEA relevance [WWW Document]. URL http://data.europa.eu/eli/dir/2010/75/oj/eng (accessed 5.17.18).

Friedrich, R., 2009. Natural and biogenic emissions of environmentally relevant atmospheric trace constituents in Europe. Atmos. Environ. 43, 1377–1379. https://doi.org/10.1016/j.atmosenv.2008.10.001

Garbariene, I., Sapolaite, J., Garbaras, A., Ezerinskis, Z., Pocevicius, M., Krikscikas, L., Plukis, A., Remeikis, V., 2016. Origin Identification of Carbonaceous Aerosol Particles by Carbon Isotope Ratio Analysis. Aerosol Air Qual. Res. 16, 1356–1365. https://doi.org/10.4209/aaqr.2015.07.0443

Gichuki, S.W., Mason, R.P., 2014. Wet and dry deposition of mercury in Bermuda. Atmos. Environ. 87, 249–257. https://doi.org/10.1016/j.atmosenv.2014.01.025

Gioda, A., Perez, U., Rosa, Z., Jimenez-Velez, B.D., 2007. Particulate matter (PM10 and PM2.5) from different areas of Puerto Rico. Fresenius Environ. Bull. 16, 861–868.

Golomb, D., Ryan, D., Eby, N., Underhill, J., Zemba, S., 1997. Atmospheric deposition of toxics onto Massachusetts Bay—I. Metals. Atmos. Environ. 31, 1349–1359. https://doi.org/10.1016/S1352-2310(96)00276-2

González-De Zayas, R., Merino-Ibarra, M., Matos-Pupo, F., Soto-Jiménez, M., 2012. Atmospheric Deposition of Nitrogen to a Caribbean Coastal Zone (Cayo Coco, Cuba): Temporal Trends and Relative Importance as a Nitrogen Source. Water. Air. Soil Pollut. 223, 1125–1136. https://doi.org/10.1007/s11270-011-0930-6

Gorka, M., Rybicki, M., Simoneit, B.R.T., Marynowski, L., 2014. Determination of multiple organic matter sources in aerosol PM10 from Wroclaw, Poland using molecular and stable carbon isotope compositions. Atmos. Environ. 89, 739–748. https://doi.org/10.1016/j.atmosenv.2014.02.064

Gorka, M., Zwolinska, E., Malkiewicz, M., Lewicka-Szczebak, D., Jedrysek, M.O., 2012. Carbon and nitrogen isotope analyses coupled with palynological data of PM10 in Wroclaw city (SW Poland) - assessment of anthropogenic impact. Isotopes Environ. Health Stud. 48, 327–344. https://doi.org/10.1080/10256016.2012.639449

Gramsch, E., Cáceres, D., Oyola, P., Reyes, F., Vásquez, Y., Rubio, M.A., Sánchez, G., 2014. Influence of surface and subsidence thermal inversion on PM2.5 and black carbon concentration. Atmos. Environ. 98, 290–298. https://doi.org/10.1016/j.atmosenv.2014.08.066

Grantz, D.A., Garner, J.H.B., Johnson, D.W., 2003. Ecological effects of particulate matter. Environ. Int. 29, 213–239. https://doi.org/10.1016/S0160-4120(02)00181-2

Grigoratos, T., Martini, G., 2015. Brake wear particle emissions: a review. Environ. Sci. Pollut. Res. 22, 2491–2504. https://doi.org/10.1007/s11356-014-3696-8

Gualtieri, G., Toscano, P., Crisci, A., Di Lonardo, S., Tartaglia, M., Vagnoli, C., Zaldei, A., Gioli, B., 2015. Influence of road traffic, residential heating and meteorological conditions on PM10 concentrations during air pollution critical episodes. Environ. Sci. Pollut. Res. 22, 19027–19038. https://doi.org/10.1007/s11356-015-5099-x

Guo, X., Li, C., Gao, Y., Tang, L., Briki, M., Ding, H., Ji, H., 2016. Sources of organic matter (PAHs and n-alkanes) in PM2.5 of Beijing in haze weather analyzed by combining the C-N isotopic and PCA-MLR analyses. Environ. Sci.-Process. Impacts 18, 314–322. https://doi.org/10.1039/c6em00037a

Harris, R., Pollman, C., Landing, W., Evans, D., Axelrad, D., Hutchinson, D., Morey, S.L., Rumbold, D., Dukhovskoy, D., Adams, D.H., Vijayaraghavan, K., Holmes, C., Atkinson, R.D., Myers, T., Sunderland, E., 2012. Mercury in the Gulf of Mexico: Sources to receptors. Mercury Mar. Ecosyst. Sources Seaf. Consum. 119, 42–52. https://doi.org/10.1016/j.envres.2012.08.001

Harrison, R.M., 1999. Understanding Our Environment: An Introduction to Environmental Chemistry and Pollution. Royal Society of Chemistry.

Heaton, T.H.E., Spiro, B., Robertson, S.M.C., 1997. Potential canopy influences on the isotopic composition of nitrogen and sulphur in atmospheric deposition. Oecologia 109, 600–607. https://doi.org/10.1007/s004420050122

Hoefs, J., 2015. Stable isotope geochemistry, Seventh edition. ed, Earth Sciences. Springer, Cham Heidelberg New York Dordrecht London.

Hopke, P.K., Ito, K., Mar, T., Christensen, W.F., Eatough, D.J., Henry, R.C., Kim, E., Laden, F., Lall, R., Larson, T.V., Liu, H., Neas, L., Pinto, J., Stolzel, M., Suh, H., Paatero, P., Thurston, G.D., 2006. PM source apportionment and health effects: 1. Intercomparison of source apportionment results. J. Expo. Sci. Environ. Epidemiol. 16, 275–286. https://doi.org/10.1038/sj.jea.7500458

Johansson, C., Norman, M., Burman, L., 2009. Road traffic emission factors for heavy metals. Atmos. Environ. 43, 4681–4688. https://doi.org/10.1016/j.atmosenv.2008.10.024

Jomolca-Parra, Y., Lima-Cazorla, L., Manduca-Artiles, M., 2014. Determination of Atmospheric Fluxes and Concentrations of Heavy Metals and Radionuclides of Environmental Concern in Total Atmospheric Deposition. Rev. Cuba. Quím. 25, 345–363.

Jones, A.M., Harrison, R.M., 2005. Interpretation of particulate elemental and organic carbon concentrations at rural, urban and kerbside sites. Atmos. Environ. 39, 7114–7126. https://doi.org/10.1016/j.atmosenv.2005.08.017

Jusino-Atresino, R., Anderson, J., Gao, Y., 2016. Ionic and elemental composition of PM2.5 aerosols over the Caribbean Sea in the Tropical Atlantic. J. Atmospheric Chem. 73, 427–457. https://doi.org/10.1007/s10874-016-9337-5

Kanakidou, M., Seinfeld, J.H., Pandis, S.N., Barnes, I., Dentener, F.J., Facchini, M.C., Van Dingenen, R., Ervens, B., Nenes, A., Nielsen, C.J., Swietlicki, E., Putaud, J.P., Balkanski, Y., Fuzzi, S., Horth, J., Moortgat, G.K., Winterhalter, R., Myhre, C.E.L., Tsigaridis, K., Vignati, E., Stephanou, E.G., Wilson, J., 2005. Organic aerosol and global climate modelling: a review. Atmos Chem Phys 5, 1053–1123. https://doi.org/10.5194/acp-5-1053-2005

Kelly, S.D., Stein, C., Jickells, T.D., 2005. Carbon and nitrogen isotopic analysis of atmospheric organic matter. Atmos. Environ. 39, 6007–6011. https://doi.org/10.1016/j.atmosenv.2005.05.030

Kim, E., Hopke, P.K., Edgerton, E.S., 2003. Source identification of Atlanta aerosol by positive matrix factorization. J. Air Waste Manag. Assoc. 53, 731–739.

Kim, H.-S., Jong-Bae, H., Philip, K.H., Holsen, T.M., Yi, S.-M., 2007. Characteristics of the major chemical constituents Of PM2.5 and smog events in Seoul, Korea in 2003 and 2004. Atmos. Environ. 41, 6762–6770. https://doi.org/10.1016/j.atmosenv.2007.04.060

Latif, M.T., Ngah, S.A., Dominick, D., Razak, I.S., Guo, X., Srithawirat, T., Mushrifah, I., 2015. Composition and source apportionment of dust fall around a natural lake. J. Environ. Sci.-China 33, 143–155. https://doi.org/10.1016/j.jes.2015.02.002

Lawrence, S., Sokhi, R., Ravindra, K., 2016. Quantification of vehicle fleet PM10 particulate matter emission factors from exhaust and non-exhaust sources using tunnel measurement techniques. Environ. Pollut. 210, 419–428. https://doi.org/10.1016/j.envpol.2016.01.011

Le Tertre, A., Medina, S., Samoli, E., Forsberg, B., Michelozzi, P., Boumghar, A., Vonk, J.M., Bellini, A., Atkinson, R., Ayres, J.G., Sunyer, J., Schwartz, J., Katsouyanni, K., 2002. Short-term effects of particulate air pollution on cardiovascular diseases in eight European cities. J. Epidemiol. Community Health 56, 773–779. https://doi.org/10.1136/jech.56.10.773

Lenes, J.M., Prospero, J.M., Landing, W.M., Virmani, J.I., Walsh, J.J., 2012. A model of Saharan dust deposition to the eastern Gulf of Mexico. Mar. Chem. 134–135, 1–9. https://doi.org/10.1016/j.marchem.2012.02.007

Li, P., Xin, J., Wang, Y., Wang, S., Shang, K., Liu, Z., Li, G., Pan, X., Wei, L., Wang, M., 2013. Time-series analysis of mortality effects from airborne particulate matter size fractions in Beijing. Atmos. Environ. 81, 253–262. https://doi.org/10.1016/j.atmosenv.2013.09.004

Librando, V., Tringali, G., 2005. Atmospheric fate of OH initiated oxidation of terpenes. Reaction mechanism of α-pinene degradation and secondary organic aerosol formation. J. Environ. Manage. 75, 275–282. https://doi.org/10.1016/j.jenvman.2005.01.001

Lin, C.C., Chen, S.J., Huang, K.L., Hwang, W.I., Chang-Chien, G.P., Lin, W.Y., 2005. Characteristics of metals in nano/ultrafine/fine/coarse particles collected beside a heavily trafficked road. Environ. Sci. Technol. 39, 8113–8122. https://doi.org/10.1021/es048182a

Liu, D.H.F., Liptak, B.G., 1999. Air Pollution. CRC Press.

Lopez-Veneroni, D., 2009. The stable carbon isotope composition of PM2.5 and PM10 in Mexico City Metropolitan Area air. Atmos. Environ. 43, 4491–4502. https://doi.org/10.1016/j.atmosenv.2009.06.036

Mari, M., Sanchez-Soberon, F., Audi-Miro, C., van Drooge, B.L., Soler, A., Grimalt, J.O., Schuhmacher, M., 2016. Source Apportionment of Inorganic and Organic PM in the Ambient Air around a Cement Plant: Assessment of Complementary Tools. Aerosol Air Qual. Res. 16, 3230–3242. https://doi.org/10.4209/aaqr.2016.06.0276

Mariani, R.L., de Mello, W.Z., 2007. PM2.5-10, PM2.5 and associated water-soluble inorganic species at a coastal urban site in the metropolitan region of Rio de Janeiro. Atmos. Environ. 41, 2887–2892. https://doi.org/10.1016/j.atmosenv.2006.12.009

Martinelli, L.A., Camargo, P.B., Lara, L.B.L.S., Victoria, R.L., Artaxo, P., 2002. Stable carbon and nitrogen isotopic composition of bulk aerosol particles in a C4 plant landscape of southeast Brazil. Atmos. Environ. 36, 2427–2432. https://doi.org/10.1016/S1352-2310(01)00454-X

Martínez Varona, M., García Roche, R., Molina Esquivel, E., Fernández Arocha, A., 2008. Comportamiento de dióxido de nitrógeno y partículas en suspensión totales en el periodo 2004-2006 en la estación del INHEM. Hig. Sanid. Ambient. 8, 343–347.

Martínez Varona, M., Guzmán Vila, M., Pérez Cabrera, A., Fernández Arocha, A., 2015a. Presencia de metales pesados en material particulado en aire. Estación de monitoreo INHEM, Centro Habana. Ecosolar 52.

Martínez Varona, M., Maldonado, G., Molina, E., 2011. Concentraciones diarias de contaminantes del aire en La Habana (Cuba). Hig. Sanid. Ambient. 11, 786–792.

Martínez Varona, M., Molina Esquivel, E., Guzmán Vila, M., Pérez Cabrera, A., Fernández Arocha, A., 2015b. Determinación de la concentración de gases en la estación de monitoreo INHEM Centro Habana (Cuba). Hig. Sanid. Ambient. 15, 1285–1290.

Martínez Varona, M., Molina Esquivel, E., Maldonado Cantillo, G., Guzmán Vila, M., Alonso, D., 2013. Comportamiento de partículas menores de 10 micras mediante dos equipos de monitoreo. Hig. Sanid. Ambient. 13, 1060–1065.

Masalaite, A., Remeikis, V., Garbaras, A., Dudoitis, V., Ulevicius, V., Ceburnis, D., 2015. Elucidating carbonaceous aerosol sources by the stable carbon delta C-13(TC) ratio in size-segregated particles. Atmospheric Res. 158, 1–12. https://doi.org/10.1016/j.atmosres.2015.01.014

Mazzei, F., D'Alessandro, A., Lucarelli, F., Nava, S., Prati, P., Valli, G., Vecchi, R., 2008. Characterization of particulate matter sources in an urban environment. Sci. Total Environ. 401, 81–89. https://doi.org/10.1016/j.scitotenv.2008.03.008

McDonald, B.C., Gouw, J.A. de, Gilman, J.B., Jathar, S.H., Akherati, A., Cappa, C.D., Jimenez, J.L., Lee-Taylor, J., Hayes, P.L., McKeen, S.A., Cui, Y.Y., Kim, S.-W., Gentner, D.R., Isaacman-VanWertz, G., Goldstein, A.H., Harley, R.A., Frost, G.J., Roberts, J.M., Ryerson, T.B., Trainer, M., 2018. Volatile chemical products emerging as largest petrochemical source of urban organic emissions. Science 359, 760–764. https://doi.org/10.1126/science.aaq0524

Meng, X., Ma, Y., Chen, R., Zhou, Z., Chen, B., Kan, H., 2013. Size-Fractionated Particle Number Concentrations and Daily Mortality in a Chinese City. Environ. Health Perspect. 121, 1174–1178. https://doi.org/10.1289/ehp.1206398

Meszaros, E., 1993. Global and regional changes in atmospheric composition / Erno Meszaros. Lewis Publishers, Boca Raton, FL.

Miao, Y., Guo, J., Liu, S., Liu, H., Li, Z., Zhang, W., Zhai, P., 2017. Classification of summertime synoptic patterns in Beijing and their associations with boundary layer structure affecting aerosol pollution. Atmos Chem Phys 17, 3097–3110. https://doi.org/10.5194/acp-17-3097-2017

Mojena López, E., Ortega González, A., Casilles Vega, E.F., Leyva Santos, J., 2015. Sahara Clouds Dust. Their presence in Cuba. Rev. Cuabana Meteorol. 21, 120–134.

Molina Esquivel, E., Pérez Zayas, G., Martínez Varona, M., Aldape Ugalde, F., Flores Maldonado, J., 2011. Comportamiento de las fracciones fina y gruesa de PM10 en la estación de monitoreo de calidad del aire en Centro Habana. Campaña 2006-2007. Hig. Sanid. Ambient. 11, 820–826.

Montero Alvarez, A., Estevez Alvarez, J.R., Padilla Alvarez, R., 2007. Heavy metal analysis of rainwaters: A comparison of TXRF and ASV analytical capabilities. J. Radioanal. Nucl. Chem. 273, 427–433. https://doi.org/10.1007/s10967-007-6895-7

Moore, H., 1977. The isotopic composition of ammonia, nitrogen dioxide and nitrate in the atmosphere. Atmospheric Environ. 1967 11, 1239–1243. https://doi.org/10.1016/0004-6981(77)90102-0

Moreno, T., Querol, X., Alastuey, A., de la Rosa, J., Sánchez de la Campa, A.M., Minguillón, M., Pandolfi, M., González-Castanedo, Y., Monfort, E., Gibbons, W., 2010. Variations in vanadium, nickel and lanthanoid element concentrations in urban air. Sci. Total Environ. 408, 4569–4579. https://doi.org/10.1016/j.scitotenv.2010.06.016

Moreno, T., Querol, X., Castillo, S., Alastuey, A., Cuevas, E., Herrmann, L., Mounkaila, M., Elvira, J., Gibbons, W., 2006. Geochemical variations in aeolian mineral particles from the Sahara-Sahel Dust Corridor. Chemosphere 65, 261–270. https://doi.org/10.1016/j.chemosphere.2006.02.052

Mukherjee, A., Agrawal, M., 2017. World air particulate matter: sources, distribution and health effects. Environ. Chem. Lett. 15, 283–309. https://doi.org/10.1007/s10311-017-0611-9

NC 39, 1999. Norma Cubana 39: 1999. CALIDAD DEL AIRE. REQUISITOS HIGIENICOSANITARIOS.

NC 111, 2004. Norma Cubana 111:2004. CALIDAD DEL AIRE—REGLAS PARA LA VIGILANCIA DE LA CALIDAD DEL AIRE EN ASENTAMIENTOS HUMANOS.

NC 1020, 2014. Norma Cubana 1020:2014. CALIDAD DEL AIRE — CONTAMINANTES — CONCENTRACIONES MÁXIMAS ADMISIBLES Y VALORES GUÍAS EN ZONAS HABITABLES.

NC-TS 803, 2004. Norma Cubana TS 803:2010 CALIDAD DEL AIRE — EMISIONES MÁXIMAS ADMISIBLES DE CONTAMINANTES A LA ATMÓSFERA EN FUENTES FIJAS PUNTUALES DE INSTALACIONES GENERADORAS DE ELECTRICIDAD Y VAPOR.

Norris, G., Duvall, R., Brown, S., Bai, S., 2014. EPA Positive Matrix Factorization (PMF) 5.0 Fundamentals and User Guide. U.S. Environmental Protection Agency National Exposure Research Laboratory, Sonoma Technology, Inc.

Okin, G.S., Baker, A.R., Tegen, I., Mahowald, N.M., Dentener, F.J., Duce, R.A., Galloway, J.N., Hunter, K., Kanakidou, M., Kubilay, N., Prospero, J.M., Sarin, M., Surapipith, V., Uematsu, M., Zhu, T., 2011. Impacts of atmospheric nutrient deposition on marine productivity: Roles of nitrogen, phosphorus, and iron. Glob. Biogeochem. Cycles 25, GB2022. https://doi.org/10.1029/2010GB003858

Oravisjärvi, K., Timonen, K.L., Wiikinkoski, T., Ruuskanen, A.R., Heinänen, K., Ruuskanen, J., 2003. Source contributions to PM2.5 particles in the urban air of a town situated close to a steel works. Atmos. Environ. 37, 1013–1022. https://doi.org/10.1016/S1352-2310(02)01048-8

Paatero, P., 1997. Least squares formulation of robust non-negative factor analysis. Chemom. Intell. Lab. Syst. 37, 23–35. https://doi.org/10.1016/S0169-7439(96)00044-5

Paatero, P., Eberly, S., Brown, S.G., Norris, G.A., 2014. Methods for estimating uncertainty in factor analytic solutions. Atmos Meas Tech 7, 781–797. https://doi.org/10.5194/amt-7-781-2014

Paatero, P., Tapper, U., 1994. Positive matrix factorization: A non-negative factor model with optimal utilization of error estimates of data values. Environmetrics 5, 111–126. https://doi.org/10.1002/env.3170050203

Park, S.S., Ondov, J.M., Harrison, D., Nair, N.P., 2005. Seasonal and shorter-term variations in particulate atmospheric nitrate in Baltimore. Atmos. Environ. 39, 2011–2020. https://doi.org/10.1016/j.atmosenc.2004.12.032

Parra, M.A., González, L., Elustondo, D., Garrigó, J., Bermejo, R., Santamaría, J.M., 2006. Spatial and temporal trends of volatile organic compounds (VOC) in a rural area of northern Spain. Sci. Total Environ. 370, 157–167. https://doi.org/10.1016/j.scitotenv.2006.06.022

Pavuluri, C.M., Kawamura, K., Tachibana, E., Swaminathan, T., 2010. Elevated nitrogen isotope ratios of tropical Indian aerosols from Chennai: Implication for the origins of aerosol nitrogen in South and Southeast Asia. Atmos. Environ. 44, 3597–3604. https://doi.org/10.1016/j.atmosenv.2010.05.039

Pérez, G., Piñera, I., Aldape, F., Flores, J.M., Martínez, M., Molina, E., Fernández, A., Ramos, M., Guibert, R., 2009. First study of airborne particulate pollution using pixe analysis in Havana city, Cuba. Int. J. PIXE 19, 157–166. https://doi.org/10.1142/S0129083509001849

Pérez, G., Piñera, I., Molina, E., Martínez, M., Ramos, M., Guibert, R., Fernández, A., Aldape, F., Flores, J.M., 2010. Caracterización Másica de Partículas Finas y Gruesas de Aerosol Urbano. Contrib Educ Prot Med Amb 9, E70–E74.

Phillips, D.L., Gregg, J.W., 2003. Source partitioning using stable isotopes: coping with too many sources. Oecologia 136, 261–269. https://doi.org/10.1007/s00442-003-1218-3

Piñera, I., Pérez, G., Aldape, F., Flores, J.M., Molina, E., Ramos, M., Martínez, M., Guibert, R., 2010. Estudio de Partículas Finas de la Atmósfera en Centro Habana. Contrib Educ Prot Med Amb 9, E39–E47.

Pope, C.A., Dockery, D.W., 2006. Health effects of fine particulate air pollution: Lines that connect. J. Air Waste Manag. Assoc. 56, 709–742.

Pöschl, U., 2005. Atmospheric aerosols: composition, transformation, climate and health effects. Angew. Chem. Int. Ed Engl. 44, 7520–7540. https://doi.org/10.1002/anie.200501122

Préndez, M., López, R., Carrillo, E., 2014. Physical and Chemical Components of Cuba's Rain: Effects on Air Quality. Int. J. Atmospheric Sci. 2014, 1–8. https://doi.org/10.1155/2014/680735

Prospero, J.M., 1999. Long-term measurements of the transport of African mineral dust to the southeastern United States: Implications for regional air quality. J. Geophys. Res.-Atmospheres 104, 15917–15927. https://doi.org/10.1029/1999JD900072

Prospero, J.M., Collard, F.-X., Molinie, J., Jeannot, A., 2014. Characterizing the annual cycle of African dust transport to the Caribbean Basin and South America and its impact on the environment and air quality. Glob. Biogeochem. Cycles 28, 757–773. https://doi.org/10.1002/2013GB004802

Prospero, J.M., Mayol-Bracero, O.L., 2013. Understanding the Transport and Impact of African Dust on the Caribbean Basin. Bull. Am. Meteorol. Soc. 94, 1329–1337. https://doi.org/10.1175/BAMS-D-12-00142.1

Prospero, J.M., Olmez, I., Ames, M., 2001. Al and Fe in PM 2.5 and PM 10 Suspended Particles in South-Central Florida: The Impact of the Long Range Transport of African Mineral Dust. Water. Air. Soil Pollut. 125, 291–317. https://doi.org/10.1023/A:1005277214288

Putaud, J.-P., Raes, F., Van Dingenen, R., Brüggemann, E., Facchini, M.-C., Decesari, S., Fuzzi, S., Gehrig, R., Hüglin, C., Laj, P., Lorbeer, G., Maenhaut, W., Mihalopoulos, N., Müller, K., Querol, X., Rodriguez, S., Schneider, J., Spindler, G., Brink, H. ten, Tørseth, K., Wiedensohler, A., 2004. A European aerosol phenomenology—2: chemical characteristics of particulate matter at kerbside, urban, rural and background sites in Europe. Atmos. Environ. 38, 2579–2595. https://doi.org/10.1016/j.atmosenv.2004.01.041

Querol, X., Alastuey, A., de la Rosa, J., Sanchez-de-la-Campa, A., Plana, F., Ruiz, C.R., 2002. Source apportionment analysis of atmospheric particulates in an industrialised urban site in southwestern Spain. Atmos. Environ. 36, 3113–3125. https://doi.org/10.1016/S1352-2310(02)00257-1

Querol, X., Alastuey, A., Rodriguez, S., Plana, F., Ruiz, C.R., Cots, N., Massagué, G., Puig, O., 2001. PM10 and PM2.5 source apportionment in the Barcelona Metropolitan area, Catalonia, Spain. Atmos. Environ. 35, 6407–6419. https://doi.org/10.1016/S1352-2310(01)00361-2

Querol, X., Alastuey, A., Rodriguez, S., Viana, M.M., Artinano, B., Salvador, P., Mantilla, E., do Santos, S.G., Patier, R.F., de La Rosa, J., de la Campa, A.S., Menendez, M., Gil, J.J., 2004. Levels of particulate matter in rural, urban and industrial sites in Spain. Sci. Total Environ. 334, 359–376. https://doi.org/10.1016/j.scitotenv.2004.04.036

Regulation (EU) 2016/2286, 2016. Regulation (EU) 2016/2286 of 15 December 2016 laying down detailed rules on the application of fair use policy and on the methodology for assessing the sustainability of the abolition of retail roaming surcharges and on the application to be submitted by a roaming provider for the purposes of that assessment (Text with EEA relevance) [WWW Document]. URL http://data.europa.eu/eli/reg_impl/2016/2286/oj/eng (accessed 5.17.18).

Richter, H., Howard, J.B., 2000. Formation of polycyclic aromatic hydrocarbons and their growth to soot - a review of chemical reaction pathways. Prog. Energy Combust. Sci. 26, 565–608. https://doi.org/10.1016/S0360-1285(00)00009-5

Rodriguez, S., Cuevas, E., Prospero, J.M., Alastuey, A., Querol, X., Lopez-Solano, J., Garcia, M.I., Alonso-Perez, S., 2015. Modulation of Saharan dust export by the North African dipole. Atmospheric Chem. Phys. 15, 7471–7486. https://doi.org/10.5194/acp-15-7471-2015

Romero-Placeres, M., Mas-Bermejo, P., Lacasana-Navarro, M., Rojo-Solis, M.M.T., Aguilar-Valdes, J., Romieu, I., 2004. Air pollution, bronchial asthma, and acute respiratory infections in children less years of age, Habana City. Salud Publica Mex. 46, 222–233. https://doi.org/10.1590/S0036-36342004000300012

Sabin, L.D., Lim, J.H., Stolzenbach, K.D., Schiff, K.C., 2006. Atmospheric dry deposition of trace metals in the coastal region of Los Angeles, California, USA. Environ. Toxicol. Chem. 25, 2334–2341. https://doi.org/10.1897/05-300R.1

Samet, J.M., Dominici, F., Curriero, F.C., Coursac, I., Zeger, S.L., 2000. Fine Particulate Air Pollution and Mortality in 20 U.S. Cities, 1987–1994. N. Engl. J. Med. 343, 1742–1749. https://doi.org/10.1056/NEJM200012143432401

Sanchez de la Campa, A.M., de la Rosa, J., Querol, X., Alastuey, A., Mantilla, E., 2007. Geochemistry and origin of PM10 in the Huelva region, Southwestern Spain. Environ. Res. 103, 305–316. https://doi.org/10.1016/j.envres.2006.06.011

Sanchez-Soberon, F., Mari, M., Kumar, V., Rovira, J., Nadal, M., Schuhmacher, M., 2015. An approach to assess the Particulate Matter exposure for the population living around a cement plant: modelling indoor air and particle deposition in the respiratory tract. Environ. Res. 143, 10–18. https://doi.org/10.1016/j.envres.2015.09.008

Seinfeld, J.H., Pandis, S.N., 2012. Atmospheric Chemistry and Physics: From Air Pollution to Climate Change. Wiley.

Seinfeld, J.H., Pankow, J.F., 2003. Organic Atmospheric Particulate Material. Annu. Rev. Phys. Chem. 54, 121–140. https://doi.org/10.1146/annurev.physchem.54.011002.103756

Silva, J., Rojas, J., Norabuena, M., Molina, C., Toro, R.A., Leiva-Guzmán, M.A., 2017. Particulate matter levels in a South American megacity: the metropolitan area of Lima-Callao, Peru. Environ. Monit. Assess. 189, 635. https://doi.org/10.1007/s10661-017-6327-2

Singh, N., Murari, V., Kumar, M., Barman, S.C., Banerjee, T., 2017. Fine particulates over South Asia: Review and meta-analysis of PM2.5 source apportionment through receptor model. Environ. Pollut. Barking Essex 1987 223, 121–136. https://doi.org/10.1016/j.envpol.2016.12.071

Sisler, J.F., Malm, W.C., 2000. Interpretation of trends of PM2.5 and reconstructed visibility from the IMPROVE network. J. Air Waste Manag. Assoc. 1995 50, 775–789.

Smithson, P.A., 2002. IPCC, 2001: climate change 2001: the scientific basis. Contribution of Working Group 1 to the Third Assessment Report of the Intergovernmental Panel on Climate Change, edited by J. T. Houghton, Y. Ding, D. J. Griggs, M. Noguer, P. J. van der Linden, X. Dai, K. Maskell and C. A. Johnson (eds). Cambridge University Press, Cambridge, UK. Int. J. Climatol. 22, 1144–1144. https://doi.org/10.1002/joc.763

Strayer, H., Smith, R., Mizak, C., Poor, N., 2007. Influence of air mass origin on the wet deposition of nitrogen to Tampa Bay, Florida—An eight-year study. BRACE Bay Reg. Atmospheric Chem. Exp. 41, 4310–4322. https://doi.org/10.1016/j.atmosenv.2006.08.060

Suárez Tamayo, S., Maldonado Cantillo, G., Cañas Ávila, N., Romero Placeres, M., 2010. Contribución de la contaminación atmosférica a la ocurrencia de enfermedades respiratorias agudas en menores de 15 años. Ciudad de La Habana, 2001-2003. Hig. Sanid. Ambient. 10, 635–644.

Sudheer, A.K., Aslam, M.Y., Upadhyay, M., Rengarajan, R., Bhushan, R., Rathore, J.S., Singh, S.K., Kumar, S., 2016. Carbonaceous aerosol over semi-arid region of western India: Heterogeneity in sources and characteristics. Atmospheric Res. 178–179, 268–278. https://doi.org/10.1016/j.atmosres.2016.03.026

Tai, A.P.K., Mickley, L.J., Jacob, D.J., 2010. Correlations between fine particulate matter (PM2.5) and meteorological variables in the United States: Implications for the sensitivity of PM2.5 to climate change. Atmos. Environ. 44, 3976–3984. https://doi.org/10.1016/j.atmosenv.2010.06.060

Taiwo, A.M., Harrison, R.M., Shi, Z., 2014. A review of receptor modelling of industrially emitted particulate matter. Atmos. Environ. 97, 109–120. https://doi.org/10.1016/j.atmosenv.2014.07.051

Thurston, G.D., Spengler, J.D., 1985. A quantitative assessment of source contributions to inhalable particulate matter pollution in metropolitan Boston. Atmospheric Environ. 1967 19, 9–25. https://doi.org/10.1016/0004-6981(85)90132-5

Tie, X., Wu, D., Brasseur, G., 2009. Lung cancer mortality and exposure to atmospheric aerosol particles in Guangzhou, China. Atmos. Environ. 43, 2375–2377. https://doi.org/10.1016/j.atmosenv.2009.01.036

Tomaz, S., Jaffrezo, J.-L., Favez, O., Perraudin, E., Villenave, E., Albinet, A., 2017. Sources and atmospheric chemistry of oxy- and nitro-PAHs in the ambient air of Grenoble (France). Atmos. Environ. 161, 144–154. https://doi.org/10.1016/j.atmosenv.2017.04.042

Trapp, J.M., Millero, F.J., Prospero, J.M., 2010. Temporal variability of the elemental composition of African dust measured in trade wind aerosols at Barbados and Miami. Mar. Chem., Aerosol chemistry and impacts on the ocean 120, 71–82. https://doi.org/10.1016/j.marchem.2008.10.004

Turekian, V.C., Macko, S.A., Keene, W.C., 2003. Concentrations, isotopic compositions, and sources of size-resolved, particulate organic carbon and oxalate in near-surface marine air at Bermuda during spring. J. Geophys. Res. Atmospheres 108, 4157. https://doi.org/10.1029/2002JD002053

Turtos Carbonell, L.M., Capote Mastrapa, G., Fonseca Rodriguez, Y., Alvarez Escudero, L., Gacita, M.S., Bezanilla Morlot, A., Borrajero Montejo, I., Meneses Ruiz, E., Pire Rivas, S., 2013. Assessment of the Weather Research and Forecasting model implementation in Cuba addressed to diagnostic air quality modeling. Atmospheric Pollut. Res. 4, 64–74. https://doi.org/10.5094/APR.2013.007

Turtos Carbonell, L.M., Meneses Ruiz, E., Carrera Doral, W., Zucchetti, M., 2010a. Global and Local Atmospheric Pollution Evaluation and Control. Challenges for a Small Island and for Developing Countries. Fresenius Environ. Bull. 19, 2354–2360.

Turtos Carbonell, L.M., Meneses Ruiz, E., Sanchez Gacita, M., Rivero Oliva, J., Diaz Rivero, N., 2007. Assessment of the impacts on health due to the emissions of Cuban power plants that use fossil fuel oils with high content of sulfur. Estimation of external costs. Atmos. Environ. 41, 2202–2213. https://doi.org/10.1016/j.atmosenv.2006.10.062

Turtos Carbonell, L.M., Sanchez Gacita, M., de Jesus Rivero Oliva, J., Curbelo Garea, L., Diaz Rivero, N., Meneses Ruiz, E., 2010b. Methodological guide for implementation of the AERMOD system with incomplete local data. Atmospheric Pollut. Res. 1, 102–111. https://doi.org/10.5094/APR.2010.013

U.S. EPA, 2016a. Particulate Matter (PM) Pollution [WWW Document]. US EPA. URL https://www.epa.gov/pm-pollution (accessed 1.13.18).

U.S. EPA, 2016b. Setting and Reviewing Standards to Control Particulate Matter (PM) Pollution [WWW Document]. US EPA. URL https://www.epa.gov/pm-

pollution/setting-and-reviewing-standards-control-particulate-matter-pm-pollution (accessed 1.25.18).

U.S. EPA, 2014. Particulate Matter Emissions. ROE Home | Report on the Environment (ROE).

U.S. EPA, 2009. Integrated Science Assessment (ISA) for Particulate Matter (Final Report, Dec 2009) (Reports & Assessments No. EPA/600/R-08/139F). U.S. Environmental Protection Agency, Washington, DC.

Utsunomiya, S., Jensen, K.A., Keeler, G.J., Ewing, R.C., 2004. Direct identification of trace metals in fine and ultrafine particles in the Detroit urban atmosphere. Environ. Sci. Technol. 38, 2289–2297. https://doi.org/10.1021/es035010p

Vallius, M., 2005. Charasteristics and sources of fine particulate matter in urban air. National Public Health Institute ; University of Kuopio, Helsinki; Kuopio.

Venero-Fernández, S.J., 2016. Saharan Dust Effects on Human Health: A Challenge for Cuba's Researchers. MEDICC Rev. 18, 32–34.

Viana, M., Kuhlbusch, T. a. J., Querol, X., Alastuey, A., Harrison, R.M., Hopke, P.K., Winiwarter, W., Vallius, A., Szidat, S., Prevot, A.S.H., Hueglin, C., Bloemen, H., Wahlin, P., Vecchi, R., Miranda, A.I., Kasper-Giebl, A., Maenhaut, W., Hitzenberger, R., 2008. Source apportionment of particulate matter in Europe: A review of methods and results. J. Aerosol Sci. 39, 827–849. https://doi.org/10.1016/j.jaerosci.2008.05.007

Viana, M., Querol, X., Alastuey, A., Cuevas, E., Rodriguez, S., 2002. Influence of African dust on the levels of atmospheric particulates in the Canary Islands air quality network. Atmos. Environ. 36, 5861–5875. https://doi.org/10.1016/S1352-2310(02)00463-6

Viard, V.B., Fu, S., 2015. The effect of Beijing's driving restrictions on pollution and economic activity. J. Public Econ. 125, 98–115. https://doi.org/10.1016/j.jpubeco.2015.02.003

Watson, Chow, 1994. Clear Sky Visibility as a Challenge for Society. Annu. Rev. Energy Environ. 19, 241–266. https://doi.org/10.1146/annurev.eg.19.110194.001325

Watson, J., Chow, J., Chen, L.-W.A., Wang, X., 2010. Measurement system evaluation for fugitive dust emissions detection and quantification.

West, J.B., Bowen, G.J., Cerling, T.E., Ehleringer, J.R., 2006. Stable isotopes as one of nature's ecological recorders. Trends Ecol. Evol. 21, 408–414. https://doi.org/10.1016/j.tree.2006.04.002

Whitby, K.T., Husar, R.B., Liu, B.Y.H., 1972. The aerosol size distribution of Los Angeles smog. J. Colloid Interface Sci. 39, 177–204. https://doi.org/10.1016/0021-9797(72)90153-1

WHO, 2016. WHO | WHO releases country estimates on air pollution exposure and health impact [WWW Document]. WHO. URL http://www.who.int/mediacentre/news/releases/2016/air-pollution-estimates/en/ (accessed 3.21.17).

WHO, 2005. WHO | Air quality guidelines for particulate matter, ozone, nitrogen dioxide and sulfur dioxide- global update 2005 [WWW Document]. WHO. URL http://www.who.int/phe/health_topics/outdoorair/outdoorair_aqg/en/ (accessed 3.6.16).

Widory, D., 2007. Nitrogen isotopes: Tracers of origin and processes affecting PM10 in the atmosphere of Paris. Atmos. Environ. 41, 2382–2390. https://doi.org/10.1016/j.atmosenv.2006.11.009

Widory, D., 2006. Combustibles, fuels and their combustion products: A view through carbon isotopes. Combust. Theory Model. 10, 831–841. https://doi.org/10.1080/13647830600720264

Widory, D., Roy, S., Le Moullec, Y., Goupil, G., Cocherie, A., Guerrot, C., 2004. The origin of atmospheric particles in Paris: a view through carbon and lead isotopes. Atmos. Environ. 38, 953–961. https://doi.org/10.1016/j.atmosenv.2003.11.001

Wilson, W.E., Suh, H.H., 1997. Fine particles and coarse particles: concentration relationships relevant to epidemiologic studies. J. Air Waste Manag. Assoc. 1995 47, 1238–1249.

Wurzler, S., Reisin, T.G., Levin, Z., 2000. Modification of mineral dust particles by cloud processing and subsequent effects on drop size distributions. J. Geophys. Res.-Atmospheres 105, 4501–4512. https://doi.org/10.1029/1999JD900980

Xie, S., Qi, L., Zhou, D., 2004. Investigation of the effects of acid rain on the deterioration of cement concrete using accelerated tests established in laboratory. Atmos. Environ. 38, 4457–4466.

Yeatman, S.G., Spokes, L.J., Dennis, P.F., Jickells, T.D., 2001. Can the study of nitrogen isotopic composition in size-segregated aerosol nitrate and ammonium be used to investigate atmospheric processing mechanisms? Atmos. Environ. 35, 1337–1345. https://doi.org/10.1016/S1352-2310(00)00457-X

Chapter 2

Chemical characterization of PM_{10} samples collected simultaneously at a rural and an urban site in the Caribbean coast: local and long-range source apportionment

This chapter reproduces the text of the following manuscript:

Morera-Gómez, Y., Elustondo, D., Lasheras, E., Alonso-Hernandez, C.M., Santamaría, J.M., 2018. Chemical characterization of PM_{10} samples collected simultaneously at a rural and an urban site in the Caribbean coast: local and long-range source apportionment. Submitted to Atmospheric Environment.

Abstract

The deterioration of the air quality is a global concern. Daily PM_{10} samples were simultaneously collected and chemically characterized between January 2015 and January 2016 at an urban and a rural site in Cienfuegos, Cuba. A source apportionment study was conducted in order to identify and quantify the main local and long-range source of contributions.

Concentrations of PM_{10} varied similarly at the urban and rural site, with annual averages of 35.4 and 24.8 $\mu g\ m^{-3}$, respectively. The highest concentrations were observed between March and August at both sites, when a strong influence of Saharan dust was identified. The PM_{10} daily limit (50 $\mu g\ m^{-3}$) established in the Cuban legislation for air quality was exceeded 3 and 8 times in the rural and urban site, respectively. The chemical characterization of PM_{10} showed important contributions of mineral matter, total carbon and secondary inorganic compounds in the region, with the highest concentrations observed at the urban site. Marine contribution, by contrast, was higher at the rural site. The highest enrichment factors were obtained for the typical road traffic tracers Mo and Cu. Positive matrix factorization (PMF) analysis coupled with conditional bivariate probability function (CBPF) and concentration weighted trajectory (CWT) identified 5 main sources in the studied sites (Saharan intrusions, marine aerosol, combustion, road traffic and cement plant). Saharan dust contribution was quantified for the first time in Cuba, proving to be one of the major components of PM_{10} at both sites. Its daily contribution, indeed, explained more than 60% of the PM_{10} recorded in 10 of the 11 exceedance events.

This study reports the first simultaneous evaluation of PM_{10} and its chemical composition in urban and rural areas of Cuba and provide the basis for environmental managers to adopt control strategies to reduce the impact of PM_{10} pollution in the region.

Keywords: PM_{10}; chemical composition; PMF 5.0; local anthropogenic sources; Saharan dust

1. Introduction

Air pollution caused by the release of particulate matter (PM) from industries, road traffic, biomass burning, oil combustion and other anthropogenic and natural sources is one of the major issues of global concern. The exposure to high levels of PM has negative implications on human health (Pope and Dockery, 2006; WHO, 2016), visibility (Kanakidou et al., 2005), climate and ecosystems (Grantz et al., 2003). Comprehensive studies on daily time series of PM levels and chemical composition are therefore necessary to evaluate the regional air quality. Such data constitute an invaluable basis of knowledge to identify and quantify the PM sources, by using robust mathematical tools. Receptor models such as Positive Matrix Factorization (PMF), are widely used for that purpose (Kim and Hopke, 2005; Querol et al., 2007; Squizzato et al., 2017).

Several studies on PM source apportionment have been carried out around the world (Amato et al., 2009; Contini et al., 2016; Kim et al., 2016; Viana et al., 2008). Results indicate that the concentration and composition of PM at a specific location depend on a large number of factors, such as the characteristics of local sources, the regional background and the meteorological conditions, among others. Thus, it has been found that urban air quality is mainly affected by emission derived from road traffic (exhaust and non-exhaust emissions), industrial activities, combustion sources and also by organic and inorganic particles formed from chemical processes involving precursor gases (Aldabe et al., 2011; Querol et al., 2007, 2004; Squizzato et al., 2017). Moreover, depending on the characteristics of the study area other important contributions may derive from the resuspension of road dust, sea-salt or construction activities. Rural air quality is mainly affected by the resuspension of soil, agricultural activities, wood burning and secondary pollutans whose precursors have been emitted from distant sources; but also by the urban background if there are populated areas nearby (Ancelet et al., 2014; Arruti et al., 2011).

There are numerous reports about the aerosols and PM measurements in the Caribbean region. Many of these studies are mainly related to the qualitative identification of the Sahara dust intrusions by using concentration of major elements, backward air trajectories and satellite data (Mojena López et al., 2015; Prospero, 1999;

Prospero et al., 2014, 2001; Prospero and Mayol-Bracero, 2013; Rodriguez et al., 2015). Saharan dust contributions to PM in the region have only been quantitatively estimated in the southern United States (Bozlaker et al., 2013). As a result of its geographical position, very close to the Tropic of Cancer, Cuba is influenced by tropical and extratropical air masses circulation and can then be affected by a large variety of PM sources including the African dust. To date, studies in Cuba are restricted to some urban location, mainly in Havana, and showed a main influence from marine aerosol and local anthropogenic sources (Cuesta-Santos et al., 2002; Martínez Varona et al., 2015; Molina Esquivel et al., 2011; Piñera et al., 2010). In a recent work carried out in the region of Camagüey, chemical composition and optical absorbing properties of PM_{10} and PM_1 were determined indicating the influence of the marine aerosol and the occurrence of Sahara dust intrusion events (Barja et al., 2013). However, as far as the authors know, there are no values reported of chemical elements in PM fractions in other regions of Cuba and background levels of several air pollutants are unknown in the entire national territory and in many regions of the Caribbean basin. This scarcity is mainly associated with technical difficulties with the local measurements based on the instrumentation maintenance and availability (Barja et al., 2013). Therefore, the identification and the apportionment of the different sources impacting both rural and urban areas are imperative to develop effective air quality management strategies in this region.

This work aims to study the concentrations, chemical composition and main sources of PM_{10} in rural and urban environments in Cienfuegos, Cuba. For that purpose, a simultaneous PM_{10} monitoring at an urban and rural site with an exhaustive chemical characterization of major and trace elements, was carried out between 2015 and 2016. Using this information, a source apportionment study, employing PMF 5.0 coupled with the conditional bivariate probability function (CBPF) and concentration weighted trajectory (CWT), was performed as an integrated approach in order to evaluate the local and long-range (Sahara dust) contributions to PM_{10} for the first time in the studied region. Additionally, similarities and differences in the chemical element correlations and the crustal enrichment factors (EFs) in the studied sites are discussed.

2. Materials and methods

2.1. Area of study

Monitoring of PM_{10} was carried out at two stations (rural and urban sites) located in the municipality of Cienfuegos, on the south central coast of Cuba (see Figure 2.1). The rural station (22º 03' 55'' N, 80º 28' 58'' W) is located in the main facilities of the Centre for Environmental Studies (CEAC), between the Caribbean Sea and the Bay of Cienfuegos, a rural area 9 km south of Cienfuegos City. A medium-size town is about 1.5 km east. The urban station is located at the CEAC facilities in the city of Cienfuegos (22º 08' 32'' N, 80º 27' 29'' W) very close to the coast of Cienfuegos Bay.

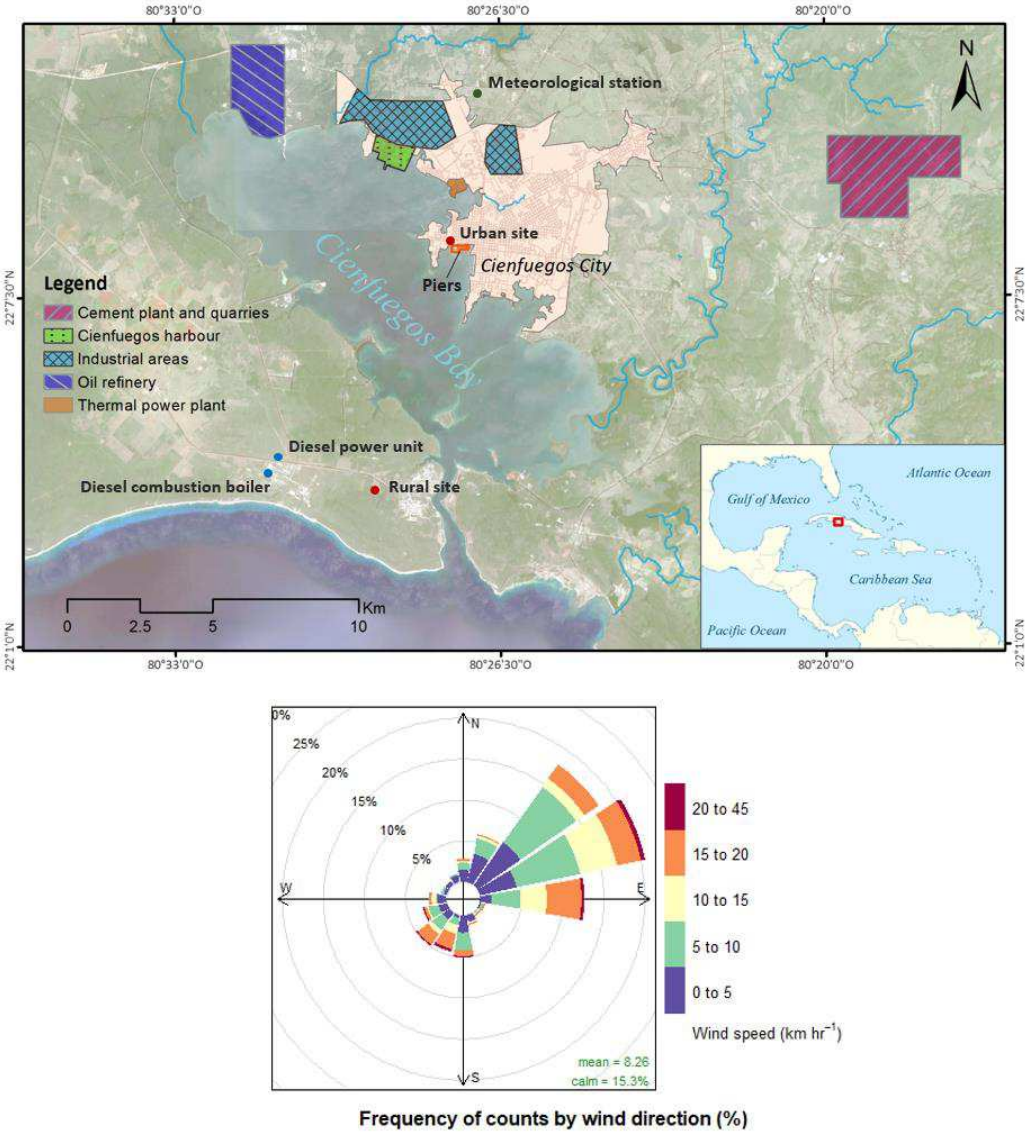

Figure 2.1. Area of study, sampling stations and wind rose for the period of study.

Cienfuegos city is currently an important tourist and industrial center in Cuba, with a population of about 147 000 inhabitants. The climate in the region is tropical with two clearly defined seasons: wet (approximately May to October) and dry (approximately November to April). In the last three decades the average annual rainfall has been 1363 mm, with about 80% produced in the wet period. The prevalent wind direction in the area during the study was ENE (see wind rose in Figure 2.1).

The main pollution sources in the area are a thermal power plant (TPP), with a capacity of ~316 MW h^{-1} and powered by sulfur-rich Cuban crude oil, an oil refinery and a cement plant (petroleum-coke powered) framed in a circular area with a radius of 15 km centered in the monitoring urban station (see Figure 2.1). This area also includes the quarries related to the cement plant activities, the harbour and other pier areas in the Bay of Cienfuegos, other industrial areas and the rural monitoring station. According to the prevailing wind direction, the urban station is mainly influenced by the city background (mainly the road traffic) and cement plant emissions. Moreover, shipping emissions can also affect this site because of its proximity to the piers area (100 – 500 m away). The rural site may be also affected by the city background, and emissions derived from the TPP, the cement plant and quarries and local sources such as a small diesel power unit (2.76 MW h^{-1}) and a diesel combustion boiler (1.76 MW) located at 4 km to the west. In addition, the frequent wood burning around this site for charcoal production will also play an important role in the chemical characteristics of PM.

2.2. PM_{10} sampling

24-hour PM_{10} samples were collected in parallel at both stations on quartz fiber filters (Munktell, 150 mm diameter) every three days from 31/01/2015 to 20/01/2016 using high-volume samplers MCV-CAV which operated at a flow rate of 30 m^3 h^{-1}. This frequency allows us to guarantee at least 50 daily determinations in a year including at least 4 determinations in each month according to the requirements of the Cuban legislation to evaluate the PM_{10} annual mean concentration (NC 1020, 2014). A total of 68 and 71 PM_{10} samples were collected at rural and urban stations, respectively. Due to a problem with the high-volume sampler, PM_{10} samples could not be taken during the period 5/08/2015 - 12/11/2015 at the rural station.

2.3. PM_{10} chemical analysis

After sampling, PM_{10} filters, previously heated at 550 °C during 4 h, were stabilized at 20 – 24 °C and 35 – 40% relative humidity before weighing. This procedure was repeated 24 h later, and finally determining the PM_{10} ambient levels by gravimetric measurements. Afterwards, filters were cut into quarters for further chemical analysis.

The chemical analysis of PM_{10} was performed using the methods described in Aldabe et al., (2013, 2011). In short, a quarter of filter was used to determine major and trace elements (Be, Na, Mg, Al, P, S, K, Ca, V, Ti, Cr, Mn, Fe, Co, Ni, Cu, Zn, As, Se, Rb, Sr, Cd, Sn, Sb, Cs, Ba, Hf, Tl, Pb, Th, U, Ge, Zr, Nb, Mo, W) by inductively coupled plasma mass spectrometry (ICP-MS, Agilent 7500a), after their extraction with HF, H_2O_2, HNO_3 and HCl (3:3:4:1 mL) in a closed microwave digestion system (CEM Co., Mars X press). A multi-elemental solution (Li, Sc, Y, In, Bi) was added to the samples as internal standard for further determination by ICP-MS. Ammonium (NH_4^+) and anions (Cl^-, NO_3^- and SO_4^{2-}) were analyzed in the soluble fraction of another quarter of filter by Ion Chromatography (Dionex ICS 1100 for ammonium and Dionex ICS 2000 for anions). The pH and conductivity (EC) were also analyzed in the soluble fraction. Punches of 4.1 cm^2 in the third portion of filter were used for the analysis of mercury (Hg) and total carbon (TC), which were determined by thermo-optical methods in a Mercury Analyzer (MA-2000 Series, Nippon) and a Carbon Analyzer (Liqui-TOC Elementar), respectively.

The quality control of the analytical procedures was carried out by repeated analysis of certified reference materials (CRM) at least every 10 samples. Certified reference material CTA-FFA1 (fine fly ash), Silty Clay Loam (0217-CM-73007) and Synthetic Carbon (No 203–029 Leco) were used for major and trace elements, Hg and TC, respectively. NH_4^+ and anions in turn were assessed by using reference standard solutions at different concentrations along the method range. Table 2.1 lists the elements measured along with element recoveries, the Relative Standard Deviation (RSD) obtained from the CRMs, the average contributions of the filter blanks evaluated and subtracted from the results, the detection limits (DLs) and percentages of values below detection limits (BDL).

Table 2.1. Recovery (%) and Relative Standard Deviation (%) obtained from the CRMs, average contribution of the filter blanks (ng m^{-3}), method detection limit (DL, ng m^{-3}) and percentages of values below the detection limit (BDL).

Element	Recovery	RSD	Filter blank	DL	% BDL	
					Urban station	Rural station
TC	97	4.4	388.8	248.7	0	0
NH_4^+	98	6.9	50.8	39.2	3	0
Cl^-	96	3.6	28.7	28.3	3	3
NO_3^-	93	5.6	42.9	41.8	0	1
SO_4^{2-}	96	5.4	79.6	59.9	0	0
Be	87	5.0	0.03	0.02	37	18
Na	90	3.6	98.2	6.1	0	0
Mg	76	8.8	59.1	1.3	0	0
Al	74	5.4	268.0	9.2	0	6
P	84	4.1	<DL	5.7	0	12
S	N.A.	6.0	97.6	33.5	0	0
K	85	5.0	11.2	6.6	0	0
Ca	92	7.6	144.2	113.7	0	9
V	89	3.8	<DL	0.5	0	0
Cr	88	3.8	4.4	0.2	3	4
Mn	92	4.4	1.7	0.1	0	3
Fe	88	3.4	45.5	6.6	0	0
Co	86	3.7	0.01	0.01	0	1
Ni	83	4.3	2.8	0.1	0	3
Cu	85	4.4	1.2	0.2	0	0
Zn	94	5.3	4.7	0.5	0	0
As	90	4.6	0.2	0.1	7	28
Se	73	13.8	0.2	0.2	44	44
Rb	64	14.8	0.2	0.04	0	7
Sr	82	8.2	0.9	0.1	0	0
Cd	79	3.7	0.01	0.01	3	16
Cs	81	4.4	<DL	0.01	4	6
Ba	74	6.9	17.1	0.2	8	43
Hf	95	2.9	0.6	0.01	15	25
Tl	N.A.	3.9	0.04	0.01	27	15
Pb	94	2.5	0.3	0.1	0	0
Th	87	6.5	0.6	0.01	30	40
U	87	3.2	0.8	0.003	0	43
Ti	94	3.5	4.3	1.2	3	0
Ge	N.A.	4.2	2.4	0.01	66	69
Zr	N.A.	4.7	14.6	0.1	41	59
Nb	N.A.	3.9	0.1	0.02	14	19
Mo	75	5.5	60.1	0.02	0	28
Sn	N.A.	2.7	0.3	0.04	3	0
Sb	96	2.9	0.1	0.02	0	0
W	91	3.8	0.1	0.01	3	6
Hg	82	8.3	<DL	0.01	0	6

N.A.: referent value not available for the CRM CTA-FFA1.

As a first approach to interpret the PM_{10} origin in the study region, carbonate (CO_3^{2-}), silica (SiO_2), alumina (Al_2O_3), marine sulphate (mSO_4^{2-}) and non-marine sulphate ($nmSO_4^{2-}$) concentrations were obtained by stoichiometry according to the literature (Sanchez de la Campa et al., 2007).

2.4. Enrichment factors

Enrichment factors (EFs) were estimated in order to determine possible contributions of anthropogenic trace elements in both sampling sites. The EF is calculated as follow:

$$EF_X = (C_X/C_R)_{PM10}/(C_X/C_R)_{Crust} \qquad (2.1)$$

where X represents the element of interest; EF_X the EF of X; C_X the concentration of X, and C_R the concentration of a reference element. In this study Ti was selected as reference element, and the mean elemental composition of the local soils was used to estimate the elemental concentration of the crustal material. We evaluated the Al and Fe as reference elements and also the database proposed by Li et al., (2009) as reference crustal material and similar EFs were observed. According to the EFs values, the elements can be considered highly enriched (EF>100), moderately enriched (10<EF<100) and poorly enriched (EF<10) (Fernandez-Olmo et al., 2016, 2015).

Chemical composition of the local soils was determined by using a total of 24 top soil samples collected in the 15 km radius study area during April 2015. Samples were dried at 45 ^oC and then sieved through a mesh of 250 μm. A subsample of 0.25 g was digested in 12 ml aqua regia (HCl/HNO_3=3:1) in the microwave system described above. Major and trace elements were determined using the same techniques described for PM_{10} analysis. The recovery from the used CRM (Silty Clay Loam 0217-CM-73007) was generally within the range of 80 – 102%, and the RSD was less than 8%.

2.5. Source apportionment with PMF

Positive Matrix Factorization (PMF) is a multivariate factor analysis tool for quantifying the contribution of sources to samples based on the detailed composition

of the samples collected in one or more sites and it has been widely described in the literature (Paatero, 1997; Paatero and Tapper, 1994).

The EPA PMF software v5.0 was used in this study (Norris et al., 2014) and for PMF reporting results we followed the recommendations from Brown et al., (2015). All available concentration values were used without any censored procedure, and the uncertainty was calculated according to equation 2.2 (Cesari et al., 2016),

$$s_{ij} = \sigma_{Bj} + h_j x_{ij} \qquad (2.2)$$

where σ_{Bj} is the standard deviation of the filter blank contributions and h_j is a constant calculated taking into account the analytical uncertainties. The uncertainties of the identified outliers (values higher than 1.5 times the 95th percentile of the data) were replaced by $4\bar{x}_{ij}$ to minimize their influence. We added a 10% of extra modeling uncertainty for the runs.

The appropriate number of extracted factors was determined by providing the best physical significance based on the following procedure:

1. Using the Signal-to-Noise (S/N) ratio computed by the model we classified the species as “Strong” (S/N≥2.0), “Weak” (0.5≤S/N<2.0) and “Bad” (S/N<0.5).
2. Species with more than 50% of the data BDL were excluded and selected as “Bad”.
3. We evaluated the species categorization after the initial runs by reviewing the linear fit (R^2) between predicted and observed concentrations (Vossler et al., 2016).
4. After steps 1 – 3, three to 7 factors solutions were tested for both stations using an initial random seed number (24 for final solution) and 30 model runs. First, we evaluate how the parameters Q robust (Q_{rob}), $Q_{rob}/Q_{expected}$ (Q_{rob}/Q_{exp}), IM and IS (maximum mean and SD values of the scaled residuals, respectively) changed with the number of factors. When changes in Q become small and/or a sharp drop in IS or IM is produced with increasing factors, it can be indicative that there may be too many factors being fit (Brown et al., 2015; Heo et al., 2009).

5. Uncertainties on estimated factor profiles and contributions under different scenarios (different numbers of factors) were evaluated using the Displacement (DISP), Bootstrap (BS) and BS-DISP methods (Paatero et al., 2014).
6. We examined the Q/Q_{exp} for individual species and the time series of Q/Q_{exp} computed by the model, to understand what samples or species were not well modeled (values greater than 2).

We found that 5 factors with 17 "Strong" species (PM_{10}, C, NH_4^+, Cl^-, NO_3^-, SO_4^{2-}, Na, Mg, Al, K, Ca, Mn, Fe, Ni, Cu, Zn, Pb, Ti and Sb) and 6 "Weak" species (Cd, Ba, V, Co, As and Mo) was the better solution for the urban station, while 4 factors with 15 "Strong" species (PM_{10}, C, NH_4^+, NO_3^-, SO_4^{2-}, Cl^-, Na, Mg, Al, K, Mn, Fe, Co, Zn and Ti) and 6 "Weak" species (Ca, V, Ni, As, Cd and Sb) was the most appropriate solution for the rural station. We also calculated the FPEAK parameter as function of the Q-value for the best found solution and observed that FPEAK = 0.0 provided the most physically meaningful solution at both stations. Once the number of factors was optimized, we tested up to 500 model runs and up to 20 random seed numbers and confirmed the solutions as a global minimum. Finally, the goodness of the fit between the measured and modeled PM_{10} mass at both the rural ($PM_{10}^{modeled}$=0.99$PM_{10}^{measured}$-0.19, R^2=0.93) and the urban ($PM_{10}^{modeled}$=0.97$PM_{10}^{measured}$+0.61, R^2=0.90) site was corroborated. From these results the unexplained PM_{10} mass resulted less than 1.8%.

2.6. Conditional bivariate probability function and concentration weighted trajectory

Source contribution estimated from PMF coupled with time resolved wind direction, wind speed and backward trajectory data were investigated by using the conditional bivariate probability function (CBPF) and concentration weighted trajectory (CWT) to better understand the local and regional source impacts. Calculations of both functions were done using the Openair package freely available for R (Carslaw, 2015).

The CBPF improves the traditional CPF (Kim et al., 2003; Kim and Hopke, 2005) by adding the wind speed as a third variable and estimates the probability that a given source contribution from a given wind direction and speed will exceed a predetermined

threshold criterion. The CBPF is defined as $CBPF = m_{\theta,l}/n_{\theta,l}$, where $m_{\theta,l}$ is the number of samples in the wind sector θ and wind speed interval l with mixing ratios greater than a threshold concentration, and $n_{\theta,l}$ is the total number of samples in the same wind direction-speed interval (Squizzato et al., 2017; Uria-Tellaetxe and Carslaw, 2014). Here, the same 24-h mass contribution of each identified source was assigned to each 3-h wind data available from the Canta Rana meteorological station located in the study area within a radius of 15 km. We used 16 wind sectors ($\theta = 22.5°$) and calm winds (≤1 km h^{-1}) were excluded from the analysis.

The CWT computes a log-mean concentration at the receptor site weighted by the residence time of the trajectory for each grid cell of the geographical domain (Cheng et al., 2013; Hsu et al., 2003). A high CWT value means that air parcels passing over a given cell would cause, on average, high concentrations at the receptor site. For our study, 120-h and 240-h back-trajectories (BTs) were computed using the Hybrid Single Particle Lagrangian Integrated Trajectory (HYSPLIT) model and the Global NOAA-NCEP/NCAR reanalysis data files (Draxler and Rolph, 2015). BTs were run at 3-h intervals with an increase of 1-h starting at a ground-level of 500 m for each day during the sampling period. The trajectory domain was divided into grid cells of 2.5x2.5° and because of this and the proximity between the sampling sites, the coordinates of the urban station were selected as the starting point.

3. Results and discussion

3.1. PM_{10} concentrations

Variation of the daily concentration of PM_{10} at both sampling sites are shown in Figure 2.2a. The concentration of PM_{10} varied between 10.7 and 69.5 μgm^{-3} (average of 24.8 μgm^{-3}) and between 15.6 and 84.5 μgm^{-3} (35.4 μgm^{-3}) at rural and urban sites, respectively. Similar values to those obtained in the urban site have been reported for urban regions in Havana (Martínez Varona et al., 2013; Molina Esquivel et al., 2011) and Camagüey (Barja et al., 2013). No more studies have been performed either in the Cienfuegos region or in other rural areas of the country. On the other hand, similar

annual average of PM_{10} has also been reported in Caribbean areas like at Cayenne (French Guiana) and Guadeloupe (Lesser Antilles) (Prospero et al., 2014).

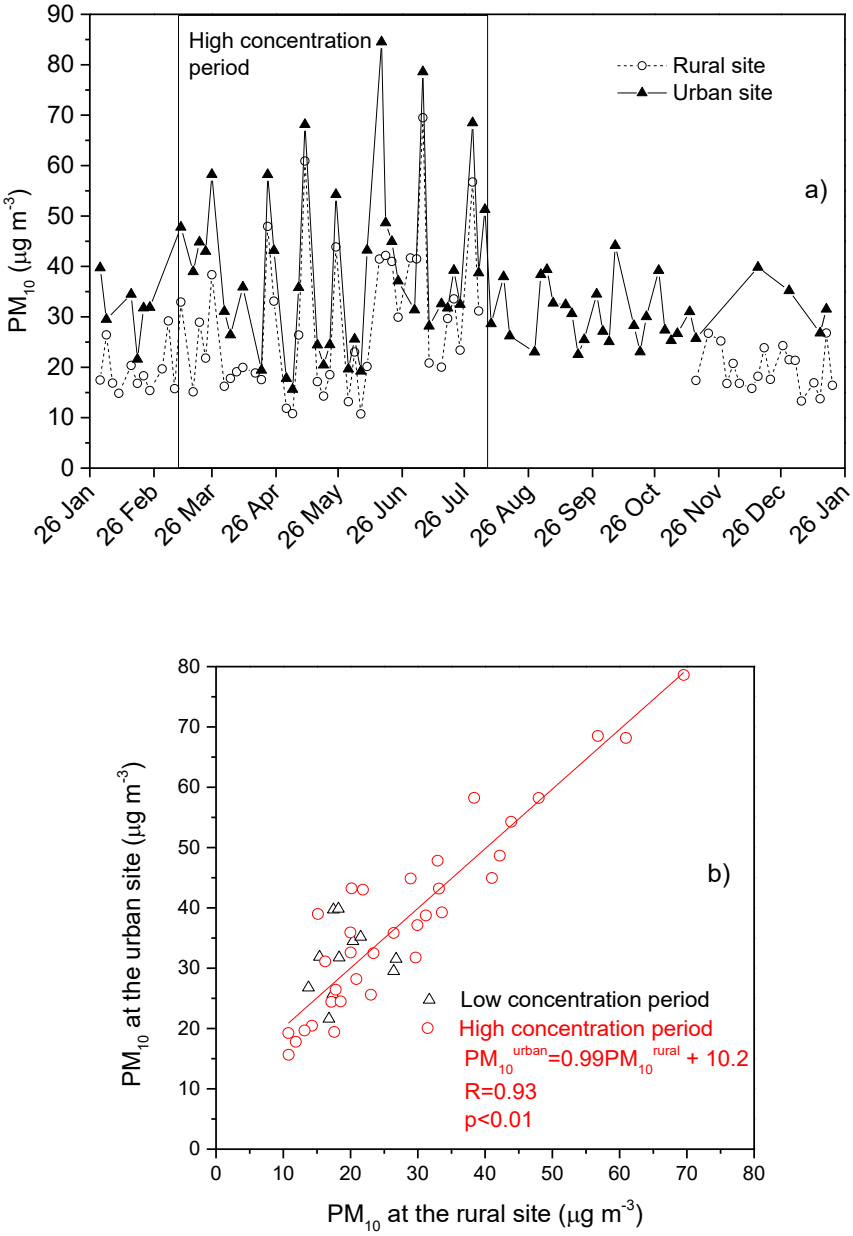

Figure 2.2. Temporal distributions of the concentration of PM_{10} at the rural and urban stations (a) and linear correlation between sites (b).

Although the temporal dynamic of PM_{10} was very similar in both sampling sites, probably as a result of the regional and global influence, the levels of PM_{10} were higher in the urban site showing and additional influence of local sources. A t-test ($p < 0.05$)

showed that there was no seasonal pattern for PM_{10} among the wet and dry season either in the rural or urban site. However, the highest PM_{10} levels were recorded during the March-August period in both sites. A significant correlation ($r = 0.93$, $p<0.01$) between the values of both stations was found in this period (Figure 2b). No such correlation was found between November and April, when PM_{10} contents were lower.

A visual examination of the filters with the highest concentration of PM_{10} from both stations revealed a yellow PM, thereby suggesting the influence of the Sahara dust which frequently affect the Caribbean region during those months (Prospero et al., 2014; Prospero and Mayol-Bracero, 2013; Rodriguez et al., 2015). The well-known seasonality of the Saharan dust clouds in Cuba (Mojena López et al., 2015), with the highest presence in the months from May to August, seems to corroborate this idea. Thus, Barja et al., (2013) also detected higher concentrations of PM_{10} between May and August in the Camagüey region (central Cuba), which they attributed to the occurrence of Saharan dust intrusions.

According to the Cuban legislation for air quality (NC 1020, 2014), the maximum admissible daily concentration of PM_{10} (MAC=50 $\mu g\ m^{-3}$), was exceeded 3 and 8 times during the sampling period at rural and urban sampling sites, respectively. All exceedance events occurred in the period of high concentrations, often coinciding with the presence of Saharan dust clouds. Similar events were also reported in other Caribbean countries and in Southern United States in the same period (Bozlaker et al., 2013; Prospero et al., 2014). Although the annual PM_{10} limit established by the Cuban legislation (30 $\mu g\ m^{-3}$) was only exceeded at the urban site, the annual value (20 $\mu g\ m^{-3}$) recommended by the World Health Organization (WHO, 2005) was also exceeded in the rural site.

3.2. Chemical composition

3.2.1. Major elements

Table 2.2 shows the statistical summary of concentration of major elements analyzed in the PM_{10} samples, which contributed 71.7% (17.8 $\mu g\ m^{-3}$) and 77.3% (27.3 $\mu g\ m^{-3}$) to the PM_{10} mass in the rural and urban sites respectively. While in the rural site

the PM_{10} mass was dominated by the mineral fraction (CO_3^{2-}+Al_2O_3+SiO_2+Ca+Fe+K+Mg) and the marine aerosol (Na+Cl^-+mSO_4^{2-}), in the urban site the mineral and TC fractions were dominant.

Table 2.2. Statistic summary of concentration of PM_{10}, major elements and estimated major components (μg m^{-3}), ΔpH and ΔEC (μS cm^{-1}) at both sampling sites. The intersite Pearson correlations (R_{IPC}) in bold represent a statistic significant at the 0.01 level.

Element	Rural station (n=68)		Urban Station (n=71)		R_{IPC}
	AVE (SD)	Range	AVE (SD)	Range	
PM_{10}	24.8 (12.1)	10.7-69.5	35.4 (13.6)	15.6-84.5	**0.91**
TC	2.60 (1.65)	1.01-9.96	5.54 (2.22)	1.54-13.26	**0.69**
NH_4^+	0.49 (0.33)	0.09-1.98	0.51 (0.3)	<DL-1.43	**0.86**
Cl^-	1.76 (1.61)	<DL-7.07	1.35 (1.3)	<DL-6.05	**0.76**
NO_3^-	0.72 (0.42)	<DL-2.07	0.77 (0.45)	0.13-2.09	**0.73**
SO_4^{2-}	2.31 (1.14)	0.2-6.81	2.39 (0.96)	0.77-6.76	**0.87**
Na	1.69 (0.94)	0.36-4.57	1.39 (0.83)	0.25-4.09	**0.87**
Mg	0.29 (0.19)	0.04-1.13	0.40 (0.25)	0.09-1.27	**0.92**
Al	0.67 (1.04)	<DL-5.35	1.13 (1.29)	0.15-6.34	**0.98**
S	0.87 (0.46)	0.26-2.73	0.96 (0.38)	0.38-2.72	**0.91**
K	0.34 (0.6)	0.07-4.93	0.36 (0.21)	0.13-1.14	**0.95**
Ca	0.51 (0.38)	<DL-1.51	1.81 (1.2)	0.13-6.66	0.18
Fe	0.32 (0.49)	0.01-2.4	0.54 (0.55)	0.07-2.71	**0.97**
CO_3^{2-}	1.72 (1.98)	0.1-10.86	3.72 (2.09)	0.44-10.87	**0.46**
Al_2O_3	1.26 (1.97)	0.01-10.09	2.14 (2.43)	0.29-11.96	**0.98**
SiO_2	3.78 (5.91)	0.03-30.28	6.41 (7.29)	0.87-35.87	**0.98**
mSO_4^{2-}	0.42 (0.24)	0.09-1.14	0.35 (0.21)	0.06-1.02	**0.87**
$nmSO_4^{2-}$	1.89 (1.14)	0.01-6.54	2.04 (0.95)	0.66-6.51	**0.88**
Mineral	8.2 (10.82)	0.54-56.63	15.38 (12.72)	3.16-66.08	**0.93**
Marine	3.87 (2.67)	0.47-11.17	3.09 (2.3)	0.38-11.16	**0.85**
Σ_{major}	17.8 (71.7)		27.3 (77.3)		
ΔpH*	-0.38 (0.49)	-1.92-0.63	0.93 (0.52)	-0.72-1.98	0.08
ΔEC*	50.4 (22.8)	12.9-109.8	58.4 (25.2)	8.13-127.4	**0.64**

Σ_{major} is the sum of all major components and the % of PM_{10} mass is given in brackets.
*ΔpH and ΔEC were calculated as the difference between blank filters (pH_{blank}=6.43 and EC_{blank}=4.75 μS cm^{-1}) and sample values.

Concentrations of major elements were generally higher in the urban station except for the marine aerosol, which indicate a major marine influence in the rural station. The average concentration ratio Cl^-/Na^+ was 0.89 and 0.81 at rural and urban sites, respectively. Comparison of these values and the ones expected for seawater (1.16) and earth's crust (0.003) (Barja et al., 2013), suggests that these elements were primarily of

marine origin. The most important contribution to the PM_{10} total mass at both sites was derived from the mineral matter, being considerably higher in the urban site. Concentrations of the typical crustal elements Al, K and Fe varied similarly during the study at both sites with the highest values observed between March and August, which probably indicated that they were mainly derived from the Saharan dust intrusions. The biggest difference was observed for Ca being about 3.5 times higher at the urban site, and could be related to the emissions coming from the cement plant and quarries located at 15 km downwind from the prevalent wind direction, and also to the wearing of roads, construction works and the handling of construction materials in the piers close to the urban sampling site. The TC contribution was significantly high in the urban site and it is likely due to the direct influence of the road traffic; nevertheless, the TC contribution in the rural station was also important, probably reflecting the impact of the wood burning for charcoal production in this area. The mean values of $nmSO_4^{2-}$, NO_3^- and NH_4^+ were slightly higher at the urban site. Concentrations of $nmSO_4^{2-}$ and NH_4^+ were significantly correlated ($r=0.84$, $p<0.01$ at both stations) suggesting the formation of ammonium sulphate of secondary origin. In both cases, however, a $nmSO_4^{2-}$ excess in the ionic balance with NH_4^+ was observed, suggesting that part of the $nmSO_4^{2-}$ may be linked to other cations.

The inter-site Pearson correlation analysis carried out on the studied element and major components revealed a significant association between the two sampling stations (Table 2.2), suggesting that both sites are subject to the impact of common sources, which is consistent with the regional influence produced by the Saharan dust. Although crustal elements showed the highest correlations (especially Al, K and Fe) no correlation was found for Ca, suggesting the existence of a local source of that element at the urban site, where the highest levels were observed. This result supports the previous conclusions about the influence of emissions derived from the cement plant and related activities as well as other local sources at the urban site.

The pH of the particulate matter extracts also showed significant differences between the sampling sites (Table 2.2), as well as correlations with the major ions. In the rural area pH variation (ΔpH) was negative (average value of -0.38) and negatively correlated with TC ($r = -0.59$, $p <0.01$), NH_4^+ ($r = -0.66$, $p <0.01$) and $nmSO_4^{2-}$ ($r = -0.61$, p

<0.01), while in the urban site was positive (average value of 0.93) and positively correlated with mineral matter fraction (r = 0.44, p <0.01) and, specially, with Ca^{2+} (r = 0.65, p <0.01). These results suggest that the alkaline water-soluble elements (probably anions that accompany Ca^{2+}, such as OH^- or HCO_3^-) neutralize acidic matter (sulfate, nitrate and carboxylic anions) in the urban station. Concerning variation of conductivity (EC), slightly higher values were observed at urban site, probably related to the highest content of total ions.

Average concentrations of Cl^-, K, NH_4^+ and NO_3^- in our sampling sites were lower than those obtained in Camagüey (Barja et al., 2013), while level of Mg was higher and Na and SO_4^{2-} were similar. Concentration of Ca was lower in our rural station but in the urban site we obtained a value twofold the reported for Camagüey. Another study carried out in Havana (Pérez et al., 2009), showed higher average concentrations of Cl^-, S and Ca, and lower of K and Fe than those found in our sampling sites. Contributions of most of the major elements in this work were in the range of variation of those reported in Jamaica (Boman and Gaita, 2015), Puerto Rico (Jusino-Atresino et al., 2016) and southern United States (Bozlaker et al., 2013; Prospero, 1999; Prospero et al., 2001). This is not an unexpected result because, despite the strong influence of the marine aerosol in this region, the Saharan dust intrusions (mainly associated with the mineral fraction) are synoptic-scale events and, consequently, they can impact large regions of the Caribbean Sea and southern and eastern United States. By contrast, the concentrations of SO_4^{2-} found in Cienfuegos were considerably higher than those reported in a rural site in Puerto Rico (Jusino-Atresino et al., 2016) and similar to the values reported for Miami (Prospero, 1999). This result may be related to SO_2 emissions from local fossil fuel combustion sources using sulfur-rich oil and the subsequent secondary processes in the atmosphere. The amount of SO_4^{2-} in the air mass is expected to grow fast as a result of the conversion of SO_2 into sulphate; this conversion is faster in high UV radiation and humidity conditions (Bove et al., 2016), two typical characteristics of the Caribbean region.

3.2.2. Trace elements

The statistical summary and the inter-site Pearson correlation of the studied trace elements are shown in Table 2.3. Trace elements represented a 0.5 % (0.12 μg m^{-3}) and 0.8 % (0.28 μg m^{-3}) of the total PM_{10} mass at the rural and urban sites, respectively. Especially, those elements typically derived from non-exhaust traffic emissions, such as Cu, Ni, Cd, Ba, Pb and Mo (Grigoratos and Martini, 2015; Querol et al., 2007), were clearly higher in the urban station.

Table 2.3. Statistic summary of concentration of trace elements (ng m^{-3}) at both sampling sites. The intersite Pearson correlations (R_{IPC}) in bold represent a statistic significant at 0.01 level.

Element	Rural station (n=68)		Urban Station (n=71)		R_{IPC}
	AVE (SD)	Range	AVE (SD)	Range	
Be	0.06 (0.05)	<DL-0.17	0.05 (0.05)	<DL-0.27	**0.83**
P	20.8 (11.9)	<DL-52.8	48.4 (17.2)	13.9-114.5	**0.44**
V	6.85 (6.33)	1.28-35.99	11.34 (7.65)	1.96-38.92	**0.47**
Cr	2.72 (2.47)	<DL-12.91	2.99 (2.09)	<DL-9.45	0.20
Mn	6.14 (8.69)	<DL-44.6	11.11 (9.86)	0.24-46.7	**0.93**
Co	0.2 (0.22)	<DL-1.07	0.37 (0.23)	0.1-1.28	**0.78**
Ni	1.88 (1.63)	<DL-8.69	4.77 (7.46)	0.31-62.1	**0.39**
Cu	13.2 (19.5)	0.61-87.5	69.4 (98.8)	7.58-640.4	**0.70**
Zn	13.4 (33.5)	1.73-277	18.1 (7.8)	6.22-45.9	0.12
As	0.38 (0.31)	<DL-1.04	0.55 (0.29)	<DL-1.24	**0.72**
Se	0.58 (0.6)	<DL-1.7	0.81 (1.04)	<DL-4.32	**0.74**
Rb	0.84 (0.78)	<DL-4.24	2.44 (1.97)	0.17-10.25	**0.96**
Sr	3.24 (2.64)	0.21-14.66	6.4 (4.18)	1.17-22.2	**0.91**
Cd	0.06 (0.05)	<DL-0.22	0.15 (0.18)	<DL-1.26	0.05
Cs	0.07 (0.05)	<DL-0.27	0.09 (0.06)	<DL-0.33	**0.96**
Ba	4.55 (6.93)	<DL-27.6	11.9 (10.4)	<DL-44.3	**0.62**
Hf	0.06 (0.05)	<DL-0.24	0.11 (0.22)	<DL-1.7	0.36
Tl	0.08 (0.09)	<DL-0.32	0.08 (0.09)	<DL-0.4	0.32
Pb	1.29 (0.72)	0.11-3.22	4.32 (2.75)	1.13-17.17	**0.47**
Th	0.09 (0.15)	<DL-0.85	0.19 (0.27)	<DL-1.27	**0.51**
U	0.04 (0.05)	<DL-0.21	0.12 (0.1)	0-0.61	0.36
Ti	39.7 (60)	2.35-287.1	51.4 (65.0)	<DL-336.9	**0.98**
Ge	0.05 (0.12)	<DL-0.61	0.05 (0.09)	<DL-0.54	0.27
Zr	1.22 (2.02)	<DL-7.9	0.94 (1.42)	<DL-7.43	**0.62**
Nb	0.22 (0.38)	<DL-2.24	0.21 (0.4)	<DL-2.21	0.34
Mo	5.83 (11.9)	<DL-58.1	28.7 (20.4)	6.48-114.9	0.36
Sn	0.46 (0.41)	0.05-1.66	0.41 (0.36)	<DL-1.55	**0.77**
Sb	0.22 (0.53)	0.04-4.38	0.25 (0.14)	0.06-0.73	-0.08
W	0.1 (0.1)	<DL-0.45	0.13 (0.15)	<DL-1	0.19
Hg	0.03 (0.02)	<DL-0.14	0.04 (0.03)	0.01-0.17	0.19
Σ_{trace}(%)	124 (0.5)		276 (0.8)		

Σ_{trace} is the sum of all trace elements and the % of PM_{10} mass is given in brackets.

When studying the relation between both sites (see R_{ipc} in Table 2.3), significant correlations were found for Mn, Rb, Sr, Cs, Ti, Be, Co and Se, elements typically found in mineral matter, and Cu, As, Ba and Sn, usual components of traffic and industrial emissions (Taiwo et al., 2014). This result, therefore, confirms the expected influence of natural sources (likely related to the Saharan intrusion as we noted before) in both sites,

but, on the other hand, it appears to suggest the existence of common anthropogenic sources. This was an expected result due to the relative positions of the studied sites and the prevalent NE wind direction in the region. In the same vein, the lack of correlation for Cr, Zn, Cd, Mo, Sb and Hg seemed to indicate preeminence of local sources.

Average level of V/Ni ratio in the rural site (4.8) was higher than the average level at urban site (3.3). This could be related to the influence of different combustion sources since these elements are often used as tracers of fossil fuel combustion processes (Viana et al., 2008). For comparison, six samples of fly ash collected at the stack of the TPP, located at northern direction from both sites, were measured in this study and showed an average V/Ni ratio of 4.4 (SD=0.2), consistent with that observed at the rural site. High V/Ni values, typically ranging from 4 to 8, are characteristic of high sulphur residues from the fossil fuel combustion (Moreno et al., 2010). In contrast, several authors have reported V/Ni ratios around 3 for shipping emissions (Pandolfi et al., 2011; Viana et al., 2014), which are more consistent with that observed at the urban site. This result is probably related to the shipping emissions from the piers area located near this sampling site.

The annual mean concentrations of the trace elements As, Cd, Hg, Ni and Pb did not exceed the annual MAC set in the Cuban legislation on air quality (10, 10, 1000, 20 and 500 ng m^{-3}, respectively) at any of the two studied sites. This legislation also regulates the 24-h concentration of As, Cd, Hg, Ni, Pb, Co, Cr and Mn (20, 20, 2000, 100, 1000, 1000 and 10 000 ng m^{-3}, respectively), and all the results obtained were below the MAC in both stations. In addition, the annual concentration for V did not exceed the WHO air quality guideline value (1000 ng m^{-3}).

When comparing the results of our study with other previously carried out in Cuba, the average concentrations of V, Cr, Mn, Ni, Zn, As, Cd and Pb found in our sampling sites were lower than those reported for a traffic station in Havana (Martínez Varona et al., 2015; Pérez et al., 2009), whereas concentrations of Cu and Ti were higher in our study. With regard to values reported for other countries, most of the trace elements reported in this study were comparable to those reported for urban areas in Houston

(Bozlaker et al., 2013) and in the range of variation of rural and urban European regions (Aldabe et al., 2011; Contini et al., 2016; Fernandez-Olmo et al., 2016; Minguillon et al., 2012). Only Mo showed remarkable differences with the above regions, with higher values especially in the urban site.

3.3. Enrichment factors

The elements' EFs of both sampling sites are shown in Figure 2.3. The elements W, Cu and Mo were highly enriched at both sites except Cu which was moderately enriched at the rural site. Comparison of the EF values at the two sites indicates that Cu and Mo, widely used as tracers of road traffic, were more enriched at the urban site, thereby indicating a greater impact of road traffic at this site. The high correlation found among these elements ($r=0.85$, $p<0.01$) at the urban site, seemed to confirm the effect of traffic. The high EFs of these elements at the rural site might be due to the influence of urban background under northerly wind directions. The elements V, Ni, Tl, Sb, Hf, Zr, Ge, Ba, Sn, Cd, S, Hg, Nb, Pb and Zn were moderately enriched at both stations being likely an anthropogenic origin. Finally, Fe, Al, Ca, Mn and Co were the least enriched elements confirming their crustal origin.

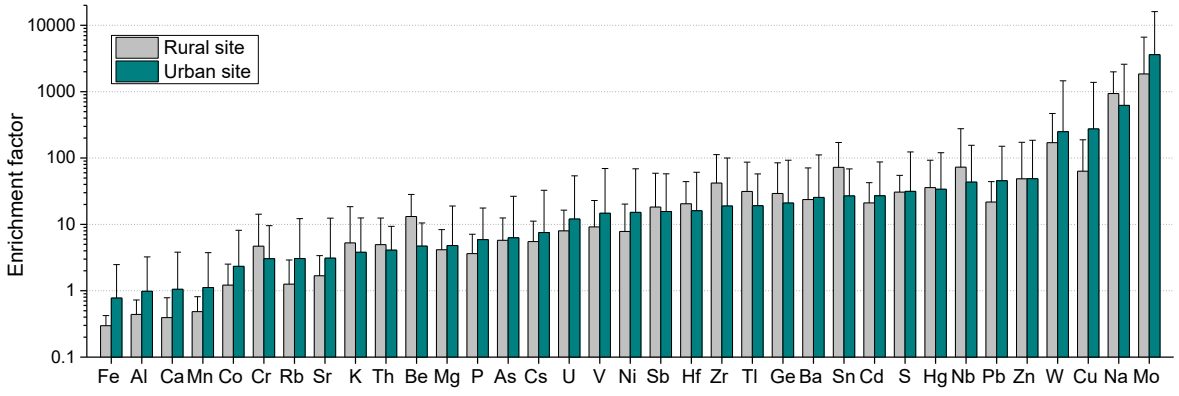

Figure 2.3. Element enrichment factors (EFs). Bars represent the 1σ standard deviation (SD).

3.4. Identification of the main sources from the PMF factors

3.4.1. Rural station

Source profiles and daily source contributions at the rural site are shown in Figure 2.4. Factor 1, characterized by high contributions of the crustal elements Al, Mn, Fe, Co and Ti, was associated with the Saharan dust intrusions. The daily PM_{10} contribution from this factor (average of 6.3 $\mu g\ m^{-3}$ for a 25.9%) was mainly produced between April and August, thereby agreeing with the Saharan dust intrusions period in our region. The highest contributions from this factor matched with the 3 PM_{10} exceedance events produced in this site, and explained more than 60% of the total PM_{10} mass obtained in those days. Similar results were observed in Houston in 2008 under Saharan dust intrusions (Bozlaker et al., 2013). The CWT plotted in Figure 2.5a confirmed the African origin of the air masses affecting the studied region during the days with the highest contributions from this factor. Factor 2 was characterized by Cl^-, Na and Mg and represents the marine aerosol contribution with a daily average of 5.1 $\mu g\ m^{-3}$ (21.1%) of PM_{10}. The CWT associated with this factor (Figure 2.5b) indicated that marine aerosol was mainly originated in the southern region of the Caribbean Sea and in the Atlantic Ocean.

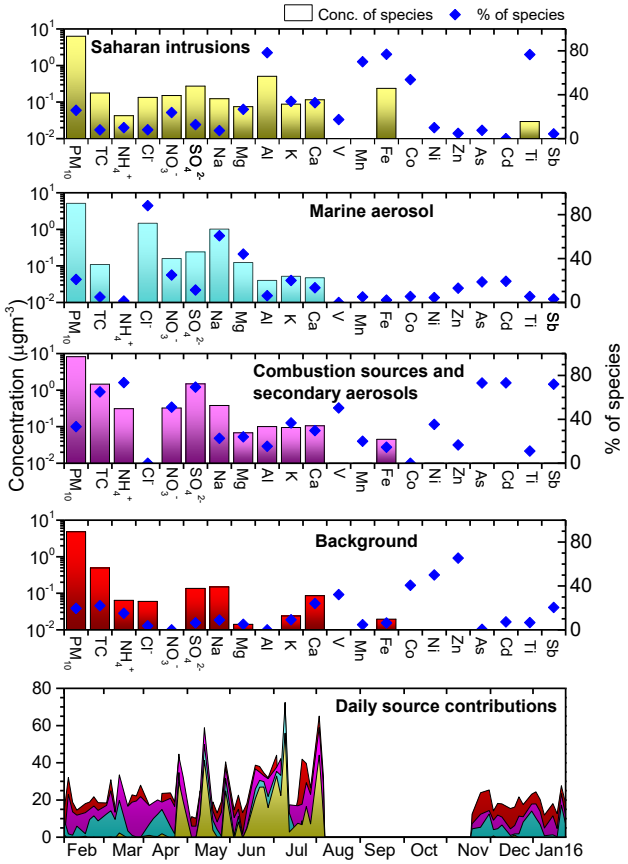

Figure 2.4. PMF factor profile and daily source contributions at the rural site.

Factor 3 was characterized by elements typically derived from combustion sources and secondary compounds, which represent a mixture of sources. In fact, this factor split into two different sources when testing the 5-factor PMF solution: one related to oil combustion (association of V, Ni, SO_4^{2-}, NH_4^+ and Sb) and the other one to wood burning (TC, NO_3^- and K). This solution was, however, discarded because it turned out to be less stable (higher uncertainties) than the 4-factor solution. Nevertheless, the origin of the contributions from this factor was later confirmed when considering two intervals of CBPF (Figure 2.6) (Uria-Tellaetxe and Carslaw, 2014). Contributions between 7.2 and 11 μg m^{-3} were observed for low wind speed and derived from sources located in the E-S sector (Figure 2.6a), reflecting the impact of local wood burning. In contrast, sources located in the sector SW-N were dominant between 11 and 22 μg m^{-3} when wind speed was higher than 10 km h^{-1} (Figure 2.6b), thereby indicating the influence of more distant sources. According to this, the potential sources were the emissions coming from the diesel power unit and diesel combustion boiler located 4 km westward and also the

emissions derived from TPP, refinery and harbour area located at northern directions. The higher contribution of SO_4^{2-} and NH_4^+ indicated the formation of secondary ammonium sulphate probably related to the primary emissions from the aforementioned sources. This factor was the most important contributor at this site with a daily average of 8.2 μg m^{-3} (33.4%) of PM_{10}.

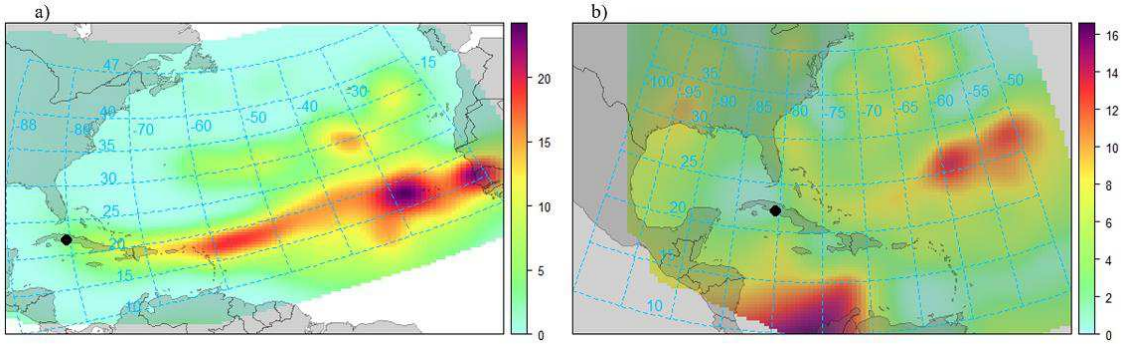

Figure 2.5. CWT of Saharan intrusions (a) and marine aerosol (b) contributions (μg m^{-3}) estimated by PMF in the studied area.

In the factor 4, Zn, V, Ni, Co, Ca and TC were dominant. V, Ni, Zn and TC are often associated with industrial and road traffic emissions while Ca and Co are crustal elements, which could be associated with activities in the cement plant and construction works. The CBPF plotted in Figure 2.6c confirmed that contributions from this factor between 4.7 and 24 μg m^{-3} were mainly derived from distant sources mainly located at NE, suggesting the influence of the urban background and cement plant emissions as potential sources in this sector. Then, we identified this factor as background with a daily average contribution of 4.8 μg m^{-3} (19.6%) of the total PM_{10} mass.

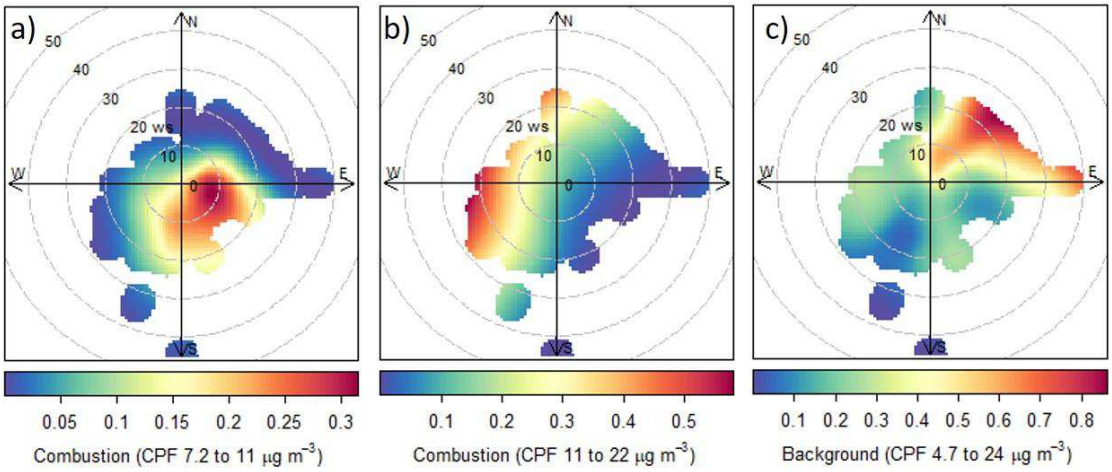

Figure 2.6. CBPF plot for different concentration intervals of Combustion (a and b) and Background (c) factor at the rural site.

3.4.2. Urban station

Source profiles and daily source contributions at the urban site are shown in Figure 2.7. Factor 1, characterized by high contributions of the crustal elements Al, Mn, Fe, Co, Ba and Ti, was identified as Sahara intrusions. The daily contribution was similar to that observed in the rural site and its maximum values explained 7 of the 8 PM_{10} exceedances observed in this site (except the event produced on 26/03/2015). This factor contributed with a daily average of 9.2 μg m^{-3} (26.3%) to the total PM_{10}. Factor 2, accounting for a 12.5% (4.3 μg m^{-3}) of the PM_{10}, was characterized by Cl^-, Na and Mg and represented the marine aerosol. Contribution from this factor was lower than that obtained for the rural site as the discussed in the section 3.2.

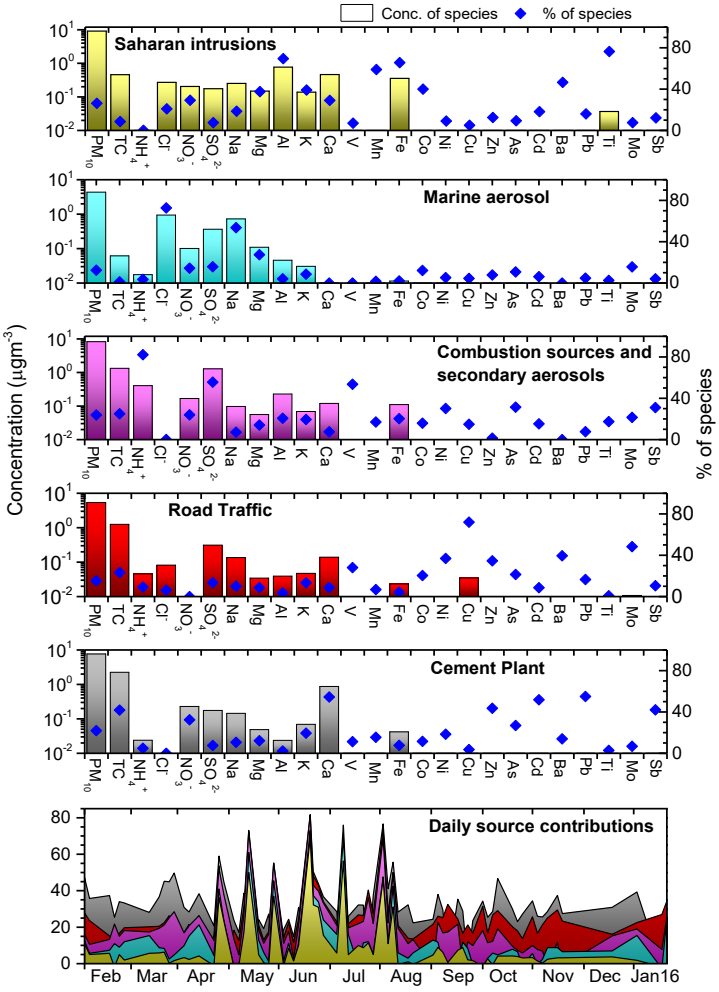

Figure 2.7. PMF factor profile and daily source contributions at urban site.

The Factor 3 was dominated by SO_4^{2-}, NH_4^+ and V with important contributions of Ni, As and Sb, elements commonly associated with secondary processes and oil combustion (Cesari et al., 2014; Querol et al., 2007). According to the CBPF (Figure 2.8a) the contributions of this factor between 7.3 and 24 μg m^{-3} were associated with sources located in the sectors N – W and W – S. It suggested the influence of emissions coming from the TPP located 2.5 km to the N, the harbour and other industries located 3 km to the NNW, and the influence of the shipping emissions produced in the piers area located at southern directions. The daily average contribution from this factor was the second most important with 8.3 μg m^{-3} (23.8%) of PM_{10}. The Factor 4 was strongly characterized by Cu, Mo, Ba, Zn, Ni and V, elements typically attributed to road traffic (Grigoratos and Martini, 2015; Querol et al., 2007), and represented the 15.4% (5.4 μg m^{-3}) of the PM_{10} at urban site. The CBPF (Figure 2.8b) clearly showed that higher contributions (8.8 – 19.0

μg m^{-3}) from this factor came mainly from the urban sector, where the road traffic is concentrated.

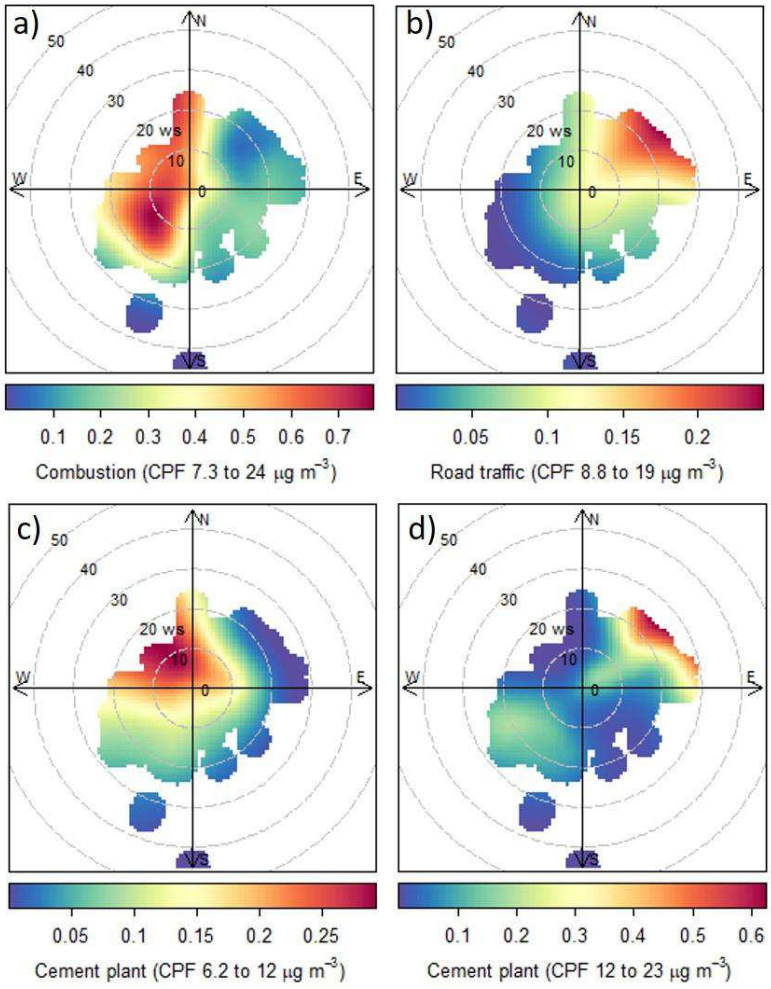

Figure 2.8. CBPF plot for different concentration intervals of Combustion (a), Road traffic (b) and Cement plant (c and d) factor at the urban site.

The last factor (Factor 5), which accounted for 21.9% (7.6 μg m^{-3}) of the total PM_{10} mass, was explained by high contributions of Ca, Pb, Cd, TC, Sb, Zn and NO_3^-. The CBPF plotted by intervals allowed us to identify 2 different sectors associated with this factor. The higher contributions (12 to 23 μg m^{-3}) were linked to sources located in the NE – E sector for wind speeds >20 km h^{-1}, pointing to the cement plant and quarries as potential sources (Figure 2.8d). The intermediate contributions (6.2 to 12 μg m^{-3}), by contrast, were associated with sources located in the N – W sector for low wind speeds (Figure 2.8c). The potential sources here could be the emissions related to the Cienfuegos harbour, where the main loading and unloading activities of the raw materials for the

cement plant (kilns, petroleum coke, among others) and the cement produced in the factory are carried out. Therefore, we identified this factor as cement plant. Contributions from Factor 5 and Factor 3 (combustion) explained 92% of the PM_{10} mass observed on 26/03/2015, when the other PM_{10} exceedance event occurred.

4. Conclusions

A PM_{10} monitoring survey was simultaneously performed in a rural and urban Caribbean coastal site in Cuba between 31/01/2015 and 20/01/2016. PM_{10} concentrations varied similarly at the two sampling sites and were mainly governed by a strong influence of the Saharan dust during the months from March to August when the highest PM_{10} concentrations were observed in both sites; however, significantly higher levels were generally observed at the urban station due to the influence of local sources. The MAC of PM_{10} established in the Cuban legislation for air quality was exceeded 3 and 8 times during the study in the rural and urban site, respectively. The annual limit established in this legislation was only exceeded in the urban site, although in the rural site it still exceeded the annual PM_{10} value recommended by WHO.

Concentrations of all major elements were higher in the urban site except for Na and Cl^-, therefore indicating a major marine influence at the rural site. In general, the mineral matter was the dominant fraction at both sites due to the regional influence produced by the Sahara dust intrusions. Meanwhile, concentrations of Ca and TC were significantly higher at the urban site because of the contributions from local sources such as the cement plant and quarries, and road traffic. In addition, an important contribution of TC was also observed at the rural site due to the influence of wood burning. Levels of $nmSO_4^{2-}$, NH_4^+ and NO_3^- were slightly higher at urban sites with a clear tendency to formation of ammonium sulfate at both sites.

Concentration of trace elements typically derived from traffic and industrial emissions, such as Cu, Ni, Cd, Ba, Pb and Mo were higher in the urban area, but were found to be significantly enriched at both sites, thereby indicating the anthropogenic origin of these elements in both stations. W, Cu and Mo were the most enriched

elements at the urban site and appear to be excellent tracers of the urban traffic emissions. The V/Ni ratios were different at the rural (4.8) and urban site (3.3) and seem to be mainly affected by the power plant and shipping emissions, respectively. The concentration of trace elements regulated in the national legislation for air quality was found to be below the MAC during the entire study period at both sites.

At the rural site 4 principal sources were identified: Saharan intrusions, marine, combustion (mainly related with emission from TPP and wood burning) and a background source representing the contribution from urban background (mainly urban traffic) and cement plant, while 5 principal sources were identified at the urban site: Saharan intrusions, marine, combustion (mainly related with shipping and industrial emissions), traffic and cement plant. Saharan dust contribution was quantified for the first time in Cuba, proving to be one of the most significant PM_{10} sources in the studied region. This contribution explained 10 of the 11 PM_{10} exceedances events observed during the study. This result confirms the scale and relevance of the long-range transport in our region; however, attention must be paid to the identified anthropogenic local sources since they represented, on average, more than 50% of the total PM_{10} recorded in the study area.

The exhaustive PM_{10} chemical composition data presented here represent the most complete report on PM in Cuba and provide the basis for environmental managers to adopt control strategies to reduce the impact of PM_{10} pollution in the studied region.

Acknowledgements

The research leading to these results has received funding from "la Caixa" Banking Foundation. This study was also supported by the IAEA TC Project CUB/7/008 “Strengthening the National System for Analysis of the Risks and Vulnerability of Cuba’s Coastal Zone Through the Application of Nuclear and Isotopic Techniques” and National Program PNUOLU /4-1/ 2 No. /2014 of the National Nuclear Agency. The authors express their gratitude to the analytical staff of the Laboratorio Integrado de Calidad Ambiental (LICA) of the University of Navarra and Centro de Estudios Ambientales de Cienfuegos (CEAC) for its assistance.

References

Aldabe, J., Elustondo, D., Santamaria, C., Lasheras, E., Pandolfi, M., Alastuey, A., Querol, X., Santamaria, J.M., 2011. Chemical characterisation and source apportionment of PM2.5 and PM10 at rural, urban and traffic sites in Navarra (North of Spain). Atmospheric Res. 102, 191–205. https://doi.org/10.1016/j.atmosres.2011.07.003

Aldabe, J., Santamaría, C., Elustondo, D., Lasheras, E., Santamaría, J.M., 2013. Application of microwave digestion and ICP-MS to simultaneous analysis of major and trace elements in aerosol samples collected on quartz filters. Anal. Methods 5, 554–559. https://doi.org/10.1039/c2ay25724f

Amato, F., Pandolfi, M., Escrig, A., Querol, X., Alastuey, A., Pey, J., Perez, N., Hopke, P.K., 2009. Quantifying road dust resuspension in urban environment by Multilinear Engine: A comparison with PMF2. Atmos. Environ. 43, 2770–2780. https://doi.org/10.1016/j.atmosenv.2009.02.039

Ancelet, T., Davy, P.K., Trompetter, W.J., Markwitz, A., Weatherburn, D.C., 2014. Particulate matter sources on an hourly timescale in a rural community during the winter. J. Air Waste Manag. Assoc. 64, 501–508. https://doi.org/10.1080/10962247.2013.813414

Arruti, A., Fernández-Olmo, I., Irabien, A., 2011. Regional evaluation of particulate matter composition in an Atlantic coastal area (Cantabria region, northern Spain): Spatial variations in different urban and rural environments. Atmospheric Res. 101, 280–293. https://doi.org/10.1016/j.atmosres.2011.03.001

Barja, B., Mogo, S., Cachorro, V.E., Carlos Antuna, J., Estevan, R., Rodrigues, A., de Frutos, A., 2013. Atmospheric particulate matter levels, chemical composition and optical absorbing properties in Camaguey, Cuba. Environ. Sci.-Process. Impacts 15, 440–453. https://doi.org/10.1039/c2em30854a

Boman, J., Gaita, S.M., 2015. Mass, black carbon and elemental composition of PM2.5 at an industrial site in Kingston, Jamaica. Nucl. Instrum. Methods Phys. Res. Sect. B-Beam Interact. Mater. At. 363, 131–134. https://doi.org/10.1016/j.nimb.2015.08.068

Bove, M.C., Brotto, P., Calzolai, G., Cassola, F., Cavalli, F., Fermo, P., Hjorth, J., Massabò, D., Nava, S., Piazzalunga, A., Schembari, C., Prati, P., 2016. PM10 source apportionment applying PMF and chemical tracer analysis to ship-borne measurements in the Western Mediterranean. Atmos. Environ. 125, 140–151. https://doi.org/10.1016/j.atmosenv.2015.11.009

Bozlaker, A., Prospero, J.M., Fraser, M.P., Chellam, S., 2013. Quantifying the Contribution of Long-Range Saharan Dust Transport on Particulate Matter Concentrations in Houston, Texas, Using Detailed Elemental Analysis. Environ. Sci. Technol. 47, 10179–10187. https://doi.org/10.1021/es4015663

Brown, S.G., Eberly, S., Paatero, P., Norris, G.A., 2015. Methods for estimating uncertainty in PMF solutions: Examples with ambient air and water quality data and guidance on reporting PMF results. Sci. Total Environ. 518, 626–635. https://doi.org/10.1016/j.scitotenv.2015.01.022

Carslaw, D.C., 2015. The Openair Manual — Open-source Tools for Analysing Air Pollution Data. Manual for version 1.1-4.

Cesari, D., Donateo, A., Conte, M., Merico, E., Giangreco, A., Giangreco, F., Contini, D., 2016. An inter-comparison of PM2.5 at urban and urban background sites: Chemical characterization and source apportionment. Atmospheric Res. 174, 106–119. https://doi.org/10.1016/j.atmosres.2016.02.004

Cesari, D., Genga, A., Ielpo, P., Siciliano, M., Mascolo, G., Grasso, F.M., Contini, D., 2014. Source apportionment of PM2.5 in the harbour-industrial area of Brindisi (Italy): Identification and estimation of the contribution of in-port ship emissions. Sci. Total Environ. 497, 392–400. https://doi.org/10.1016/j.scitotenv.2014.08.007

Cheng, I., Zhang, L., Blanchard, P., Dalziel, J., Tordon, R., 2013. Concentration-weighted trajectory approach to identifying potential sources of speciated atmospheric mercury at an urban coastal site in Nova Scotia, Canada. Atmospheric Chem. Phys. 13, 6031–6048. https://doi.org/10.5194/acp-13-6031-2013

Contini, D., Cesari, D., Conte, M., Donateo, A., 2016. Application of PMF and CMB receptor models for the evaluation of the contribution of a large coal-fired power plant to PM10 concentrations. Sci. Total Environ. 560, 131–140. https://doi.org/10.1016/j.scitotenv.2016.04.031

Cuesta-Santos, O., Wallo Vázquez, A., Collazo Aranda, A., Sánchez Navarro, P., González González, M., Labrador Montero, R., 2002. Aspectos de la composicion quimica del aire en la zona de la ribera este de la bahia de la Habana. Rev. Cuabana Meteorol. 9, 90–99.

Draxler, R.R., Rolph, G.D., 2015. HYSPLIT (HYbrid Single-Particle Lagrangian Integrated Trajectory) Model access via NOAA ARL READY Website (http://www.arl.noaa.gov/HYSPLIT.php). NOAA Air Resources Laboratory, College Park, MD.

Fernandez-Olmo, I., Andecochea, C., Ruiz, S., Antonio Fernandez-Ferreras, J., Irabien, A., 2016. Local source identification of trace metals in urban/industrial mixed land-use areas with daily PM10 limit value exceedances. Atmospheric Res. 171, 92–106. https://doi.org/10.1016/j.atmosres.2015.12.010

Fernandez-Olmo, I., Puente, M., Irabien, A., 2015. A comparative study between the fluxes of trace elements in bulk atmospheric deposition at industrial, urban, traffic, and rural sites. Environ. Sci. Pollut. Res. 22, 13427–13441. https://doi.org/10.1007/s11356-015-4562-z

Grantz, D.A., Garner, J.H.B., Johnson, D.W., 2003. Ecological effects of particulate matter. Environ. Int. 29, 213–239. https://doi.org/10.1016/S0160-4120(02)00181-2

Grigoratos, T., Martini, G., 2015. Brake wear particle emissions: a review. Environ. Sci. Pollut. Res. 22, 2491–2504. https://doi.org/10.1007/s11356-014-3696-8

Heo, J.-B., Hopke, P.K., Yi, S.-M., 2009. Source apportionment of PM2.5 in Seoul, Korea. Atmospheric Chem. Phys. 9, 4957–4971.

Hsu, Y.K., Holsen, T.M., Hopke, P.K., 2003. Comparison of hybrid receptor models to locate PCB sources in Chicago. Atmos. Environ. 37, 545–562. https://doi.org/10.1016/S1352-2310(02)00886-5

Jusino-Atresino, R., Anderson, J., Gao, Y., 2016. Ionic and elemental composition of PM2.5 aerosols over the Caribbean Sea in the Tropical Atlantic. J. Atmospheric Chem. 73, 427–457. https://doi.org/10.1007/s10874-016-9337-5

Kanakidou, M., Seinfeld, J.H., Pandis, S.N., Barnes, I., Dentener, F.J., Facchini, M.C., Van Dingenen, R., Ervens, B., Nenes, A., Nielsen, C.J., Swietlicki, E., Putaud, J.P., Balkanski, Y., Fuzzi, S., Horth, J., Moortgat, G.K., Winterhalter, R., Myhre, C.E.L., Tsigaridis, K., Vignati, E., Stephanou, E.G., Wilson, J., 2005. Organic aerosol and global climate modelling: a review. Atmos Chem Phys 5, 1053–1123. https://doi.org/10.5194/acp-5-1053-2005

Kim, B.M., Lee, S.-B., Kim, J.Y., Kim, S., Seo, J., Bae, G.-N., Lee, J.Y., 2016. A multivariate receptor modeling study of air-borne particulate PAHs: Regional contributions in a roadside environment. Chemosphere 144, 1270–1279. https://doi.org/10.1016/j.chemosphere.2015.09.087

Kim, E., Hopke, P.K., 2005. Identification of fine particle sources in mid-Atlantic US area. Water. Air. Soil Pollut. 168, 391–421. https://doi.org/10.1007/s11270-005-1894-1

Kim, E., Hopke, P.K., Edgerton, E.S., 2003. Source identification of Atlanta aerosol by positive matrix factorization. J. Air Waste Manag. Assoc. 53, 731–739.

Li, C., Kang, S., Zhang, Q., 2009. Elemental composition of Tibetan Plateau top soils and its effect on evaluating atmospheric pollution transport. Environ. Pollut. 157, 2261–2265. https://doi.org/10.1016/j.envpol.2009.03.035

Martínez Varona, M., Guzmán Vila, M., Pérez Cabrera, A., Fernández Arocha, A., 2015. Presencia de metales pesados en material particulado en aire. Estación de monitoreo INHEM, Centro Habana. Ecosolar 52.

Martínez Varona, M., Molina Esquivel, E., Maldonado Cantillo, G., Guzmán Vila, M., Alonso, D., 2013. Comportamiento de partículas menores de 10 micras mediante dos equipos de monitoreo. Hig. Sanid. Ambient. 13, 1060–1065.

Minguillon, M.C., Querol, X., Baltensperger, U., Prevot, A.S.H., 2012. Fine and coarse PM composition and sources in rural and urban sites in Switzerland: Local or regional pollution? Sci. Total Environ. 427, 191–202. https://doi.org/10.1016/j.scitotenv.2012.04.030

Mojena López, E., Ortega González, A., Casilles Vega, E.F., Leyva Santos, J., 2015. Sahara Clouds Dust. Their presence in Cuba. Rev. Cuabana Meteorol. 21, 120–134.

Molina Esquivel, E., Pérez Zayas, G., Martínez Varona, M., Aldape Ugalde, F., Flores Maldonado, J., 2011. Comportamiento de las fracciones fina y gruesa de PM10 en la estación de monitoreo de calidad del aire en Centro Habana. Campaña 2006-2007. Hig. Sanid. Ambient. 11, 820–826.

Moreno, T., Querol, X., Alastuey, A., de la Rosa, J., Sánchez de la Campa, A.M., Minguillón, M., Pandolfi, M., González-Castanedo, Y., Monfort, E., Gibbons, W., 2010. Variations in vanadium, nickel and lanthanoid element concentrations in urban air. Sci. Total Environ. 408, 4569–4579. https://doi.org/10.1016/j.scitotenv.2010.06.016

NC 1020, 2014. Norma Cubana 1020:2014. CALIDAD DEL AIRE — CONTAMINANTES — CONCENTRACIONES MÁXIMAS ADMISIBLES Y VALORES GUÍAS EN ZONAS HABITABLES.

Norris, G., Duvall, R., Brown, S., Bai, S., 2014. EPA Positive Matrix Factorization (PMF) 5.0 Fundamentals and User Guide. U.S. Environmental Protection Agency National Exposure Research Laboratory, Sonoma Technology, Inc.

Paatero, P., 1997. Least squares formulation of robust non-negative factor analysis. Chemom. Intell. Lab. Syst. 37, 23–35. https://doi.org/10.1016/S0169-7439(96)00044-5

Paatero, P., Eberly, S., Brown, S.G., Norris, G.A., 2014. Methods for estimating uncertainty in factor analytic solutions. Atmos Meas Tech 7, 781–797. https://doi.org/10.5194/amt-7-781-2014

Paatero, P., Tapper, U., 1994. Positive matrix factorization: A non-negative factor model with optimal utilization of error estimates of data values. Environmetrics 5, 111–126. https://doi.org/10.1002/env.3170050203

Pandolfi, M., Gonzalez-Castanedo, Y., Alastuey, A., de la Rosa, J.D., Mantilla, E., de la Campa, A.S., Querol, X., Pey, J., Amato, F., Moreno, T., 2011. Source apportionment of PM10 and PM2.5 at multiple sites in the strait of Gibraltar by PMF: impact of shipping emissions. Environ. Sci. Pollut. Res. 18, 260–269. https://doi.org/10.1007/s11356-010-0373-4

Pérez, G., Piñera, I., Aldape, F., Flores, J.M., Martínez, M., Molina, E., Fernández, A., Ramos, M., Guibert, R., 2009. First study of airborne particulate pollution using pixe analysis in Havana city, Cuba. Int. J. PIXE 19, 157–166. https://doi.org/10.1142/S0129083509001849

Piñera, I., Pérez, G., Aldape, F., Flores, J.M., Molina, E., Ramos, M., Martínez, M., Guibert, R., 2010. Estudio de Partículas Finas de la Atmósfera en Centro Habana. Contrib Educ Prot Med Amb 9, E39–E47.

Pope, C.A., Dockery, D.W., 2006. Health effects of fine particulate air pollution: Lines that connect. J. Air Waste Manag. Assoc. 56, 709–742.

Prospero, J.M., 1999. Long-term measurements of the transport of African mineral dust to the southeastern United States: Implications for regional air quality. J. Geophys. Res.-Atmospheres 104, 15917–15927. https://doi.org/10.1029/1999JD900072

Prospero, J.M., Collard, F.-X., Molinie, J., Jeannot, A., 2014. Characterizing the annual cycle of African dust transport to the Caribbean Basin and South America and its impact on the environment and air quality. Glob. Biogeochem. Cycles 28, 757–773. https://doi.org/10.1002/2013GB004802

Prospero, J.M., Mayol-Bracero, O.L., 2013. Understanding the Transport and Impact of African Dust on the Caribbean Basin. Bull. Am. Meteorol. Soc. 94, 1329–1337. https://doi.org/10.1175/BAMS-D-12-00142.1

Prospero, J.M., Olmez, I., Ames, M., 2001. Al and Fe in PM 2.5 and PM 10 Suspended Particles in South-Central Florida: The Impact of the Long Range Transport of African Mineral Dust. Water. Air. Soil Pollut. 125, 291–317. https://doi.org/10.1023/A:1005277214288

Querol, X., Alastuey, A., Rodriguez, S., Viana, M.M., Artinano, B., Salvador, P., Mantilla, E., do Santos, S.G., Patier, R.F., de La Rosa, J., de la Campa, A.S., Menendez, M., Gil, J.J., 2004. Levels of particulate matter in rural, urban and industrial sites in Spain. Sci. Total Environ. 334, 359–376. https://doi.org/10.1016/j.scitotenv.2004.04.036

Querol, X., Viana, M., Alastuey, A., Amato, F., Moreno, T., Castillo, S., Pey, J., de la Rosa, J., Sánchez de la Campa, A., Artíñano, B., Salvador, P., García Dos Santos, S., Fernández-Patier, R., Moreno-Grau, S., Negral, L., Minguillón, M.C., Monfort, E., Gil, J.I., Inza, A., Ortega, L.A., Santamaría, J.M., Zabalza, J., 2007. Source origin of trace elements in PM from regional background, urban and industrial sites of Spain. Atmos. Environ. 41, 7219–7231. https://doi.org/10.1016/j.atmosenv.2007.05.022

Rodriguez, S., Cuevas, E., Prospero, J.M., Alastuey, A., Querol, X., Lopez-Solano, J., Garcia, M.I., Alonso-Perez, S., 2015. Modulation of Saharan dust export by the North African dipole. Atmospheric Chem. Phys. 15, 7471–7486. https://doi.org/10.5194/acp-15-7471-2015

Sanchez de la Campa, A.M., de la Rosa, J., Querol, X., Alastuey, A., Mantilla, E., 2007. Geochemistry and origin of PM10 in the Huelva region, Southwestern Spain. Environ. Res. 103, 305–316. https://doi.org/10.1016/j.envres.2006.06.011

Squizzato, S., Cazzaro, M., Innocente, E., Visin, F., Hopke, P.K., Rampazzo, G., 2017. Urban air quality in a mid-size city - PM2.5 composition, sources and identification of impact areas: From local to long range contributions. Atmospheric Res. 186, 51–62. https://doi.org/10.1016/j.atmosres.2016.11.011

Taiwo, A.M., Harrison, R.M., Shi, Z., 2014. A review of receptor modelling of industrially emitted particulate matter. Atmos. Environ. 97, 109–120. https://doi.org/10.1016/j.atmosenv.2014.07.051

Uria-Tellaetxe, I., Carslaw, D.C., 2014. Conditional bivariate probability function for source identification. Environ. Model. Softw. 59, 1–9. https://doi.org/10.1016/j.envsoft.2014.05.002

Viana, M., Hammingh, P., Colette, A., Querol, X., Degraeuwe, B., Vlieger, I. de, van Aardenne, J., 2014. Impact of maritime transport emissions on coastal air quality in Europe. Atmos. Environ. 90, 96–105. https://doi.org/10.1016/j.atmosenv.2014.03.046

Viana, M., Kuhlbusch, T. a. J., Querol, X., Alastuey, A., Harrison, R.M., Hopke, P.K., Winiwarter, W., Vallius, A., Szidat, S., Prevot, A.S.H., Hueglin, C., Bloemen, H., Wahlin, P., Vecchi, R., Miranda, A.I., Kasper-Giebl, A., Maenhaut, W., Hitzenberger, R., 2008. Source apportionment of particulate matter in Europe: A review of methods and results. J. Aerosol Sci. 39, 827–849. https://doi.org/10.1016/j.jaerosci.2008.05.007

Vossler, T., Cernikovsky, L., Novak, J., Williams, R., 2016. Source apportionment with uncertainty estimates of fine particulate matter in Ostrava, Czech Republic using Positive Matrix Factorization. Atmospheric Pollut. Res. 7, 503–512. https://doi.org/10.1016/j.apr.2015.12.004

WHO, 2016. WHO | WHO releases country estimates on air pollution exposure and health impact [WWW Document]. WHO. URL http://www.who.int/mediacentre/news/releases/2016/air-pollution-estimates/en/ (accessed 3.21.17).

WHO, 2005. WHO | Air quality guidelines for particulate matter, ozone, nitrogen dioxide and sulfur dioxide- global update 2005 [WWW Document]. WHO. URL http://www.who.int/phe/health_topics/outdoorair/outdoorair_aqg/en/ (accessed 3.6.16).

Chapter 3

Lanthanoid elements as geochemical tracers of atmospheric aerosol in a Caribbean region

This chapter reproduces the text of the following manuscript:

Morera-Gómez, Y., Alonso-Hernandez, C.M., Lasheras, E., Santamaría, J.M., Elustondo, D., 2018. Lanthanoid elements as geochemical tracers of atmospheric aerosol in a Caribbean region. Submitted to Chemosphere.

Abstract

This study investigates the content, pattern and sources of lanthanoid elements (La to Lu) in PM_{10} to better understand the atmospheric pollution dynamics in a Caribbean region. The PM_{10} sampling was simultaneously conducted at a rural and an urban site in Cienfuegos, Cuba. Concentrations of total lanthanoid elements were in the range <0.01–13.4 ng m^{-3} and 0.51–18.8 ng m^{-3} at the rural and urban sites, respectively, showing a similar temporal distribution. The highest concentrations, observed between April and August in both sites, showed a clear linear relationship with the PM_{10} mass. This result was attributed to the Saharan dust intrusions events that occurred during this period, as illustrated by concentration-weighted trajectory plots and LaCeSm triangular diagrams. The large fractionation of La/Ce and La/Sm ratios as well as the higher enrichment factors of heavier lanthanoids, evidenced the influence of anthropogenic sources, especially in the period with lowest concentration. Most samples showed low La/V values <0.1 in both sampling sites, suggesting the dominant influence of fuel oil and petroleum-coke combustion sources rather than refinery emissions. This hypothesis was investigated using LaCeV triangular diagrams, which confirmed that both sites were affected by similar sources, consisting in a mixture of crustal matter (driven by Saharan dust and local soils), oil combustion (power plant and shipping emissions), petroleum-coke combustion (cement plant) and urban road traffic, but not by emissions from the refinery located nearby. Finally, the application of the conditional probability function identified these sources in accordance with their contribution to the total content of lanthanoid elements.

Keywords: PM_{10}; lanthanoid elements; Sahara dust; fossil fuel combustion; Cuba

1. Introduction

The studies on source apportionment and environmental assessment of PM (specially PM_{10} and $PM_{2.5}$) have received increasing attention in the last two decades due to their known negative effects on human health (Pope and Dockery, 2006; WHO, 2016), visibility (Kanakidou et al., 2005), climate (Pöschl, 2005) and ecosystems (Grantz et al., 2003). Composition of PM is very complex and distinctly associated with different sources, so their chemical components can be used for identifying emission sources. Trace metals, PM_{10} and $PM_{2.5}$, despite accounting for only 10% of the total mass of particles, have been widely used for the identification of sources since most of ionic components, carbon and major crustal elements are present in most of common sources. In this regard, the use of some trace metals like lanthanoid elements (La to Lu, (Moreno et al., 2008a)) has proved to be a suitable tool to accurately identify PM sources, although their use have been fairly limited because of analytical limitations (Wang and Liang, 2014). Thus, the study of the geochemistry of lanthanoid elements in air can help understand the sources of atmospheric pollution (Hsu et al., 2016; Kulkarni et al., 2006; Moreno et al., 2008b).

Lanthanoid elements form a coherent group of elements with similar chemical properties that are often found together in mineral deposits. Although the concentration and fractionation of lanthanoids have been widely used to investigate geochemical processes in the lithosphere and hydrosphere, little attention has been paid to the analysis of their chemical signature in atmospheric particles.

Nevertheless, patterns of lanthanoids have been used to confirm the regions of origin of aerosols collected on the Tibetan Plateau (Li et al., 2009), the sources of dust deposited near Beijing (Tang et al., 2013) and the transportation process involving Sahara dust in the Mediterranean and Caribbean areas (Moreno et al., 2006; Pourmand et al., 2014). Moreover, La/Sm/Ce/V ratios have been used to identify emissions from oil refineries using zeolitic fluid catalytic converters (FCC) due to they are typically enriched in La (Kulkarni et al., 2007, 2006). All these evidences have been confirmed by source apportionment modelling (Bozlaker et al., 2013; Kulkarni et al., 2007, 2006), air mass classifications derived from air mass back trajectories (Moreno et al., 2008a) and

non-parametric wind regression (Du and Turner, 2015). Other studies have also identified additional anthropogenic sources of lanthanoid elements in air, here including emissions from power stations (Kitto et al., 1992), manufacture and use of fertilizers (Wen et al., 2001), fugitive dusts from mines (Dolgopolova et al., 2006; Wang and Liang, 2014), steelworks emissions (Geagea et al., 2007) and the use of catalytic converters in road traffic (Huang et al., 1994; Kulkarni et al., 2006). As these studies showed, concentrations of lanthanoids elements in the atmosphere are typically dominated by emissions from natural sources such as resuspended crustal material, but anthropogenic processes, including the motor vehicle emissions, oil combustion, and refinery activities, can be significant contributors.

The aforementioned studies reveal the growing interest in the use of lanthanoid elements to track both natural and anthropogenic emissions impact. But, in spite of that, published information on the concentration of lanthanoids and their distribution pattern in atmospheric PM is still fairly limited in small and poorly industrialized urban regions and, especially, in rural areas.

This study aims 1) to analyze the content and pattern of lanthanoid constituents in PM_{10} in a rural and an urban region of Cuba and 2) to identify the possible sources of lanthanoids-bearing PM_{10} in order to better understand the aerosol properties and the processes that pollutants undergo in the atmosphere. To that end, we employed multiple approaches, which included the analysis of the lanthanoid fractionations and enrichment factors (EFs) and the application of the conditional bivariate probability function (CBPF) and concentration-weighted trajectory (CWT) coupled with the lanthanoid elements concentrations data.

2. Materials and methods

2.1. Site description and sampling

Cienfuegos is currently an important tourist and industrial area of Cuba, activities that are mainly distributed around its Bay. The climate in the region is tropical with two

clearly defined seasons: wet (approximately from May to October) and dry (approximately from November to April). The most frequent wind direction is NE. The main potential sources of contamination in the area are: a thermal power plant (TPP), a refinery and a cement plant (see Figure 3.1 for more details). Included in the studied area are also relevant the quarries related to cement plant activities, the Cienfuegos Harbour, the maritime traffic in the Bay, the road traffic in the Cienfuegos city and other industrial areas on the northern outskirts of the city.

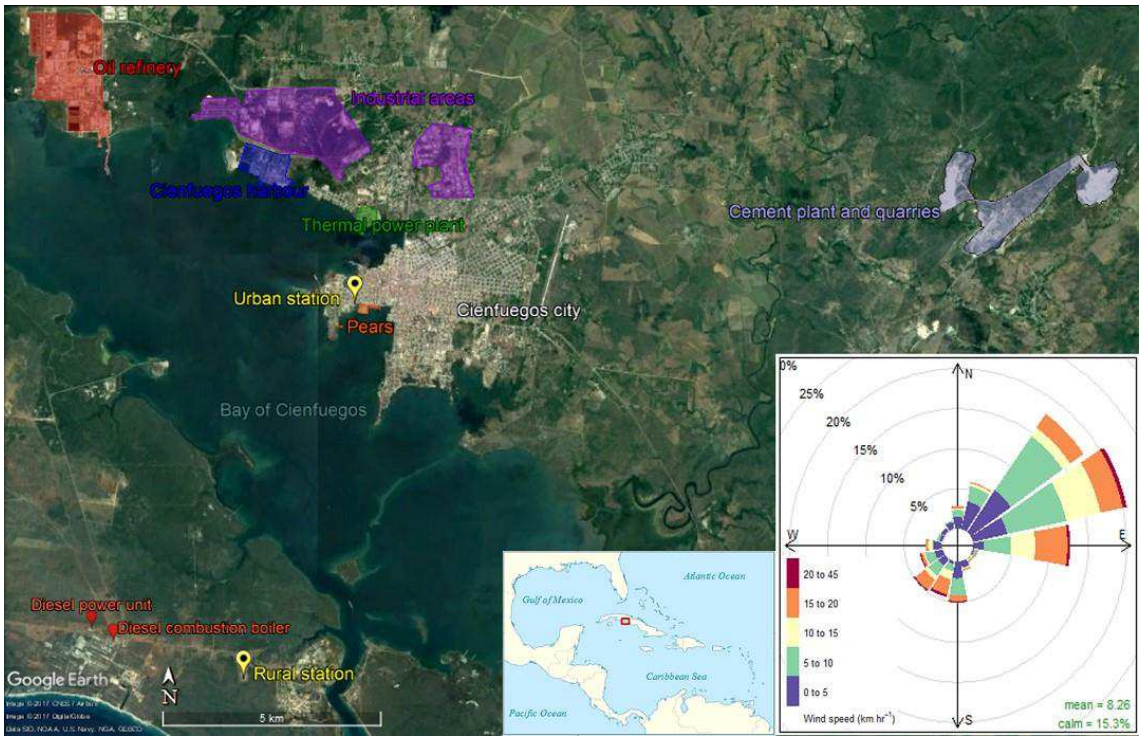

Figure 3.1. Area of study and sampling sites.

Sampling of PM_{10} was simultaneously carried out between 31/01/2015 and 20/01/2016 at two stations (rural and urban sites) located in the municipality of Cienfuegos, in the central south coast of Cuba (see Figure 3.1). The rural station (22˚ 03' 55'' N, 80˚ 28' 58'' W) is located at the main facilities of the Centre for Environmental Studies (CEAC), and the urban station is located at the CEAC facilities in the Cienfuegos city (22˚ 08' 32'' N, 80˚ 27' 29'' W).

Samples were obtained using gravimetric PM_{10} high-volume samplers operating at a flow rate of 30 m^3 h^{-1} on pre-combusted (4h at 550 ˚C) quartz micro-fiber filters (Munktell, 150 mm diameter). 24 h-samples were collected every three days in order to

obtain a sufficient number of samples for every day of the week. A total amount of 68 and 71 PM_{10} samples were collected at rural and urban stations, respectively. Due to a technical problem with the high-volume sampler located in the rural station, between 5/08/2015 and 12/11/2015 samples could not be collected.

For comparison purposes, several samples from potential sources were collected and analysed: fly ash from the stacks of the TPP (6 samples), petroleum-coke burned in the cement plant (1), local soils (16) and road dust from the main roads of the Cienfuegos city (31). Likewise, an annual sample of bulk atmospheric deposition from the vicinity of the cement plant was also taken.

2.2. Chemical analysis

Analysis of the lanthanoid elements in PM_{10} was performed using the method described by Aldabe et al., (2013, 2011). Firstly, a quarter of each filter was digested in Teflon tubes by adding HF, H_2O_2, HNO_3 and HCl (3:3:4:1 mL) in a closed microwave system. A multi-elemental solution (Li, Sc, Y, In and Bi) was added as internal standard for further determination by ICP-MS. At the same time, several filter blanks were analyzed and later subtracted from the sample concentrations. This method allows the simultaneous analysis of major and trace elements (including lanthanoid elements) by inductively coupled plasma mass spectrometry (ICP-MS). The PM_{10} and most of major and trace element data (including V data used in this study) are reported in a paper recently submitted (Morera-Gómez et al., 2018). In this article, we focus on the lanthanoid elements geochemistry.

For the analysis of the samples from potential sources of contamination the same methodology was applied, but using 50 mg of sample.

The quality control of the analytical procedure was carried out by repeated analysis of the standard reference material CTA-FFA1 (fine fly ash). Table 3.1 shows the measured lanthanoid elements together with their recoveries, relative standard deviation (RSD), the average of the filter blanks contribution evaluated and subtracted from the results, the method detection limits (DLs) and the percentages of values below

the detection limit (BDL). The obtained recoveries (75 – 85%) and DLs (1 – 10 pg m^{-3}) were similar to those reported in the literature (Celo et al., 2012; Du and Turner, 2015)

Table 3.1. Recoveries (%) and relative standard deviation (RSD in %) obtained from the SRM CTA-FFA1, average contribution of the filter blanks (ng m^{-3}), method detection limit (DL, ng m^{-3}) and percentages of values below the detection limit (BDL).

Elements	Recovery	RSD	Filter blank	DL	% BDL	
					Urban station	Rural station
La	80	5.2	0.3	0.01	0	18
Ce	78	9.4	0.6	0.01	0	15
Pr	N.A.	5.2	0.1	0.002	7	15
Nd	76	4.6	0.3	0.01	0	19
Sm	82	4.6	0.1	0.005	13	21
Eu	83	4.0	0.03	0.001	7	34
Gd	78	3.9	0.3	0.003	0	26
Dy	75	3.8	0.4	0.002	0	32
Ho	N.A.	3.6	0.1	0.001	10	13
Er	84	3.5	0.2	0.002	7	18
Tm	79	3.6	0.02	0.001	3	53
Yb	85	3.5	0.1	0.002	8	32
Lu	81	3.6	0.02	0.002	14	50

N.A.: referent value not available for the SRM CTA-FFA1.

2.3. Enrichment factors

The analysis of the enrichment factors (EFs) of lanthanoid elements was conducted in order to evaluate the effect of anthropogenic activities in each station and also to compare the sampling sites. The EF is defined as follows:

$$EF_X = (C_X/C_R)_{PM10}/(C_X/C_R)_{Crust} \qquad (3.1)$$

where X represents the element of interest; EF_X the EF of X; C_X the concentration of X, and C_R the concentration of a reference element. In this study, Ti was selected as the reference material, and the average of local top soil composition was used as the elemental composition of the crustal material.

2.4. Concentration weighted trajectory and conditional bivariate probability function.

Potential sources of lanthanoid elements were investigated by using the concentration weighted trajectory (CWT) approach and conditional bivariate probability function (CBPF). Calculations of these functions were done with the total lanthanoid concentration data coupled with time-resolved wind direction-speed and back-trajectory data using the Openair package, freely available for R (Carslaw, 2015).

The CWT computes a logarithmic mean of concentration at the receptor site weighted by the residence time of the trajectory for each grid cell of the geographical domain (Cheng et al., 2013; Hsu et al., 2003). A high value of CWT means that air parcels passing over a given cell would, on average, cause high concentrations at the receptor site. For our study, 10-day back-trajectories (BTs) were computed using the Hybrid Single Particle Lagrangian Integrated Trajectory (HYSPLIT) model and the Global NOAA-NCEP/NCAR reanalysis data archives (Draxler and Rolph, 2015). The BTs were run at 3-h intervals with 1-h increment starting at the height of 500 m above ground level for every day during the sampling period. The trajectory domain was divided into 2.5x2.5^{o} grid cells and, due to that and the proximity between the sampling sites, the coordinates of the urban station were selected as the starting point.

The CBPF improves the traditional conditional probability function (CPF, (Kim et al., 2003; Kim and Hopke, 2005)) by adding the wind speed as a third variable and estimates the probability that a given source contribution from a given wind direction and speed will exceed a predetermined threshold criterion. The CBPF is defined as $CBPF = m_{\theta,l}/n_{\theta,l}$, where $m_{\theta,l}$ is the number of samples in the wind sector θ and wind speed interval l with mixing ratios greater than a threshold concentration, and $n_{\theta,l}$ is the total number of samples in the same wind direction-speed interval (Squizzato et al., 2017; Uria-Tellaetxe and Carslaw, 2014). Here, the same 24-h lanthanoid concentration determined in the PM_{10} total mass was assigned to each 3-h wind data available from the Canta Rana meteorological station located in the Cienfuegos city. We used 16 wind sectors ($\theta = 22.5°$).

3. Results and discussion

3.1. Total lanthanoids concentration and PM_{10} mass

Table 3.2 shows the average concentration of PM_{10} and lanthanoid elements at both sampling sites. Total lanthanoid (TLoid) contents were in the range <0.01 – 13.4 ng m^{-3} and 0.51 – 18.8 ng m^{-3} at the rural and urban site, respectively. Levels at both sites were similar to those found in Mexico City (Moreno et al., 2008b) and Puertollano, Spain (Moreno et al., 2008a), locations with characteristics similar to our sampling sites in terms of the proximity of rural and urban areas or the presence of petrochemical complexes and oil power stations, among other industries.

Table 3.2. Statistic summary of concentration of lanthanoid elements (ng m^{-3}) at both sampling sites. The inter-site Pearson's correlations (R_{IPC}) in bold represent a statistic significant at the 0.01 level.

Element	Rural station (n=68)		Urban Station (n=71)		R_{IPC}
	AVE (SD)	Range	AVE (SD)	Range	
PM_{10}	24.8 (12.1)	10.7-69.5	35.4 (13.6)	15.6-84.5	**0.91**
V	6.85 (6.33)	1.28-35.99	11.34 (7.65)	1.96-38.92	**0.47**
La	0.34 (0.57)	<DL-2.77	0.56 (0.71)	0.02-3.50	**0.97**
Ce	0.69 (1.18)	<DL-5.72	1.29 (1.73)	0.17-8.88	**0.99**
Pr	0.08 (0.13)	<DL-0.67	0.09 (0.13)	<DL-0.64	**0.99**
Nd	0.29 (0.50)	<DL-2.51	0.55 (0.68)	0.07-3.38	**0.96**
Sm	0.07 (0.09)	<DL-0.49	0.11 (0.13)	<DL-0.61	**0.86**
Eu	0.02 (0.02)	<DL-0.10	0.02 (0.02)	<DL-0.12	**0.88**
Gd	0.05 (0.07)	<DL-0.39	0.15 (0.13)	0.03-0.59	**0.69**
Dy	0.04 (0.05)	<DL-0.31	0.18 (0.12)	0.05-0.69	**0.54**
Ho	0.02 (0.01)	<DL-0.06	0.01 (0.01)	<DL-0.06	**0.90**
Er	0.02 (0.03)	<DL-0.18	0.05 (0.05)	<DL-0.22	**0.70**
Tm	0.01 (0.01)	<DL-0.06	0.01 (0.01)	<DL-0.04	**0.67**
Yb	0.02 (0.03)	<DL-0.16	0.04 (0.04)	<DL-0.19	**0.77**
Lu	0.01 (0.01)	<DL-0.06	0.01 (0.01)	<DL-0.04	**0.70**
TLoid	1.64 (2.66)	<0.01-13.4	3.08 (3.69)	0.51-18.8	**0.96**
La/Ce	0.57 (0.47)	0.12-3.61	0.47 (0.12)	0.09-0.87	
La/Sm	3.67 (2.97)	0.16-14.1	5.50 (3.60)	0.52-23.9	
La/V	0.06 (0.09)	0.001-0.36	0.07 (0.09)	0.01-0.39	

TLoid is the sum of the lanthanoid elements concentration.

Figure 3.2a shows the temporal distribution of TLoid during the period of study at both sites. It can be noted that both sampling sites showed similar trends, therefore

suggesting the influence of common sources, probably on a regional scale. The highest concentrations (> 5 ng m^{-3}) were observed between middle April and early August at both sites. The amount of TLoid in this period accounted for 87 and 68% of the TLoid recorded during the study at rural and urban sites, respectively. The urban site showed intermediate values (in the range of 2 – 5 ng m^{-3}) in February and on 11th March, while concentration values lay around 1-2 ng m^{-3} during the rest of the year. At the rural site, concentrations of TLoid were lower and usually below the detection limit (see Table 3.1), except precisely between April and August, when the highest concentration were observed. The main differences between both sites may be linked to the influence of local urban sources like the road traffic.

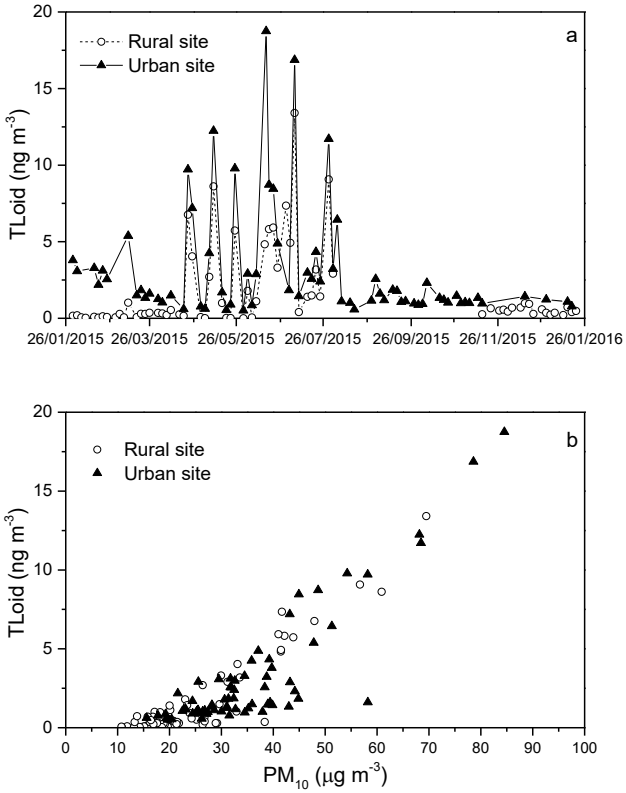

Figure 3.2. Temporal distribution of concentration of total lanthanoid (a) and total lanthanoid concentrations versus PM_{10} mass (b) at the rural and urban sampling sites.

Figure 3.2b shows a clear positive correlation between the PM_{10} mass and TLoid concentration in both rural ($r=0.92$, $p<0.01$) and urban ($r=0.87$, $p<0.01$) sites. This linear relationship was especially evidenced by the highest concentrations of PM_{10}, which usually exceeded the maximum admissible concentration of 50 μg m^{-3} established in the

Cuban legislation for air quality (NC 1020, 2014). This coincidence suggested a marked regional influence during this period, which was related to the Saharan dust intrusions occurring in the Caribbean region (Prospero et al., 2014). In fact, when coupling the CWT with the TLoid data in both sampling sites (see Figure 3.3), it may be observed that air masses causing the highest concentration of TLoid in the study area came from the East through the Atlantic Ocean, thus reflecting their African origin. Previous studies have shown the influence of African dust intrusions in Cuba in the period between March and August (Mojena López et al., 2015; Rodriguez et al., 2015) and their relation with high PM_{10} concentrations (Barja et al., 2013). On the basis of these results, we may deduce that Saharan dust was an important source of lanthanoid elements in PM_{10}, mainly in the period 22/04/2015 – 05/08/2015. This suggests that lanthanoid elements can be used as a signature for African dust transported in Cuba, as has also been reported in close regions such as Miami or Barbados (Trapp et al., 2010).

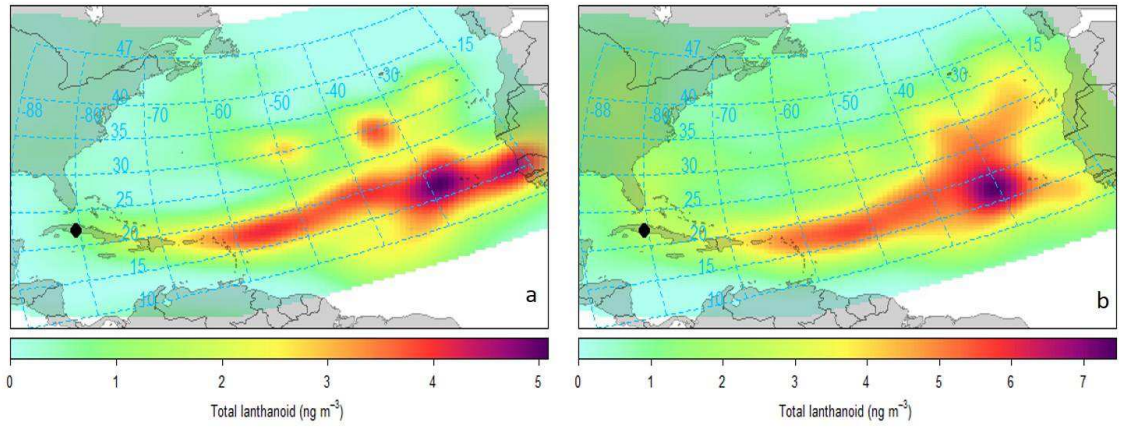

Figure 3.3. CWT for total lanthanoid concentration at rural (a) and urban (b) sampling sites.

3.2. Lanthanoid elements in ambient PM_{10}

As a result of the geochemical differences between the lighter and heavier lanthanoid elements, the abundance of the lighter lanthanoid Ce and La in crustal materials is, respectively, 10 and 5 times higher than the heavier lanthanoid Sm, which is in turn nearly twice as abundant as Yb. In addition, the odd-numbered lanthanoids are less abundant than their even-numbered neighbours (the Oddo-Harkins rule), explaining why Ce (atomic number 58) is twice as common as its immediate neighbour La (atomic number 57) (Moreno et al., 2008b). Thus, in most crustal materials such as natural dusts,

the commoner lanthanoids occur in the following order of abundance: Ce>La>Nd>Pr>Sm>Yb>Lu.

Data collected at our sampling sites (see Table 3.2) do not entirely reflect these features, thereby supporting the conclusion that the level of lanthanoids in the study area was not exclusively from a crustal origin. This conclusion was demonstrated by the existence of La/Ce ratios abnormally high or low when compared to the typical range of natural La/Ce values (0.4–0.6) in uncontaminated rocks, soils and minerals (Moreno et al., 2010). The wide variation found in the La/Ce ratios of the rural (0.12 – 3.61) and urban (0.09 – 0.87) sites showed enrichments in both elements (see Table 3.2). About 46% of the samples from the rural site and 56% from the urban site showed La/Ce ratios in the expected range for crustal composition (0.4–0.6), which indicated that in almost half of the samples this ratio was clearly influenced by anthropogenic emissions. Thus, 13% of the samples showed La enrichment (La/Ce>0.6) in the urban site, increasing up to 29% in the rural site, where La>Ce ratios reached values higher than 1. On the other hand, 25% and 31% of the samples presented Ce enrichment (La/Ce<0.4) in the rural and urban sites, respectively.

The statistical summary of La/Sm ratios shown in Table 3.2 exhibited a fractionation similar to that found for the La/Ce ratios (here crustal values of La/Sm lie within the range 5–7). It can be noted that La/Sm ratios varied in a wide range at both sampling sites, with more than 50% of samples showing values out of the crustal range.

The LaCeSm triangular diagrams shown in Figure 3.4 further illustrate this fractionation of lanthanoid elements. These ternary plots, traditionally used by geologists to illustrate the compositional variations in minerals and rocks, have also been widely used to show geochemical patterns in atmospheric PM (Moreno et al., 2008b, 2008a). In this case, the concentrations of La and Sm were adjusted to place crustal abundances of the three components in the centre of the triangle. In order to evaluate possible local or long-range crustal origins, we also added to the ternary plots the concentrations of lanthanoid elements of the local soils as well as information found in studies carried out in the Sahara-Sahel Dust Corridor (Moreno et al., 2006).

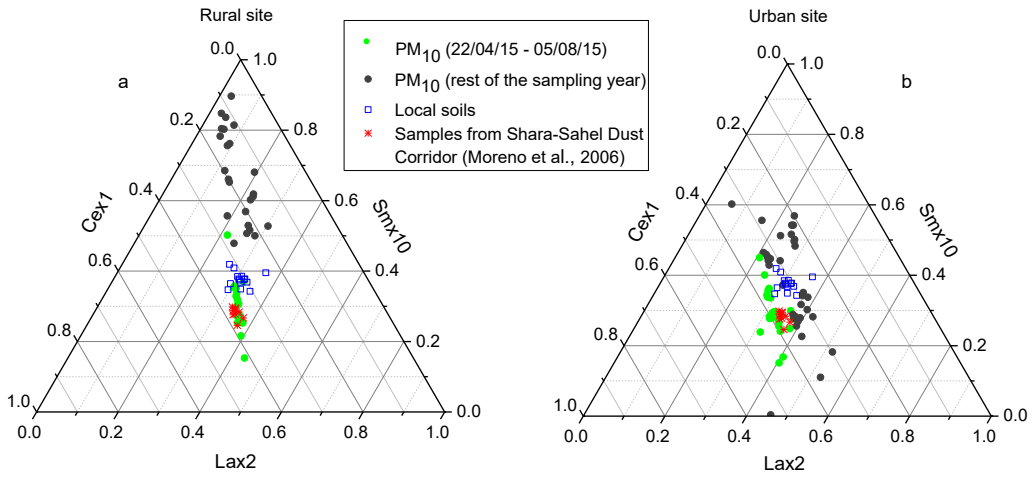

Figure 3.4. Ternary plots of LaCeSm for PM_{10} data from rural (a) and urban (b) sampling sites. PM_{10} data were divided into two groups: samples collected in the period 22/04/15 – 05/08/15 (corresponding to the highest TLoid, green circles) and data collected during the rest of the year (corresponding to the lowest TLoid, dark circles). Results for local soils and the Sahara–Sahel Dust Corridor (Moreno et al., 2006) have been included.

At the rural site, the LaCeSm diagram showed a clear fractionation into two groups (Figure 3.4a). The first group encompassed the samples with highest concentrations, collected between April and August (22/04/15 – 05/08/15, green circles). These samples were located in the centre of the triangle, next to the local soil samples and the Sahara dust data, but slightly moved toward the Saharan region. This distribution confirmed the prevalent regional influence during this period, driven by the Saharan dust intrusions and suggested a lower influence of the local soil resuspension. The second group (rest of the samples, dark circles) represents the anthropogenic nature of the LaCeSm composition as demonstrated by the displacement of the data from the center of the triangle towards the Sm apex.

Similarly, the rural site (Figure 3.4b) showed a fractionation of data too, but with a slightly different pattern, probably caused by the influence of urban sources. Thus, most of the samples corresponding to the period of highest TLoid showed a displacement towards the Sahara–Sahel Dust Corridor data similar to that observed in the rural site. However, contrary to that observed in the rural site where the rest of data were mostly located in the upper part of the triangle (highest values of Sm), the samples collected outside the April-August period spread along the Sm axis, with many samples located in

the central part of the triangle. In other words, a large number of samples are grouped along with the local soils and the samples of Saharan dust, which appears to be related to the crustal PM deposited on roads that is later suspended by the action of traffic.

3.3. Enrichment factors of lanthanoid elements

In order to determine the impact of natural and anthropogenic sources on the studied region, lanthanoid elements with EF ≤1.0 were considered of crustal origin and elements having EF in the range 1.0 – 10 were identified as originating from both anthropogenic and crustal sources (Hsu et al., 2016, 2010). Figure 3.5 shows the average enrichment factors of lanthanoid elements in two periods: from April to August (22/04/2015 – 05/08/2015), where the highest concentrations of TLoid were found, and the rest of the year, with lower concentrations of TLoid.

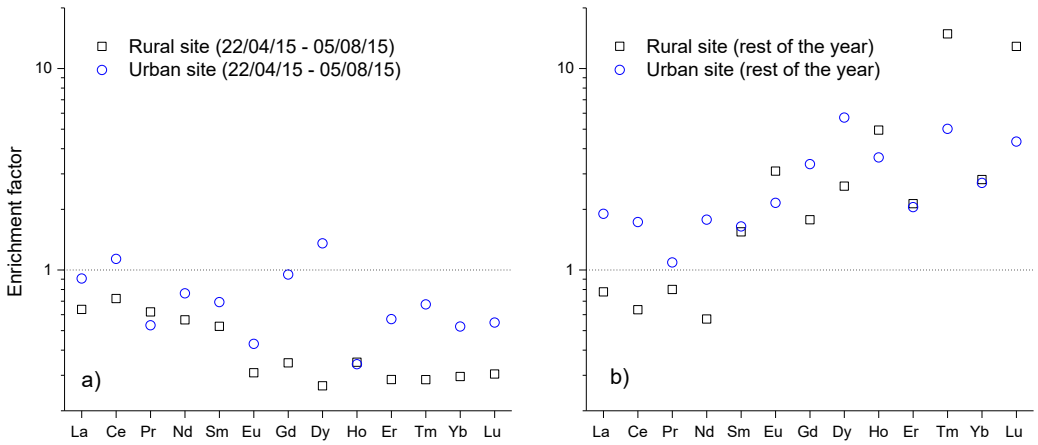

Figure 3.5. Enrichment factor of lanthanoid elements at the rural and urban sites. The EFs were separated in to two different periods according to the concentration of TLoid: a) 22/04/2015 – 05/08/2015 (higher concentration of TLoid) and b) rest of the year (lower concentration of TLoid).

Figure 3.5a shows that most of lanthanoid elements had EF<1.0 between April and August in both sampling sites, thus confirming their crustal origin in this period where the most important Saharan dust intrusion events occurred. In contrast, samples collected during the rest of the year (with low influence of Saharan dust intrusions) generally showed higher EFs at both sampling sites (Figure 3.5b). Additionally, a similar fractionation between the lighter (La - Sm) and heavier (Eu - Lu) lanthanoids was

observed in this period in both sites. The lighter lanthanoids showed EF around 1.0, thereby indicating the prevalent crustal origin in this period whereas heavier lanthanoids presented higher EFs (generally EF>2) probably related to the additional influence of anthropogenic sources. It is likely that these sources were common at both sampling sites, which produced the similar EFs fractionation.

A similar fractionation between the lighter and heavier lanthanoid elements was observed in the inter-site Pearson correlations (see Table 3.2). In general, all elements were significantly correlated between sites at the 0.01 level, which confirmed the influence of common sources in both sampling sites. However, the light lanthanoids were more strongly correlated ($r \geq 0.96$) because of their prevalent crustal origin on all year, whereas the heavy lanthanoids presented lower correlations ($0.90 \geq r \geq 0.54$). This last observation is probably the result of the effect of the local anthropogenic sources under different meteorological conditions, such as wind direction and wind speed.

3.4. La/V ratios

Vanadium, in conjunction with metals like Ni or La, is often used as a tracer of emission sources related to fossil fuel combustion and oil refining processes (Celo et al., 2012; Moreno et al., 2010, 2008a; Viana et al., 2008). Specifically, V-rich emissions derived from fuel oil and petroleum-coke combustion usually exhibit very low La/V ratios (<0.1) as compared to those of mineral PM coming from uncontaminated crustal materials or coal combustion (La/V = 0.2 – 0.3 (Moreno et al., 2008a)). On the contrary, atmospheric emissions of PM in the flue gas from the fluid catalytic converters (FCC) of refinery regenerators commonly show much greater La/V ratios, reaching values significantly high like those obtained by Kulkarni et al., (2006) beside an oil refinery in Houston during a FCC pollution event (average $PM_{2.5}$ La/V values of 1.8).

The data obtained in Cienfuegos showed atmospheric La/V values exclusively below 0.4 at both stations (see Table 3.2), with more than 80% of data showing values <0.1. These results suggest the dominance of anthropogenic emissions from industries with oil and/or petroleum-coke combustion processes (with low La/V) rather than from refineries. On the other hand, samples showing La/V values in the crustal range presented mean TLoid concentrations of 5.9 and 8.9 ng m^{-3} in the rural and urban sites,

respectively. Such high TLoid values were obtained in the samples collected between April and August, which are directly linked to the atmospheric intrusions of Saharan dust in the study area, as it was noted before.

Despite the above, it is already known that the usefulness of La/V ratios to track refinery emissions can be limited in industrial areas with multiple air pollution sources and different PM chemical composition. This is because the combined effect of these sources (e.g., oil burning (low La/V) and FCC (high La/V) emissions) counteract each other and can produce apparently 'natural' crustal La/V ratios (Kulkarni et al., 2006; Moreno et al., 2008a). This limitation can be overcome by using a LaCeV triangular diagram (Figure 3.6), adjusting the lanthanoid values to place crustal abundances of the three components in the centre of the triangle. For comparison purposes, published and local information about the composition of relevant emissions (Kulkarni et al., 2006; Moreno et al., 2006; Olmez et al., 1988) has been added in the Figure 3.6a.

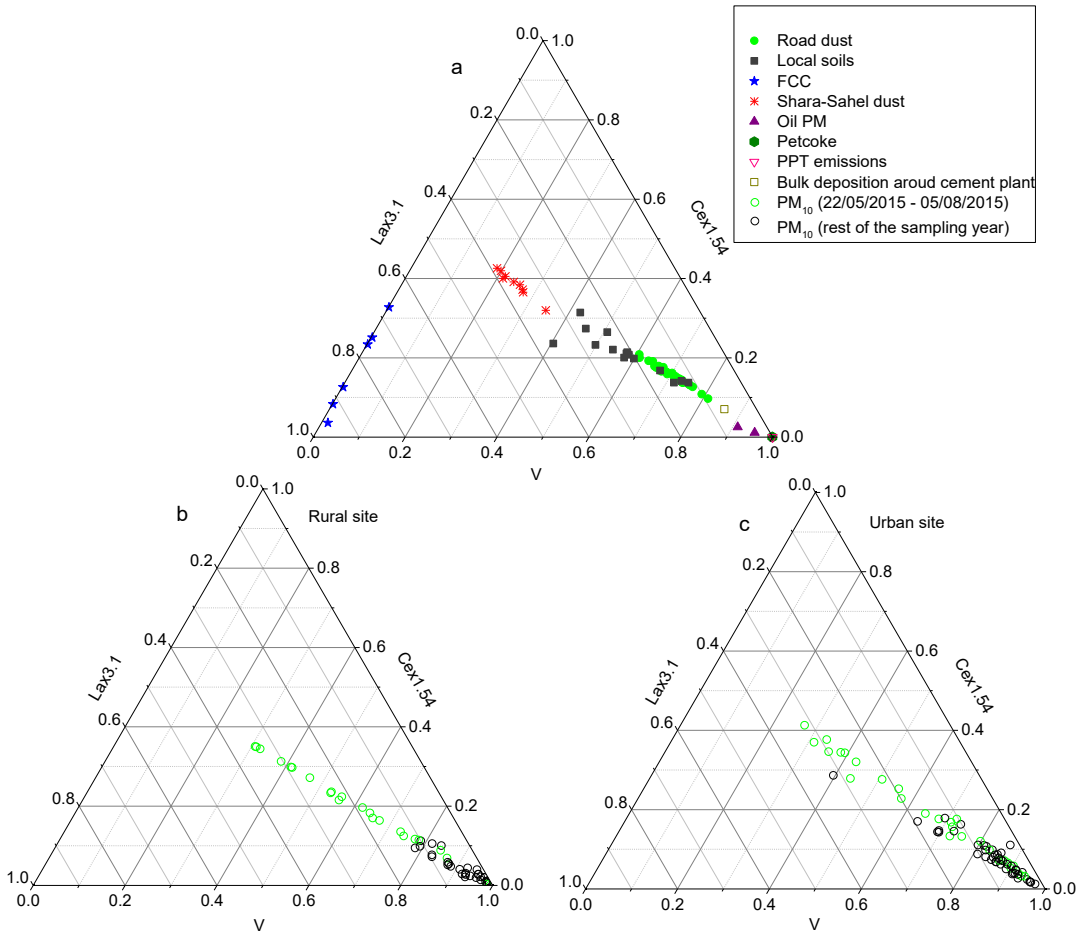

Figure 3.6. Comparison of published and local data a) on LaCeV compositions of FCC (Kulkarni et al., 2006), oil PM (Olmez et al., 1988), Sahara–Sahel Dust Corridor (Moreno et al., 2006), TPP emissions, petroleum-coke, bulk deposition around cement plant, local soil and road dust with Cienfuegos PM_{10} data from b) rural and c) urban sampling site.

Data of both sampling sites (Figures 3.6b and 3.6c) showed a well-defined linear tendency from the centre of the triangle (crustal region) towards the V apex (oil combustion). When we compare these results with the published and local data (Figure 3.6a), it can be observed that the linear trends were consistent with a mixture of crustal (local soil and Sahara dust) and anthropogenic (road dust, petroleum-coke and oil combustion) composition. Thus, the samples collected during the April-August period (green circles in Figures 3.6b and 3.6c) ranged from Sahara dust to oil PM composition with a clear prevalence for the crustal composition. This result indicates that, despite the dominant crustal origin of the PM_{10} during this period, there was also a remarkable anthropogenic influence, which seemed to be strongly diluted by the presence of

natural crustal materials. In contrast, the samples collected during the period of lowest concentration of TLoid (black circles in Figures 3.6b and 3.6c) were displaced toward the V apex, thereby reflecting an exclusive anthropogenic influence in both sampling sites. Most of these samples were located in the extreme of the linear tendency, matching with PM compositions typical of emissions coming from the power plant and harbour areas (oil combustion), and from the cement plant (petroleum-coke combustion). In addition, several samples of the urban site were slightly displaced toward the road dust composition, which probably reflects the impact of the resuspension produced by the road traffic. This pattern was also observed in a few samples of the rural site and probably reflects the influence of the urban background under northerly wind direction.

In general, the similar linear trends observed at both sampling sites confirmed the influence of common sources and indicated that, besides crustal matter (driven by Saharan dust intrusions), the combustion of oil and petroleum-coke and the emissions caused by traffic turned out to be important contributors of lanthanoid elements in the PM_{10} fraction in the study area. Following these results, the lack of any strong influence from refinery emissions at both sampling sites was then clear.

3.5. Lanthanoids source origin: CBPF

We computed the CBPF by intervals of concentration in order to investigate the influence of different potential sources based on different concentration intervals of lanthanoid elements. Intervals were investigated in accordance to the methodology described in Uria-Tellaetxe and Carslaw (2014) and the most likely sources detected for each concentration range are reported in Figure 3.7.

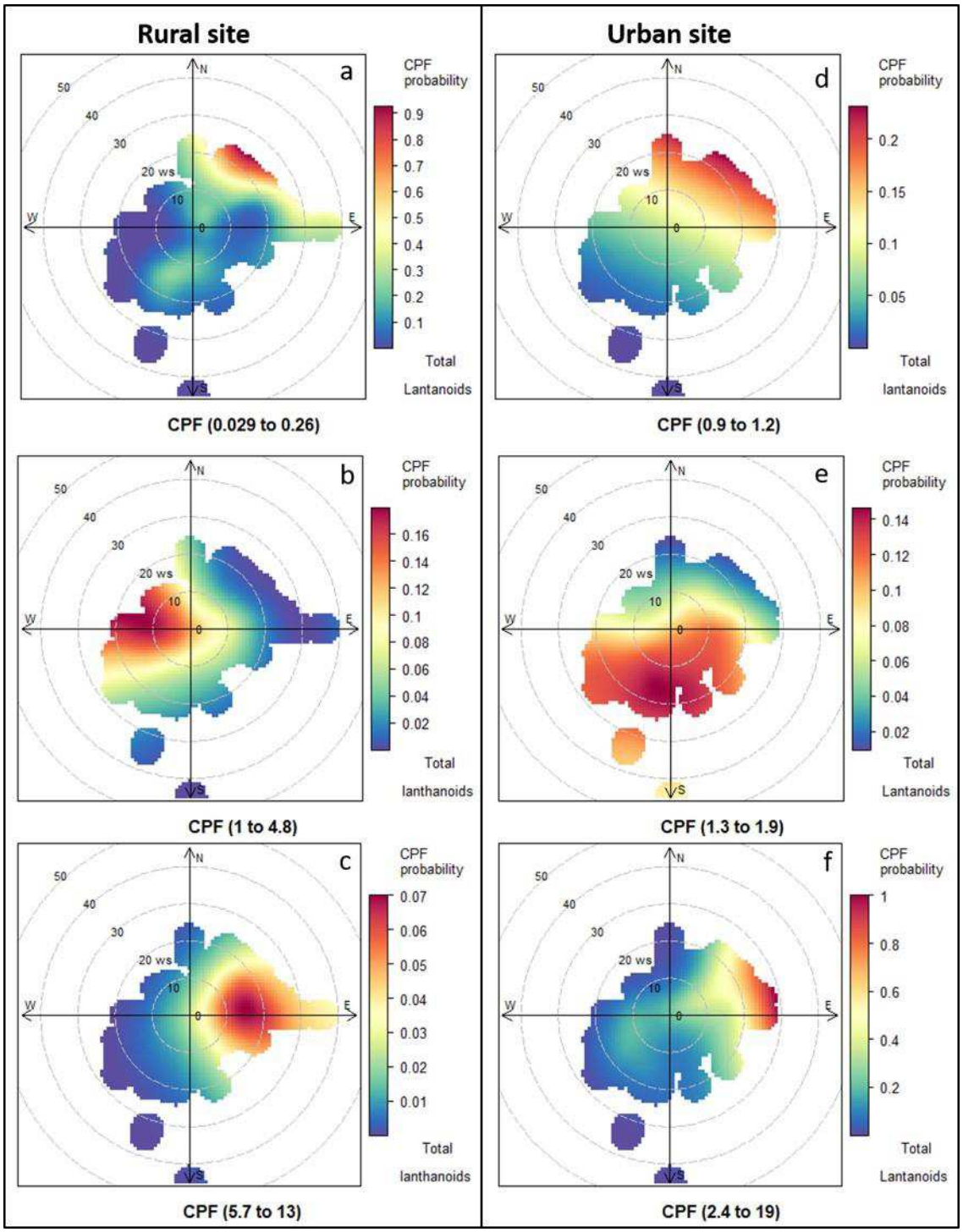

Figure 3.7. CBPF plots for different concentration intervals of total lanthanoids. Rural site: dominant sources located to the NE in the range 0.029 – 0.26 ng m^{-3} (a), dominant sources to the west in the range 1.0 – 4.8 ng m^{-3} (b) and dominant sources to de east for concentrations higher than 5.7 ng m^{-3} (c). Urban site: dominant sources from N to E directions in the range 0.9 – 1.2 ng m^{-3} (d), dominant sources to southern directions in the range 1.3 – 1.9 ng m^{-3} (e) and dominant sources to the east for concentrations higher than 4.9 ng m^{-3} (f).

Figure 3.7a displays that sources located to the NNE from the rural site were dominant at the lowest concentrations of TLoid found in the rural site (from 0.015 to 0.062 ng m^{-3}) and for higher wind speed. This means that the potential sources must be located away from the sampling site. The most likely sources are the TPP and industries (oil combustion emissions) located between 10 and 12 km northward, the city of Cienfuegos (urban background, traffic and shipping related emissions) located 9 km to the NNE and the cement plant and quarries located about 25 km to the NE. Similarly, the sources associated to the lowest concentrations of TLoid (0.9 to 1.2 ng m^{-3}) in the urban site (Figure 3.7d) were traffic-related emissions, mostly generated in the urban sector from N and E directions. However, potential influence of oil combustion emissions from the TPP and the industrial area located to the N should not be excluded.

Figure 3.7b shows a clear dominance of western pollution sources for concentrations between 1.0 – 4.8 ng m^{-3} and a wide range of wind speed in the rural site. The most likely source from this sector was the resuspension of soil particles by the agricultural activities carried out mainly to the W and NW. Other additional sources could be the diesel power unit and the diesel combustion boiler located 4 km to the West. On the other hand, dominant sources for intermediate concentrations in the urban site (from 1.3 – 1.9 ng m^{-3}) were associated to the sector E – S (Figure 3.7e), which probably reflect the influence of the shipping and maritime traffic emissions generated in this area.

Finally, the highest concentrations of TLoid in both the rural (from 5.7 to 13 ng m^{-3}) and urban (from 4.9 – 19 ng m^{-3}) sites, were associated to easterly wind directions (Figures 3.7c and 3.7f, respectively). It totally agrees with the strong association observed on CWT between the highest concentrations of TLoid and the African intrusions arriving from the East through the Atlantic Ocean. It is also quite likely that this source be mixed with material resuspended in the cement plant and the associated quarry when the wind blows from the east. This would explain the wider concentration range of TLoid observed in the urban site with respect to that found in the rural one.

4. Conclusions

Lanthanoid elements were measured in PM_{10} samples simultaneously collected in a rural and an urban site in Cienfuegos, Cuba. The analysis of the results led the following conclusions:

Concentration of total lanthanoids presented a similar distribution pattern in both sampling sites and were slightly higher in the urban site, because of the emissions from local traffic and industries. The highest concentrations (exceeding 13 ngm^{-3} in both sites) were observed between April and August, showing a clear linear relationship with the PM_{10} mass. We attributed this result to the dominance of a crustal origin governed by the Saharan dust intrusion events.

Lanthanoid elements were not exclusively from a crustal origin. When their concentrations were low in both sites, the influence of anthropogenic emissions was obvious, as demonstrated by the strong fractionation of the natural crustal ratios between the lanthanoids elements (La/Ce and La/Sm), and the increase of their EF, especially for the heavier lanthanoids.

Using the LaCeV triangular diagrams we illustrated the nature of the sources in the area resulting in a mixture of crustal material (Sahara dust and local soils composition) and anthropogenic emissions (road dust, petroleum-coke and oil combustion). The linear tendency observed in those diagrams clearly proved the lack of any strong influence from refinery emissions and confirmed the prevalence of emissions from common sources in both sampling sites. The CBPF, computed by intervals, allowed the identification of these sources according to their level of contributions.

The results presented in this paper provide the first dataset published on the concentration of lanthanoid elements in aerosols in Cuba and improve our understanding of the aerosol properties and the atmospheric pollution dynamics in the Cienfuegos region.

Acknowledgements

The research leading to these results has received funding from "la Caixa" Banking Foundation. This study was also supported by the IAEA TC Project CUB/7/008 “Strengthening the National System for Analysis of the Risks and Vulnerability of Cuba’s Coastal Zone Through the Application of Nuclear and Isotopic Techniques” and National Program PNUOLU /4-1/ 2 No. /2014 of the National Nuclear Agency. The authors express their gratitude to the analytical staff of the Laboratorio Integrado de Calidad Ambiental (LICA) of the University of Navarra and Centro de Estudios Ambientales de Cienfuegos (CEAC) for its assistance.

References

Aldabe, J., Elustondo, D., Santamaria, C., Lasheras, E., Pandolfi, M., Alastuey, A., Querol, X., Santamaria, J.M., 2011. Chemical characterisation and source apportionment of PM2.5 and PM10 at rural, urban and traffic sites in Navarra (North of Spain). Atmospheric Res. 102, 191–205. https://doi.org/10.1016/j.atmosres.2011.07.003

Aldabe, J., Santamaría, C., Elustondo, D., Lasheras, E., Santamaría, J.M., 2013. Application of microwave digestion and ICP-MS to simultaneous analysis of major and trace elements in aerosol samples collected on quartz filters. Anal. Methods 5, 554–559. https://doi.org/10.1039/c2ay25724f

Barja, B., Mogo, S., Cachorro, V.E., Carlos Antuna, J., Estevan, R., Rodrigues, A., de Frutos, A., 2013. Atmospheric particulate matter levels, chemical composition and optical absorbing properties in Camaguey, Cuba. Environ. Sci.-Process. Impacts 15, 440–453. https://doi.org/10.1039/c2em30854a

Bozlaker, A., Buzcu-Güven, B., Fraser, M.P., Chellam, S., 2013. Insights into PM10 sources in Houston, Texas: Role of petroleum refineries in enriching lanthanoid metals during episodic emission events. Atmos. Environ. 69, 109–117. https://doi.org/10.1016/j.atmosenv.2012.11.068

Carslaw, D.C., 2015. The Openair Manual — Open-source Tools for Analysing Air Pollution Data. Manual for version 1.1-4.

Celo, V., Dabek-Zlotorzynska, E., Zhao, J., Bowman, D., 2012. Concentration and source origin of lanthanoids in the Canadian atmospheric particulate matter: a case study. Atmospheric Pollut. Res. 3, 270–278. https://doi.org/10.5094/APR.2012.030

Cheng, I., Zhang, L., Blanchard, P., Dalziel, J., Tordon, R., 2013. Concentration-weighted trajectory approach to identifying potential sources of speciated atmospheric mercury at an urban coastal site in Nova Scotia, Canada. Atmospheric Chem. Phys. 13, 6031–6048. https://doi.org/10.5194/acp-13-6031-2013

Dolgopolova, A., Weiss, D.J., Seltmann, R., Dulski, P., 2006. Dust dispersal and Pb enrichment at the rare-metal Orlovka-Spokoinoe mining and ore processing site: insights from REE patterns and elemental ratios. J. Hazard. Mater. 132, 90–97. https://doi.org/10.1016/j.jhazmat.2005.11.086

Draxler, R.R., Rolph, G.D., 2015. HYSPLIT (HYbrid Single-Particle Lagrangian Integrated Trajectory) Model access via NOAA ARL READY Website (http://www.arl.noaa.gov/HYSPLIT.php). NOAA Air Resources Laboratory, College Park, MD.

Du, L., Turner, J., 2015. Using PM2.5 lanthanoid elements and nonparametric wind regression to track petroleum refinery FCC emissions. Sci. Total Environ. 529, 65–71. https://doi.org/10.1016/j.scitotenv.2015.05.034

Geagea, M.L., Stille, P., Millet, M., Perrone, T., 2007. REE characteristics and Pb, Sr and Nd isotopic compositions of steel plant emissions. Sci. Total Environ. 373, 404–419. https://doi.org/10.1016/j.scitotenv.2006.11.011

Grantz, D.A., Garner, J.H.B., Johnson, D.W., 2003. Ecological effects of particulate matter. Environ. Int. 29, 213–239. https://doi.org/10.1016/S0160-4120(02)00181-2

Hsu, C.-Y., Chiang, H.-C., Lin, S.-L., Chen, M.-J., Lin, T.-Y., Chen, Y.-C., 2016. Elemental characterization and source apportionment of PM10 and PM2.5 in the western coastal area of central Taiwan. Sci. Total Environ. 541, 1139–1150. https://doi.org/10.1016/j.scitotenv.2015.09.122

Hsu, S.C., Liu, S.C., Tsai, F., Engling, G., Lin, I.I., Chou, C.K.C., Kao, S.J., Lung, S.C.C., Chan, C.Y., Lin, S.C., Huang, J.C., Chi, K.H., Chen, W.N., Lin, F.J., Huang, C.H., Kuo, C.L., Wu, T.C., Huang, Y.T., 2010. High wintertime particulate matter pollution over an offshore island (Kinmen) off southeastern China: An overview. J. Geophys. Res.-Atmospheres 115, D17309. https://doi.org/10.1029/2009JD013641

Hsu, Y.K., Holsen, T.M., Hopke, P.K., 2003. Comparison of hybrid receptor models to locate PCB sources in Chicago. Atmos. Environ. 37, 545–562. https://doi.org/10.1016/S1352-2310(02)00886-5

Huang, X., Olmez, I., Aras, N.K., Gordon, G.E., 1994. Emissions of trace elements from motor vehicles: Potential marker elements and source composition profile. Atmos. Environ. 28, 1385–1391. https://doi.org/10.1016/1352-2310(94)90201-1

Kanakidou, M., Seinfeld, J.H., Pandis, S.N., Barnes, I., Dentener, F.J., Facchini, M.C., Van Dingenen, R., Ervens, B., Nenes, A., Nielsen, C.J., Swietlicki, E., Putaud, J.P., Balkanski, Y., Fuzzi, S., Horth, J., Moortgat, G.K., Winterhalter, R., Myhre, C.E.L., Tsigaridis, K., Vignati, E., Stephanou, E.G., Wilson, J., 2005. Organic aerosol and global climate modelling: a review. Atmos Chem Phys 5, 1053–1123. https://doi.org/10.5194/acp-5-1053-2005

Kim, E., Hopke, P.K., 2005. Identification of fine particle sources in mid-Atlantic US area. Water. Air. Soil Pollut. 168, 391–421. https://doi.org/10.1007/s11270-005-1894-1

Kim, E., Hopke, P.K., Edgerton, E.S., 2003. Source identification of Atlanta aerosol by positive matrix factorization. J. Air Waste Manag. Assoc. 53, 731–739.

Kitto, M.E., Anderson, D.L., Gordon, G.E., Olmez, I., 1992. Rare earth distributions in catalysts and airborne particles. Environ. Sci. Technol. 26, 1368–1375. https://doi.org/10.1021/es00031a014

Kulkarni, P., Chellam, S., Fraser, M.P., 2007. Tracking petroleum refinery emission events using lanthanum and lanthanides as elemental markers for PM2.5. Environ. Sci. Technol. 41, 6748–6754. https://doi.org/10.1021/es062888i

Kulkarni, P., Chellam, S., Fraser, M.P., 2006. Lanthanum and lanthanides in atmospheric fine particles and their apportionment to refinery and petrochemical operations in Houston, TX. Atmos. Environ. 40, 508–520. https://doi.org/10.1016/j.atmosenv.2005.09.063

Li, C., Kang, S., Zhang, Q., 2009. Elemental composition of Tibetan Plateau top soils and its effect on evaluating atmospheric pollution transport. Environ. Pollut. 157, 2261–2265. https://doi.org/10.1016/j.envpol.2009.03.035

Mojena López, E., Ortega González, A., Casilles Vega, E.F., Leyva Santos, J., 2015. Sahara Clouds Dust. Their presence in Cuba. Rev. Cuabana Meteorol. 21, 120–134.

Moreno, T., Querol, X., Alastuey, A., de la Rosa, J., Sánchez de la Campa, A.M., Minguillón, M., Pandolfi, M., González-Castanedo, Y., Monfort, E., Gibbons, W., 2010. Variations in vanadium, nickel and lanthanoid element concentrations in urban air. Sci. Total Environ. 408, 4569–4579. https://doi.org/10.1016/j.scitotenv.2010.06.016

Moreno, T., Querol, X., Alastuey, A., Gibbons, W., 2008a. Identification of FCC refinery atmospheric pollution events using lanthanoid- and vanadium-bearing aerosols. Atmos. Environ. 42, 7851–7861. https://doi.org/10.1016/j.atmosenv.2008.07.013

Moreno, T., Querol, X., Alastuey, A., Pey, J., Minguillon, M.C., Perez, N., Bernabe, R.M., Blanco, S., Cardenas, B., Gibbons, W., 2008b. Lanthanoid geochemistry of urban atmospheric particulate matter. Environ. Sci. Technol. 42, 6502–6507. https://doi.org/10.1021/es800786z

Moreno, T., Querol, X., Castillo, S., Alastuey, A., Cuevas, E., Herrmann, L., Mounkaila, M., Elvira, J., Gibbons, W., 2006. Geochemical variations in aeolian mineral particles from the Sahara-Sahel Dust Corridor. Chemosphere 65, 261–270. https://doi.org/10.1016/j.chemosphere.2006.02.052

Morera-Gómez, Y., Elustondo, D., Lasheras, E., Alonso-Hernandez, C.M., Santamaría, J.M., 2018. Chemical characterization of PM10 samples collected simultaneously at a rural and an urban site in the Caribbean coast: local and long-range source apportionment. Atmospheric Environ. Submitted.

NC 1020, 2014. Norma Cubana 1020:2014. CALIDAD DEL AIRE — CONTAMINANTES — CONCENTRACIONES MÁXIMAS ADMISIBLES Y VALORES GUÍAS EN ZONAS HABITABLES.

Olmez, I., Sheffield, A.E., Gordon, G.E., Houck, J.E., Pritchett, L.C., Cooper, J.A., Dzubay, T.G., Bennett, R.L., 1988. Compositions of Particles from Selected Sources in Philadelphia for Receptor Modeling Applications. JAPCA 38, 1392–1402. https://doi.org/10.1080/08940630.1988.10466479

Pope, C.A., Dockery, D.W., 2006. Health effects of fine particulate air pollution: Lines that connect. J. Air Waste Manag. Assoc. 56, 709–742.

Pöschl, U., 2005. Atmospheric aerosols: composition, transformation, climate and health effects. Angew. Chem. Int. Ed Engl. 44, 7520–7540. https://doi.org/10.1002/anie.200501122

Pourmand, A., Prospero, J.M., Sharifi, A., 2014. Geochemical fingerprinting of trans-Atlantic African dust based on radiogenic Sr-Nd-Hf isotopes and rare earth element anomalies. Geology 42, 675–678. https://doi.org/10.1130/G35624.1

Prospero, J.M., Collard, F.-X., Molinie, J., Jeannot, A., 2014. Characterizing the annual cycle of African dust transport to the Caribbean Basin and South America and its impact on the environment and air quality. Glob. Biogeochem. Cycles 28, 757–773. https://doi.org/10.1002/2013GB004802

Rodriguez, S., Cuevas, E., Prospero, J.M., Alastuey, A., Querol, X., Lopez-Solano, J., Garcia, M.I., Alonso-Perez, S., 2015. Modulation of Saharan dust export by the North African dipole. Atmospheric Chem. Phys. 15, 7471–7486. https://doi.org/10.5194/acp-15-7471-2015

Squizzato, S., Cazzaro, M., Innocente, E., Visin, F., Hopke, P.K., Rampazzo, G., 2017. Urban air quality in a mid-size city - PM2.5 composition, sources and identification of impact areas: From local to long range contributions. Atmospheric Res. 186, 51–62. https://doi.org/10.1016/j.atmosres.2016.11.011

Tang, Y., Han, G., Wu, Q., Xu, Z., 2013. Use of rare earth element patterns to trace the provenance of the atmospheric dust near Beijing, China. Environ. Earth Sci. 68, 871–879. https://doi.org/10.1007/s12665-012-1791-z

Trapp, J.M., Millero, F.J., Prospero, J.M., 2010. Temporal variability of the elemental composition of African dust measured in trade wind aerosols at Barbados and Miami. Mar. Chem., Aerosol chemistry and impacts on the ocean 120, 71–82. https://doi.org/10.1016/j.marchem.2008.10.004

Uria-Tellaetxe, I., Carslaw, D.C., 2014. Conditional bivariate probability function for source identification. Environ. Model. Softw. 59, 1–9. https://doi.org/10.1016/j.envsoft.2014.05.002

Viana, M., Kuhlbusch, T. a. J., Querol, X., Alastuey, A., Harrison, R.M., Hopke, P.K., Winiwarter, W., Vallius, A., Szidat, S., Prevot, A.S.H., Hueglin, C., Bloemen, H., Wahlin, P., Vecchi, R., Miranda, A.I., Kasper-Giebl, A., Maenhaut, W., Hitzenberger, R., 2008. Source apportionment of particulate matter in Europe: A review of methods and results. J. Aerosol Sci. 39, 827–849. https://doi.org/10.1016/j.jaerosci.2008.05.007

Wang, L., Liang, T., 2014. Accumulation and fractionation of rare earth elements in atmospheric particulates around a mine tailing in Baotou, China. Atmos. Environ. 88, 23–29. https://doi.org/10.1016/j.atmosenv.2014.01.068

Wen, B., Yuan, D., Shan, X., Li, F., Zhang, S., 2001. The influence of rare earth element fertilizer application on the distribution and bioaccumulation of rare earth

elements in plants under field conditions. Chem. Speciat. Bioavailab. 13, 39–48. https://doi.org/10.3184/095422901783726825

WHO, 2016. WHO | WHO releases country estimates on air pollution exposure and health impact [WWW Document]. WHO. URL http://www.who.int/mediacentre/news/releases/2016/air-pollution-estimates/en/ (accessed 3.21.17).

Chapter 4

Carbon and nitrogen isotopes unravels sources of aerosol contamination at Caribbean rural and urban coastal sites

This chapter reproduces the text of the following paper:

Morera-Gómez, Y., Santamaría, J.M., Elustondo, D., Alonso-Hernández, C.M., Widory, D., 2018. Carbon and nitrogen isotopes unravels sources of aerosol contamination at Caribbean rural and urban coastal sites. Sci. Total Environ. 642, 723–732. https://doi.org/10.1016/j.scitotenv.2018.06.106.

Abstract

The constant increase of anthropogenic emissions of aerosols, usually resulting from a complex mixture from various sources, leads to a deterioration of the ambient air quality. The stable isotope compositions ($\delta^{13}C$ and $\delta^{15}N$) of total carbon (TC) and nitrogen (TN) in both PM_{10} and emissions from potential sources were investigated for first time in a rural and an urban Caribbean costal sites in Cuba to better constrain the origin of the contamination. Emissions from road traffic, power plant and shipping emissions were discriminated by coupling their C and N contents and corresponding isotope signatures. Other sources (soil, road dust and cement plant), in contrast, presented large overlapping ranges for both C and N isotope compositions. $\delta^{13}C_{PM10}$ isotope compositions in the rural (average of -25.4 ± 1.2‰) and urban (average of -24.8 ± 1.2‰) sites were interpreted as a mixture of contributions from two main contributors: i) fossil fuel combustion and ii) cement plant and quarries. Results also showed that this last source is impacting more air quality at the urban site. A strong influence from local wood burning was also identified at the rural site. These conclusions were comforted by a statistical analysis using a conditional bivariate probability function. TN and $\delta^{15}N$ values from the urban site demonstrated that nitrogen in PM_{10} was generated by secondary processes through the formation of $(NH_4)_2SO_4$. The exchange in the $(NH_4)_2SO_4$ molecule between gaseous NH_3 and particle NH_4^+ under stoichiometric equilibrium may control the observed ^{15}N enrichment. At low nitrogen concentrations in the aerosols, representing PM_{10} with both the highest primary N and lowest secondary N proportions, comparison with the $\delta^{15}N$ of potential sources indicate that emissions from diesel car and power plant emissions may represent the major vectors of primary nitrogen.

Keywords: PM_{10}, $\delta^{13}C$, $\delta^{15}N$, Fossil fuel combustion, Cement plant, Secondary nitrogen

1. Introduction

Deterioration of air quality is usually associated to the increase in traffic and industrial emissions, the increase in uncontrolled urban growth and urban population, the reduction in forest areas and the increase in biomass burning (Kim et al., 2015; Reisen et al., 2013; Squizzato et al., 2017). To date, and in spite of many efforts to reduce and limit the atmospheric anthropogenic emissions (WHO, 2005), this issue remains a global concern. Atmospheric particulate matter (PM) of 10 μm or less in diameter (PM_{10}) has become one of the major air pollutants in urban, suburban and even in rural and remote regions of the world (Mukherjee and Agrawal, 2017; WHO, 2016). Due to its size, those particles can penetrate into the human breathing apparatus, with smaller ones more easily reaching the deepest parts of the lungs, and therefore being more lethal for human health (Pope and Dockery, 2006). Their concentration and toxicity also depend on their composition as well as on the presence of other pollutants, which in turn is strongly related to their origin and source type.

The analysis of stable carbon ($\delta^{13}C$) and nitrogen ($\delta^{15}N$) isotope compositions have widely been used for decoding and tracking biogeochemical processes in oceanography and limnology (Cifuentes L. A. et al., 1988; Naru et al., 2007; Peng et al., 2015) but also for tracing sources and cycling of specific elements through the atmosphere. Several studies have used carbon and nitrogen stable isotopes to establish the sources and reaction processes in gases, aerosols and atmospheric particles. Pioneering studies differentiated anthropogenic from natural (marine and continental) particulate emissions based on their $\delta^{13}C$ (Cachier et al., 1985; Chesselet et al., 1981). $\delta^{15}N$ in aerosols have been used to investigate atmospheric N cycling and to help elucidate the sources of primary and possibly secondary nitrogen (Moore, 1977; Pavuluri et al., 2010; Widory, 2007; Yeatman et al., 2001). Coupled $\delta^{13}C$ and $\delta^{15}N$ have been studied in aerosols to discern between inputs from C-3 and C-4 vegetation type in remote areas (Kelly et al., 2005; Martinelli et al., 2002). More recently, this dual-isotope approach has also been used to trace the sources of atmospheric particles in the urban environment (Chen et al., 2017; Gorka et al., 2012; X. Guo et al., 2016; Lopez-Veneroni, 2009; Sudheer et al., 2016; Widory et al., 2004).

To our knowledge, there is no study that combines C and N stable isotope approaches to address air quality issues in the Caribbean region. In addition, in many areas of the Caribbean basin and, especially in Cuba, atmospheric contamination issues regarding PM have been poorly investigated, arising the need for implementing tools in order to better constrain sources of contamination. The present study follows recent research that collected and chemically characterized PM_{10} samples in Cienfuegos, Cuba (Morera-Gómez et al., 2018). Our study presents the first carbon and nitrogen stable isotope data for aerosols in Cuba and the nearby islands. Our main objectives were (I) to determine the C and N contents and isotope compositions ($\delta^{13}C$ and $\delta^{15}N$) of PM_{10} samples from a rural and an urban coastal stations in Cienfuegos, (II) to chemically/isotopically characterize potential sources of aerosols in the studied region and (III) to identify the main sources of air contamination and, when possible, to estimate their respective contributions. In order to confront the conclusions drawn from this study of our chemical and isotope dataset, we also applied a statistical approach using a conditional bivariate probability function (CBPF) that coupled isotope data with time-resolved wind directions and wind speed data.

2. Methods

Description of the sampling sites, climatic conditions, PM_{10} samples collection, analytical procedures and results for the PM_{10} chemical constituents used in this work are provided in details in Morera-Gómez et al., (2018).

2.1. Sample collection

PM_{10} sampling was performed in parallel between 31/01/2015 and 20/01/2016 at two monitoring stations (rural and urban sites) located in the municipality of Cienfuegos, in the central south coast of Cuba (Figure 4.1). The rural station (22º 03’ 55’’ N, 80º 28’ 58’’ W) is located at the main facilities of the Centre for Environmental Studies (CEAC in Spanish) 9 km south from Cienfuegos city. The urban station is located at the CEAC facilities within the city of Cienfuegos (22º 08’ 32’’ N, 80º 27’ 29’’ W). PM_{10} samples were collected on pre-combusted (4 hours at 550 ºC) quartz fiber filters (Munktell, 150 mm

diameter) for 24-h every three days using MCV-CAV high-volume samplers operating at a flow rate of 30 m^3 h^{-1}. A total of 68 and 71 PM_{10} samples were collected at the rural and urban stations, respectively. Due to technical issues with one of the high-volume samplers no samples were collected between 5/08/2015 and 12/11/2015 at the rural station. Ten blank filters, disseminated randomly along the one-year study, were collected and analyzed. In parallel several samples, described below, were collected from the main potential sources located within 15 km from the urban sampling site.

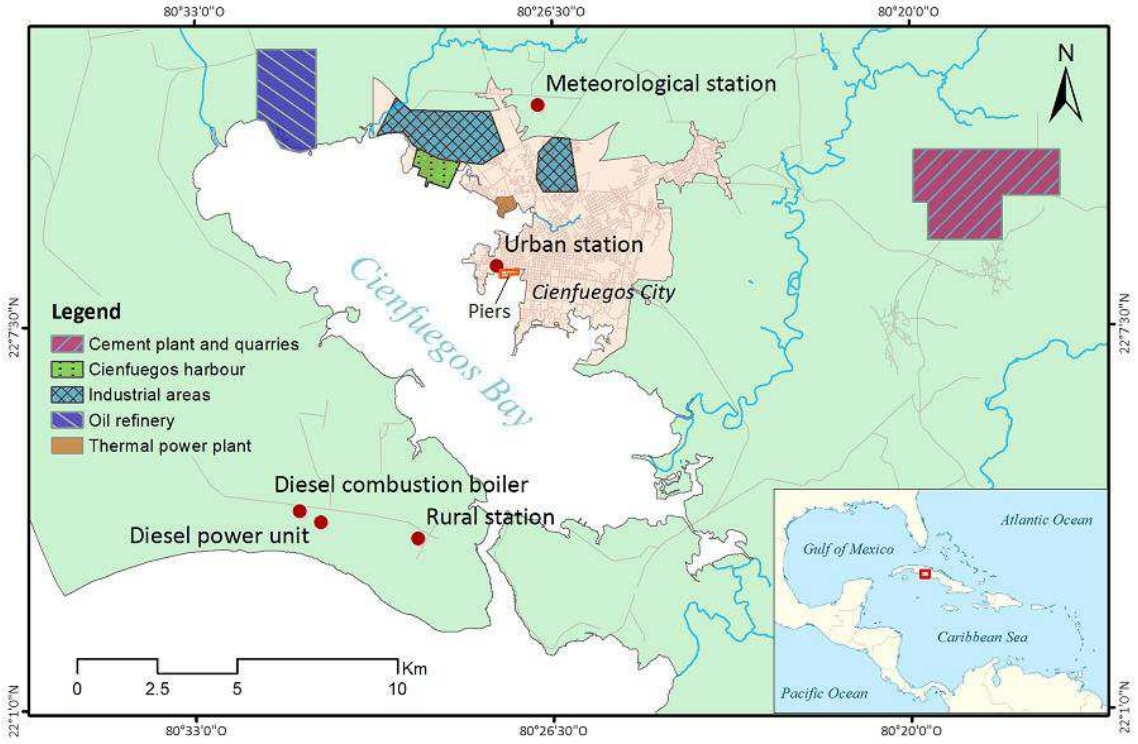

Figure 4.1. Map showing the sampling sites and main pollution sources.

6 fly ash samples were collected on quartz filters from the stacks of a thermal power plant (TPP). This power plant has a ~316 MW h^{-1} capacity, is located 2 km north of the urban sampling site and uses sulfur-rich Cuban crude oil as fuel (Turtos Carbonell et al., 2007).

A total of 31 samples of road dust were collected from the main roads of Cienfuegos city by sweeping an area of about 1.0mx0.5m from pavement edges using a plastic dustpan and brushes. These samples were dried at 45°C, passed through a 50 μm sieve and stored in polyethylene bags until further analysis.

1 sample of bulk atmospheric deposition was obtained from the vicinity of the cement plant located 15 km E-NE from the urban sampling site. Monthly samples of bulk deposition were collected during the year 2016 using a 0.25 m^2-area plastic collector. After collection, samples were transported to the laboratory and evaporated to dryness. A final sample was generated by adding all of the 12-month dried samples. A sample representative of the petroleum-coke combusted in the cement plant was also obtained. This petroleum-coke is stored in a large outdoor area, open to winds, near the cement plant, which also facilitates its eventual resuspension in the atmosphere by wind.

Soot samples resulting from the incomplete combustion of RON 83 regular gasoline (1 sample from a car) and diesel (1 sample from a car and 1 from a ship) were obtained by scraping directly at the end of tailpipes, and stored in polyethylene bags.

Top layer soils were collected at 18 different locations within 15km around the sampling sites. Samples were taken using a spatula and placed into polyethylene bags. Once in the laboratory, they were dried at 45 ^{o}C, passed through a 250 μm sieve and stored until further analysis.

2.2. Total carbon, total nitrogen and C and N stable isotopes analysis

Total carbon (TC), total nitrogen (TN) and their corresponding stable isotope compositions (δ^{13}C and δ^{15}N) were determined using an Elemental Analyzer (Vario MICRO Cube, Elementar, Hanau, Germany) coupled to an Isotope Ratio Mass Spectrometer (IsoPrime 100, Cheadle, UK) operating in continuous flow mode. The inorganic carbon fraction (carbonate) was not removed prior to the isotope analysis. TC and TN fractions measured in PM_{10} are expressed in percent (%) by normalizing the carbon and nitrogen contents with the PM_{10} total mass, respectively. For the δ^{13}C analysis either a punch of 1.3 cm^2 taken on each PM_{10} quartz filter or about 1 to 4 mg (for the emission sources and soil samples) were packed into a tin capsule. For the δ^{15}N analysis a punch of 3.0 cm^2 taken on each PM_{10} quartz filter or about 4 to 10 mg (for the emission sources and soil samples) were packed into a tin capsule with tungsten oxide (WO_3) to achieve complete combustion. δ^{15}N were not determined in PM_{10} samples

from the rural site as the TN contents were usually too low for its quantification (peak height lower than 1nA). Isotope compositions are expressed as $\delta^{13}C$ and $\delta^{15}N$ values, which represents the relative difference expressed in per mil (‰) between the isotope ratio of the sample and that of a standard (Pee Dee Belemnite (PDB) for carbon and atmospheric N_2 for nitrogen):

$$\delta^{13}C\ (‰\ \text{vs. PDB}) = \left[\left(R_{sample}/R_{standard} - 1\right)\right] x\ 1000 \qquad (4.1)$$

$$\delta^{15}N\ (‰\ \text{vs. AIR}) = \left[\left(R_{sample}/R_{standard} - 1\right)\right] x\ 1000 \qquad (4.2)$$

where $R = {}^{13}C/{}^{12}C$ or ${}^{15}N/{}^{14}N$.

The analytical quality control was performed by routinely analysis of interspersed international carbon and nitrogen isotope standards (IAEA, Vienna, Austria) and interlaboratory-calibrated alga reference material 1452 B (University of Barcelona). We also ran several samples in duplicates; the obtained reproducibility was <0.2‰ for C and <0.3‰ for N isotopes. Similarly, analytical uncertainties for TC and TN concentrations were within 3 and 4% of the reported values, respectively. TC concentrations were corrected for mean blank values, while no blank correction was made for TN as the N content in blanks were considered negligible. No blank correction was made for $\delta^{13}C$ and $\delta^{15}N$ as their corresponding IRMS peaks height (typically <0.5 nA) were below the calibration range (1 – 10 nA).

2.3. Meteorological data and conditional bivariate probability function

Meteorological data were obtained from the meteorological station located within 15 km of the study area (Figure 4.1). Wind directions and speeds were recorded every 3 hours and the other parameters (temperature, precipitation, pressure and relative humidity) every 24 hours.

Daily $\delta^{13}C$ fluctuations coupled to time-resolved wind direction and speed were investigated by applying the conditional bivariate probability function (CBPF), in order to better understand the impact of local and regional sources. Calculations were made using the Openair package free available for R (Carslaw, 2015).

The CBPF improves the traditional conditional probability function (CPF; (Kim et al., 2003; Kim and Hopke, 2005)) by adding the wind speed as a third variable. The CBPF estimates the probability that the contribution from a given source for a given wind direction and speed will exceed a predetermined threshold (Squizzato et al., 2017; Uria-Tellaetxe and Carslaw, 2014). The CBPF is defined as: $CBPF = m_{\theta,l}/n_{\theta,l}$, where $m_{\theta,l}$ is the number of samples in the wind sector θ and wind speed interval l with mixing ratios greater than a threshold concentration. $n_{\theta,l}$ is the total number of samples in the same wind direction-speed interval. As wind data were recorded every 3 hours and $\delta^{13}C$ every 24 hours, we decided to assign this $\delta^{13}C$ to all the wind data recorded on that same day. We used a total of 16 wind sectors ($\theta = 22.5°$).

3. Results

3.1. Samples from potential sources

3.1.1. TC content and $\delta^{13}C$ isotope composition

Table 4.1 reports the chemical (TC and TN) and isotope ($\delta^{13}C$ and $\delta^{15}N$) characteristics of samples from both the potential sources of contamination and ambient PM_{10} collected in Cienfuegos (individual values for ambient PM_{10} are reported in Table S4.1 and S4.2 in Supplementary Material). Average carbon concentrations from pollution sources display large fluctuations ranging from 9.0 to 78.2%. Petroleum-coke presents the highest carbon content (78.2%) coupled with the lowest $\delta^{13}C$ value (-31.0‰). Particles from the TPP stacks show a large range of carbon concentrations from 36.9 to 71.9% (average of 50.7 ± 18.6%), but with a very narrow range of $\delta^{13}C$ from -27.3 to -26.8‰ (average of -27.1 ± 0.2‰). The 2 soot particle samples from the diesel and gasoline road traffic contain 66.5 and 51.5% of carbon, respectively. Their corresponding $\delta^{13}C$ values are -26.3 and -25.2‰, respectively. Soot particles emitted by the diesel ship present lower carbon concentrations (17.0%) with an intermediate $\delta^{13}C$ value (-25.7‰). Carbon concentrations in road dust particles vary between 7.3 and 10.9% (average of 9.0 ± 1.0%) while their $\delta^{13}C$ range from -18.0 to -9.4‰ (average of -13.1 ± 2.0‰). Soil

samples show carbon concentrations from 3.7 to 16.7% (average of 10.2 ± 4.4%) and $\delta^{13}C$ values ranging from -28.0 to -14.1‰ (average of -20.5 ± 4.8‰). The bulk deposition sample collected in the vicinity of the cement plant yields a carbon concentration of 15.5% with a $\delta^{13}C$ value of -15.3‰.

Table 4.1. Average concentrations for total carbon (TC) and total N (TN) and their corresponding stable isotope compositions ($\delta^{13}C$ and $\delta^{15}N$) in aerosol samples from potential sources of contamination and in ambient PM_{10} in Cienfuegos. Number between brackets show the standard deviation from the average (1σ).

	Particles origin	TC (%)	$\delta^{13}C$ (‰)	TN (%)	$\delta^{15}N$ (‰)
TPP stacks (n=6)	Cuban crude oil combustion	50.7 (18.6)	-27.1 (0.2)	1.0 (0.2)	11.4 (3.4)
Road dust (n=31)	Paved roads of Cienfuegos city	9.0 (1.0)	-13.1 (2.0)	0.2 (0.1)	-5.0 (5.6)
Bulk deposition (n=1)	Deposited particles around cement plant	15.5	-15.3	1.1	5.6
Petroleum-coke (n=1)	Petroleum-coke burnt in cement plant	78.2	-31.0	1.8	3.8
Car tailpipe (n=1)	Diesel	66.5	-26.3	1.6	1.7
Car tailpipe (n=1)	Gasoline	51.5	-25.2	1.2	-1.8
Ship tailpipe (n=1)	Diesel	17.0	-25.7	0.6	3.0
Top soil (n=18)	Local soils	10.2 (4.4)	-20.5 (4.8)	0.6 (0.3)	1.0 (2.8)
Rural PM_{10} (n=68)	Aerosol	12.9 (6.5)	-25.4 (1.2)		
Urban PM_{10} (n=71)	Aerosol	19.3 (7.1)	-24.8 (1.2)	2.5 (0.8)	9.2 (4.4)

Emission sources combusting fossil fuel cannot, thus, be segregated by their sole carbon concentrations, except for shipping emissions that present lowest C concentration (17.0%). However, the $\delta^{13}C$ values are significantly differentiated between crude oil combustion (TPP) and diesel or gasoline combustion by about 1 – 2‰. Widory et al., (2004) observed a 2‰ difference between particles from diesel and gasoline (regular and unleaded) combustion in Paris (France), which is in the same order of magnitude than the 1.1‰ difference we are observing here (Table 4.1). The $\delta^{13}C$ values for diesel and gasoline road traffic in our study are very similar to those reported for a diesel car (-26.2‰) and an unleaded gasoline car (-25.3‰) in Barcelona (Mari et al., 2016), as well as those from diesel (-27.2 to -26.0‰) and unleaded gasoline (-25.8 to -22.6‰) vehicles in Paris (Widory et al., 2004) and diesel (-26.32 to -23.57‰) and gasoline (-26.26 to -25.19‰) vehicles in Nanjing, China (Z. Guo et al., 2016). The $\delta^{13}C$ measured in the bulk deposition sample collected in the vicinity of the cement plant (-15.3‰) is higher than the one reported for a similar sample obtained in Barcelona (-24.5

± 0.3‰), but similar to the isotope compositions measured for cement (-11.6 ± 2.0‰) and kiln (-15.5 ± 0.5‰) dust collected in that same cement plant (Mari et al., 2016). Soil samples collected around Cienfuegos show $\delta^{13}C$ values similar to those obtained in Mexico (Lopez-Veneroni, 2009) and Japan (Kawashima and Haneishi, 2012). Road dust samples present a ^{13}C enrichment of 3.9 and 4.3‰ with respect to the values reported in those Mexico and Japan studies, respectively.

3.1.2. TN content and $\delta^{15}N$ isotope composition

Average TN concentrations in samples from contamination sources show a narrow range, from 0.2 to 1.8 %. In contrast, $\delta^{15}N$ show a wide range of values from -5.0 to 13.8‰. As for carbon, petroleum-coke presents the highest nitrogen content (1.8%) with a corresponding $\delta^{15}N$ of 3.8‰. Samples from the TPP stacks have similar nitrogen concentrations from 0.7 to 1.1% (average of 1.0 ± 0.2%), but the corresponding $\delta^{15}N$ greatly vary between 5.9 and 13.8‰ (average of 11.4 ± 3.4‰). Soot particles from the diesel and gasoline cars present TN contents of 1.6 and 1.2% and $\delta^{15}N$ of 1.7 and -1.8‰, respectively. Soot particles from the ship show a TN of 0.6% and a $\delta^{15}N$ of 3.0‰. The road dust samples have the lowest nitrogen concentrations, ranging from 0.1 to 0.5% (average of 0.2 ± 0.1%) with $\delta^{15}N$ widely fluctuating from -20.5 to 7.1‰ (average of -5.0 ± 5.6‰). Nitrogen contents in soil samples vary from 0.2 to 1.4% (average of 0.6 ± 0.3%), whereas their $\delta^{15}N$ range from -3.0 to 7.1‰ (average of 1.0 ± 2.8‰). Finally, the bulk deposition sample from the vicinity of the cement plant present a TN of 1.1% and a $\delta^{15}N$ of 5.6‰.

As for carbon, the sole use of the nitrogen content cannot discriminate the potential sources, but their $\delta^{15}N$ values present significant differences that allow discriminating between road traffic, industrial (TPP) and shipping emissions. These differences in nitrogen isotope compositions could be related to difference in the combustion conditions (temperature of combustion, O_2 supply…; (Widory, 2007)). Soot samples from diesel (1.7‰) and gasoline (-1.8‰) combustion in our study show $\delta^{15}N$ values that are lower than the diesel exhaust (3.9 to 5.4‰) and unleaded gasoline exhaust (4.6‰) emissions in Paris (Widory, 2007). Proemse et al., (2012) reported ammonium and nitrate $\delta^{15}N$ in $PM_{2.5}$ emissions from stack in the Athabasca Oil Sands Region (Alberta,

Canada) ranging from -4.5 to 20.1‰ and from 9.6 to 17.9‰, respectively. Our $\delta^{15}N$ from the TPP stack (11.4 ± 3.4‰) is consistent with those ranges, which may suggest similar formation processes.

3.2. Atmospheric PM_{10}

3.2.1. Carbon and nitrogen concentrations and corresponding isotope compositions in PM_{10}

Carbon concentrations in PM_{10} at the rural and urban sites (see Table 4.1) range from 4.4 to 35.5% (average of 12.9 ± 6.5%) and from 5.2 to 32.7% (average of 19.3 ± 7.1%), respectively. Their corresponding $\delta^{13}C$ range between -27.1 and -20.9‰ (average of -25.4 ± 1.2‰) and from -27.5 to -19.3‰ (average of -24.8 ± 1.2‰), respectively. The carbon contents and isotope compositions show large and similar variations during this one-year survey at both sampling sites. However, on average, samples from the urban site present higher carbon contents and higher $\delta^{13}C$ compared to those of the rural site. For both sites, a *t*-test showed that there is no statistical difference ($p>0.05$) between the dry and wet seasons for both carbon content and $\delta^{13}C$ values. Thus, the fluctuations mentioned above probably reflect the daily variations in the amount of carbonaceous aerosol emitted by the main local sources. We also obtained a weak positive significant correlation ($r=0.3$, $p<0.05$) between the $\delta^{13}C$ values measured daily at both sites, which may indicate the impact of common sources.

Total nitrogen concentrations and $\delta^{15}N$ values were only measured at the urban site and vary between 1.0 and 4.6% (average of 2.5 ± 0.8%) and between 1.5 and 19.1‰ (average of 9.2 ± 4.4‰), respectively. No seasonal variation was also observed neither for the nitrogen content or for the $\delta^{15}N$ values.

Table 4.2 provides a synthesis of the C and N isotope compositions measured in PM_{10} samples in our and other studies around the world. To our knowledge, there is no carbon or nitrogen isotope compositions measured in Cuban aerosols available in the literature. Our average $\delta^{13}C$ in Cienfuegos is comparable to those reported for the cities of Wroclaw (Poland; Gorka et al., 2014, 2012), Baoji (China; Wang et al., 2010), Delhi, Varanasi and Kolkata (India; Sharma et al., 2007) and Mexico City (Lopez-Veneroni, 2009). However,

our data shows a wider range with a clear tendency toward a ^{13}C enrichment compared to other cities. This may either reflect carbon isotope differences in the combustibles burnt or indicate the implication of distinct sources, including marine aerosols that have typical $\delta^{13}C$ between -23.0 and -19.0‰ (Ceburnis et al., 2016, 2011; Chesselet et al., 1981; Miyazaki et al., 2011; Turekian et al., 2003). This ^{13}C enrichment could also identify the emission inputs from the cement plant and quarries located under the prevalent wind direction and/or from the road and soil dust. These latest sources yielded $\delta^{13}C$ usually higher than -20.0‰ (Table 4.1).

Table 4.2. Carbon ($\delta^{13}C$) and nitrogen ($\delta^{15}N$) isotope compositions in PM_{10} collected at different sites around the world.

Location	Form of C and N	$\delta^{15}N$(‰)		$\delta^{13}C$(‰)		Reference
		(min, max)	Mean ± SD	(min, max)	Mean ± SD	
Xiamen, China	TC/TN	(5.5, 12.5)		(-27.2, -25.4)		(Chen et al., 2017)
Wroclaw, Poland	TC/TN	(5.0, 13.7)	9.9 ± 2.0	(-26.9, -25.1)	-26.1 ± 0.1	(Gorka et al., 2012)
				(-27.6, -25.3)	-26.6 ± 0.7	(Gorka et al., 2014)
Baoji city, China	TC/TN	(8.8, 23.1)[a]		(-24.4, -22.5)[a]		(Wang et al., 2010)
Delhi, India	TC/TN	(3.3, 14.3)	9.6 ± 2.8	(-26.4, -24.8)	-25.5 ± 0.5	(Sharma et al., 2015)
Varanasi, India	TC/TN	(2.8, 11.0)	6.8 ± 2.4	(-26.4, -23.3)	-25.4 ± 0.8	
Kolkata, India	TC/TN	(2.8, 11.5)	7.4 ± 2.7	(-26.6, -24.9)	-26.0 ± 0.4	
Chennai, India	TN	(15.7, 31.2)	23.9 ± 3.3			(Pavuluri et al., 2010)
Mexico city, Mexico	TC			(-29.5, -24.3)	-25.4 ± 1.3	(Lopez-Veneroni, 2009)
Paris, France	TC/TN	(5.3, 16.1)	10.7 ± 3.1	(-26.7, -24.5)	-26.2 ± 0.5	(Widory et al., 2004; Widory, 2007)
Barcelona, Spain	TC				-25.8 ± 0.4	(Mari et al., 2016)
Cienfuegos (rural), Cuba	TC/TN			(-27.1, -20.9)	-25.4 ± 1.2	This study
Cienfuegos (urban), Cuba	TC/TN	(1.5, 19.1)	9.2 ± 4.4	(-27.5, -19.3)	-24.8 ± 1.2	

[a]Range of average values by season

While our $\delta^{15}N$ in PM_{10} are slightly enriched in ^{15}N compared to Xiamen (Chen et al., 2017) and Varanasi and Kalkota (Sharma et al., 2007), they are similar to the ones observed in Paris, where fossil fuel combustion acts as a dominant source but also where secondary processes are expected to significantly shift the $\delta^{15}N$ (Widory, 2007). In contrast, our $\delta^{15}N$ are relatively depleted in ^{15}N with respect to values from Baoji (China) and Chennai (India; (Pavuluri et al., 2010)), where fugitive dust, coal burning, animal excreta and bio-fuel/biomass burning were identified as the main vectors of aerosols. These authors also demonstrated that secondary nitrogen processes lead to enrichments in ^{15}N (Pavuluri et al., 2010).

4. Discussion

4.1. Carbon isotope compositions

The analysis of the carbon concentrations and $\delta^{13}C$ in our PM_{10} show that carbon at both study sites can be interpreted as a mixture of contributions from different sources (Figure 4.2a and 4.2b). About 70% of the samples collected at the rural site (Figure 4.2a) are consistent with the carbon isotope compositions of emissions from fossil fuel combustion ($\delta^{13}C$ ranging from -27.3 to -25.2‰). This isotope range includes emissions from the TPP, from road traffic and from ships, but also possibly emission from a small diesel-powered unit and a diesel-powered boiler located 4 km west of the study site (Figure 4.1). Local C3 plant (*Lysiloma latisiliquum*) burnt for producing charcoal, that typically presents $\delta^{13}C$ between -32.0 and 24.0‰ (Garbaras et al., 2015; Z. Guo et al., 2016; Martinelli et al., 2002), could also impact air quality at this rural area. Values around -27.0‰ have been reported for charcoal and firewood burning in Japan and China (X. Guo et al., 2016; Kawashima and Haneishi, 2012). As most of these sources display overlapping $\delta^{13}C$ ranges, their respective influences cannot be discriminated in Figure 4.2a. Nevertheless, samples from March 20th and April 19th, which yield the highest carbon concentrations appear discriminated from the other rural samples. They were collected under similar meteorological conditions with the wind blowing

predominantly from the southern direction (forest area) at very low wind speed (<3 kmh^{-1}) suggesting that local wood burning may most likely be the source of contamination.

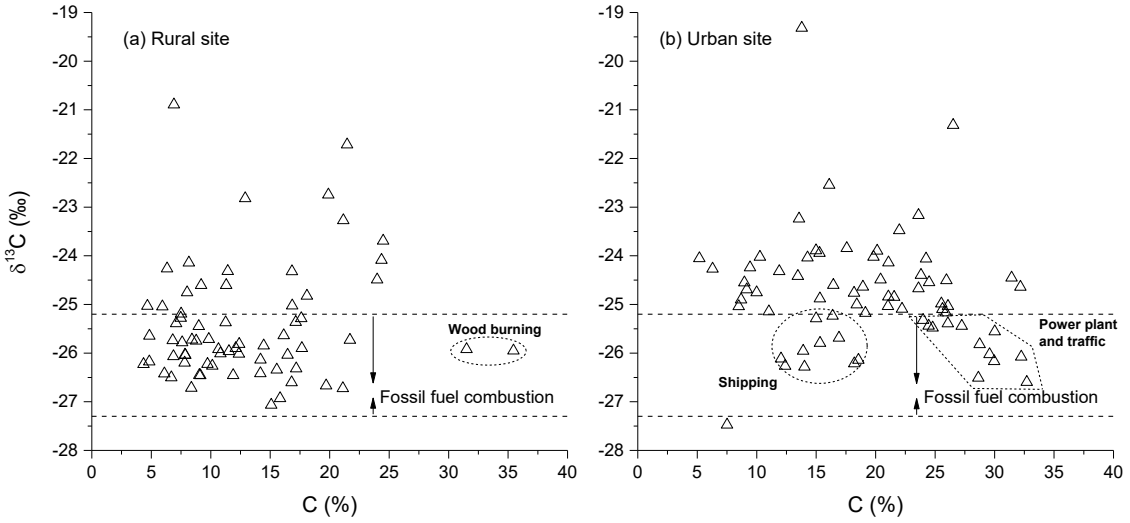

Figure 4.2. $\delta^{13}C$ versus carbon concentrations measured in PM_{10} samples at the rural (a) and urban (b) sites in Cienfuegos. The isotope ranges delimited by horizontal dashed lines indicate the range we obtained for particles generated by fossil fuel combustion.

For the rest of the rural samples that display $\delta^{13}C$> -25.2‰ (Figure 4.2a) at least another source of aerosol is required to explain their higher carbon isotope compositions. Due to the closeness with the sea, inputs of marine aerosols may be expected but no correlation between $\delta^{13}C$ and typical marine constituents (Na, Cl or Mg) was found. Instead, for these samples having $\delta^{13}C$>-25.2‰, we observed a significant statistical correlation with Ca (r=0.5, p<0.05; Table 4.3). This positive correlation probably suggests the influence of emissions from the cement plant and quarries under northeasterly wind directions. This hypothesis may also be supported by the positive correlation observed with the wind speed (r= 0.3, p<0.01), as these sources are located about 25 km northeast from the sampling site, but it could also suggest a contribution from soil dust resuspension, which showed an average $\delta^{13}C$ of -20.5 ± 4.8‰ (Table 4.1). Other significant correlations were observed with Sn, Cd, ΔpH and relative humidity (RH). The positive correlation with Sn and Cd may be indicative of industrial emissions (Taiwo et al., 2014), and thus probably relate to the cement plant, comforted by the fact

that the highest concentrations for Sn and Cd were obtained under northeasterly winds and high wind speeds.

At the urban site (Figure 4.2b), only 33% of the PM_{10} samples have $\delta^{13}C$ compatible with the isotope range previously defined for fossil fuel combustion (-27.3 to -25.2‰), which suggests that carbonaceous matter there is controlled by other sources of contamination. Similarly to the rural site, within the $\delta^{13}C$ range of -27.3 to -25.2‰ two distinct groups of PM_{10} samples can be defined based on their carbon content: samples with low (<20%) and high (>25%) carbon concentrations. Samples with low carbon contents were all collected when winds were blowing from the east-south and south-west sectors and generally with relatively low speeds, which may indicate the influence of shipping emissions coming from the harbor area located very close to the sampling site in those sectors and the overall maritime traffic in the same area of the bay. Samples displaying the high carbon contents (>25%) were collected when prevalent winds were blowing from northern directions with an average wind speed of 3 kmh^{-1}. It may indicate the influence of particle emissions from both the power plant and road traffic. These results are corroborated by the agreement in carbon concentration with the soot samples representative of emission from road traffic, shipping and combustion residues from the TPP stacks (Table 4.1). This conclusion is confirmed by the significant correlation we observed between $\delta^{13}C$ and typical tracers of these sources (Table 4.3): negative correlation (i.e. depletion in ^{13}C when the element concentrations increases) with Cu, Mo, W, S and SO_4^{2-}. Cu, Mo and W are specific tracers of road traffic emissions (Grigoratos and Martini, 2015; Johansson et al., 2009), while S is mainly emitted as SO_2 during fossil fuel combustion and rapidly reacts once in the atmosphere to form secondary sulfate (SO_4^{2+}) (Bove et al., 2016).

Table 4.3. Correlation coefficients (r) and *p*-values obtained between $\delta^{13}C$ or $\delta^{15}N$ and both some chemical elements in the PM_{10} samples and meteorological variables for the rural and urban sites in Cienfuegos (Morera-Gómez et al., 2018). The significant correlations (p <0.05) are in bold.

Variable	$\delta^{13}C$ Rural site		$\delta^{13}C$ Urban site		$\delta^{15}N$ Urban site	
	r	*p*-value	r	*p*-value	r	*p*-value
C (%)	0.135	0.274	-0.153	0.205	**0.257**	**0.045**
N (%)	–	–	-0.250	0.052	**0.522**	**0.000**
Na (%)	0.086	0.486	-0.173	0.152	-0.189	0.142
Cl^- (%)	0.135	0.271	-0.119	0.326	-0.196	0.126
Mg (%)	0.096	0.436	0.008	0.951	**-0.283**	**0.026**
Ca (%)	**0.467**[a]	**0.038**	**0.708**	**0.000**	-0.045	0.729
S (%)	0.072	0.560	**-0.394**	**0.001**	**0.467**	**0.000**
NH_4^+	0.075	0.542	-0.157	0.196	**0.618**	**0.000**
SO_4^{2-} (%)	-0.021	0.864	**-0.340**	**0.004**	**0.571**	**0.000**
Cd (%)	**0.261**	**0.032**	-0.069	0.573	**-0.254**	**0.047**
Sr (%)	0.015	0.904	**0.412**	**0.000**	-0.041	0.749
Cu (%)	-0.189	0.122	**-0.344**	**0.004**	-0.007	0.956
Mo (%)	0.064	0.603	**-0.409**	**0.000**	0.074	0.568
Sn (%)	**0.377**	**0.002**	**0.354**	**0.003**	-0.040	0.757
W (%)	-0.077	0.533	**-0.356**	**0.002**	0.020	0.880
ΔpH[b]	**-0.280**	**0.021**	**0.678**	**0.000**	-0.196	0.127
Wind speed (km h^{-1})	**0.345**	**0.004**	0.112	0.356	**-0.354**	**0.005**
Relative humidity (%)	**-0.400**	**0.001**	**-0.487**	**0.000**	-0.037	0.773

[a]Determined only for samples having $\delta^{13}C$>-25.2‰ (n=20).
[b]pH variation calculated as the pH difference between the PM_{10} sample and a blank filter.

Samples enriched in ^{13}C ($\delta^{13}C$ > -25.2‰) represent the largest group at the urban site and, similarly to the rural site, we found them to be related with atmospheric emissions from the cement plant and quarries located 15 km E-NE of the study site. This is also corroborated by the strong correlations observed between their $\delta^{13}C$ and both their Ca contents and ΔpH (Table 4.3). In contrast to the rural station, the correlation with ΔpH was positive. This may be explained by an excess of carbonates in the urban PM_{10}, which once again points out to atmospheric emissions from the cement plant that buffer acidic matter by addition of their inherent carbonates (Galindo et al., 2011). In addition, these samples were collected in days with northeasterly and easterly prevalent winds and higher wind speeds (frequently >10 kmh^{-1}) indicating the influence of a distant source in that sector. We also observed a positive correlation between $\delta^{13}C$ and both Sn and Sr

(Table 4.3), indicative of the presence of industrial and mineral fractions in the urban PM_{10} that is consistent with the influence of emissions from the cement plant and quarries. The high Sn and Sr concentrations were observed under easterly winds and higher wind speed, which agrees with this conclusion as it corresponds to the location of these emission sources.

Conditional probability functions have mostly been used in conjunction with stable isotope compositions to elucidate the breeding origins of migratory animals (Royle and Rubenstein, 2004; Wunder et al., 2005), but to our knowledge not yet to track sources of aerosol contamination. We ran separate CBPF analysis on our rural and urban datasets (including $\delta^{13}C$ as a variable). For each dataset we distinguished the 2 groups defined in Figure 4.3 (based on their $\delta^{13}C$, with a threshold set at -25.2‰): Figures 4.3a (rural) and 4.3c (urban) with all samples having $\delta^{13}C \leq$ -25.2‰ indicate local (generally associated to low wind speeds) contamination by fossil fuel burning, including wood burning in the case of the rural site. Figures 4.3b (rural) and 4.3d (urban) with all samples having $\delta^{13}C >$ -25.2‰ identify a contamination from more distant sources along the northeast direction, where the cement plant and quarries are located.

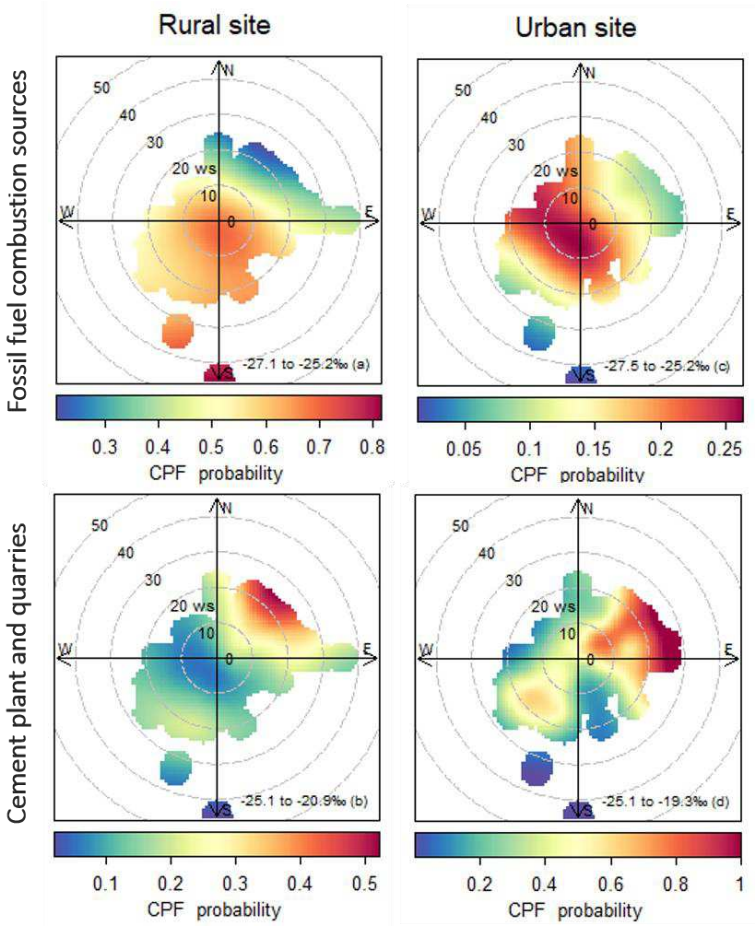

Figure 4.3. Conditional bivariate probability function plots obtained at the rural and urban sites in Cienfuegos. For each study site, the distinction between the two graphs created is made based on the PM_{10} carbon isotope compositions with a threshold set at $\delta^{13}C$=-25.2‰. "Ws" corresponds to wind speed.

We can then model mixing relationships for these two end-members using mass balance equations, and ultimately estimate their respective contributions for each sample. The equation of mixing for a k component system for isotope ratios "I" can be expressed in the following way (Douglass and Schilling, 2000):

$$I = \sum_{i=1}^{k} z_i n_i I_i \Big/ \sum_{i=1}^{k} z_i n_i \qquad (4.3)$$

With $\sum_{i=1}^{k} z_i = 1$ and $0 \leq z_i \leq 1$, and where I is the isotope ratio in the mixture, I_i the isotope ratio in each end-member component, z_i the mass fraction of component 1, 2, 3… and n_i the relative enrichment of element I in component 1, 2, 3… relative to component k (i.e. $n_i = c_i/c_k$; where c is the concentration of element I). In our model

we considered the following characteristics: -26.5 ± 1.0‰ for fossil fuel burning and -20.0 ± 1.0‰ for the cement plant. This latest value is considered a representative $\delta^{13}C$ estimation of emissions from the cement plant that considers all the carbon-containing compounds related to the fabrication of cement: emissions from the cement plant, quarries, transportations and storage of petroleum coke… Results indicate that the average relative contribution of the cement plant and quarries to the carbon content in PM_{10} was estimated to be 6 – 30% and 12 – 40% at the rural and urban sites, respectively. These results confirm that the daily $\delta^{13}C$ observed in PM_{10} in Cienfuegos are mainly governed by aerosol emissions from local sources, with a clear prevalence of fossil fuel combustion contributions at both sites (70 – 94% at the rural site and 60 – 88% at the urban site).

4.2. Nitrogen isotope compositions

Figure 4.4a reports the TN and $\delta^{15}N$ isotope compositions of both PM_{10} aerosols and particles emitted by potential sources of contamination. The high variability observed in the $\delta^{15}N$ (between 1.5 and 19.1‰; Table 4.2) in Cienfuegos PM_{10} could reveal either that multiple sources of (primary) nitrogen are involved or that secondary processes undergo in the atmosphere post-emission that induce nitrogen isotope fractionation (nitrogen in the aerosols is then of secondary origin; (Ciezka et al., 2016; Widory, 2007)). The hypothesis that post-emission processes may generate secondary nitrogen is also supported by the fact that our PM_{10} samples all have TN concentrations higher than those measured in particles from the sources of contamination, clearly indicating the presence of a N excess in the aerosols. Ultimately the $\delta^{15}N$ measured in the PM_{10} may also result from a mixture of both primary and secondary nitrogen. However, the significant positive correlation observed between the $\delta^{15}N$ in PM_{10} and the TN and NH_4^+ concentrations (Table 4.3) suggest that secondary processes are the dominant pathway to generate nitrogen in the aerosols (Bikkina et al., 2016; Pavuluri et al., 2010). At the urban site, inorganic nitrogen ($N\text{-}NH_4^+$ + $N\text{-}NO_3^-$, obtained from Morera-Gómez et al., (2018)) represents on average 65% of the TN, and $N\text{-}NH_4^+$ is the major inorganic fraction (71%). It is thus likely that one source of NH_4^+ and/or the exchange between gas (NH_3) and particle (NH_4^+) controls the $\delta^{15}N$ of the total nitrogen in PM_{10}.

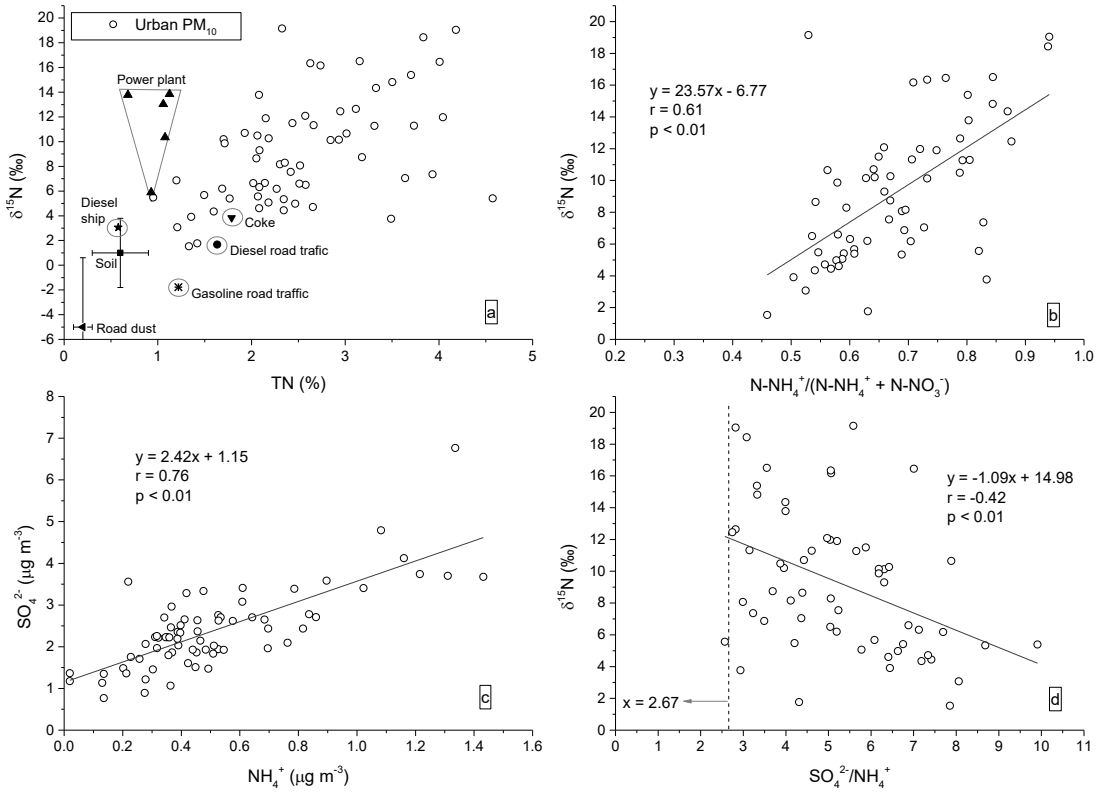

Figure 4.4. Nitrogen characteristics in PM_{10} samples from Cienfuegos. a) Total nitrogen (TN) and $\delta^{15}N$. Characteristics of particles from the main sources of contamination are also reported (bars represents the standard deviation with 1σ). b) $\delta^{15}N$ vs. $N\text{-}NH_4^+$ relative inorganic fraction. c) SO_4^{2-} vs. NH_4^+ concentrations. d) $\delta^{15}N$ vs. SO_4^{2-}/NH_4^+ ratios.

The positive trend observed between $\delta^{15}N$ and the relative N inorganic fraction (e.g. $N\text{-}NH_4^+$; Figure 4.4b) strongly suggests that NH_4^+ controls the final $\delta^{15}N$ in PM_{10}. We observe a significant ^{15}N enrichment (almost 17‰) positively correlated with the relative $N\text{-}NH_4^+$ content during the year of sampling. NH_4^+ is also positively correlated with SO_4^{2-} (Figure 4.4c), suggesting the formation of ammonium sulfate ($(NH_4)_2SO_4$). In addition, these two species (NH_4^+ and SO_4^{2-}) are correlated with V (r=0.4, p<0.01 for both NH_4^+ and SO_4^{2-} (Morera-Gómez et al., 2018)), indicating that they are mainly formed during fossil fuel combustion (Moreno et al., 2010). As nitrogen in aerosols, mainly present under the forms of ammonium and nitrate ions, is mostly generated from gaseous precursors (i.e., NH_3 and NO_x produced during fossil fuel combustion), the trend observed in Figure 4.4b may finally suggest that $\delta^{15}N$ in PM_{10} traces the formation of secondary nitrogen using gaseous precursors from fossil fuel combustion.

Heaton et al., (1997) exposed H_2SO_4-containing filters to an NH_3-rich atmosphere for various periods of time. While results showed that for short exposure periods (1 to 3 min) the final $\delta^{15}N$ of the generated NH_4^+ was lower than the isotope composition of the initial NH_3, for longer exposure periods (>10 min), when equilibrium conditions were reached, the final $\delta^{15}N$-NH_4^+ became higher than the one of the initial NH_3. ^{15}N-enrichments of up to 33‰ were reported (Heaton et al., 1997). The authors concluded that, at the onset, the reaction between NH_3 and H_2SO_4 is unidirectional (i.e. kinetic isotope fractionation) and favors the lighter isotopes (^{14}N) in the $(NH_4)_2SO_4$ formed. But when the reaction reaches the stoichiometric equilibrium (~6 min), a NH_3/NH_4^+ equilibrium isotope exchange takes place, resulting in a final $\delta^{15}N$-NH_4^+ higher than the one of the initial NH_3.

PM_{10} aerosols in Cienfuegos present an average SO_4^{2-}/NH_4^+ molar ratios of 5.1 $\pm$ 1.7 showing a SO_4^{2-}enrichment (Morera-Gómez et al., 2018) probably resulting from the use of sulfur-rich crude oil in the TPP, as well as the fast conversion of SO_2 into sulphate catalyzed by high UV radiation and humidity conditions (Bove et al., 2016), that are typical of the Caribbean region. Figure 4.4d shows that $\delta^{15}N$ values are negatively correlated with SO_4^{2-}/NH_4^+. It suggests that when NH_3 reaches a stoichiometric equilibrium with $(NH_4)_2SO_4$ (reached for a SO_4^{2-}/NH_4^+ molar ratio of 2.67) it enhances ^{15}N enrichment in agreement with Heaton et al., (1997). A similar trend have been recently observed over the Bay of Bengal, in which the $\delta^{15}N$ of TN in $PM_{2.5}$ (10.4 to 31.7‰) has been shown to significantly be influenced by the exchange reaction of gaseous NH_3 and particulate NH_4^+ during the formation of ammonium sulfate aerosols (Bikkina et al., 2016). In general, a ^{15}N isotope fractionation have been suggested in aerosol (Pavuluri et al., 2010) and rainwater samples (Ciezka et al., 2016) collected around the world during the equilibrium exchange between NH_3 and NH_4^+.

As discussed in Widory, (2007), if the trend observed between $\delta^{15}N$ and TN reflects the formation of secondary nitrogen in PM_{10}, it can be assumed that the aerosols having the lowest TN are the closest representatives of the primary nitrogen origin (e.g. their TN is mostly controlled by primary nitrogen and include low secondary nitrogen). If we consider this hypothesis, the $\delta^{15}N$ of low-TN in PM_{10} are consistent with the isotope

ranges we measured in 3 potential sources of contamination (Figure 4.4a): diesel road traffic, TPP (crude oil combustion) and petroleum-coke. Ultimately it comes that, taking into account the previous findings (i.e. secondary nitrogen formation linked to gaseous precursors from fossil fuel combustion), our results identify diesel road traffic and TTP emissions as the main sources of primary nitrogen in the PM_{10} collected in Cienfuegos. This conclusion is consistent with the fact that most of the transportation vehicles in Cuba are running on diesel fuel, and that thus gasoline road traffic is expected to have a lower impact.

Finally, the weak but significant negative correlation observed between the $\delta^{15}N$ and wind speed (Table 4.3) reinforces our conclusion that the $\delta^{15}N$ enrichment we are observing in PM_{10} under low wind speeds is most probably generated by particle and gas emissions from local anthropogenic sources rather than from regional or long-range transportation. This is consistent with our $\delta^{13}C$ results (section 4.1), indicating that the C and N present in aerosols in Cienfuegos share common origins (i.e. mainly the combustion of fossil fuels). This conclusion is also in agreement with the Positive Matrix Factorization (PMF) analysis undertaken to apportion sources of aerosol contamination in the study area (Morera-Gómez et al., 2018), and confirm the added value of the carbon and nitrogen stable isotope approaches for tracing sources and secondary processes controlling the budget of the aerosols in rural and urban atmospheres.

5. Conclusions

Aerosols (PM_{10}) from a rural and an urban sites and particles emitted by sources of contamination in Cienfuegos have been chemically (TC and TN) and isotopically ($\delta^{13}C$ and $\delta^{15}N$) characterized for first time in Cuba. Results lead to the following conclusions:

I. While carbon concentration in particles emitted by sources of contamination displayed a large range of values (9.0 – 78.2%), nitrogen concentration showed a narrower range (0.2 – 1.8 %). In comparison, carbon contents in PM_{10} were significantly lower at both the rural (12.9 ± 6.5%) and urban (19.3

± 7.1%) sites. For nitrogen, concentrations were higher at the urban site (2.5 ± 0.8%), which suggests secondary formation.

II. Carbon and nitrogen isotope compositions discriminated particle emissions between road traffic, industrial (TPP) and shipping. Meanwhile, other sources (soil, road dust and atmospheric deposition around cement plant) presented large ranges of variation that usually overlapped.

III. $\delta^{13}C$ at both sites result of mixing contributions from two main emitters: fossil fuel combustion and cement plant and quarries. The relative contribution of the cement plant and quarries was estimated to be 6 – 30% and 12 – 40% at the rural and urban site, respectively. Additionally, coupling carbon concentration in PM_{10} having a $\delta^{13}C$<-25.2‰ (which corresponds to the isotope range of emissions from fossil fuel combustion) with prevalent meteorological conditions at the time of sampling helped distinguish the influence of shipping, traffic and power plant emissions at the urban site and the influence of local wood burning at the rural site.

IV. $\delta^{15}N$ values at the urban site were positively correlated with TN, NH_4^+ and SO_4^{2-} concentrations, indicating the formation of secondary nitrogen under the form of $(NH_4)_2SO_4$. Exchange between gas (NH_3) and particle (NH_4^+) under stoichiometric equilibrium in $(NH_4)_2SO_4$ can explain the ^{15}N enrichment observed in PM_{10}. By comparing $\delta^{15}N$ values in PM_{10} at lower nitrogen concentrations with those measured in samples from potential sources of contamination we concluded that primary nitrogen may mainly be generated by diesel road traffic and the power plant emissions.

Acknowledgments

The authors express their gratitude to the analytical staff of the GEOTOP research center at UQAM for its assistance. This research has received funding from "la Caixa" Banking Foundation. The study was also supported by the IAEA TC Project CUB/7/008 “Strengthening the National System for Analysis of the Risks and Vulnerability of Cuba’s Coastal Zone Through the Application of Nuclear and Isotopic Techniques” and National Program PNUOLU /4-1/ 2 No. /2014 of the National Nuclear Agency.

References

Bikkina, S., Kawamura, K., Sarin, M., 2016. Stable carbon and nitrogen isotopic composition of fine mode aerosols (PM2.5) over the Bay of Bengal: impact of continental sources. Tellus B Chem. Phys. Meteorol. 68, 31518. https://doi.org/10.3402/tellusb.v68.31518

Bove, M.C., Brotto, P., Calzolai, G., Cassola, F., Cavalli, F., Fermo, P., Hjorth, J., Massabò, D., Nava, S., Piazzalunga, A., Schembari, C., Prati, P., 2016. PM10 source apportionment applying PMF and chemical tracer analysis to ship-borne measurements in the Western Mediterranean. Atmos. Environ. 125, 140–151. https://doi.org/10.1016/j.atmosenv.2015.11.009

Cachier, H., Buat-Menard, P., Fontugne, M., Rancher, J., 1985. Source terms and source strengths of the carbonaceous aerosol in the tropics. J. Atmospheric Chem. 3, 469–489. https://doi.org/10.1007/BF00053872

Carslaw, D.C., 2015. The Openair Manual — Open-source Tools for Analysing Air Pollution Data. Manual for version 1.1-4.

Ceburnis, D., Garbaras, A., Szidat, S., Rinaldi, M., Fahrni, S., Perron, N., Wacker, L., Leinert, S., Remeikis, V., Facchini, M.C., Prevot, A.S.H., Jennings, S.G., Ramonet, M., O'Dowd, C.D., 2011. Quantification of the carbonaceous matter origin in submicron marine aerosol by 13C and 14C isotope analysis. Atmos Chem Phys 11, 8593–8606. https://doi.org/10.5194/acp-11-8593-2011

Ceburnis, D., Rinaldi, M., Ovadnevaite, J., Martucci, G., Giulianelli, L., O'Dowd, C.D., 2016. Marine submicron aerosol gradients, sources and sinks. Atmospheric Chem. Phys. 16, 12425–12439. https://doi.org/10.5194/acp-16-12425-2016

Chen, Y., Du, W., Chen, J., Hong, Y., Zhao, J., Xu, L., Xiao, H., 2017. Chemical composition, structural properties, and source apportionment of organic macromolecules in atmospheric PM10 in a coastal city of Southeast China. Environ. Sci. Pollut. Res. 24, 5877–5887. https://doi.org/10.1007/s11356-016-8314-5

Chesselet, R., Fontugne, M., Buat-Ménard, P., Ezat, U., Lambert, C.E., 1981. The origin of particulate organic carbon in the marine atmosphere as indicated by its stable carbon isotopic composition. Geophys. Res. Lett. 8, 345–348. https://doi.org/10.1029/GL008i004p00345

Ciezka, M., Modelska, M., Gorka, M., Trojanowska-Olichwer, A., Widory, D., 2016. Chemical and isotopic interpretation of major ion compositions from precipitation: a one-year temporal monitoring study in Wroclaw, SW Poland. J. Atmospheric Chem. 73, 61–80. https://doi.org/10.1007/s10874-015-9316-2

Cifuentes L. A., Sharp J. H., Fogel Marilyn L., 1988. Stable carbon and nitrogen isotope biogeochemistry in the Delaware estuary. Limnol. Oceanogr. 33, 1102–1115. https://doi.org/10.4319/lo.1988.33.5.1102

Douglass, J., Schilling, J.G., 2000. Systematics of three-component, pseudo-binary mixing lines in 2D isotope ratio space representations and implications for mantle plume-ridge interaction. Chem. Geol. 163, 1–23. https://doi.org/10.1016/S0009-2541(99)00070-4

Galindo, N., Yubero, E., Nicolas, J.F., Crespo, J., Pastor, C., Carratala, A., Santacatalina, M., 2011. Water-soluble ions measured in fine particulate matter next to cement works. Atmos. Environ. 45, 2043–2049. https://doi.org/10.1016/j.atmosenv.2011.01.059

Garbaras, A., Masalaite, A., Garbariene, I., Ceburnis, D., Krugly, E., Remeikis, V., Puida, E., Kvietkus, K., Martuzevicius, D., 2015. Stable carbon fractionation in size-segregated aerosol particles produced by controlled biomass burning. J. Aerosol Sci. 79, 86–96. https://doi.org/10.1016/j.jaerosci.2014.10.005

Gorka, M., Rybicki, M., Simoneit, B.R.T., Marynowski, L., 2014. Determination of multiple organic matter sources in aerosol PM10 from Wroclaw, Poland using molecular and stable carbon isotope compositions. Atmos. Environ. 89, 739–748. https://doi.org/10.1016/j.atmosenv.2014.02.064

Gorka, M., Zwolinska, E., Malkiewicz, M., Lewicka-Szczebak, D., Jedrysek, M.O., 2012. Carbon and nitrogen isotope analyses coupled with palynological data of PM10 in Wroclaw city (SW Poland) - assessment of anthropogenic impact. Isotopes Environ. Health Stud. 48, 327–344. https://doi.org/10.1080/10256016.2012.639449

Grigoratos, T., Martini, G., 2015. Brake wear particle emissions: a review. Environ. Sci. Pollut. Res. 22, 2491–2504. https://doi.org/10.1007/s11356-014-3696-8

Guo, X., Li, C., Gao, Y., Tang, L., Briki, M., Ding, H., Ji, H., 2016. Sources of organic matter (PAHs and n-alkanes) in PM2.5 of Beijing in haze weather analyzed by combining the C-N isotopic and PCA-MLR analyses. Environ. Sci.-Process. Impacts 18, 314–322. https://doi.org/10.1039/c6em00037a

Guo, Z., Jiang, W., Chen, S., Sun, D., Shi, L., Zeng, G., Rui, M., 2016. Stable isotopic compositions of elemental carbon in PM1.1 in north suburb of Nanjing Region, China. Atmospheric Res. 168, 105–111. https://doi.org/10.1016/j.atmosres.2015.09.006

Heaton, T.H.E., Spiro, B., Robertson, S.M.C., 1997. Potential canopy influences on the isotopic composition of nitrogen and sulphur in atmospheric deposition. Oecologia 109, 600–607. https://doi.org/10.1007/s004420050122

Johansson, C., Norman, M., Burman, L., 2009. Road traffic emission factors for heavy metals. Atmos. Environ. 43, 4681–4688. https://doi.org/10.1016/j.atmosenv.2008.10.024

Kawashima, H., Haneishi, Y., 2012. Effects of combustion emissions from the Eurasian continent in winter on seasonal δ13C of elemental carbon in aerosols in Japan. Atmos. Environ. 46, 568–579. https://doi.org/10.1016/j.atmosenv.2011.05.015

Kelly, S.D., Stein, C., Jickells, T.D., 2005. Carbon and nitrogen isotopic analysis of atmospheric organic matter. Atmos. Environ. 39, 6007–6011. https://doi.org/10.1016/j.atmosenv.2005.05.030

Kim, B.M., Park, J.-S., Kim, S.-W., Kim, H., Jeon, H., Cho, C., Kim, J.-H., Hong, S., Rupakheti, M., Panday, A.K., Park, R.J., Hong, J., Yoon, S.-C., 2015. Source apportionment of PM10 mass and particulate carbon in the Kathmandu Valley, Nepal. Atmos. Environ. 123, 190–199. https://doi.org/10.1016/j.atmosenv.2015.10.082

Kim, E., Hopke, P.K., 2005. Identification of fine particle sources in mid-Atlantic US area. Water. Air. Soil Pollut. 168, 391–421. https://doi.org/10.1007/s11270-005-1894-1

Kim, E., Hopke, P.K., Edgerton, E.S., 2003. Source identification of Atlanta aerosol by positive matrix factorization. J. Air Waste Manag. Assoc. 53, 731–739.

Lopez-Veneroni, D., 2009. The stable carbon isotope composition of PM2.5 and PM10 in Mexico City Metropolitan Area air. Atmos. Environ. 43, 4491–4502. https://doi.org/10.1016/j.atmosenv.2009.06.036

Mari, M., Sanchez-Soberon, F., Audi-Miro, C., van Drooge, B.L., Soler, A., Grimalt, J.O., Schuhmacher, M., 2016. Source Apportionment of Inorganic and Organic PM in the Ambient Air around a Cement Plant: Assessment of Complementary Tools. Aerosol Air Qual. Res. 16, 3230–3242. https://doi.org/10.4209/aaqr.2016.06.0276

Martinelli, L.A., Camargo, P.B., Lara, L.B.L.S., Victoria, R.L., Artaxo, P., 2002. Stable carbon and nitrogen isotopic composition of bulk aerosol particles in a C4 plant landscape of southeast Brazil. Atmos. Environ. 36, 2427–2432. https://doi.org/10.1016/S1352-2310(01)00454-X

Miyazaki, Y., Kawamura, K., Jung, J., Furutani, H., Uematsu, M., 2011. Latitudinal distributions of organic nitrogen and organic carbon in marine aerosols over the western North Pacific. Atmos Chem Phys 11, 3037–3049. https://doi.org/10.5194/acp-11-3037-2011

Moore, H., 1977. The isotopic composition of ammonia, nitrogen dioxide and nitrate in the atmosphere. Atmospheric Environ. 1967 11, 1239–1243. https://doi.org/10.1016/0004-6981(77)90102-0

Moreno, T., Querol, X., Alastuey, A., de la Rosa, J., Sánchez de la Campa, A.M., Minguillón, M., Pandolfi, M., González-Castanedo, Y., Monfort, E., Gibbons, W., 2010. Variations in vanadium, nickel and lanthanoid element concentrations in urban air. Sci. Total Environ. 408, 4569–4579. https://doi.org/10.1016/j.scitotenv.2010.06.016

Morera-Gómez, Y., Elustondo, D., Lasheras, E., Alonso-Hernandez, C.M., Santamaría, J.M., 2018. Simultaneous monitoring and chemical characterization of PM10 in rural and urban Caribbean coastal sites: local and long-range source apportionment. Atmospheric Environ. Submitt.

Mukherjee, A., Agrawal, M., 2017. World air particulate matter: sources, distribution and health effects. Environ. Chem. Lett. 15, 283–309. https://doi.org/10.1007/s10311-017-0611-9

Naru, D., Harmelin-Vivien, M., Gomoiu, M.T., Onciu, T.M., 2007. Influence of the Danube River inputs on C and N stable isotope ratios of the Romanian coastal waters and sediment (Black Sea). Mar. Pollut. Bull. 54, 1385–1394.

Pavuluri, C.M., Kawamura, K., Tachibana, E., Swaminathan, T., 2010. Elevated nitrogen isotope ratios of tropical Indian aerosols from Chennai: Implication for the origins of aerosol nitrogen in South and Southeast Asia. Atmos. Environ. 44, 3597–3604. https://doi.org/10.1016/j.atmosenv.2010.05.039

Peng, T.-R., Liang, W.-J., Liu, T.-S., Lin, Y.-W., Zhan, W.-J., 2015. Assessing the authenticity of commercial deep-sea drinking water by chemical and isotopic approaches. Isotopes Environ. Health Stud. 51, 322–331. https://doi.org/10.1080/10256016.2015.1016431

Pope, C.A., Dockery, D.W., 2006. Health effects of fine particulate air pollution: Lines that connect. J. Air Waste Manag. Assoc. 56, 709–742.

Proemse, B.C., Mayer, B., Chow, J.C., Watson, J.G., 2012. Isotopic characterization of nitrate, ammonium and sulfate in stack PM2.5 emissions in the Athabasca Oil Sands Region, Alberta, Canada. Atmos. Environ. 60, 555–563. https://doi.org/10.1016/j.atmosenv.2012.06.046

Reisen, F., Meyer, C.P., Keywood, M.D., 2013. Impact of biomass burning sources on seasonal aerosol air quality. Atmos. Environ. 67, 437–447. https://doi.org/10.1016/j.atmosenv.2012.11.004

Royle, J.A., Rubenstein, D.R., 2004. The role of species abundance in determining breeding origins of migratory birds with stable isotopes. Ecol. Appl. 14, 1780–1788.

Sharma, H., Jain, V.K., Khan, Z.H., 2007. Characterization and source identification of polycyclic aromatic hydrocarbons (PAHs) in the urban environment of Delhi. Chemosphere 66, 302–310. https://doi.org/10.1016/j.chemosphere.2006.05.003

Squizzato, S., Cazzaro, M., Innocente, E., Visin, F., Hopke, P.K., Rampazzo, G., 2017. Urban air quality in a mid-size city - PM2.5 composition, sources and identification of impact areas: From local to long range contributions. Atmospheric Res. 186, 51–62. https://doi.org/10.1016/j.atmosres.2016.11.011

Sudheer, A.K., Aslam, M.Y., Upadhyay, M., Rengarajan, R., Bhushan, R., Rathore, J.S., Singh, S.K., Kumar, S., 2016. Carbonaceous aerosol over semi-arid region of western India: Heterogeneity in sources and characteristics. Atmospheric Res. 178–179, 268–278. https://doi.org/10.1016/j.atmosres.2016.03.026

Taiwo, A.M., Harrison, R.M., Shi, Z., 2014. A review of receptor modelling of industrially emitted particulate matter. Atmos. Environ. 97, 109–120. https://doi.org/10.1016/j.atmosenv.2014.07.051

Turekian, V.C., Macko, S.A., Keene, W.C., 2003. Concentrations, isotopic compositions, and sources of size-resolved, particulate organic carbon and oxalate in near-surface marine air at Bermuda during spring. J. Geophys. Res. Atmospheres 108, 4157. https://doi.org/10.1029/2002JD002053

Turtos Carbonell, L.M., Meneses Ruiz, E., Sanchez Gacita, M., Rivero Oliva, J., Diaz Rivero, N., 2007. Assessment of the impacts on health due to the emissions of Cuban power plants that use fossil fuel oils with high content of sulfur. Estimation of external costs. Atmos. Environ. 41, 2202–2213. https://doi.org/10.1016/j.atmosenv.2006.10.062

Uria-Tellaetxe, I., Carslaw, D.C., 2014. Conditional bivariate probability function for source identification. Environ. Model. Softw. 59, 1–9. https://doi.org/10.1016/j.envsoft.2014.05.002

Wang, G., Xie, M., Hu, S., Gao, S., Tachibana, E., Kawamura, K., 2010. Dicarboxylic acids, metals and isotopic compositions of C and N in atmospheric aerosols from inland China: implications for dust and coal burning emission and secondary aerosol formation. Atmospheric Chem. Phys. 10, 6087–6096. https://doi.org/10.5194/acp-10-6087-2010

WHO, 2016. WHO | WHO releases country estimates on air pollution exposure and health impact [WWW Document]. WHO. URL http://www.who.int/mediacentre/news/releases/2016/air-pollution-estimates/en/ (accessed 3.21.17).

WHO, 2005. WHO | Air quality guidelines for particulate matter, ozone, nitrogen dioxide and sulfur dioxide- global update 2005 [WWW Document]. WHO. URL http://www.who.int/phe/health_topics/outdoorair/outdoorair_aqg/en/ (accessed 3.6.16).

Widory, D., 2007. Nitrogen isotopes: Tracers of origin and processes affecting PM10 in the atmosphere of Paris. Atmos. Environ. 41, 2382–2390. https://doi.org/10.1016/j.atmosenv.2006.11.009

Widory, D., Roy, S., Le Moullec, Y., Goupil, G., Cocherie, A., Guerrot, C., 2004. The origin of atmospheric particles in Paris: a view through carbon and lead isotopes. Atmos. Environ. 38, 953–961. https://doi.org/10.1016/j.atmosenv.2003.11.001

Wunder, M.B., Kester, C.L., Knopf, F.L., Rye, R.O., 2005. A test of geographic assignment using isotope tracers in feathers of known origin. Oecologia 144, 607–617. https://doi.org/10.1007/s00442-005-0071-y

Yeatman, S.G., Spokes, L.J., Dennis, P.F., Jickells, T.D., 2001. Can the study of nitrogen isotopic composition in size-segregated aerosol nitrate and ammonium be used to investigate atmospheric processing mechanisms? Atmos. Environ. 35, 1337–1345. https://doi.org/10.1016/S1352-2310(00)00457-X

Supplementary material

Table S4.1. Concentrations of total carbon (TC) and their corresponding stable isotope compositions ($\delta^{13}C$) measured in ambient PM_{10} samples in the studied rural site in Cienfuegos, Cuba.

Date	$\delta^{13}C$(‰)	TC(%)
31/01/2015	-23.27	21.15
03/02/2015	-23.69	24.50
06/02/2015	-22.74	19.89
09/02/2015	-25.36	17.15
15/02/2015	-21.71	21.46
18/02/2015	-25.28	7.47
21/02/2015	-24.60	11.30
24/02/2015	-26.45	9.05
02/03/2015	-25.45	9.00
05/03/2015	-24.32	16.83
08/03/2015	-25.78	7.59
11/03/2015	-22.82	12.89
17/03/2015	-25.90	17.66
20/03/2015	-25.95	35.45
23/03/2015	-24.49	23.99
26/03/2015	-24.09	24.36
01/04/2015	-25.90	12.11
04/04/2015	-24.32	11.43
07/04/2015	-24.60	9.19
10/04/2015	-26.42	6.11
16/04/2015	-24.82	18.09
19/04/2015	-25.92	31.51
22/04/2015	-26.46	11.89
25/04/2015	-24.14	8.16
01/05/2015	-25.29	17.61
04/05/2015	-26.60	16.80
07/05/2015	-25.82	12.39
10/05/2015	-25.04	5.93
16/05/2015	-20.89	6.90
19/05/2015	-25.75	8.78
22/05/2015	-25.73	21.71
25/05/2015	-25.74	6.80
31/05/2015	-26.93	15.83
03/06/2015	-26.26	10.13
06/06/2015	-26.67	19.71
09/06/2015	-25.96	11.53
15/06/2015	-25.73	8.42
18/06/2015	-24.26	6.33
21/06/2015	-25.64	4.84
24/06/2015	-26.20	7.80
30/06/2015	-26.03	7.84
03/07/2015	-26.46	9.12
06/07/2015	-25.03	4.67
09/07/2015	-25.19	7.51
15/07/2015	-26.01	12.37
18/07/2015	-26.72	21.11
21/07/2015	-26.23	4.35
24/07/2015	-26.42	14.17
30/07/2015	-26.17	4.83
02/08/2015	-26.14	14.19
15/11/2015	-27.07	15.09
21/11/2015	-26.04	16.47
27/11/2015	-26.07	6.87
30/11/2015	-25.71	9.84
03/12/2015	-25.64	16.14
06/12/2015	-25.37	11.26
12/12/2015	-26.01	10.81
15/12/2015	-26.32	17.19
18/12/2015	-26.34	15.56
21/12/2015	-26.04	7.87
27/12/2015	-26.72	8.37
30/12/2015	-25.92	10.65
02/01/2016	-25.39	7.09
05/01/2016	-24.75	8.02
11/01/2016	-25.02	16.85
14/01/2016	-25.85	14.45
17/01/2016	-26.50	6.68
20/01/2016	-26.23	9.73
Average	*-25.45*	*12.92*
SD	*1.19*	*6.46*
Min	*-27.07*	*4.4*
Max	*-20.89*	*35.5*
5th	*-26.70*	*5.22*
95th	*-22.98*	*24.23*

Table S4.2. Concentrations of total carbon (TC), total N (TN) and their corresponding stable isotope compositions ($\delta^{13}C$ and $\delta^{15}N$) measured in ambient PM_{10} samples in the studied urban site in Cienfuegos, Cuba.

Date	$\delta^{13}C$(‰)	TC(%)	$\delta^{15}N$(‰)	TN(%)
31/01/2015	-23.48	21.99	6.5	2.6
03/02/2015	-23.17	23.61	6.6	2.5
15/02/2015	-21.31	26.52	--	--
18/02/2015	-26.28	14.02	16.5	4.0
21/02/2015	-24.14	21.07	8.1	2.5
24/02/2015	-22.54	16.10	8.2	2.3
11/03/2015	-23.24	13.57	7.0	3.6
17/03/2015	-24.02	19.82	6.9	1.2
20/03/2015	-24.06	24.24	11.3	2.7
23/03/2015	-25.03	26.09	5.6	2.1
26/03/2015	-24.67	23.61	16.2	2.7
01/04/2015	-23.84	17.58	8.7	3.2
04/04/2015	-23.89	14.99	11.9	2.2
10/04/2015	-24.04	14.28	10.7	3.0
19/04/2015	-25.29	15.00	5.4	4.6
22/04/2015	-24.32	11.90	5.5	1.0
25/04/2015	-24.02	10.27	1.8	1.4
01/05/2015	-25.09	22.22	--	--
04/05/2015	-26.51	28.64	3.8	3.5
07/05/2015	-24.76	18.19	10.2	1.7
10/05/2015	-24.69	9.16	19.1	2.3
16/05/2015	-25.69	16.92	12.0	4.0
19/05/2015	-24.85	21.55	--	--
22/05/2015	-25.39	26.07	10.5	2.1
25/05/2015	-25.04	8.49	--	--
31/05/2015	-24.55	24.50	--	--
03/06/2015	-26.14	18.55	--	--
06/06/2015	-26.02	29.58	--	--
09/06/2015	-19.32	13.79	6.2	1.7
16/06/2015	-24.05	5.18	1.5	1.3
18/06/2015	-24.75	10.00	5.7	1.5
21/06/2015	-24.90	8.68	4.3	1.6
24/06/2015	-25.14	11.03	5.1	2.2
02/07/2015	-25.79	15.33	4.4	2.3
06/07/2015	-24.27	6.29	3.1	1.2
09/07/2015	-24.88	15.31	5.0	2.5
15/07/2015	-24.40	23.81	12.6	3.1
18/07/2015	-26.11	12.04	7.5	2.4
21/07/2015	-26.21	18.21	16.5	3.2
24/07/2015	-24.84	21.07	14.8	3.5
30/07/2015	-24.55	8.97	10.7	1.9
02/08/2015	-25.18	19.14	8.3	2.4
05/08/2015	-24.24	9.44	3.9	1.4
08/08/2015	-25.23	16.38	16.3	2.6
14/08/2015	--	--	9.3	2.1
17/08/2015	-23.94	15.29	10.1	2.8
29/08/2015	-24.42	13.46	6.6	2.0
01/09/2015	-24.64	18.93	12.1	2.6
04/09/2015	-26.17	29.96	12.5	2.9
07/09/2015	-25.17	25.90	18.4	3.8
13/09/2015	-24.49	20.42	15.4	3.7
16/09/2015	-25.00	18.41	6.7	2.1
19/09/2015	-26.26	12.39	6.2	2.3
22/09/2015	-25.04	21.04	14.3	3.3
28/09/2015	-25.48	24.79	19.0	4.2
01/10/2015	-24.60	16.44	11.3	3.7
04/10/2015	-25.96	13.90	11.5	2.4
07/10/2015	-23.90	20.12	13.8	2.1
16/10/2015	-24.45	31.43	4.7	2.7
19/10/2015	-24.64	32.18	7.4	3.9
22/10/2015	-24.50	25.95	4.6	2.1
28/10/2015	-25.44	24.46	10.3	2.2
31/10/2015	-25.44	27.25	11.3	3.3
03/11/2015	-25.56	30.01	10.1	2.9
06/11/2015	-25.32	24.00	5.4	1.8
12/11/2015	-24.98	25.52	6.3	2.1
15/11/2015	-25.10	25.62	5.3	2.3
15/12/2015	-26.08	32.25	8.6	2.1
30/12/2015	-25.82	28.75	9.9	1.7
14/01/2016	-26.60	32.71	--	--
17/01/2016	-27.47	7.51	--	--
Average	*-24.81*	*19.31*	*9.18*	*2.53*
SD	*1.19*	*7.13*	*4.37*	*0.83*
Min	*-27.5*	*5.2*	*1.5*	*1.0*
Max	*-19.3*	*32.7*	*19.1*	*4.6*
5th	*-26.27*	*8.58*	*3.77*	*1.33*
95th	*-23.20*	*30.79*	*16.50*	*4.00*

Chapter 5

Determination and source apportionment of major and trace elements in atmospheric bulk depositions in a Caribbean rural area

This chapter reproduces the text of the following manuscript:

Morera-Gómez, Y., Santamaría, J.M., Elustondo, D., Lasheras, E., Alonso-Hernandez, C.M., 2018. Determination and source apportionment of major and trace elements in atmospheric bulk depositions in a Caribbean rural area. Submitted to Atmospheric Environment.

Abstract

Atmospheric deposition is considered to be the major pathway by which substances from the atmosphere enter to the terrestrial and aquatic ecosystems. This study constitutes the first exhaustive report on trace metal deposition in Cuba and is aimed to determine the monthly atmospheric flux of 47 major and trace elements in a Caribbean coastal site and investigate their main sources of contribution.

Bulk depositions (average of 46 018 μg m^{-2} day^{-1}) and fluxes of studied elements showed a high variability and no seasonality with the dry and wet periods, result that we attributed to the fluctuations of the emissions from their main sources rather than to meteorological factors controlling the deposition processes. However, stronger correlations were found between typical crustal elements, which showed a marked seasonality with the presence of Saharan cloud dust in the Caribbean. Most of the analyzed elements were found in the range of variation of those reported in rural environments around the world but, the elements V, Ni, As and Sb presented higher levels, typically founded in urban and industrial areas. The elements Sb, Pb, W, Sn, S, Cu, Mo, Nb and P were moderately enriched (10<EF<100) and Zn was highly enriched (EF>100), indicating they were mainly derived from anthropogenic sources. The La/V ratios were found to be exclusively lower than 0.06 suggesting the prevalence of anthropogenic emissions from industries with oil and/or petroleum-coke combustion processes rather than from refineries. In this direction, we corroborated that our data was consistent with LaCeV compositions characteristic of emissions related to industries in the studied area such as the thermal power plant, cement plant and also with emission from the road traffic. Finally, Principal Component, Multilinear Regression and Cluster analyses led the identification of 5 main sources contributing to the bulk depositions: crustal matter (39.5%), marine aerosol (38.2%), combustions including the wastes incineration, wood and fossil fuel burning (6.7%), industries (8.7%) and road traffic (1.4%).

Keywords: Atmospheric bulk deposition; Trace elements; Enrichment factors; PCA-MLRA; Saharan dust; Cuba

1. Introduction

Atmospheric particulate matter (PM) is generally defined as a mixture of solid and/or liquid particles that remain individually dispersed in air and it is identified as one of the most significant air pollutants in terms of environmental and health impacts (Grantz et al., 2003; Kanakidou et al., 2005; Okin et al., 2011; Pope and Dockery, 2006). Wet and dry deposition are important processes for removing PM and other pollutants from the atmosphere on urban, regional, and global scales (U.S. EPA, 2009). The residence time of particles (and associated trace elements) in the atmosphere depends on their size. While the rate of deposition is slower for fine particles, the coarse particles settle out quickly near their sources by sedimentation or impaction processes. Thus, deposition is a significant pathway for transferring trace elements from the atmosphere to the terrestrial surfaces and aquatic ecosystems. It is important for PM and its elemental concentrations and compositions to be measured, monitored and determined in rural, urban and industrial regions in order to assess whether it has negative effects on biotic or abiotic environments.

Bulk deposition sampling (i.e., sampling the total deposition fluxes without separating as wet or dry), provides some advantages compared to ambient air monitoring, such as being low cost, and simple, having no needed for electrical power, and low maintenance (Dämmgen et al., 2005; Shanquan et al., 2016). The deposition fluxes of atmospheric PM and the ratio of wet to dry deposition are controlled by emission sources, atmospheric concentrations, distance to receptor sites, and meteorological conditions (i.e. wind speed, prevailing wind directions, frequency, amount and intensity of precipitation) (Mijić et al., 2010; Okubo et al., 2013). Then, the characterization of bulk deposition samples is important for identifying the variability and sources of the atmospheric pollutants.

In the last decades, many studies on the deposition fluxes of trace elements in rural, urban and industrial areas have been widely used to estimate the influence of atmospheric inputs of trace elements to the environmental compartments (Castillo et al., 2013a, 2013b; D'Alessandro et al., 2013; Golomb et al., 1997; Kara et al., 2014; Mijić et al., 2010; Sharma et al., 2008). Some studies have indicated that trace elements

particularly emitted from anthropogenic sources can be persistent, toxic, widely dispersed in the environment (air, water and soil compartments), and interact with different natural components, cause threat to human health and have harmful effects on the biosphere (Baker and Jickells, 2017; Gao et al., 2016; Mason et al., 2006; Morel and Price, 2003; Okin et al., 2011).

The atmospheric depositions in the Gulf of Mexico and southern and eastern coast United States have been largely studied (Golomb et al., 1997; Harris et al., 2012; Strayer et al., 2007). Many of these studies have been not only focused on the input amount of several pollutants, such as heavy metals from anthropogenic and natural local sources, but also on long-range contributions, mainly due to the African transported dust that affects these regions every year (Prospero, 1999; Prospero and Mayol-Bracero, 2013; Trapp et al., 2010). Nutrients associated with African dust deposition have been linked to toxic algal blooms in the Gulf of Mexico and the coastal environment of South Florida (Lenes et al., 2012; Walsh et al., 2006). However, few studies on atmospheric depositions in the Caribbean basin have been published.

Cuba is the major island in the Caribbean Sea. Scarce reports on pollutants in atmospherics depositions are available, limiting the national and regional evaluations. Some of these studies have been indirectly carried out using dated marine sediment cores (Diaz-Asencio et al., 2014, 2009). To our knowledge, only some heavy metal (Jomolca-Parra et al., 2014), nitrogen compounds (Cuesta-Santos et al., 2001; González-De Zayas et al., 2012) and radionuclides (Alonso-Hernández et al., 2014, 2006) have been directly measured in atmospheric depositions. As a consequence, at present, the understanding of the chemicals elements deposition along the island are quite limited, and studies on the main pollutant sources and factor controlling the atmospheric deposition processes have not been addressed.

In this framework, the objectives of this study were (1) to determine and characterize the levels and seasonal variations of monthly atmospheric bulk depositions and atmospheric fluxes of major and trace elements in a coastal rural region in Cienfuegos Province (Cuba) and (2) to identify and quantify the main sources of major and trace elements in bulk depositions in this area.

2. Materials and methods

2.1. Study area and sampling site

The Cienfuegos region, with a population of ~150 000 inhabitants, is located in the south center part of Cuba on the coast of the Caribbean Sea and contains a number of significant air pollution sources including a large petroleum refinery, a thermal power plant (TPP), a cement plant, a fertilizer plant, a harbour, large pier areas and ship breaking yards, coal storage and packing, scrap storage and classification sites, heavy road traffic, very intense transportation activities including ferrous scrap trucks and busy ports used for transportation. Several villages and agricultural areas and some resorts are also located within the region. The region is mainly classified within the local climate of the Caribbean Sea that is characterized by dry (approximately from May to October) and wet (November to April) seasons. While the annual rainfall in this study reached to 1166 mm, the average rainfall were 820 and 226 mm for wet and dry sampling periods, respectively. Monthly average temperatures during the sampling periods were measured as 25.4 ˚C, max (27.6 ˚C) and min (21.6 ˚C). The wind roses generated for the sampling periods and the main pollution sources are shown in Figure 5.1.

In the present study, the bulk deposition samples were collected at the Environmental Study Centre Facilities (22˚ 03’ N, 80˚ 29’ W) located in a rural area. This sampling site is one of the air monitoring stations in the Environmental Radiological Surveillance Network (RNVRA, Spanish acronyms), established in Cuba in 1990, with the support of the International Atomic Energy Agency (IAEA). Samples collected through this network were used in this study. Locations of the sampling site and settlements in the region are illustrated in Figure 5.1.

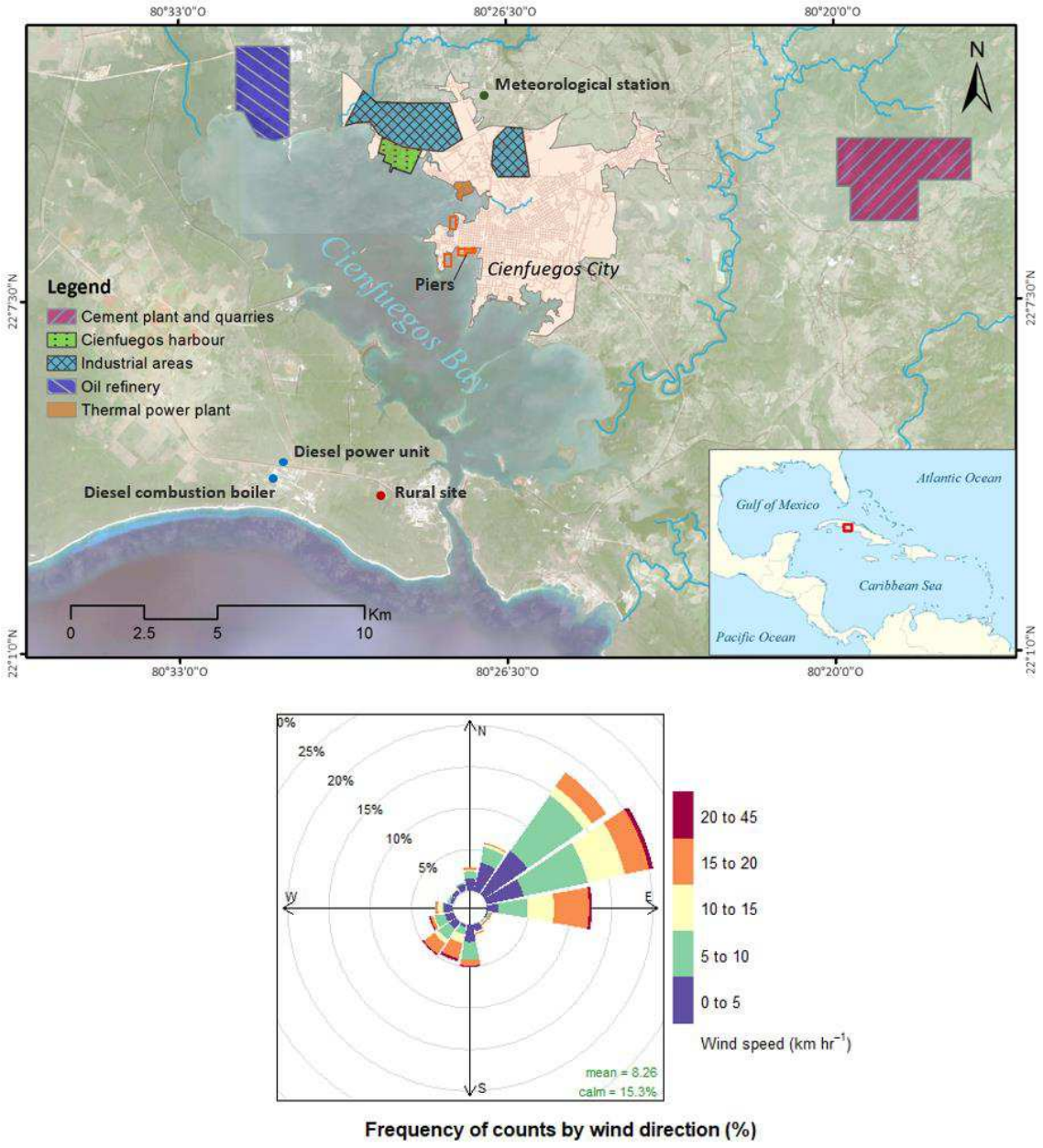

Figure 5.1. Map showing the sampling site, wind rose for the sampling period and main pollution sources in Cienfuegos, Cuba.

2.2. Sample collection and analysis

Sampling of bulk atmospheric deposition (wet + dry) was carried out between March, 2014 and November, 2016. Bulk deposition samples were collected using five bulk rain collectors (50 L polyethylene and 0.25 m^2 of surface area each one). The collectors were installed on a small building roof (about 5 m high of the ground) in the CEAC facilities, and acidified prior to deployment with concentrated HCl. After monthly periods the samples were collected rinsing the walls of collectors twice with distilled

water and combined all into plastic bottles; then the collectors were acidified and deployed again. The samples were immediately transported to the laboratory where they were evaporated to dryness and weighed (before and after the evaporation) to obtain the mass of total deposited particles. The residual particles were ground to a fine powder and stored until chemical analysis.

Determination of chemicals elements was performed by inductively coupled plasma mass spectrometry (ICP-MS, Agilent 7500a), after their acid extraction in closed microwave digestion (CEM Co., Mars X press) adding 0.25 g of sample and 12 ml of aqua regia (HCl/HNO_3=3:1). A multi-elemental solution (Li, Sc, Y, In, Bi, Inorganic Ventures 71D) was added to the samples as internal standard for further determination by ICP-MS. A total of 47 elements, including 13 lanthanoids elements (La to Lu), were simultaneously quantified in all samples using this procedure.

For comparison purposes, several samples from potential sources were collected and analysed: fly ash from the stacks of the thermal power plant (6 samples), petroleum-coke burned in the cement plant (1), local soils (16) and road dust from the main roads of the Cienfuegos city (31). Likewise, an annual sample of bulk atmospheric deposition from the vicinity of the cement plant was also taken.

Table 5.1. Element recoveries (%) and relative standard deviations (RSD, %) of CRM CTA-FFA1 (n=6), and method detection limits (DL*, ng/g) for elements in the dissolved blank samples (n=9) measured by ICP-MS.

Element	Recovery	RSD	DL	Element	Recovery	RSD	DL
Be	88.38	12.40	0.02	Pr	N.A.		0.01
Na	88.07	6.10	23.67	Nd	73.36	6.67	0.05
Mg	104.86	5.13	4.67	Sm	75.88	5.13	0.02
Al	74.83	7.86	50.15	Eu	80.36	4.32	0.002
P	94.15	3.33	3.51	Gd	71.32	5.61	0.01
S	N.A.		843.51	Dy	63.25	6.64	0.01
K	78.30	6.49	13.94	Ho	N.A.		0.01
Ca	91.17	6.96	1271.68	Er	70.13	6.95	0.01
V	94.62	7.52	0.11	Tm	65.51	8.16	0.01
Cr	104.21	10.27	0.28	Yb	69.01	7.44	0.01
Mn	110.77	2.82	0.65	Lu	63.30	7.90	0.01
Fe	103.32	6.09	25.84	Tl	N.A.		0.05
Co	98.71	11.60	0.02	Pb	84.69	1.86	0.16
Ni	89.72	2.84	0.39	Th	67.47	6.55	0.03
Cu	94.30	2.42	1.14	U	82.05	8.32	0.01
Zn	100.65	5.35	1.02	Ti	68.23	6.11	1.53
As	95.78	10.61	0.14	Ge	N.A.		0.19
Rb	88.92	3.18	0.11	Zr	N.A.		0.17
Sr	95.19	1.57	0.07	Nb	N.A.		0.01
Cd	66.46	5.73	0.02	Mo	77.05	5.04	0.01
Cs	70.01	1.86	0.02	Sn	N.A.		0.30
Ba	77.74	10.89	1.02	Sb	93.54	6.59	0.17
La	81.81	3.70	0.06	W	72.87	2.23	0.01
Ce	84.64	3.17	0.12				

*DLs were calculated as 3x standard deviation of blank samples.
N.A.: reference value not available for the SRM CTA-FFA1.

The quality control of the analytical procedures was carried out by repeated analysis of the certified reference materials (CRM) CTA-FFA1 (fine fly ash). The recovery of major and trace elements was generally within the range of 80–110%, and the relative standard deviations (RSDs) less than 12%. Table 5.1 provides the element recoveries, RSDs and method detection limits (DLs).

The monthly atmospheric fluxes (F, in μg m^{-2} day^{-1}) for the studied elements were calculated as follows:

$$F = \frac{C * m}{S * T} \quad (5.1)$$

where: C is the measured concentration (in μg g^{-1}), m is the total deposited dry mass (in g), S is the total surface area of the collectors (in m^2) and T is the duration of the sampling period (in days). The atmospheric bulk deposition rate (μg m^{-2} day^{-1}, hereinafter bulk deposition) was calculated by the same formula (Eq. 5.1) without the parameter C.

We also calculated the Eu anomaly (Eu/Eu*) as in Eq. 5.2 (Pourmand et al., 2014) in order to identify different origins of the PM.

$$Eu/Eu^{*} = \frac{Eu_N}{\sqrt{Sm_N Gd_N}} \quad (5.2)$$

Here, N mean that values are normalized to Post Archean Australian Shale (Gromet et al., 1984).

2.3. Enrichment factors

An analysis of the elements enrichment factors (EFs) was conducted in order to distinguish typical anthropogenic elements in bulk depositions. The EFs is defined as follow:

$$EF_X = (C_X/C_R)_{bulk}/(C_X/C_R)_{Crust} \quad (5.3)$$

where X represents the element of interest; EF_X the EF of X; C_X the concentration of X, and C_R the concentration of a reference element. In this study Fe was selected as the reference material, and the average of local top soil composition was used as the elemental composition of the crustal material. We evaluate the Al and Ti as reference elements and also the database proposed by Li et al. (2009) as reference crustal material and similar results were observed. According to the EF values, the elements were considered highly enriched (EF>100), moderately enriched (10<EF<100) and less enriched (EF<10) (Fernandez-Olmo et al., 2014).

2.4. Statistical analyses

We performed Pearson's correlation and t-test analysis at the probability level of 0.05 between bulk deposition, flux of the studied elements and meteorological variables

to identify possible seasonal variations. Meteorological data (temperature, precipitation, pressure, relative humidity and wind speed all collected every 24 hours and monthly averaged) were obtained from a meteorological station located in Cienfuegos city.

Principal component analysis (PCA) with VARIMAX rotation and Kaiser normalization was used to identify the main element contribution sources in the study area. Prior to statistical analyses, the data set distribution was evaluated using the Kolmogorov-Smirnov method; when the distribution was not normal, the data was log-transformed (Zhong et al., 2014). Principal components were extracted from the variables with eigenvalues >1 and the PCA results were only accepted when the sum of those principal components accounted for more than 75% of the total variance of the dataset, and all the communality values were greater than 0.6. Contributions from the identified sources were quantitatively derived applying a multi-linear regression analysis (MLRA), using the bulk deposition values as the dependent variable and absolute factor scores from the PCA analysis as independent variables.

Clustering analysis (CA) was also performed to help in the association of the principal components (from the PCA results) with the main anthropogenic or natural sources in the study area. A CA using the Ward method and the Pearson correlations as similarity was applied. The statistical analyses were carried out using the SPSS 15.0 statistical software package.

3. Results and discussion

3.1. Bulk depositions

Figure 5.2 shows the monthly variation of the bulk depositions and amount of rainfall during the study. Monthly fluxes ranged from 23 129 to 97 224 $\mu g\ m^{-2}\ day^{-1}$ (averaging 46 018 $\mu g\ m^{-2}\ day^{-1}$). These values were lower than those reported in an urban site in Havana (86 460 $\mu g\ m^{-2}\ day^{-1}$) (Jomolca-Parra et al., 2014) but comparable to some reported in other coastal regions around the world (Huston et al., 2012; Rossini et al.,

2005). Nonetheless, we generally found higher values reported in the literature (Castillo et al., 2013b; Kara et al., 2014; Shanquan et al., 2016). As in most of the countries, bulk depositions are not regulated in Cuba; nevertheless, we found all our monthly depositions to be below the Australian guideline of 4 g m^{-2} $month^{-1}$ (130 000 μg m^{-2} day^{-1}) for deposited dust (Huston et al., 2012).

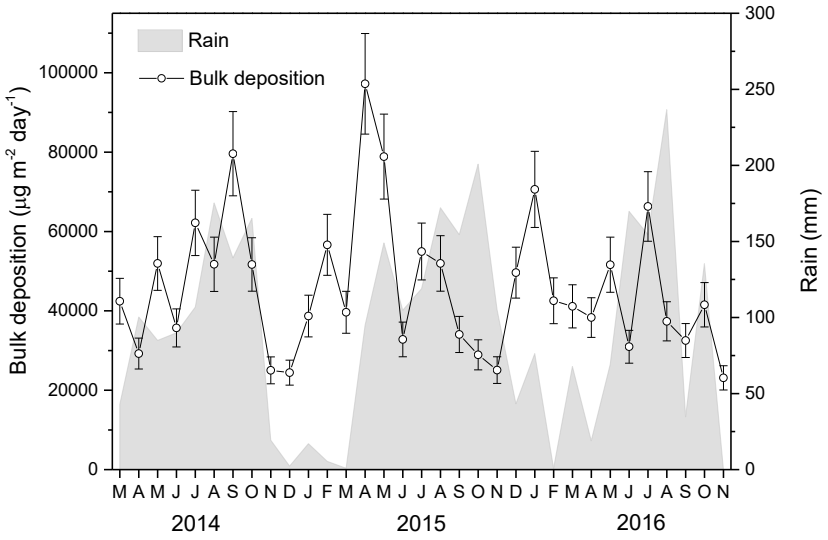

Figure 5.2. Monthly variation of atmospheric bulk depositions and rain in Cienfuegos.

There was no significant correlation between the monthly bulk depositions and the meteorological variables and there were no differences between the bulk depositions among the wet and dry season (*t*-test, $p<0.05$). We observed a wide variation of bulk depositions with maximum values in both typically wet and dry months. However, the annual bulk depositions during the study (2014–2016), 16.6, 17.9 and 15.8 g m^{-2} $year^{-1}$, respectively, showed fluctuations similar to the annual precipitation (1010, 1166 and 964 mm, respectively). In fact, when we included the annual flux values corresponding to the years 2010–2013 (unpublished values) we obtained a significant correlation ($r=0.8$, $p<0.05$) with the annual amount of precipitation. These results suggest that monthly variations of the bulk depositions probably reflected the variations in the amount of PM emitted from their major sources, while the annual variations reflected the changes in the meteorological conditions in the studied site like the precipitations.

3.2. Atmospheric flux of major and trace elements

Average and range of variation of atmospheric monthly fluxes of major and trace elements are reported in Table 5.2. The average monthly fluxes of major elements followed the order Ca>Na>S>K≈Al>Fe>Mg, whereas the average fluxes of trace metals were dominated by elements in the following order P>Zn>Ti>Mn>V>Sr≈Cu>Pb>Ba>Ni>Cr≈Rb≈Sb>As. These rankings are commonly found in rural regions around the world with the exception of V and Sb, which presented high levels compared with typical values reported in this environment (Castillo et al., 2013b; Fernandez-Olmo et al., 2015; Kyllonen et al., 2009).

Wide variation in the monthly fluxes of all elements was observed, which explains their high standard deviations. This may be attributed mainly to weather conditions (amount of precipitations, height of mixing layers, and the origin of air masses, among others) that strongly affected the dispersion and deposition of air pollutants, as well as to variation of emission of pollutants. However, similar to the bulk depositions, no significant correlation (at p=0.05) was observed between the monthly fluxes of the studied elements and the meteorological variables. Additionally, a *t*-test showed that there were no significant differences (at p=0.05) of atmospheric fluxes of any studied elements between the wet and dry season. This appeared to suggest that the monthly deposition fluxes of the studied elements were mostly affected by fluctuations of the emissions from their sources.

Table 5.2. Descriptive statistics for the monthly atmospheric flux (μg m^{-2} day^{-1}, n=33) of major and trace elements in Cienfuegos, Cuba.

Element	Mean	Min	Max	SD	Element	Mean	Min	Max	SD
Ca	3259	1692	8051	1456	La	0.27	0.06	0.78	0.17
Na	2801	1027	8008	1389	Nd	0.24	0.06	0.71	0.15
S	1127	445	2224	437	Cd	0.073	0.019	0.239	0.056
K	637	232	1085	241	Pr	0.064	0.015	0.190	0.041
Al	677	154	1921	347	Nb	0.053	0.010	0.184	0.043
Fe	581	169	1651	295	Sm	0.050	0.013	0.146	0.030
Mg	493	205	1247	225	Th	0.049	0.010	0.155	0.037
P	103	33	315	60	Gd	0.046	0.012	0.133	0.026
Zn	60	6	302	77	W	0.039	0.008	0.400	0.067
Ti	30	8	91	17	Cs	0.039	0.008	0.250	0.043
Mn	15.2	4.8	50.1	8.5	Dy	0.036	0.010	0.104	0.020
V	10.7	2.4	22.6	5.0	Ge	0.031	0.004	0.138	0.027
Sr	9.0	3.5	42.9	6.7	U	0.024	0.008	0.062	0.014
Cu	8.8	1.9	50.2	10	Er	0.020	0.006	0.057	0.010
Pb	6.4	1.1	34.3	6.6	Yb	0.018	0.005	0.049	0.009
Ba	5.1	1.8	14.1	2.8	Be	0.015	0.004	0.048	0.010
Ni	3.5	1.3	9.1	1.5	Ho	0.014	0.002	0.049	0.014
Cr	2.8	0.7	8.3	1.6	Tl	0.013	0.001	0.066	0.014
Rb	2.49	1.21	5.51	0.92	Eu	0.013	0.003	0.036	0.007
Sb	2.3	0.1	12.5	3.1	Tm	0.003	0.001	0.008	0.001
As	1.2	0.1	6.0	1.5	Lu	0.003	0.001	0.007	0.001
Ce	0.53	0.12	1.58	0.35	La/Ce	0.52	0.48	0.84	0.07
Zr	0.47	0.13	1.48	0.27	La/Sm	5.28	4.36	8.19	0.79
Sn	0.35	0.06	1.71	0.33	La/V	0.03	0.01	0.05	0.01
Mo	0.31	0.08	1.92	0.34	V/Ni	3.17	1.59	5.95	1.09
Co	0.27	0.08	0.84	0.14					

A similar temporal trend between the flux of the typical crustal elements was observed (see Figure 5.3). In general, atmospheric fluxes of the elements Al, P, Cr, Mn, Fe, Co, Rb, Cs, Ba, Th, U, Ti, Ge, Zr, Nb and lanthanoid elements were significantly higher (*t*-test, $p<0.05$) between March and August than during the rest of the year. The highest fluxes were obtained in July each year of study and in April 2015. This result may indicate a strong association with the seasonality of African dust clouds in the Caribbean region (Prospero and Mayol-Bracero, 2013; Rodriguez et al., 2015). The presence and characteristics of Sahara clouds dust in Cuba have been reported for each province based on the information obtained from different satellites and sensors (Mojena López et al., 2015). In the case of Cienfuegos, the presence of the Sahara dust clouds was

mainly reported from March until August with the highest presence in June and July, which agree with our results.

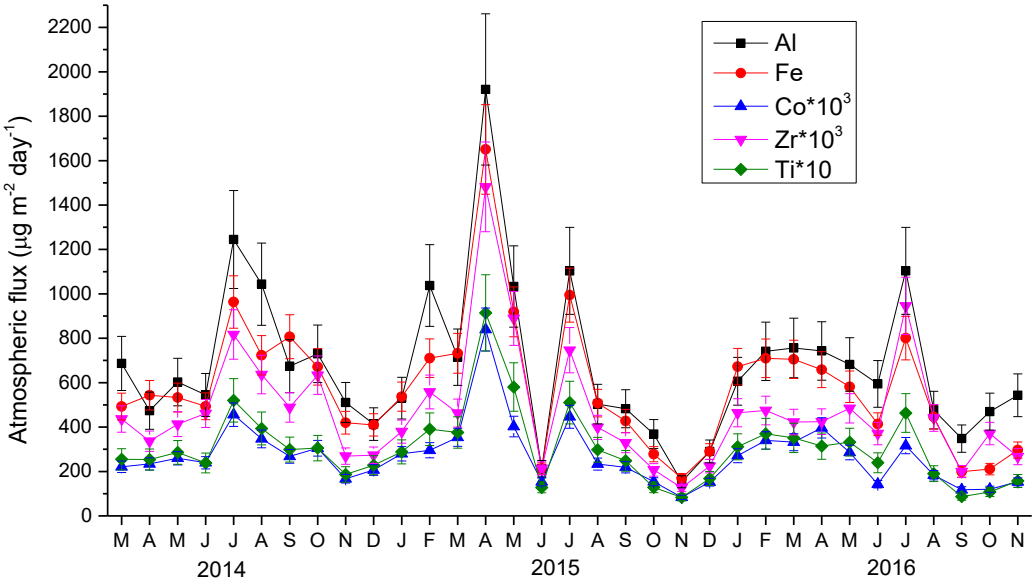

Figure 5.3. Temporal trend of selected crustal elements.

The stronger correlations ($r>0.9$, $p<0.001$) were found between the typical crustal elements Al–Fe, Al–Co, Al–lanthanoid elements, Al–Ti, Al–Zr, Cr–Fe, Cr–Co, Cr–Ti, Mn–Fe, Mn–Co, Mn–Ni, Mn–Ti, Fe–Co, Fe–Rb, Fe–Ti, Fe–Zr and Co–Ti, which corroborated that these elements had a predominantly common origin. Important correlations ($0.7<r<0.9$, $p<0.01$) were observed between Mg, Ca, S, Ba, Th, U and Nb and most of the above crustal elements, probably reflecting an important contributions of these elements from the crustal matter. A strong correlation was also observed for As–Sb ($r=0.98$, $p<0.0001$) and Cu–W ($r=0.8$, $p<0.0001$), probably indicating a common origin of these pairs of elements. Additionally, there was a significant correlation for V–Ni ($r=0.66$, $p<0.0001$), which are typical markers of fossil fuel combustion sources (Moreno et al., 2010). No correlation between the metals typically associated to traffic and industrial emissions (Cu, Zn, Cd, Pb, Mo and Sn) and crustal elements was found; however, statistically significant correlations ($0.4<r<0.6$, $p<0.01$) for Zn–Sn, Cu–Cd, Cd–Sn and Pb–Sn, were observed.

In Figure 5.4a are compared the average monthly fluxes of elements measured in the present study with those determined in other worldwide regions at rural environments (Castillo et al., 2013b; Fernandez-Olmo et al., 2015; Fowler et al., 2006; Hovmand and Kystol, 2013; Kara et al., 2014; Kyllonen et al., 2009; Rossini et al., 2005). The atmospheric fluxes of most of the studied elements in Cienfuegos were within and, in some cases below (e.g. lanthanoid elements), the range of variation found in those sites. However, the fluxes of the elements V, Ni, Sb and As were higher in our studied site. These elements are typically associated to fossil fuel combustion sources (Querol et al., 2007; Viana et al., 2008), and their high flux values probably reflects the influence of emissions derived from local anthropogenic sources. A comparison with values reported in urban (Bermudez et al., 2012; Castillo et al., 2013b; Fernandez-Olmo et al., 2014; Gao et al., 2016; Huston et al., 2012; Kara et al., 2014; Mijić et al., 2010; Rossini et al., 2005) and industrial (Castillo et al., 2013a; Fernandez-Olmo et al., 2015; Kara et al., 2014; Rossini et al., 2005) sites around the world (Figures 5.4b and 5.4c) confirmed that atmospheric fluxes of these elements in Cienfuegos were in the range of variation observed in those environments.

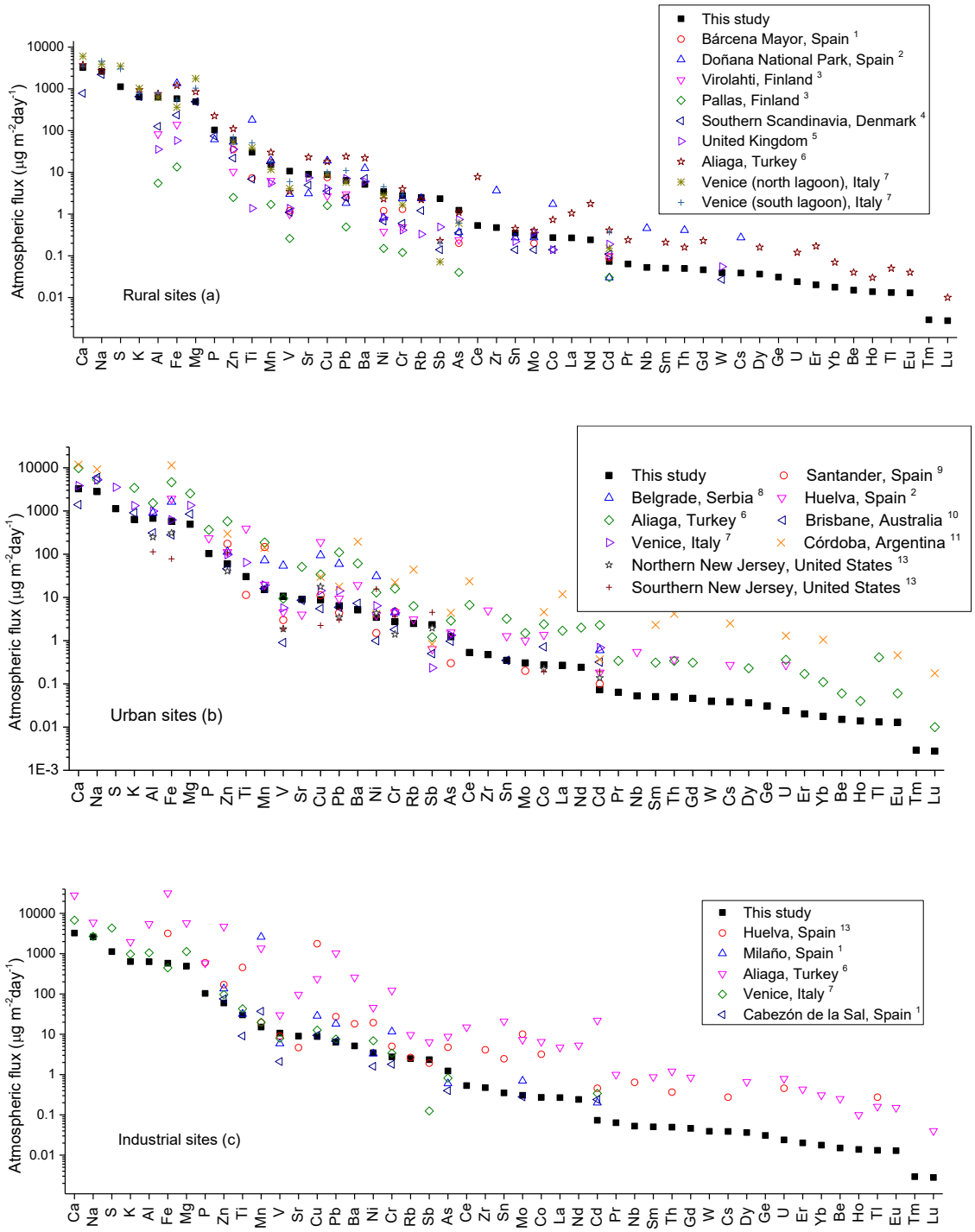

Figure 5.4. Comparison of atmospheric fluxes of major and trace elements in a rural site in Cienfuegos with values reported in rural (a), urban (b) and industrial (c) sites around the world: 1 (Fernandez-Olmo et al., 2015); 2 (Castillo et al., 2013b); 3 (Kyllonen et al., 2009); 4 (Hovmand and Kystol, 2013); 5 (Fowler et al., 2006); 6 (Kara et al., 2014), 7 (Rossini et al., 2005), 8 (Mijić et al., 2010), 9 (Fernandez-Olmo et al., 2014), 10 (Huston et al., 2012), 11 (Bermudez et al., 2012), 12 (Gao et al., 2016) and 13 (Castillo et al., 2013a).

3.3. Lanthanoid elements

In most unpolluted crustal materials such as natural dusts, the commoner lanthanoids occur in the following order of abundance: Ce>La>Nd>Pr>Sm>Yb>Lu (Moreno et al., 2008b). Our data (Table 5.2) also reflected the same order and supported the conclusion that the levels of lanthanoid elements in the studied area were mostly of natural origin. In Table 5.2 is also provided the statistical summary of La/Ce and La/Sm ratios, which showed narrow ranges of variation: 0.5–0.8 (average of 0.5) and 4.4–8.2 (average of 5.3), respectively. These values were in the typical range of natural La/Ce (0.4–0.6) and La/Sm (5–7) values in uncontaminated rocks, soils and minerals (Moreno et al., 2010), confirming their prevalent crustal origin.

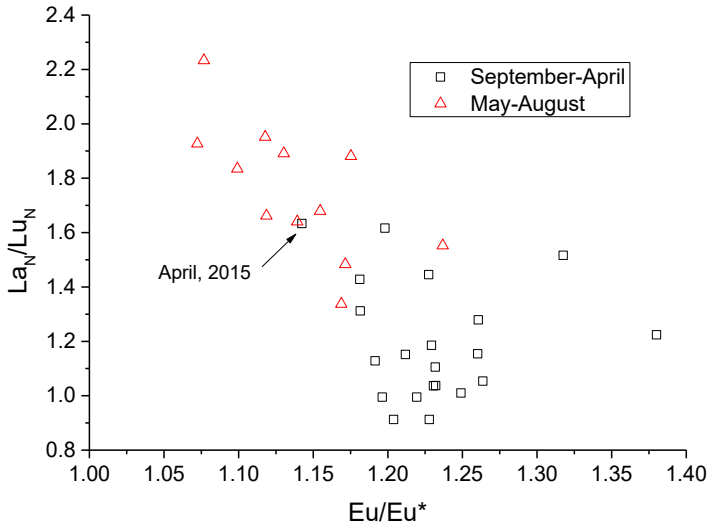

Figure 5.5. Eu anomalies versus La_N/Lu_N ratios in bulk deposition samples collected in Cienfuegos between 2014 and 2016.

To identify different origins of the particulate matter in Cienfuegos, we plotted the Eu anomalies versus La_N/Lu_N ratios (Figure 5.5). Most of samples from May–August, a period of high presence of Sahara dust clouds in Cienfuegos (Mojena López et al., 2015), showed the lowest Eu anomaly values and the highest La_N/Lu_N ratios. A similar result was observed in North African aerosols collected in Barbados (Pourmand et al., 2014). Thus, this result revealed the influence of the African dust intrusions in the geochemical composition of bulk deposition in Cienfuegos governed by a clear seasonality. The sample collected on April 2015 presented similar geochemical signatures to samples

from May–August, suggesting an important influence of African dust. This hypothesis was corroborated by back trajectory frequency analysis (not shown), which showed the frequent arrival of air masses from Northeast Africa in late April. This fact would explain the higher fluxes of crustal elements obtained in that month (see Figure 5.3).

As discussed in Chapter 3, the La/V ratio values in atmospheric particles can be used to distinguish the emission sources related to the fossil fuel combustion and oil refining processes. V-rich emissions derived from fuel oil and petroleum coke combustion usually exhibit very low La/V ratios (<0.1) compared to those of mineral particulate matter coming from uncontaminated crustal materials or coal combustion (La/V = 0.2–0.3) (Celo et al., 2012; Moreno et al., 2008a). On the contrary, atmospheric emissions of PM in the flue gas from the fluid catalytic converters (FCC) refinery regenerator commonly show much greater La/V values (Kulkarni et al., 2007). Our data from Cienfuegos showed atmospheric La/V values exclusively below 0.06 (see Table 5.2) suggesting the prevalence of anthropogenic emissions from industries with oil and/or petroleum-coke combustion processes rather than from refineries. We confirmed that using a LaCeV triangular diagram (Figure 5.6) and comparing with local and published data (Kulkarni et al., 2006; Moreno et al., 2006; Olmez et al., 1988). Samples from Cienfuegos (Figure 5.6a) showed a clear displacement toward the V apex indicating a strong influence of oil and/or petroleum-coke combustion sources. According to that, the potential sources affecting the studied region (see Figure 5.6b) were the TPP, shipping emissions, the diesel power unit and diesel combustion boiler located 4 km west of the sampling site (all these sources use diesel as fuel) and the cement plant that use petroleum-coke as fuel. The influence of urban road traffic was also possible due to some samples presented similar LaCeV composition.

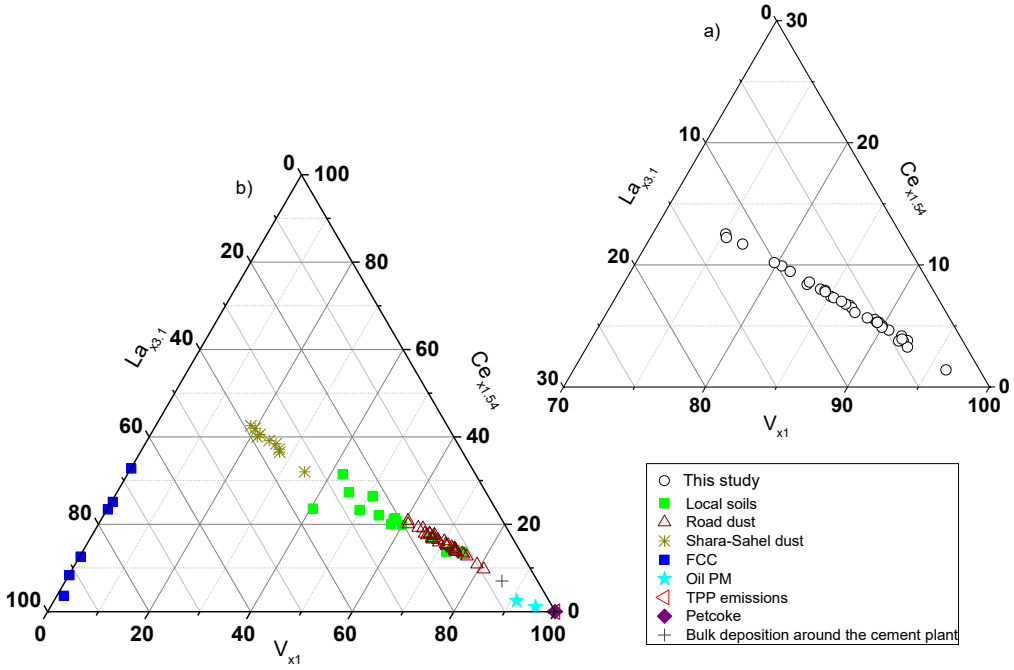

Figure 5.6. (a): Triangular diagram of LaCeV compositions of bulk deposition samples collected in Cienfuegos. (b): LaCeV compositions of published data of FCC (Kulkarni et al., 2006), oil PM (Olmez et al., 1988), Sahara–Sahel Dust Corridor (Moreno et al., 2006), and local data of power plant emissions, petroleum-coke burned in the cement plant, local soils, road dust and a bulk deposition sample collected around the cement plant.

3.4. Enrichment factors

The monthly average of EFs values for the studied elements are displayed in Figure 5.7. Sodium and Zn were highly enriched (EF>100). The high value for Na indicated the strong marine influence while the high EF values of Zn may be related to the scrap storage, classification and transportation activities in Cienfuegos city. The elements Sb, Pb and W were moderately enriched (10<EF<100) but, sometimes they reached values higher than 100 indicating a dominant anthropogenic origin. Tin, S, Cu, Mo, Nb and P were also moderately enriched indicating they had a significant anthropogenic influence. Copper, W and Mo are typical tracers of road traffic (Grigoratos and Martini, 2015; Johansson et al., 2009; Querol et al., 2007), so their moderate enrichment could be due to the influence of the urban traffic emissions in the studied site under northerly wind directions. The S-enrichment probably reflected the use of sulfur-rich Cuban crude oil and diesel in industries (Turtos Carbonell et al., 2007). Due to lead gasoline not being

used in Cuba since 1990, the Pb-enrichment was probably related to industrial emissions, mainly by fossil fuel combustion and other anthropogenic activities.

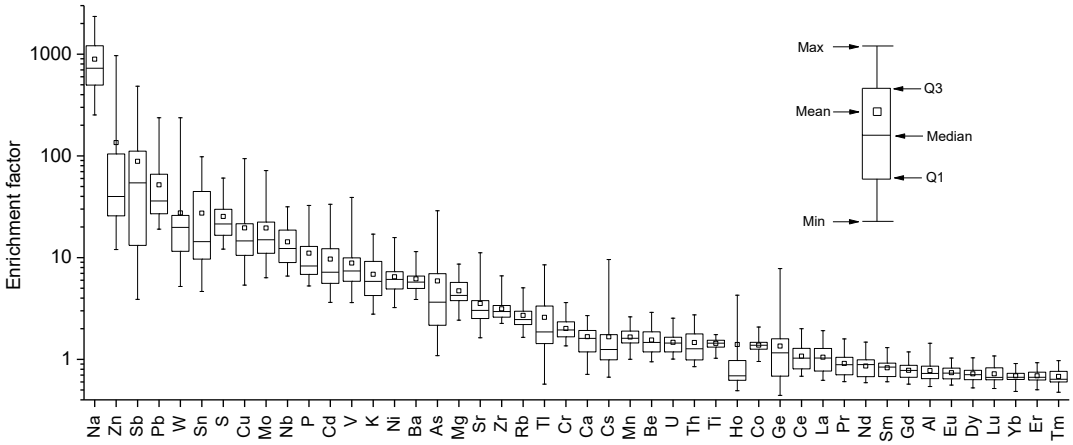

Figure 5.7. Element enrichment factors in bulk deposition samples collected in Cienfuegos between 2014 and 2016.

Cadmium, V, Ni, K, Ba and As, with average EFs below 10, appeared to be mainly of crustal origin, but they sometimes presented values higher than 10 suggesting the influence of anthropogenic sources. Vanadium and Ni are often used as tracers of fossil fuel combustion processes (Viana et al., 2008) and their slight enrichments probably reflected the influence of these kind of sources. The average V/Ni in our samples was 3.2 ± 1.1, which is lower than the V/Ni ratio found in fly ash samples collected in the TPP stacks (4.4 ± 0.2) but, within the range of variation of those reported in the literature for shipping emissions (values around 3) (Moreno et al., 2010; Pandolfi et al., 2011; Viana et al., 2014). Slightly enrichment of K could be due to the wood burning for charcoal. The rest of elements were less enriched, specially the lanthanoid elements, which presented the lowest EFs confirming their prevailing crustal origin.

3.5. Source identification and source apportionment

3.5.1. PCA-MLRA

The PCA results shown 5 principal components with eigenvalues greater than 1 accounting for 82.7% of the total variance (Table 5.3). The obtained chemical profiles,

based on the factor loadings greater than 0.6, were used to identify the most probable sources.

Table 5.3. Result of the PCA carried out with VARIMAX rotation. Factor loadings >0.6 are highlighted in bold.

Variables	Factors				
	F1	F2	F3	F4	F5
Al	**0.90**	0.13	0.22	0.19	-0.02
Tloid*	**0.89**	0.36	0.07	0.03	0.12
Zr	**0.87**	0.30	0.16	0.24	0.06
Ti	**0.85**	0.36	0.24	0.10	0.06
Fe	**0.83**	0.37	0.26	0.18	0.08
Ni	**0.81**	0.02	0.30	0.29	0.08
Co	**0.80**	0.36	0.24	0.13	0.10
Nb	**0.76**	0.55	-0.01	0.05	0.06
Ba	**0.75**	0.47	0.17	0.25	0.01
Mn	**0.74**	0.28	0.31	0.22	0.11
Rb	**0.73**	0.34	0.45	0.09	0.28
V	**0.72**	-0.22	0.17	0.07	0.14
Cr	**0.66**	0.40	0.26	0.35	0.26
Tl	0.60	0.40	-0.07	0.40	-0.06
S	0.51	0.42	0.43	0.20	0.22
As	0.40	**0.78**	0.20	0.26	-0.14
Sb	0.26	**0.78**	0.19	0.27	-0.27
P	0.42	0.54	0.24	0.04	0.31
Na	0.05	0.00	**0.89**	0.23	0.07
Mg	0.52	0.31	**0.71**	0.22	0.04
Ca	0.51	0.16	**0.64**	0.18	0.19
K	0.41	0.34	0.58	0.08	0.16
Cu	0.20	0.07	0.25	**0.86**	0.08
W	0.17	0.24	0.19	**0.83**	0.06
Sn	0.20	-0.23	0.05	0.21	**0.88**
Zn	-0.15	-0.08	0.04	-0.15	**0.86**
Pb	0.34	0.26	0.28	0.24	**0.65**
Cd	0.36	0.28	0.20	0.53	0.54
Percentage of variance (%)	*57.77*	*9.75*	*6.55*	*4.59*	*4.06*
Cumulative (%)	*57.77*	*67.52*	*74.07*	*78.66*	*82.72*

*TLoid: The sum of lanthanoid elements flux.

F1 (Crustal), accounting for 57.8% of the variance, was dominated by the typical elements from the Earth's crust Al, lanthanoid elements, Zr, Ti, Fe, Ni and Co. Other elements highlighted in this factor were Nb, Ba, Mn, Rb, V and Cr. The source of these

elements may be related to the impact of Saharan dust intrusion and to the resuspension of soil. F2 (Combustion), with 9.8% of the variance, was represented by higher loading of As and Sb. The origin of this factor is not clear but may be related to the incineration of solid wastes that take place in an outdoor dump located about 1 km N of the sampling site and other burnings including fossil fuel combustion. In the literature, these elements have been related to the contribution from waste incinerators and oil combustion (Gao et al., 2002; Venturini et al., 2013). F3 (Marine) accounted for 6.6% of the variance and was represented by the typical constituents of the marine aerosol Na and Mg. F4 (Traffic), with 4.6% of the variance, is dominated by Cu and W, which are typical tracers of non-exhaust traffic emissions (Grigoratos and Martini, 2015; Johansson et al., 2009). The last factor F5 (Industrial) was associated to the elements Sn, Zn and Pb explaining 4.1% of the variance. In the literature these elements have been often linked with metal, cement and asphalt production and also with combustion in industries (Taiwo et al., 2014). The most likely sources in the region may be the emissions coming from the industrial activities in Cienfuegos city including scrap storage, classification and transportation activities and from the cement plant located 25 km at NE.

The monthly average contributions of the different sources, calculated by MLRA, are shown in Figure 5.8. The crustal and marine sources were dominant, contributing with 39.5 and 38.2% of the bulk atmospheric deposition, respectively, while 6.7% were derived from the combustion sources, 8.7% related to industrial activities, 1.4% from road traffic and 5% undetermined. Although natural sources dominated the atmospheric depositions, the source apportionment demonstrated the influence of the anthropogenic emissions in the studied rural site.

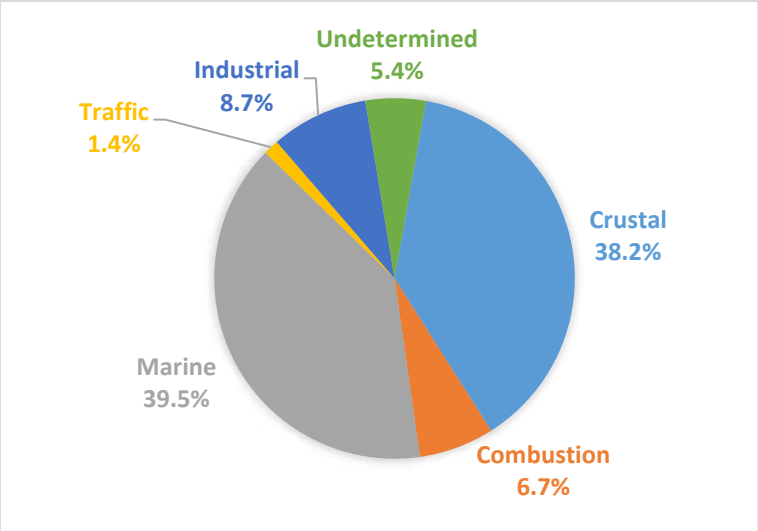

Figure 5.8. Average contribution of the different sources determined by PCA-MLRA to the bulk atmospheric deposition in the period 2014 – 2016 in Cienfuegos.

3.5.2. Cluster analysis

The dendrogram in Figure 5.9 shows the result of the CA. For its interpretation have been highlighted 5 distinct clusters which are consistent with each identified factor from the PCA analysis. Some of the highlighted elements clusters may contribute to a better interpretation of the identified major sources (from the PCA analysis).

In cluster 1 the elements As, Sb, S, Tl, P and K are associated, representing the influence of different burnings. In addition to the waste incineration (As and Sb), this cluster reveals the influence of the wood burning (K and Tl), probably related to the charcoal production around the sampling site, and the fossil fuel combustion as a result of the use of S-rich Cuban crude oil and diesel in the TPP, other industries, trucks and ships.

The elements Al, Zr, Fe, Ti, Rb, Ba, Nb, TLoid, Cr, Mn, Co and Ni were grouped in cluster 2 indicating a common crustal origin. High fluxes of most of these elements were associated to the Saharan dust intrusions in this study, a result similar to that reported in nearby areas (Prospero et al., 2001). The high dissimilarity of V with respect to the rest of elements in this cluster is probably related to some anthropogenic contributions of this element as noted when we discussed the EFs.

Finally, clusters 3 (Na, Mg and Ca), 4 (Cu and W) and 5 (Cd, Sn, Pb and Zn) clearly represent the marine, traffic and industrial influence, respectively.

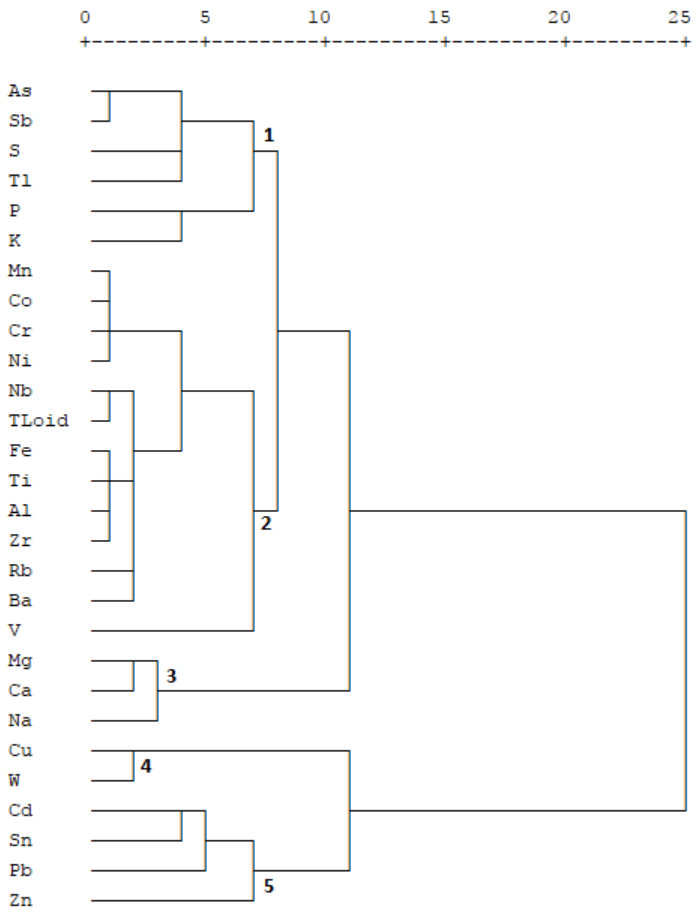

Figure 5.9. Hierarchical clustering on variables for major and trace elements in bulk atmospheric deposition (using the Ward method).

4. Conclusions

In this study we monitored and chemically characterized the monthly bulk atmospheric depositions in a coastal rural site in Cienfuegos (Cuba). No significant correlation was found between meteorological factors (precipitation, temperature or relative humidity) and the monthly bulk depositions or the monthly flux of major and trace elements. We attributed this result to the fluctuations of the emissions from their main sources rather than to meteorological factors controlling the deposition processes. No seasonality was observed with the dry and wet periods. However, strong correlations

were found between typical crustal elements, which showed a marked seasonality with the presence of Saharan cloud dust in the Caribbean.

Most of the studied elements were found in the range of variation of those reported in rural environments around the world, but some trace elements such as V, Ni, As and Sb presented higher levels, typical of urban and industrial areas. Atmospheric depositions were highly enriched (EF>100) with Zn and moderately enriched (10<EF<100) with Sb, Pb, W, Sn, S, Cu, Mo, Nb and P, indicating significant contributions of these elements from anthropogenic sources. The rest of the elements were less enriched confirming their predominant crustal origin. The La/V ratio values were found to be exclusively lower than 0.06 suggesting the prevalence of anthropogenic emissions from industries with oil and/or petroleum-coke combustion processes rather than from the refinery. We corroborated the consistence of our data with a LaCeV composition characteristic of emissions related to the TPP, cement plant and, eventually, road dust.

Five main sources of elements were identified by multivariate statistical analyses (PCA-MLRA and CA): crustal matter (39.5% of the bulk deposition), marine aerosol (38.2%), combustion including waste incineration, wood and fossil fuel burning (6.7%), industrial emissions (8.7%) and road traffic (1.4%).

This study represents the first exhaustive report on element deposition fluxes directly measured in bulk deposition in Cuba and significantly expand the database for the Caribbean region. The evidences and results provided here could be of help to establish efficient environmental strategies for the improvement of the quality of the air and ecosystems.

Acknowledgements

The authors express their gratitude to the analytical staff of the Laboratorio Integrado de Calidad Ambiental (LICA) of the Department of Chemistry of the University of Navarra and of the Centro de Estudios Ambientales de Cienfuegos (CEAC) for its assistance. This research has received funding from "la Caixa" Banking Foundation. This study was also supported by the IAEA TC Project CUB/7/008 “Strengthening the National

System for Analysis of the Risks and Vulnerability of Cuba's Coastal Zone Through the Application of Nuclear and Isotopic Techniques" and National Program PNUOLU /4-1/ 2 No. /2014 of the National Nuclear Agency.

References

Alonso-Hernández, C.M., Cartas Águila, H., Diaz-Asencio, M., Muños-Caravaca, A., Martín-Pérez, J., Sibello-Hernández, R., 2006. Atmospheric deposition of 137Cs between 1994 and 2002 at Cienfuegos, Cuba. J. Environ. Radioact. 88, 199–204.

Alonso-Hernández, C.M., Morera-Gómez, Y., Cartas-Águila, H., Guillén-Arruebarrena, A., 2014. Atmospheric deposition patterns of 210Pb and 7Be in Cienfuegos, Cuba. J. Environ. Radioact. 138, 149–155. https://doi.org/10.1016/j.jenvrad.2014.08.023

Baker, A.R., Jickells, T.D., 2017. Atmospheric deposition of soluble trace elements along the Atlantic Meridional Transect (AMT). Prog. Oceanogr., The Atlantic Meridional Transect programme (1995-2016) 158, 41–51. https://doi.org/10.1016/j.pocean.2016.10.002

Bermudez, G.M.A., Jasan, R., Pla, R., Pignata, M.L., 2012. Heavy metals and trace elements in atmospheric fall-out: Their relationship with topsoil and wheat element composition. J. Hazard. Mater. 213, 447–456. https://doi.org/10.1016/j.jhazmat.2012.02.023

Castillo, S., de la Rosa, J.D., Sanchez de la Campa, A.M., Gonzalez-Castanedo, Y., Fernandez-Caliani, J.C., Gonzalez, I., Romero, A., 2013a. Contribution of mine wastes to atmospheric metal deposition in the surrounding area of an abandoned heavily polluted mining district (Rio Tinto mines, Spain). Sci. Total Environ. 449, 363–372. https://doi.org/10.1016/j.scitotenv.2013.01.076

Castillo, S., de la Rosa, J.D., Sanchez de la Campa, A.M., Gonzalez-Castanedo, Y., Fernandez-Camacho, R., 2013b. Heavy metal deposition fluxes affecting an Atlantic coastal area in the southwest of Spain. Atmos. Environ. 77, 509–517. https://doi.org/10.1016/j.atmosenv.2013.05.046

Celo, V., Dabek-Zlotorzynska, E., Zhao, J., Bowman, D., 2012. Concentration and source origin of lanthanoids in the Canadian atmospheric particulate matter: a case study. Atmospheric Pollut. Res. 3, 270–278. https://doi.org/10.5094/APR.2012.030

Cuesta-Santos, O., Collazo, A., Wallo, A., Labrador, R., Gonzalez, M., Ortiz, P., 2001. Deposition of atmospheric nitrogen compounds in humid tropical Cuba. Sci. World J. 1, 238–244.

D'Alessandro, W., Katsanou, K., Lambrakis, N., Bellomo, S., Brusca, L., Liotta, M., 2013. Chemical and isotopic characterisation of bulk deposition in the Louros basin (Epirus, Greece). Atmospheric Res. 132–133, 399–410. https://doi.org/10.1016/j.atmosres.2013.07.007

Dämmgen, U., Erisman, J.W., Cape, J.N., Grünhage, L., Fowler, D., 2005. Practical considerations for addressing uncertainties in monitoring bulk deposition. Environ. Pollut. 134, 535–548. https://doi.org/10.1016/j.envpol.2004.08.013

Diaz-Asencio, M., Alonso-Hernández, C.M., Bolaños-Álvarez, Y., Gómez-Batista, M., Pinto, V., Morabito, R., Hernández-Albernas, J.I., Eriksson, M., Sanchez-Cabeza, J.A., 2009. One century sedimentary record of Hg and Pb pollution in the Sagua estuary (Cuba) derived from 210 Pb and 137 Cs chronology. Mar. Pollut. Bull. 59, 108–115.

Diaz-Asencio, M., Sanchez-Cabeza, J.-A., Bolanos-Alvarez, Y., Carolina Ruiz-Fernandez, A., Gomez-Batista, M., Morabito, R., Alonso-Hernandez, C., 2014. One century of sedimentation and Hg pollution at the mouth of the Sagua la Grande River (Cuba). Cienc. Mar. 40, 321–337. https://doi.org/10.7773/cm.v40i4.2472

Fernandez-Olmo, I., Puente, M., Irabien, A., 2015. A comparative study between the fluxes of trace elements in bulk atmospheric deposition at industrial, urban, traffic, and rural sites. Environ. Sci. Pollut. Res. 22, 13427–13441. https://doi.org/10.1007/s11356-015-4562-z

Fernandez-Olmo, I., Puente, M., Montecalvo, L., Irabien, A., 2014. Source contribution to the bulk atmospheric deposition of minor and trace elements in a Northern Spanish coastal urban area. Atmospheric Res. 145, 80–91. https://doi.org/10.1016/j.atmosres.2014.04.002

Fowler, D., McDonald, A.G., Crossley, A., Nemitz, E., Leaver, D., Cape, J.N., Smith, R.I., Anderson, D., Rowland, P., Ainsworth, G., 2006. UK heavy metal monitoring network (No. AS 06/07). NERC/Centre for Ecology and Hydrology.

Gao, Y., Mukherjee, P., Jusino-Atresino, R., 2016. The Air-Coastal Sea Chemical Exchange: A Case Study on the New Jersey Coast. Aquat. Geochem. 22, 275–289. https://doi.org/10.1007/s10498-015-9285-8

Gao, Y., Nelson, E.D., Field, M.P., Ding, Q., Li, H., Sherrell, R.M., Gigliotti, C.L., Van Ry, D.A., Glenn, T.R., Eisenreich, S.J., 2002. Characterization of atmospheric trace elements on PM2.5 particulate matter over the New York–New Jersey harbor estuary. Atmos. Environ. 36, 1077–1086. https://doi.org/10.1016/S1352-2310(01)00381-8

Golomb, D., Ryan, D., Eby, N., Underhill, J., Zemba, S., 1997. Atmospheric deposition of toxics onto Massachusetts Bay—I. Metals. Atmos. Environ. 31, 1349–1359. https://doi.org/10.1016/S1352-2310(96)00276-2

González-De Zayas, R., Merino-Ibarra, M., Matos-Pupo, F., Soto-Jiménez, M., 2012. Atmospheric Deposition of Nitrogen to a Caribbean Coastal Zone (Cayo Coco, Cuba): Temporal Trends and Relative Importance as a Nitrogen Source. Water. Air. Soil Pollut. 223, 1125–1136. https://doi.org/10.1007/s11270-011-0930-6

Grantz, D.A., Garner, J.H.B., Johnson, D.W., 2003. Ecological effects of particulate matter. Environ. Int. 29, 213–239. https://doi.org/10.1016/S0160-4120(02)00181-2

Grigoratos, T., Martini, G., 2015. Brake wear particle emissions: a review. Environ. Sci. Pollut. Res. 22, 2491–2504. https://doi.org/10.1007/s11356-014-3696-8

Gromet, L., Dymek, R., Haskin, L., Korotev, R., 1984. The North-American Shale Composite - Its Compilation, Major and Trace-Element Characteristics. Geochim. Cosmochim. Acta 48, 2469–2482. https://doi.org/10.1016/0016-7037(84)90298-9

Harris, R., Pollman, C., Landing, W., Evans, D., Axelrad, D., Hutchinson, D., Morey, S.L., Rumbold, D., Dukhovskoy, D., Adams, D.H., Vijayaraghavan, K., Holmes, C., Atkinson, R.D., Myers, T., Sunderland, E., 2012. Mercury in the Gulf of Mexico: Sources to receptors. Mercury Mar. Ecosyst. Sources Seaf. Consum. 119, 42–52. https://doi.org/10.1016/j.envres.2012.08.001

Hovmand, M.F., Kystol, J., 2013. Atmospheric element deposition in southern Scandinavia. Atmos. Environ. 77, 482–489. https://doi.org/10.1016/j.atmosenv.2013.03.008

Huston, R., Chan, Y.C., Chapman, H., Gardner, T., Shaw, G., 2012. Source apportionment of heavy metals and ionic contaminants in rainwater tanks in a subtropical urban area in Australia. Water Res. 46, 1121–1132. https://doi.org/10.1016/j.watres.2011.12.008

Johansson, C., Norman, M., Burman, L., 2009. Road traffic emission factors for heavy metals. Atmos. Environ. 43, 4681–4688. https://doi.org/10.1016/j.atmosenv.2008.10.024

Jomolca-Parra, Y., Lima-Cazorla, L., Manduca-Artiles, M., 2014. Determination of Atmospheric Fluxes and Concentrations of Heavy Metals and Radionuclides of Environmental Concern in Total Atmospheric Deposition. Rev. Cuba. Quím. 25, 345–363.

Kanakidou, M., Seinfeld, J.H., Pandis, S.N., Barnes, I., Dentener, F.J., Facchini, M.C., Van Dingenen, R., Ervens, B., Nenes, A., Nielsen, C.J., Swietlicki, E., Putaud, J.P., Balkanski, Y., Fuzzi, S., Horth, J., Moortgat, G.K., Winterhalter, R., Myhre, C.E.L., Tsigaridis, K., Vignati, E., Stephanou, E.G., Wilson, J., 2005. Organic aerosol and global climate modelling: a review. Atmos Chem Phys 5, 1053–1123. https://doi.org/10.5194/acp-5-1053-2005

Kara, M., Dumanoglu, Y., Altiok, H., Elbir, T., Odabasi, M., Bayram, A., 2014. Seasonal and spatial variations of atmospheric trace elemental deposition in the Aliaga industrial region, Turkey. Atmospheric Res. 149, 204–216. https://doi.org/10.1016/j.atmosres.2014.06.009

Kulkarni, P., Chellam, S., Fraser, M.P., 2007. Tracking petroleum refinery emission events using lanthanum and lanthanides as elemental markers for PM2.5. Environ. Sci. Technol. 41, 6748–6754. https://doi.org/10.1021/es062888i

Kulkarni, P., Chellam, S., Fraser, M.P., 2006. Lanthanum and lanthanides in atmospheric fine particles and their apportionment to refinery and petrochemical operations in Houston, TX. Atmos. Environ. 40, 508–520. https://doi.org/10.1016/j.atmosenv.2005.09.063

Kyllonen, K., Karlsson, V., Ruoho-Airola, T., 2009. Trace element deposition and trends during a ten year period in Finland. Sci. Total Environ. 407, 2260–2269. https://doi.org/10.1016/j.scitotenv.2008.11.045

Lenes, J.M., Prospero, J.M., Landing, W.M., Virmani, J.I., Walsh, J.J., 2012. A model of Saharan dust deposition to the eastern Gulf of Mexico. Mar. Chem. 134–135, 1–9. https://doi.org/10.1016/j.marchem.2012.02.007

Li, C., Kang, S., Zhang, Q., 2009. Elemental composition of Tibetan Plateau top soils and its effect on evaluating atmospheric pollution transport. Environ. Pollut. 157, 2261–2265. https://doi.org/10.1016/j.envpol.2009.03.035

Mason, R.P., Heyes, D., Sveinsdottir, A., 2006. Methylmercury concentrations in fish from tidal waters of the Chesapeake bay. Arch. Environ. Contam. Toxicol. 51, 425–437. https://doi.org/10.1007/s00244-004-0230-x

Mijić, Z., Stojić, A., Perišić, M., Rajšić, S., Tasić, M., Radenković, M., Joksić, J., 2010. Seasonal variability and source apportionment of metals in the atmospheric deposition in Belgrade. Atmos. Environ. 44, 3630–3637. https://doi.org/10.1016/j.atmosenv.2010.06.045

Mojena López, E., Ortega González, A., Casilles Vega, E.F., Leyva Santos, J., 2015. Sahara Clouds Dust. Their presence in Cuba. Rev. Cuabana Meteorol. 21, 120–134.

Morel, F.M.M., Price, N.M., 2003. The Biogeochemical Cycles of Trace Metals in the Oceans. Science 300, 944–947. https://doi.org/10.1126/science.1083545

Moreno, T., Querol, X., Alastuey, A., de la Rosa, J., Sánchez de la Campa, A.M., Minguillón, M., Pandolfi, M., González-Castanedo, Y., Monfort, E., Gibbons, W., 2010. Variations in vanadium, nickel and lanthanoid element concentrations in urban air. Sci. Total Environ. 408, 4569–4579. https://doi.org/10.1016/j.scitotenv.2010.06.016

Moreno, T., Querol, X., Alastuey, A., Gibbons, W., 2008a. Identification of FCC refinery atmospheric pollution events using lanthanoid- and vanadium-bearing aerosols. Atmos. Environ. 42, 7851–7861. https://doi.org/10.1016/j.atmosenv.2008.07.013

Moreno, T., Querol, X., Alastuey, A., Pey, J., Minguillon, M.C., Perez, N., Bernabe, R.M., Blanco, S., Cardenas, B., Gibbons, W., 2008b. Lanthanoid geochemistry of urban atmospheric particulate matter. Environ. Sci. Technol. 42, 6502–6507. https://doi.org/10.1021/es800786z

Moreno, T., Querol, X., Castillo, S., Alastuey, A., Cuevas, E., Herrmann, L., Mounkaila, M., Elvira, J., Gibbons, W., 2006. Geochemical variations in aeolian mineral particles from the Sahara-Sahel Dust Corridor. Chemosphere 65, 261–270. https://doi.org/10.1016/j.chemosphere.2006.02.052

Okin, G.S., Baker, A.R., Tegen, I., Mahowald, N.M., Dentener, F.J., Duce, R.A., Galloway, J.N., Hunter, K., Kanakidou, M., Kubilay, N., Prospero, J.M., Sarin, M., Surapipith, V., Uematsu, M., Zhu, T., 2011. Impacts of atmospheric nutrient deposition on marine productivity: Roles of nitrogen, phosphorus, and iron. Glob. Biogeochem. Cycles 25, GB2022. https://doi.org/10.1029/2010GB003858

Okubo, A., Takeda, S., Obata, H., 2013. Atmospheric deposition of trace metals to the western North Pacific Ocean observed at coastal station in Japan. Atmospheric Res. 129–130, 20–32. https://doi.org/10.1016/j.atmosres.2013.03.014

Olmez, I., Sheffield, A.E., Gordon, G.E., Houck, J.E., Pritchett, L.C., Cooper, J.A., Dzubay, T.G., Bennett, R.L., 1988. Compositions of Particles from Selected Sources in Philadelphia for Receptor Modeling Applications. JAPCA 38, 1392–1402. https://doi.org/10.1080/08940630.1988.10466479

Pandolfi, M., Gonzalez-Castanedo, Y., Alastuey, A., de la Rosa, J.D., Mantilla, E., de la Campa, A.S., Querol, X., Pey, J., Amato, F., Moreno, T., 2011. Source apportionment of PM10 and PM2.5 at multiple sites in the strait of Gibraltar by PMF: impact of shipping emissions. Environ. Sci. Pollut. Res. 18, 260–269. https://doi.org/10.1007/s11356-010-0373-4

Pope, C.A., Dockery, D.W., 2006. Health effects of fine particulate air pollution: Lines that connect. J. Air Waste Manag. Assoc. 56, 709–742.

Pourmand, A., Prospero, J.M., Sharifi, A., 2014. Geochemical fingerprinting of trans-Atlantic African dust based on radiogenic Sr-Nd-Hf isotopes and rare earth element anomalies. Geology 42, 675–678. https://doi.org/10.1130/G35624.1

Prospero, J.M., 1999. Long-term measurements of the transport of African mineral dust to the southeastern United States: Implications for regional air quality. J. Geophys. Res.-Atmospheres 104, 15917–15927. https://doi.org/10.1029/1999JD900072

Prospero, J.M., Mayol-Bracero, O.L., 2013. Understanding the Transport and Impact of African Dust on the Caribbean Basin. Bull. Am. Meteorol. Soc. 94, 1329–1337. https://doi.org/10.1175/BAMS-D-12-00142.1

Prospero, J.M., Olmez, I., Ames, M., 2001. Al and Fe in PM 2.5 and PM 10 Suspended Particles in South-Central Florida: The Impact of the Long Range Transport of African Mineral Dust. Water. Air. Soil Pollut. 125, 291–317. https://doi.org/10.1023/A:1005277214288

Querol, X., Viana, M., Alastuey, A., Amato, F., Moreno, T., Castillo, S., Pey, J., de la Rosa, J., Sánchez de la Campa, A., Artíñano, B., Salvador, P., García Dos Santos, S.,

Fernández-Patier, R., Moreno-Grau, S., Negral, L., Minguillón, M.C., Monfort, E., Gil, J.I., Inza, A., Ortega, L.A., Santamaría, J.M., Zabalza, J., 2007. Source origin of trace elements in PM from regional background, urban and industrial sites of Spain. Atmos. Environ. 41, 7219–7231. https://doi.org/10.1016/j.atmosenv.2007.05.022

Rodriguez, S., Cuevas, E., Prospero, J.M., Alastuey, A., Querol, X., Lopez-Solano, J., Garcia, M.I., Alonso-Perez, S., 2015. Modulation of Saharan dust export by the North African dipole. Atmospheric Chem. Phys. 15, 7471–7486. https://doi.org/10.5194/acp-15-7471-2015

Rossini, P., Guerzoni, S., Molinaroli, E., Rampazzo, G., De Lazzari, A., Zancanaro, A., 2005. Atmospheric bulk deposition to the lagoon of Venice: Part I. Fluxes of metals, nutrients and organic contaminants. Environ. Int., Lagoon of Venice: Loads, Distribution, and Effects of Nutrients and Pollutants 31, 959–974. https://doi.org/10.1016/j.envint.2005.05.006

Shanquan, L., Ganlin, Z., Jinling, Y., Nan, J., 2016. Multi-Source Characteristics of Atmospheric Deposition in Nanjing, China, as Controlled by East Asia Monsoons and Urban Activities. Pedosphere 26, 374–385. https://doi.org/10.1016/S1002-0160(15)60050-9

Sharma, R.K., Agrawal, M., Marshall, F.M., 2008. Heavy metal (Cu, Zn, Cd and Pb) contamination of vegetables in urban India: a case study in Varanasi. Environ. Pollut. Barking Essex 1987 154, 254–263. https://doi.org/10.1016/j.envpol.2007.10.010

Strayer, H., Smith, R., Mizak, C., Poor, N., 2007. Influence of air mass origin on the wet deposition of nitrogen to Tampa Bay, Florida—An eight-year study. BRACE Bay Reg. Atmospheric Chem. Exp. 41, 4310–4322. https://doi.org/10.1016/j.atmosenv.2006.08.060

Taiwo, A.M., Harrison, R.M., Shi, Z., 2014. A review of receptor modelling of industrially emitted particulate matter. Atmos. Environ. 97, 109–120. https://doi.org/10.1016/j.atmosenv.2014.07.051

Trapp, J.M., Millero, F.J., Prospero, J.M., 2010. Temporal variability of the elemental composition of African dust measured in trade wind aerosols at Barbados and Miami. Mar. Chem., Aerosol chemistry and impacts on the ocean 120, 71–82. https://doi.org/10.1016/j.marchem.2008.10.004

Turtos Carbonell, L.M., Meneses Ruiz, E., Sanchez Gacita, M., Rivero Oliva, J., Diaz Rivero, N., 2007. Assessment of the impacts on health due to the emissions of Cuban power plants that use fossil fuel oils with high content of sulfur. Estimation of external costs. Atmos. Environ. 41, 2202–2213. https://doi.org/10.1016/j.atmosenv.2006.10.062

U.S. EPA, 2009. Integrated Science Assessment (ISA) for Particulate Matter (Final Report, Dec 2009) (Reports & Assessments No. EPA/600/R-08/139F). U.S. Environmental Protection Agency, Washington, DC.

Venturini, E., Vassura, I., Ferroni, L., Raffo, S., Passarini, F., Beddows, D.C.S., Harrison, R.M., 2013. Bulk deposition close to a Municipal Solid Waste incinerator: One source among many. Sci. Total Environ. 456, 392–403. https://doi.org/10.1016/j.scitotenv.2013.03.097

Viana, M., Hammingh, P., Colette, A., Querol, X., Degraeuwe, B., Vlieger, I. de, van Aardenne, J., 2014. Impact of maritime transport emissions on coastal air quality in Europe. Atmos. Environ. 90, 96–105. https://doi.org/10.1016/j.atmosenv.2014.03.046

Viana, M., Kuhlbusch, T. a. J., Querol, X., Alastuey, A., Harrison, R.M., Hopke, P.K., Winiwarter, W., Vallius, A., Szidat, S., Prevot, A.S.H., Hueglin, C., Bloemen, H., Wahlin, P., Vecchi, R., Miranda, A.I., Kasper-Giebl, A., Maenhaut, W., Hitzenberger, R., 2008. Source apportionment of particulate matter in Europe: A review of methods and results. J. Aerosol Sci. 39, 827–849. https://doi.org/10.1016/j.jaerosci.2008.05.007

Walsh, J.J., Jolliff, J.K., Darrow, B.P., Lenes, J.M., Milroy, S.P., Remsen, A., Dieterle, D.A., Carder, K.L., Chen, F.R., Vargo, G.A., Weisberg, R.H., Fanning, K.A., Muller-Karger, F.E., Shinn, E., Steidinger, K.A., Heil, C.A., Tomas, C.R., Prospero, J.S., Lee, T.N., Kirkpatrick, G.J., Whitledge, T.E., Stockwell, D.A., Villareal, T.A., Jochens, A.E., Bontempi, P.S., 2006. Red tides in the Gulf of Mexico: Where, when, and why? J. Geophys. Res. 111, 1–46. https://doi.org/10.1029/2004JC002813

Zhong, C., Yang, Z., Jiang, W., Yu, T., Hou, Q., Li, D., Wang, J., 2014. Annual input fluxes and source identification of trace elements in atmospheric deposition in Shanxi Basin: the largest coal base in China. Environ. Sci. Pollut. Res. 21, 12305–12315. https://doi.org/10.1007/s11356-014-3052-z

Chapter 6

General discussion

1. Air quality and environmental implications

Particulate matter (PM) is a complex mixture of extremely small particles and liquid droplets suspended in the atmosphere originated from a wide range of sources such as traffic, industry, energy production, arid regions, domestic combustion or biomass burning, among others (U.S. EPA, 2016). Consequently, its composition and size is widely variable in space and time (Cheng et al., 2016; Seinfeld and Pandis, 2012). Nowadays, particles, and particularly those with mean aerodynamic diameter below 10 μm (PM_{10}), are a concern because they are related with many adverse effects on human health, ecosystems and climate (Grantz et al., 2003; Kanakidou et al., 2005; Mukherjee and Agrawal, 2017; Pope and Dockery, 2006).

In the present thesis both the concentration and the chemical composition of atmospheric particulate matter have been studied in the coastal region in Cienfuegos, Cuba. The levels of PM_{10} and bulk atmospheric depositions, their chemical and isotopic compositions and their main sources of contribution have been assessed in Chapters 2, 3, 4 and 5. In this chapter we discuss the implications of the results obtained in those chapters for air quality and the environment.

The results presented in this dissertation provide, to our knowledge, the largest datasets published so far on atmospheric chemical element concentrations and depositional flux measurements in Cuba. The levels and composition of aerosol samples in a rural area and the concentration of elements such as Be, total carbon (TC), Al, P, Co, Se, Rb, Sr, Cs, Ba, Hf, Tl, Th, U, Ge, Zr, Nb, Mo, Sn, Sb, W, Hg and lanthanoid elements (La to Lu) in an urban area are reported for the first time in Cuba. Stable carbon and nitrogen isotope composition in aerosols and most of the atmospheric fluxes of the studied elements are also reported for the first time in the country. Therefore, these results expand significantly the existing datasets in Cuba so far, providing a useful information to study air quality and the potential impact of air pollutants on human health and on terrestrial and aquatic ecosystems.

Figure 6.1 shows the concentration range of PM_{10} and major and trace elements measured in PM_{10} in this study (results shown in Chapter 2) that are regulated in the

Cuban legislation for air quality (NC 1020, 2014). Additionally, the Cuban ranges (see Tables 1.5 and 1.6) for the elements determined in PM_{10} have been included. The obtained values are within the range of variation, and in some cases below (As and Cd), of those reported in other regions of the country. Although all major and trace elements in PM_{10} determined in this study were below the MAC established in the Cuban legislation for air quality (NC 1020, 2014), this was not the case for the total content of particulate matter.

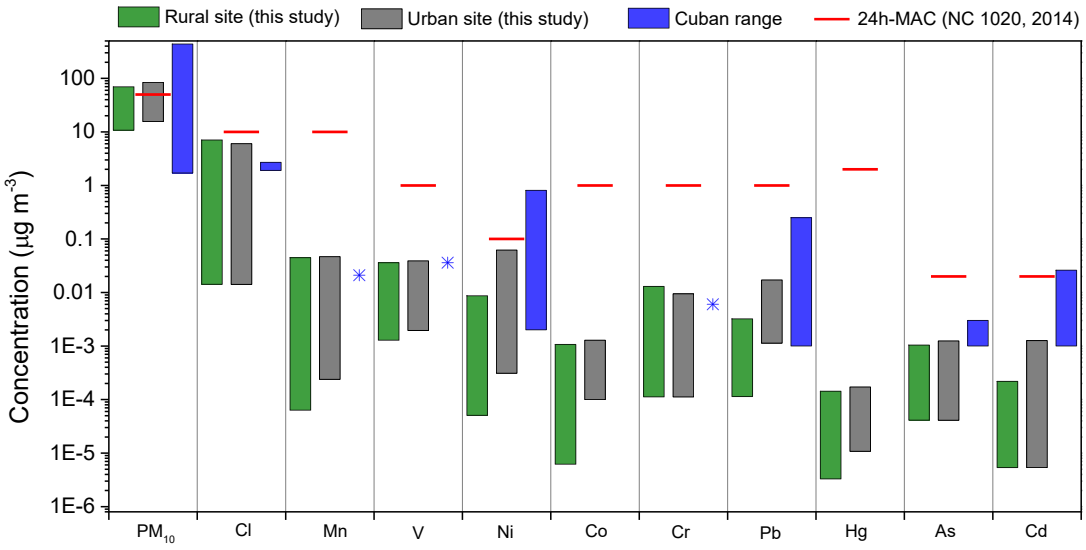

Figure 6.1. Concentration range of PM_{10} and major and trace elements in the studied sites in Cienfuegos. Concentration ranges obtained in different studies carried out in Cuba (see Tables 1.5 and 1.6) (Barja et al., 2013; Cuesta Santos et al., 2014; Martínez Varona et al., 2015, 2013; Molina Esquivel et al., 2011; Pérez et al., 2009; Romero Placeres et al., 2006; Suárez Tamayo et al., 2010) and the 24h-MAC set in the Cuban legislation for air quality (NC 1020, 2014).

Levels of PM_{10} measured in the rural sampling site (24.8 ± 12.1 µg m^{-3}) were lower than those measured in the urban site (35.4 ± 13.6 µg m^{-3}). Even though the annual MAC (30 µg m^{-3}) established by the Cuban legislation was only exceeded in the urban station, the annual PM_{10} value in both studied sites fell below the limits of WHO Air quality guideline (20 µg m^{-3}). The PM_{10} daily limit (50 µg m^{-3}) established in the Cuban legislation was exceeded 3 and 8 times in the rural and urban site, respectively. In a PM_{10} monitoring study that we carried out in 2016 at 3 different sites in the city of Cienfuegos (traffic, urban and sub-urban background sites, see Figure 6.2 and Annex I), we found

similar values to those recorded in 2015. In that monitoring campaign the lower values were observed in the sub-urban background site where, according to the prevalent wind direction, a lower impact of road traffic, shipping and power plant emissions was expected. Highest values were observed the other two sites (traffic and urban background), in each of which an exceedance event occurred.

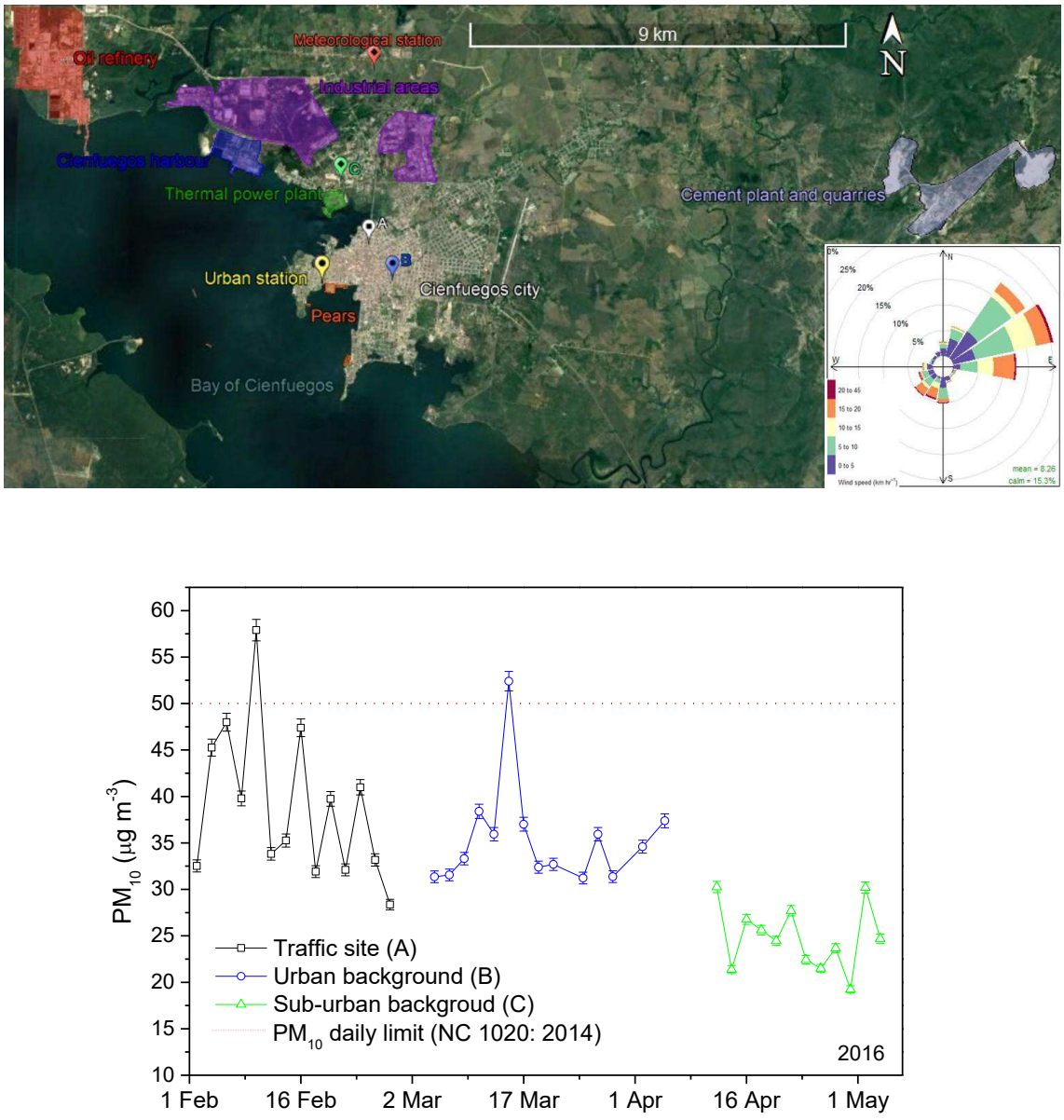

Figure 6.2. PM_{10} in a traffic (A), urban (B) and sub-urban (C) background sites in Cienfuegos in 2016.

Similar results have been also reported in urban sites in Havana and Camagüey during the last 12 years, which in turn were very different from those reported before 2006, when higher PM_{10} (>60 µg m^{-3}) levels were recorded (see Table 1.5). These results,

and the existence of similar meteorological conditions throughout the island, may suggest that there are similarities in terms of air quality in different cities of the country over the last years, which in turn, may be related to a regional impact governed by the Saharan dust intrusions (Mojena López et al., 2015). In this regard, our results can provide the basis for environmental managers to adopt control strategies in order to reduce the impact of PM_{10} pollution, not only in the studied region but also in the rest of the country.

The maximum value recorded for PM_{10} in the rural and the urban sites was, respectively, 69.5 and 84.5 μg m^{-3}. According to these values, the Air Quality Index (ICA), included in the legislation NC 111: 2004 (NC 111, 2004) and calculated using the Equation 1.14, was 139 and 169, thereby indicating a "deficient" air quality at both sites. According to this legislation, these values still do not lead to a "situation of attention" (200<ICA<299: "poor" air quality) or "alert" (300<ICA<499: "very poor" air quality); nevertheless, under such conditions, a slight increase in the frequency and severity of acute and chronic adverse health effects can occur in the general population and, especially, in people with cardiovascular, respiratory and allergic diseases (NC 111, 2004). In that case, the legislation proposes the establishment of environmental programs to prevent the increase of air pollution and achieve their progressive reduction until reaching an ICA<80.

In general, the establishment of environmental programs to reduce or limit the emission of air pollutants involves the identification of the main pollution sources, their contributions and temporal variation (seasonality), among other features. The analytical and statistical approaches employed to carry out the studies presented in the previous Chapters allowed the identification and the chemical and isotopic characterization and quantification of the main local and long-range pollution sources contributing to the PM pollution in Cienfuegos.

As stated in Chapter 2, the PMF source apportionment analysis and the use of integrated statistical approaches and atmospheric transport models (CBPF and CWT) led to the identification of 5 main PM_{10} sources in the studied sites: Saharan dust intrusions, marine aerosol, combustion sources, road traffic and cement plant and quarries. Major

contributions were estimated to be derived from crustal matter (Saharan dust) and combustion sources (wood and fossil fuel burning) in both the rural and urban sites (see Figure 6.3). Globally, contributions related to anthropogenic sources (considered as the sum of combustion sources, road traffic and the cement plant and related activities) accounted, on average, for 53 and 61% of the total PM_{10} mass in the rural and urban sites, respectively. These results reveal the strong anthropogenic influence in the rural site, largely determined by activities developed in the urban area. Consequently, this site cannot be considered as a rural background area.

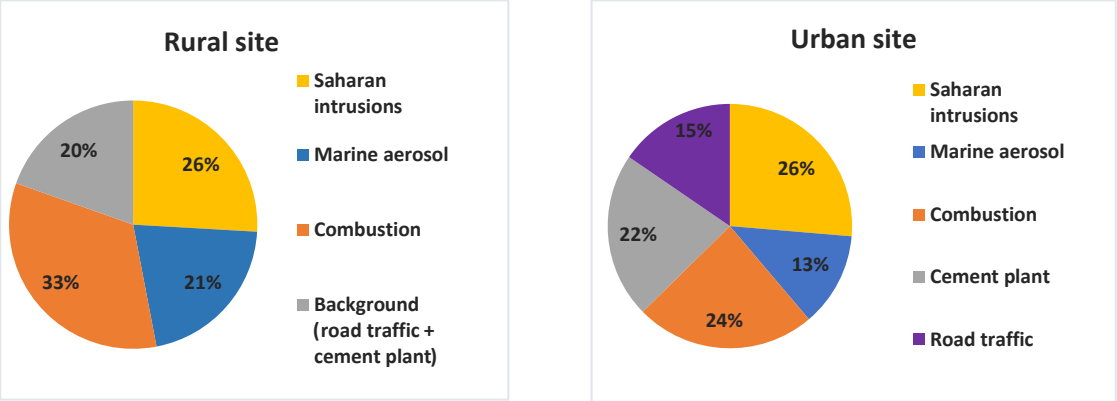

Figure 6.3. PM_{10} mass contribution from the identified sources in Cienfuegos after the PMF source apportionment analysis.

In the same way, the study of lanthanoid elements (Chapter 3) and the C and N stable isotope composition of PM_{10} (Chapter 4) provided a very useful information to understand the sources of atmospheric pollution in Cienfuegos. The lanthanoid dataset from Cienfuegos was consistent with a mixture of crustal (dominated by Saharan dust) and anthropogenic contributions (oil combustion), producing a similar trace elements composition in both sites that was illustrated on diagrams such as Figures 3.4 and 3.6. These results corroborated the influence of common sources and revealed the lack of any strong influence from refinery emissions at both sites. On the other hand, $\delta^{13}C$ and $\delta^{15}N$ signatures (Tables 4.1 and 4.2) were particularly useful to help elucidate the primary sources of contribution of these elements (dominated by emissions related to fossil fuel combustion and cement plant and quarries) and the secondary atmospheric processes [formation of $(NH_4)_2SO_4$] affecting the final content and isotope fractionation

of N in ambient PM_{10}. These results also confirmed the strong influence of combustion sources in both sites.

In view of these results, it is clear the dominance of local anthropogenic sources, especially at the urban site. Nevertheless, special attention should be paid to the Saharan dust contributions. Since the amount of crustal PM present in Cienfuegos air depends on controlling factors such as the seasonality of Saharan dust intrusions and therefore the climatic conditions in the region, the early prediction and identification of such events, as well as the quantification of their contribution, is essential in order to develop effective air quality management strategies.

Evidences discussed in Chapter 2 demonstrated that Saharan dust reached the country between April and August 2015 and had a major impact on air quality, even overwhelming local anthropogenic emissions in many sampling days. Indeed, the Saharan dust contribution (Figures 2.4 and 2.7) represented more than 60% of the total PM_{10} mass measured when its daily limit was exceeded, making clear the importance of the long-range transported dust when assessing air quality. Despite of the growing interest in relation to this issue and in the Caribbean region (Bozlaker et al., 2018, 2013; Prospero et al., 2014) and particularly in Cuba (Venero-Fernández, 2016), the impact of this pollution source on human health has not been adequately addressed. There are still difficulties to discriminate between local and global dust sources.

The tracing of dust aerosols to specific sources based on composition characteristics is difficult because of the diversity of soils and the complexity of the soil emission processes which can lead to a fractionation of different mineral components (Bozlaker et al., 2018). Moreover, the mixing of dust from different locations during transport across thousands of kilometers throughout a period of days to a week or more tends to smooth out the compositional differences in dust from different regions (Kumar et al., 2014; Pourmand et al., 2014). Additionally, dust-loaded air masses can also mix with aerosols emitted from other natural (e.g. marine emissions and wildfires) and anthropogenic (e.g. ships and industrial emissions) sources during atmospheric transport, thereby altering the bulk mineral and chemical composition of PM. These difficulties are added to the fact that the link between air quality and health is largely

based on studies in urban regions, where the atmospheric concentration of species is strongly linked to anthropogenic activities and also to the absence of routine air quality monitoring programs in many sites of interest, like pristine or rural areas (Prospero et al., 2014).

To our knowledge, this is the first work where the impact of African dust on rural and urban ambient PM has been identified and quantified simultaneously in the Caribbean region. Thus, our evidences and approaches will assist regulatory agencies in isolating and quantifying long-range transport dust events and developing targeted management strategies to comply with air quality regulations. More specifically, they will be a valuable tool to review the current legislation on air quality assessment in Cuba and they will allow, where appropriate, exceptions when local PM levels exceed national standards under "exceptional circumstances" (e.g. high contributions from a natural origin like African dust outbreaks). In order to account for the impact of such events, it is necessary to develop a set of diagnostic indicators for African dust (Amodio et al., 2012; Prospero, 1999; Querol et al., 2009). The PM_{10} elemental composition, more specifically the concentration of the crustal elements Al, Fe and Ti (Figures 2.4 and 2.7), the total content of lanthanoid elements (Figure 3.3) and the lanthanoid elements composition (Figures 3.4 and 3.6), all coupled with atmospheric transport models discussed in Chapters 2 and 3, appear to be particularly useful to that end.

Other implications of the long-range transported African dust lie in its impact on coastal ecosystems. Nutrients associated with African dust have been linked to toxic algal blooms (usually presented as red tides) in the Gulf of Mexico and the coastal environment of South Florida (Lenes et al., 2012; Walsh et al., 2006). During summer 2015, between 23 and of 26 July, around 60 cases of skin lesions (most of them in children) were recorded from some popular beaches in Cienfuegos Bay. These lesions were linked to toxic algal blooms that appeared as reddish-brown patches near the shore of the affected beaches and persisted until middle September (Moreira González et al., 2016). In our study (results presented in Chapter 2) the major Saharan dust intrusions (PM_{10} values above 40 μg m^{-3}) were detected in the same region in late June and July 2015, being more than 50% of the total mass of PM_{10} attributable to Saharan dust (see Figures 2.4 and 2.7). Although these results are not conclusive, the input of

nutrients from long-range transported dust and the extreme weather conditions in Cuba in this period (high salinity, temperature, irradiance and water residence time) could be an optimal scenario for algal bloom-forming. Thus, there is a clear need for coordinated studies on long-range dust events. This implies the execution of integrated projects to relate the concentration of nutrients in PM, to the content of these elements in sea water samples and to the algal bloom events occurring in the coastal zone. The approaches used in this thesis can also serve to adequately address this issue in the studied region or in other similar regions affected by long-range transport of particulate matter.

In this sense, the study of the particles removed from the atmosphere, mainly by wet and dry deposition processes at urban, regional, and global scales (U.S. EPA, 2009), provides the basis to better understand the dynamics and origin of several pollutants in the environment, as well as their impact. The study presented in Chapter 5, allowed us to estimate the monthly transfer of elements from the atmosphere to the Earth surface in the Cienfuegos region. This kind of information has proved to be especially useful to study the sedimentation and deposition of nutrients in aquatic and terrestrial ecosystems (Cao et al., 2011; Castillo et al., 2013; Cundy et al., 2003; Sabin et al., 2006), the direct effects on metabolic processes of plant foliage, soil biogeochemistry and microbiology and marine productivity, as well as the contribution to total organics loading resulting in bioaccumulation and biomagnification across trophic levels (Grantz et al., 2003; Okin et al., 2011; U.S. EPA, 2009).

As mentioned in Chapter 5, the monthly deposition of inorganic elements varied greatly throughout the study and no seasonality was observed, which were attributed to the fluctuations of the emissions rather than to meteorological factors controlling the deposition processes. Atmospheric fluxes of typical crustal elements such as Al, Fe, Ti, Co and Zr showed very similar distributions (Figure 5.3), with flux peaks in April and July 2015, coinciding with the occurrence of several African dust intrusions as described above (see Figures 2.4 and 2.7). The high flux of mineral materials observed in July (Figure 5.3), considerably higher than those observed in the rest of summer months, demonstrated that there was a significant contribution of nutrients to the aquatic ecosystems in the region, supporting the idea discussed earlier about the implication of

the Saharan dust on the occurrence of algal blooms in the beaches of the Cienfuegos Bay.

Atmospheric deposition has been regarded as the primary source of heavy metals and nutrients entering into the soil and water reservoirs in many sites around the world (Ayars and Gao, 2007; Gray et al., 2003; Pereira et al., 2007; Yi et al., 2018). The annual flux of nutrients and pollutants over terrestrial and aquatic ecosystems is thus an issue of primary concern. Table 6.1 provided the annual fluxes of the elements studied in Chapter 5. Results have been estimated as the annual pondered sum of the monthly fluxes in each year of study. It should be noted that typical crustal elements (Al, Fe, Mg, Ti, Mn, Rb and Co) and nutrients such as TC and P presented the highest fluxes in 2015, when skin lesions were reported in some beaches in Cienfuegos Bay. It is also important to note the decrease observed for Cu, Mo and W, typical tracers of traffic emissions, probably indicating a lower impact in recent years. In contrast, industrial markers such as Pb, Zn, Sn and V increased. Therefore, environmental managers could adopt strategic measures to improve air quality based on the knowledge of the main pollution sources and associated emissions and depositions in the region, their inter- and intra-annual behavior and their relation with local and regional conditions, all provided in this study.

Table 6.1. Annual bulk deposition (BD) and annual flux of elements determined in a rural site in Cienfuegos, Cuba.

	2014	2015	2016		2014	2015	2016
Kg ha^{-1} y^{-1}				mg ha^{-1} y^{-1}			
BD	166 ± 53	180 ± 63	157 ± 53	**Cd**	278 ± 116	252 ± 115	275 ± 120
TC	37.2 ± 12.3	41.6 ± 15.1	36.5 ± 12.7	**W**	257 ± 122	106 ± 55	85.0 ± 42.2
Ca	12.1 ± 5.1	11.6 ± 5.4	11.9 ± 5.3	**Pr**	236 ± 96	246 ± 109	220 ± 94
Na	9.2 ± 3.8	11.1 ± 5	9.9 ± 4.3	**Nb**	202 ± 108	213 ± 124	163 ± 91
TN	4.7 ± 1.6	4.6 ± 1.7	3.8 ± 1.3	**Th**	201 ± 80	196 ± 85	150 ± 62
S	4.2 ± 2	4.3 ± 2.3	3.8 ± 1.9	**Sm**	184 ± 72	192 ± 83	180 ± 74
Al	2.5 ± 1.4	2.6 ± 1.6	2.3 ± 1.4	**Gd**	166 ± 65	175 ± 75	167 ± 68
K	2.3 ± 0.9	2.4 ± 1	2.3 ± 0.9	**Dy**	129 ± 54	137 ± 62	134 ± 58
Fe	2.2 ± 0.9	2.3 ± 1	1.9 ± 0.8	**Ge**	127 ± 64	123 ± 68	92 ± 49
Mg	1.7 ± 0.7	2.0 ± 0.8	1.6 ± 0.7	**Cs**	109 ± 43	104 ± 45	219 ± 91
g ha^{-1} y^{-1}				**U**	105 ± 40	87.1 ± 36.6	72.3 ± 29.1
P	381 ± 161	415 ± 192	344 ± 152	**Er**	70.9 ± 29.5	75.7 ± 34.5	74.4 ± 32.4
Ti	109 ± 65	126 ± 82	96.7 ± 60.3	**Tl**	66.3 ± 42.2	48.0 ± 33.5	31.2 ± 20.8
Zn	70.0 ± 27.4	330 ± 142	235 ± 97	**Yb**	62.1 ± 25.9	66.1 ± 30.2	66.0 ± 28.9
Mn	56.1 ± 19.9	60.9 ± 23.6	49.5 ± 18.4	**Be**	61.8 ± 24.1	60.6 ± 25.8	43.4 ± 17.7
Cu	54.4 ± 22.2	24.2 ± 10.8	20.6 ± 8.8	**Hf**	52.2 ± 62.8	52.3 ± 68.9	48.8 ± 61.5
Sr	40.0 ± 16.6	29.9 ± 13.6	29.3 ± 12.7	**Eu**	47.1 ± 18.6	48.6 ± 21	46.2 ± 19.1
V	33.7 ± 12.9	36.8 ± 15.4	45.7 ± 18.3	**Ho**	25.0 ± 8.9	33.9 ± 13.3	91.8 ± 34.4
Ba	22.1 ± 8.5	19.3 ± 8.1	15.4 ± 6.2	**Te**	19.1 ± 15.7	19.7 ± 17.7	8.9 ± 7.6
Pb	19.6 ± 8.3	20.2 ± 9.4	31.2 ± 13.9	**Tm**	10.0 ± 4.1	10.7 ± 4.8	11.4 ± 4.8
Ni	12.4 ± 4.9	13.6 ± 5.8	11.9 ± 4.9	**Lu**	9.2 ± 3.6	10.3 ± 4.5	11.1 ± 4.6
Cr	10.6 ± 4.6	11.7 ± 5.6	8.0 ± 3.7				
Sb	9.8 ± 3.8	14.5 ± 6.1	0.9 ± 0.4				
Rb	8.9 ± 3.4	9.3 ± 3.9	9.1 ± 3.7				
As	4.5 ± 1.8	7.5 ± 3.2	1.3 ± 0.5				
Ce	2.0 ± 0.8	2.0 ± 0.9	1.9 ± 0.8				
Mo	1.7 ± 0.9	0.7 ± 0.4	1.0 ± 0.5				
Zr	1.7 ± 0.8	1.8 ± 0.9	1.6 ± 0.7				
Co	1.0 ± 0.4	1.1 ± 0.4	0.9 ± 0.3				
La	1.0 ± 0.4	1.0 ± 0.4	1.0 ± 0.4				
Sn	0.9 ± 0.6	0.9 ± 0.7	2.0 ± 1.5				
Nd	0.9 ± 0.4	0.9 ± 0.4	0.9 ± 0.4				

Note: Total carbon (TC) and total nitrogen (TN) were not included in Chapter 5 but due to their importance they have been included here (see Annex I). They were measured according to the methodology described in Chapter 4.

As in the PM_{10} samples, the study of the atmospheric bulk deposition samples revealed the anthropogenic origin of several elements such as Zn, Sb, Pb, W, Sn, S, Cu and Mo (Figure 5.7), typically related to the industrial and road traffic emissions (Grigoratos and Martini, 2015; Johansson et al., 2009; Querol et al., 2007; Taiwo et al.,

2014). Such results and the application of different statistical approaches such as PCA-MLRA source apportionment or cluster analysis, allowed to identify 5 main contributors to the bulk atmospheric depositions collected in the rural site (Figure 5.8): crustal matter (39.5%), marine aerosol (38.2%), combustion (6.7%), industrial activities (8.7%) and traffic (1.4%). These sources were similar to those isolated by the PMF analysis on PM_{10} samples (Figure 6.3). The main differences observed in the estimated contributions are attributed to the different particle fractions studied. It is expected that in bulk deposition, the concentration of coarse particles (greater than 10 μm) be significant, as a consequence of the mechanical disruption of large particles by crushing or grinding, the bursting bubbles in the ocean (sea spray) or the dust resuspension (Cao et al., 2013; Cesari et al., 2012). As a result, higher crustal and marine fractions were observed in bulk depositions.

In addition to the separate evaluation of the impact of the aerosols and atmospheric depositions, the simultaneous monitoring of PM_{10} and bulk deposition samples during 2015 have relevant implications on assessing the impact on air quality and terrestrial and aquatic ecosystems. Both approaches can be used to calculate the total (wet plus dry) deposition velocity (V_d) of the studied elements, a critical parameter for environmental modeling purposes (Chance et al., 2015; Maro et al., 2014; Roupsard et al., 2013). Taking into account that data required for the calculations of V_d are often limited, empirical estimates of V_d and calculations using radiotracers like ^{7}Be and ^{210}Pb have been usually applied to improve the parametrization of deposition models (Chance et al., 2015; Laguionie et al., 2014; Percot et al., 2013; Roupsard et al., 2013; U.S. EPA, 2009). Then, our results are very suitable to alleviate these limitations and expand the existing databases.

The V_d for any element can be determined by the ratio between the total flux (F) of an element to the Earth's surface and its concentration in air (C) at the Earth surface ($V_d = F/C$) (Dueñas et al., 2005). The average V_d of the studied elements, estimated by taking into account the fluxes of bulk deposition and the concentrations in atmospheric PM_{10} provided in Chapter 2, 3 and 5, are shown in Figure 6.4. The total deposition velocity generated in this way is, therefore, a function of aerosol particle sizes (e.g. elements with higher velocities such as Ca, Mn, Fe, La, Ce, Rb and Al, are partially

attributed to the dominance of the largest aerosol particles dominated by gravitational settling) and environmental conditions such as precipitations (amount of rainfall, number of rainy days, duration, among other parameters) and wind speed (that can induce resuspension).

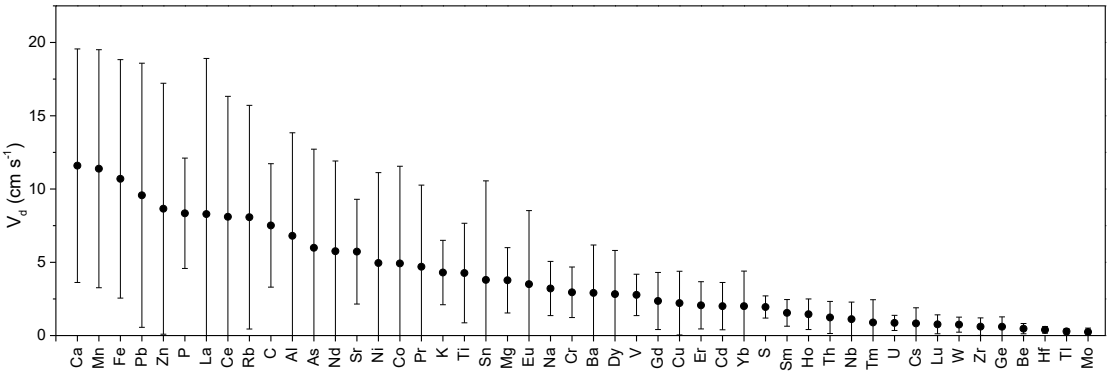

Figure 6.4. Average total deposition velocity (V_d) determined in a rural site of Cienfuegos during 2015. Bars represent the standard deviation (1σ).

Once calculated, V_d can be used to determine the fluxes of pollutants to the Earth's surface from the concentration of these pollutants in air (Gao et al., 2016; Ioannidou, 2012) or, in our case, to determine the concentration of air pollutants from their fluxes (reported in Chapter 5 from 2014 to 2016). Figure 6.4 shows the estimated average concentrations of the studied elements in 2014 and 2016 along with the average concentration of 2015. Although the estimated concentrations were derived from deposition velocities directly calculated for each element, bulk deposition varied temporally depending on many factors. Therefore, it is likely that these values have an associated uncertainty. For most of the elements, the estimated concentrations are comparable to the values measured in 2015, although slightly lower. The highest differences are observed in crustal elements like Al, Fe, Ti, Ce and La. As described in Chapters 2 and 3, the high concentrations of these elements are associated to Saharan dust intrusions, indicating a stronger long-range transport influence in 2015.

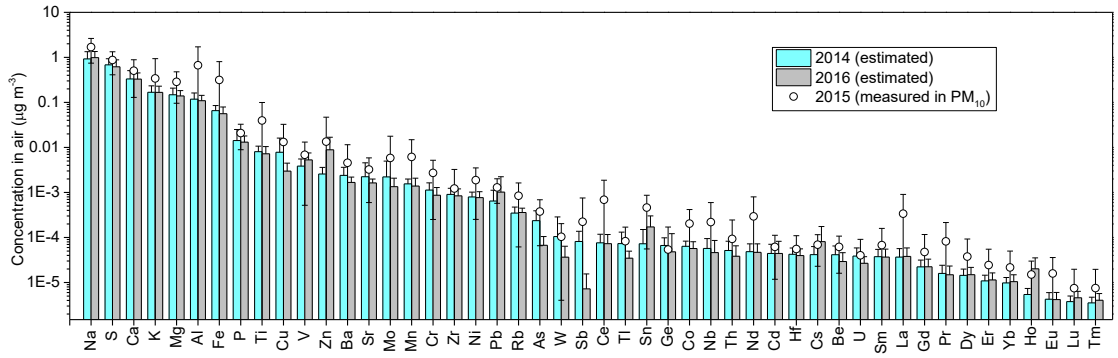

Figure 6.5. Estimated average concentrations of the studied elements in 2014 and 2016 and average concentration measured in 2015 in the rural site in Cienfuegos. Bars represent the standard deviation (1σ).

On the other hand, dry particulate deposition, especially of heavy metals, base cations, and organic contaminants, is a complex and poorly characterized process (Dämmgen et al., 2005; U.S. EPA, 2009). For the determination of the atmospheric dry deposition fluxes of trace elements in aerosols is necessary to have the dry deposition velocity (V_{dd}), instead of the V_d. As our data are based in monthly bulk deposition (wet plus dry), it is not possible to determine V_{dd}; nevertheless, for specific purposes, a rough estimation, based on data from the months without precipitation (or having little precipitation, e.g. <20mm) could be addressed. However, we recommend to modify the approaches used in this work in order to monitor dry and wet depositions separately.

Finally, the emissions from different pollution sources (power plant, traffic and shipping exhaust emissions, road dust, top soils, bulk deposition around a cement plant and petroleum-coke from the cement plant) were chemically and isotopically ($\delta^{13}C$ and $\delta^{15}N$) characterized, which can be the basis for future studies on air pollution and environmental impact assessment. These results are very suitable for 1) calculation of both receptor and source-oriented models (Amato et al., 2009; Gibson et al., 2013; Kim and Hopke, 2005; Turtos Carbonell et al., 2007) and for 2) establishing specific tracers, capable of discriminating different pollution sources (Lopez-Veneroni, 2009; Moreno et al., 2010; Viana et al., 2009; Widory et al., 2004). Based on the knowledge acquired on PM sources and the chemical/isotopic profiles provided by the measurement of samples collected directly in several of these sources, we strongly recommend to preform

constrained source apportionment analyses (Amato et al., 2016; Cesari et al., 2016) and dispersion model calculations in order to continue improving the understanding on aerosol properties and the processes that pollutants undergo in the atmosphere.

References

Amato, F., Favez, O., Pandolfi, M., Alastuey, A., Querol, X., Moukhtar, S., Bruge, B., Verlhac, S., Orza, J.A.G., Bonnaire, N., Le Priol, T., Petit, J.-F., Sciare, J., 2016. Traffic induced particle resuspension in Paris: Emission factors and source contributions. Atmos. Environ. 129, 114–124. https://doi.org/10.1016/j.atmosenv.2016.01.022

Amato, F., Pandolfi, M., Escrig, A., Querol, X., Alastuey, A., Pey, J., Perez, N., Hopke, P.K., 2009. Quantifying road dust resuspension in urban environment by Multilinear Engine: A comparison with PMF2. Atmos. Environ. 43, 2770–2780. https://doi.org/10.1016/j.atmosenv.2009.02.039

Amodio, M., Andriani, E., de Gennaro, G., Loiotile, A.D., Di Gilio, A., Placentino, M.C., 2012. An integrated approach to identify the origin of PM10 exceedances. Environ. Sci. Pollut. Res. 19, 3132–3141. https://doi.org/10.1007/s11356-012-0804-5

Ayars, J., Gao, Y., 2007. Atmospheric nitrogen deposition to the Mullica River-Great Bay Estuary. Mar. Environ. Res. 64, 590–600. https://doi.org/10.1016/j.marenvres.2007.06.004

Barja, B., Mogo, S., Cachorro, V.E., Carlos Antuna, J., Estevan, R., Rodrigues, A., de Frutos, A., 2013. Atmospheric particulate matter levels, chemical composition and optical absorbing properties in Camaguey, Cuba. Environ. Sci.-Process. Impacts 15, 440–453. https://doi.org/10.1039/c2em30854a

Bozlaker, A., Prospero, J.M., Fraser, M.P., Chellam, S., 2013. Quantifying the Contribution of Long-Range Saharan Dust Transport on Particulate Matter Concentrations in Houston, Texas, Using Detailed Elemental Analysis. Environ. Sci. Technol. 47, 10179–10187. https://doi.org/10.1021/es4015663

Bozlaker, A., Prospero, J.M., Price, J., Chellam, S., 2018. Linking Barbados Mineral Dust Aerosols to North African Sources Using Elemental Composition and Radiogenic Sr, Nd, and Pb Isotope Signatures. J. Geophys. Res. Atmospheres 123, 2017JD027505. https://doi.org/10.1002/2017JD027505

Cao, J.J., Chow, J.C., Lee, F.S.C., Watson, J.G., 2013. Evolution of PM2.5 measurements and standards in the U.S. and future perspectives for China.

Cao, Z., Yang, Y., Lu, J., Zhang, C., 2011. Atmospheric particle characterization, distribution, and deposition in Xi'an, Shaanxi Province, Central China. Environ. Pollut. 159, 577–584. https://doi.org/10.1016/j.envpol.2010.10.006

Castillo, S., de la Rosa, J.D., Sanchez de la Campa, A.M., Gonzalez-Castanedo, Y., Fernandez-Camacho, R., 2013. Heavy metal deposition fluxes affecting an Atlantic coastal area in the southwest of Spain. Atmos. Environ. 77, 509–517. https://doi.org/10.1016/j.atmosenv.2013.05.046

Cesari, D., Contini, D., Genga, A., Siciliano, M., Elefante, C., Baglivi, F., Daniele, L., 2012. Analysis of raw soils and their re-suspended PM10 fractions: Characterisation of source profiles and enrichment factors. Appl. Geochem. 27, 1238–1246. https://doi.org/10.1016/j.apgeochem.2012.02.029

Cesari, D., Donateo, A., Conte, M., Merico, E., Giangreco, A., Giangreco, F., Contini, D., 2016. An inter-comparison of PM2.5 at urban and urban background sites: Chemical characterization and source apportionment. Atmospheric Res. 174, 106–119. https://doi.org/10.1016/j.atmosres.2016.02.004

Chance, R., Jickells, T.D., Baker, A.R., 2015. Atmospheric trace metal concentrations, solubility and deposition fluxes in remote marine air over the south-east Atlantic. Mar. Chem. 177, 45–56. https://doi.org/10.1016/j.marchem.2015.06.028

Cheng, Z., Luo, L., Wang, S., Wang, Y., Sharma, S., Shimadera, H., Wang, X., Bressi, M., de Miranda, R.M., Jiang, J., Zhou, W., Fajardo, O., Yan, N., Hao, J., 2016. Status and characteristics of ambient PM2.5 pollution in global megacities. Environ. Int. 89–90, 212–221. https://doi.org/10.1016/j.envint.2016.02.003

Cuesta Santos, O., Collazo Aranda, A., Sánchez Navarro, P., Manrique Suárez, R., Fonseca Hernández, M., Rodríguez Valdés, D., Sánchez Díaz, A., Miló López, M.V., Díaz Díaz, J.M., Victorero Hernández, A., González Jaime, Y., Sosa Pérez, C., 2014. Air quality of Pinar del Rio city. Experimental values. Rev. Cuabana Meteorol. 20, 98–113.

Cundy, A.B., Croudace, I.W., Cearreta, A., Irabien, M.J., 2003. Reconstructing historical trends in metal input in heavily-disturbed, contaminated estuaries: studies from Bilbao, Southampton Water and Sicily. Appl. Geochem. 18, 311–325. https://doi.org/10.1016/S0883-2927(02)00127-0

Dämmgen, U., Erisman, J.W., Cape, J.N., Grünhage, L., Fowler, D., 2005. Practical considerations for addressing uncertainties in monitoring bulk deposition. Environ. Pollut. 134, 535–548. https://doi.org/10.1016/j.envpol.2004.08.013

Dueñas, C., Fernández, M.C., Carretero, J., Liger, E., Cañete, S., 2005. Deposition velocities and washout ratios on a coastal site (southeastern Spain) calculated from 7Be and 210Pb measurements. Atmos. Environ. 39, 6897–6908.

Gao, Y., Mukherjee, P., Jusino-Atresino, R., 2016. The Air-Coastal Sea Chemical Exchange: A Case Study on the New Jersey Coast. Aquat. Geochem. 22, 275–289. https://doi.org/10.1007/s10498-015-9285-8

Gibson, M.D., Kundu, S., Satish, M., 2013. Dispersion model evaluation of PM2.5, NOX and SO2 from point and major line sources in Nova Scotia, Canada using AERMOD Gaussian plume air dispersion model. Atmospheric Pollut. Res. 4, 157–167. https://doi.org/10.5094/APR.2013.016

Grantz, D.A., Garner, J.H.B., Johnson, D.W., 2003. Ecological effects of particulate matter. Environ. Int. 29, 213–239. https://doi.org/10.1016/S0160-4120(02)00181-2

Gray, C.W., McLaren, R.G., Roberts, A.H.C., 2003. Atmospheric accessions of heavy metals to some New Zealand pastoral soils. Sci. Total Environ. 305, 105–115. https://doi.org/10.1016/S0048-9697(02)00404-7

Grigoratos, T., Martini, G., 2015. Brake wear particle emissions: a review. Environ. Sci. Pollut. Res. 22, 2491–2504. https://doi.org/10.1007/s11356-014-3696-8

Ioannidou, A., 2012. 7 Be aerosols and their deposition on the sea: a possible method to estimate trace metals deposition on the sea. J. Environ. Radioact. 108, 29–32.

Johansson, C., Norman, M., Burman, L., 2009. Road traffic emission factors for heavy metals. Atmos. Environ. 43, 4681–4688. https://doi.org/10.1016/j.atmosenv.2008.10.024

Kanakidou, M., Seinfeld, J.H., Pandis, S.N., Barnes, I., Dentener, F.J., Facchini, M.C., Van Dingenen, R., Ervens, B., Nenes, A., Nielsen, C.J., Swietlicki, E., Putaud, J.P., Balkanski, Y., Fuzzi, S., Horth, J., Moortgat, G.K., Winterhalter, R., Myhre, C.E.L., Tsigaridis, K., Vignati, E., Stephanou, E.G., Wilson, J., 2005. Organic aerosol and global climate modelling: a review. Atmos Chem Phys 5, 1053–1123. https://doi.org/10.5194/acp-5-1053-2005

Kim, E., Hopke, P.K., 2005. Identification of fine particle sources in mid-Atlantic US area. Water. Air. Soil Pollut. 168, 391–421. https://doi.org/10.1007/s11270-005-1894-1

Kumar, A., Abouchami, W., Galer, S.J.G., Garrison, V.H., Williams, E., Andreae, M.O., 2014. A radiogenic isotope tracer study of transatlantic dust transport from Africa to the Caribbean. Atmos. Environ. 82, 130–143. https://doi.org/10.1016/j.atmosenv.2013.10.021

Laguionie, P., Roupsard, P., Maro, D., Solier, L., Rozet, M., Hebert, D., Connan, O., 2014. Simultaneous quantification of the contributions of dry, washout and rainout deposition to the total deposition of particle-bound Be-7 and Pb-210 on an urban catchment area on a monthly scale. J. Aerosol Sci. 77, 67–84. https://doi.org/10.1016/j.jaerosci.2014.07.008

Lenes, J.M., Prospero, J.M., Landing, W.M., Virmani, J.I., Walsh, J.J., 2012. A model of Saharan dust deposition to the eastern Gulf of Mexico. Mar. Chem. 134–135, 1–9. https://doi.org/10.1016/j.marchem.2012.02.007

Lopez-Veneroni, D., 2009. The stable carbon isotope composition of PM2.5 and PM10 in Mexico City Metropolitan Area air. Atmos. Environ. 43, 4491–4502. https://doi.org/10.1016/j.atmosenv.2009.06.036

Maro, D., Connan, O., Flori, J.P., Hébert, D., Mestayer, P., Olive, F., Rosant, J.M., Rozet, M., Sini, J.F., Solier, L., 2014. Aerosol dry deposition in the urban environment: Assessment of deposition velocity on building facades. J. Aerosol Sci. 69, 113–131. https://doi.org/10.1016/j.jaerosci.2013.12.001

Martínez Varona, M., Guzmán Vila, M., Pérez Cabrera, A., Fernández Arocha, A., 2015. Presencia de metales pesados en material particulado en aire. Estación de monitoreo INHEM, Centro Habana. Ecosolar 52.

Martínez Varona, M., Molina Esquivel, E., Maldonado Cantillo, G., Guzmán Vila, M., Alonso, D., 2013. Comportamiento de partículas menores de 10 micras mediante dos equipos de monitoreo. Hig. Sanid. Ambient. 13, 1060–1065.

Mojena López, E., Ortega González, A., Casilles Vega, E.F., Leyva Santos, J., 2015. Sahara Clouds Dust. Their presence in Cuba. Rev. Cuabana Meteorol. 21, 120–134.

Molina Esquivel, E., Pérez Zayas, G., Martínez Varona, M., Aldape Ugalde, F., Flores Maldonado, J., 2011. Comportamiento de las fracciones fina y gruesa de PM10 en la estación de monitoreo de calidad del aire en Centro Habana. Campaña 2006-2007. Hig. Sanid. Ambient. 11, 820–826.

Moreira González, A., Abilio Comas, A., Valle Pombrol, A., Seisdedo, M., 2016. Bloom of Vulcanodinium rugosum linked to skin lesions in Cienfuegos Bay, Cuba. HARMFUL ALGAE NEWS 55.

Moreno, T., Querol, X., Alastuey, A., de la Rosa, J., Sánchez de la Campa, A.M., Minguillón, M., Pandolfi, M., González-Castanedo, Y., Monfort, E., Gibbons, W., 2010. Variations in vanadium, nickel and lanthanoid element concentrations in urban air. Sci. Total Environ. 408, 4569–4579. https://doi.org/10.1016/j.scitotenv.2010.06.016

Mukherjee, A., Agrawal, M., 2017. World air particulate matter: sources, distribution and health effects. Environ. Chem. Lett. 15, 283–309. https://doi.org/10.1007/s10311-017-0611-9

NC 111, 2004. Norma Cubana 111:2004. CALIDAD DEL AIRE—REGLAS PARA LA VIGILANCIA DE LA CALIDAD DEL AIRE EN ASENTAMIENTOS HUMANOS.

NC 1020, 2014. Norma Cubana 1020:2014. CALIDAD DEL AIRE — CONTAMINANTES — CONCENTRACIONES MÁXIMAS ADMISIBLES Y VALORES GUÍAS EN ZONAS HABITABLES.

Okin, G.S., Baker, A.R., Tegen, I., Mahowald, N.M., Dentener, F.J., Duce, R.A., Galloway, J.N., Hunter, K., Kanakidou, M., Kubilay, N., Prospero, J.M., Sarin, M., Surapipith, V., Uematsu, M., Zhu, T., 2011. Impacts of atmospheric nutrient deposition on marine productivity: Roles of nitrogen, phosphorus, and iron. Glob. Biogeochem. Cycles 25, GB2022. https://doi.org/10.1029/2010GB003858

Percot, S., Ruban, V., Roupsard, P., Maro, D., Millet, M., 2013. Use of beryllium-7 as a surrogate to determine the deposition of metal and polycyclic aromatic hydrocarbon through urban aerosols in Nantes, France. Atmos. Environ. 74, 338–345. https://doi.org/10.1016/j.atmosenv.2013.03.056

Pereira, P.A. de P., Lopes, W.A., Carvalho, L.S., da Rocha, G.O., Bahia, N. de C., Loyola, J., Quiterio, S.L., Escaleira, V., Arbilla, G., de Andrade, J.B., 2007. Atmospheric concentrations and dry deposition fluxes of particulate trace metals in Salvador, Bahia, Brazil. Atmos. Environ. 41, 7837–7850. https://doi.org/10.1016/j.atmosenv.2007.06.013

Pérez, G., Piñera, I., Aldape, F., Flores, J.M., Martínez, M., Molina, E., Fernández, A., Ramos, M., Guibert, R., 2009. First study of airborne particulate pollution using pixe analysis in Havana city, Cuba. Int. J. PIXE 19, 157–166. https://doi.org/10.1142/S0129083509001849

Pope, C.A., Dockery, D.W., 2006. Health effects of fine particulate air pollution: Lines that connect. J. Air Waste Manag. Assoc. 56, 709–742.

Pourmand, A., Prospero, J.M., Sharifi, A., 2014. Geochemical fingerprinting of trans-Atlantic African dust based on radiogenic Sr-Nd-Hf isotopes and rare earth element anomalies. Geology 42, 675–678. https://doi.org/10.1130/G35624.1

Prospero, J.M., 1999. Long-term measurements of the transport of African mineral dust to the southeastern United States: Implications for regional air quality. J. Geophys. Res.-Atmospheres 104, 15917–15927. https://doi.org/10.1029/1999JD900072

Prospero, J.M., Collard, F.-X., Molinie, J., Jeannot, A., 2014. Characterizing the annual cycle of African dust transport to the Caribbean Basin and South America and its impact on the environment and air quality. Glob. Biogeochem. Cycles 28, 757–773. https://doi.org/10.1002/2013GB004802

Querol, X., Pey, J., Pandolfi, M., Alastuey, A., Cusack, M., Pérez, N., Moreno, T., Viana, M., Mihalopoulos, N., Kallos, G., Kleanthous, S., 2009. African dust contributions to mean ambient PM10 mass-levels across the Mediterranean Basin. Atmos. Environ. 43, 4266–4277. https://doi.org/10.1016/j.atmosenv.2009.06.013

Querol, X., Viana, M., Alastuey, A., Amato, F., Moreno, T., Castillo, S., Pey, J., de la Rosa, J., Sánchez de la Campa, A., Artíñano, B., Salvador, P., García Dos Santos, S., Fernández-Patier, R., Moreno-Grau, S., Negral, L., Minguillón, M.C., Monfort, E., Gil, J.I., Inza, A., Ortega, L.A., Santamaría, J.M., Zabalza, J., 2007. Source origin of trace elements in PM from regional background, urban and industrial sites of Spain. Atmos. Environ. 41, 7219–7231. https://doi.org/10.1016/j.atmosenv.2007.05.022

Romero Placeres, M., Diego Olite, F., Álvarez Toste, M., 2006. La contaminación del aire: su repercusión como problema de salud. Rev. Cuba. Hig. Epidemiol. 44, 0–0.

Roupsard, P., Amielh, M., Maro, D., Coppalle, A., Branger, H., Connan, O., Laguionie, P., Hebert, D., Talbaut, M., 2013. Measurement in a wind tunnel of dry deposition velocities of submicron aerosol with associated turbulence onto rough and smooth urban surfaces. J. Aerosol Sci. 55, 12–24. https://doi.org/10.1016/j.jaerosci.2012.07.006

Sabin, L.D., Lim, J.H., Stolzenbach, K.D., Schiff, K.C., 2006. Atmospheric dry deposition of trace metals in the coastal region of Los Angeles, California, USA. Environ. Toxicol. Chem. 25, 2334–2341. https://doi.org/10.1897/05-300R.1

Seinfeld, J.H., Pandis, S.N., 2012. Atmospheric Chemistry and Physics: From Air Pollution to Climate Change. Wiley.

Suárez Tamayo, S., Maldonado Cantillo, G., Cañas Ávila, N., Romero Placeres, M., 2010. Contribución de la contaminación atmosférica a la ocurrencia de enfermedades respiratorias agudas en menores de 15 años. Ciudad de La Habana, 2001-2003. Hig. Sanid. Ambient. 10, 635–644.

Taiwo, A.M., Harrison, R.M., Shi, Z., 2014. A review of receptor modelling of industrially emitted particulate matter. Atmos. Environ. 97, 109–120. https://doi.org/10.1016/j.atmosenv.2014.07.051

Turtos Carbonell, L.M., Meneses Ruiz, E., Sanchez Gacita, M., Rivero Oliva, J., Diaz Rivero, N., 2007. Assessment of the impacts on health due to the emissions of Cuban power plants that use fossil fuel oils with high content of sulfur. Estimation of external costs. Atmos. Environ. 41, 2202–2213. https://doi.org/10.1016/j.atmosenv.2006.10.062

U.S. EPA, 2016. Particulate Matter (PM) Pollution [WWW Document]. US EPA. URL https://www.epa.gov/pm-pollution (accessed 1.13.18).

U.S. EPA, 2009. Integrated Science Assessment (ISA) for Particulate Matter (Final Report, Dec 2009) (Reports & Assessments No. EPA/600/R-08/139F). U.S. Environmental Protection Agency, Washington, DC.

Venero-Fernández, S.J., 2016. Saharan Dust Effects on Human Health: A Challenge for Cuba's Researchers. MEDICC Rev. 18, 32–34.

Viana, M., Amato, F., Alastuey, A., Querol, X., Moreno, T., Garcia Dos Santos, S., Dolores Herce, M., Fernandez-Patier, R., 2009. Chemical Tracers of Particulate Emissions from Commercial Shipping. Environ. Sci. Technol. 43, 7472–7477. https://doi.org/10.1021/es901558t

Walsh, J.J., Jolliff, J.K., Darrow, B.P., Lenes, J.M., Milroy, S.P., Remsen, A., Dieterle, D.A., Carder, K.L., Chen, F.R., Vargo, G.A., Weisberg, R.H., Fanning, K.A., Muller-Karger, F.E., Shinn, E., Steidinger, K.A., Heil, C.A., Tomas, C.R., Prospero, J.S., Lee, T.N., Kirkpatrick, G.J., Whitledge, T.E., Stockwell, D.A., Villareal, T.A., Jochens, A.E., Bontempi, P.S., 2006. Red tides in the Gulf of Mexico: Where, when, and why? J. Geophys. Res. 111, 1–46. https://doi.org/10.1029/2004JC002813

Widory, D., Roy, S., Le Moullec, Y., Goupil, G., Cocherie, A., Guerrot, C., 2004. The origin of atmospheric particles in Paris: a view through carbon and lead isotopes. Atmos. Environ. 38, 953–961. https://doi.org/10.1016/j.atmosenv.2003.11.001

Yi, K., Fan, W., Chen, J., Jiang, S., Huang, S., Peng, L., Zeng, Q., Luo, S., 2018. Annual input and output fluxes of heavy metals to paddy fields in four types of contaminated areas in Hunan Province, China. Sci. Total Environ. 634, 67–76. https://doi.org/10.1016/j.scitotenv.2018.03.294

General conclusions

The evaluation of the obtained results in the present thesis lead to the following main conclusions:

1. Annual concentrations of PM_{10} in the rural and urban sites of Cienfuegos reached 24.8 and 35.4 $\mu g\ m^{-3}$, respectively. The highest concentrations were observed between March and August at both sites, as a result of the Saharan dust intrusions.

2. Analyses of PM_{10} showed significant contributions of mineral matter, total carbon and secondary inorganic compounds in the region, with highest concentrations in the urban site. By contrast, marine contribution was higher in the rural site.

3. The PM_{10} daily limit of 50 $\mu g\ m^{-3}$, established in the Cuban legislation for air quality, was exceeded 3 and 8 times in the rural and urban sites, respectively. However, concentrations of trace elements in both sites were below the maximum admissible concentration set in this legislation.

4. According to the levels of PM_{10} and the current regulation NC 111: 2004, the Air Quality is classified as “deficient” in both studied sites in Cienfuegos.

5. The applied statistical and model tools identified 5 main sources contributing to the total PM_{10} in the studied region: Saharan dust, marine aerosol, combustion, road traffic and cement plant and quarries.

6. Saharan dust contribution was quantified for the first time in Cuba, proving to be one of the most important pollution sources. In fact, the contribution of this source explained more than 60% of the PM_{10} in 10 of the 11 exceedance events.

7. Contributions from anthropogenic sources accounted, on average, for 53% and 61% of the total PM_{10} mass in the rural and urban sites, respectively. Consequently, the studied rural site cannot be considered as a rural background area.

8. Concentrations of lanthanoid elements were strongly modulated by the seasonality of Saharan dust intrusions in the Caribbean, which suggest they can be used as a signature for African dust. However, the origin of these elements was not exclusively crustal, showing the influence of different anthropogenic sources.

9. $\delta^{13}C$ signature in PM_{10} in Cienfuegos revealed the mixing contributions from two main emitters: fossil fuel combustion and cement plant and quarries.

10. $\delta^{15}N$ signature in PM_{10} in Cienfuegos suggested the formation of secondary nitrogen under the form of $(NH_4)_2SO_4$. Exchange between gas (NH_3) and particle (NH_4^+) under stoichiometric equilibrium in $(NH_4)_2SO_4$ can explain the ^{15}N enrichment observed. However, primary nitrogen seemed to be generated by diesel road traffic and power plant emissions.
11. Bulk depositions and fluxes of major and trace elements showed a high temporal variability, although without showing any significant relation to dry and wet periods. However, crustal elements showed a marked seasonality with the presence of Saharan dust intrusions in the Caribbean.
12. Most of the elements in bulk depositions showed similar values to those reported in rural environments around the world. On the contrary, V, Ni, As and Sb presented higher levels than those typically found in urban and industrial areas. In addition, samples were significantly enriched in Zn, Sb, Pb, W, Sn, S, Cu, Mo, Nb and P, thereby revealing their anthropogenic origin.
13. Annual flux tendency of trace elements revealed a decrease of road traffic emissions and an increase of industrial ones in the last years.
14. Statistical analyses enabled the identification of 5 main sources contributing to bulk deposition: crustal matter (39.5%), marine aerosol (38.2%), combustion of wastes, wood and fossil fuel (6.7%), industries (8.7%) and road traffic (1.4%).
15. The results presented in this thesis expand significantly the datasets already existing in Cuba, providing a useful information to study air quality and the potential impact of air pollutants on terrestrial and aquatic ecosystems.

Annexes

Annex I

IAEA TC Project CUB/7/008 and National Program PNUOLU /4-1/ 2 No. /2014.

The field samplings, samples treatments and PM_{10} levels determinations undertaken in this thesis involved to the Centro de Estudios Ambientales de Cienfuegos (CEAC) staff and their facilities and were carried out in the framework of the IAEA TC Project CUB/7/008 "Strengthening the National System for Analysis of the Risks and Vulnerability of Cuba's Coastal Zone Through the Application of Nuclear and Isotopic Techniques" and the National Program PNUOLU /4-1/ 2 No. /2014 of the National Nuclear Agency "Soluciones a problemas específicos del manejo integrado de cuencas y áreas costeras en Cuba, a través de técnicas isotópicas y nucleares (TIN): Acidificación del Mar, Ciclo y Secuestro de CO_2, Florecimiento de Algas Toxicas, Especies Invasivas, Contaminación ambiental, Erosión-Sedimentación-Transporte de Nutrientes y Contaminantes, Eutrofización y Calidad de embalses de aguas".

The main aim of these projects is to reduce specific problems for the sustainable management of watersheds and coastal areas in Cuba, their conservation and adaptation to climate change, with the introduction, development and validation of nuclear and isotopic technologies.

To contribute to that goal, and in addition to the research studies presented in this thesis, during this period (between 2014 and 2018) other research activities have been carried out in close collaboration with the *Laboratorio Integrado de Calidad Ambiental (LICA)*. Although in the present PhD only a part of the findings related to those investigations have been discussed, it is important to highlight the obtained results since they constitute research lines in which we continue working:

a. Three epiphytic bromeliad species (*Tillandsia recurvata L, Tillandsia fasciculata and Tillandsia bulbosa*) were monitored during 2015 in 24 sampling sites around the Bay of Cienfuegos in order to evaluate their feasibility for air pollution biomonitoring surveys. The only species found inside the Cienfuegos city (*Tillandsia recurvata L*) was additionally monitored every three months at 4 sampling sites during 2015 and 2016. In parallel, and simultaneously, this specie was monitoring at 5 sampling sites in the Santa Clara city (located at 50 km at NE

of Cienfuegos). All collected samples were analyzed for their major and trace elements (a total of 54 elements), TC and TN tissue contents, and their stable C and N isotope composition ($\delta^{13}C$ and $\delta^{15}N$).

At the same time, top soil samples were collected in the same sampling sites and analyzed for the same elements in order to evaluate their contribution by resuspension. This led to the exhaustive characterization of top soil layers in the studied areas. These results have been partially presented in Chapters 3 and 4 and they were employed for the calculation of the EFs presented in Chapters 2, 3 and 5.

b. Monthly bulk deposition samples, addressed in Chapter 5 for major and trace elements, were also analyzed for TC and TN content and their stable isotope composition ($\delta^{13}C$ and $\delta^{15}N$). These results have been partially presented in Chapter 6. Additionally, these samples were analyzed to determine the concentration of the atmospheric radionuclides ^{7}Be, ^{210}Pb, ^{137}Cs and ^{40}K and to calculate their monthly atmospheric depositional fluxes.

   At the same time, 48h-PM_{10} samples were collected every 15 days in 2015 at the urban and rural studied sites in order to determine the concentration of atmospheric radiotracers (^{7}Be, ^{210}Pb, ^{137}Cs and ^{40}K). Similar to the discussed in Chapter 6, these results can serve to calculate the total deposition velocity (Eq. 6.1) and to evaluate the feasibility of these radionuclides to trace processes of transport and deposition of pollutants in the atmosphere.

c. A PM_{10} monitoring (24h-PM_{10} samples every 2 days) was carried out at a traffic, urban and sub-urban background sites in the Cienfuegos city during February, March and April 2016, respectively. The main aim is to evaluate the PM_{10} levels variability along the city and the influence of different sources of contamination. Collected samples have been analyzed for their TC and TN content and their stable isotope composition ($\delta^{13}C$ and $\delta^{15}N$), NH_4^+, SO_4^{2-}, NO_3^-, Cl^-, pH and conductivity according to the methodologies described in Chapters 2 and 4. These results have been partially presented in Chapter 6.

d. A total of 31 road dust samples were collected in the main roads of the Cienfuegos city in summer 2016. These samples were chemically characterized for major and trace elements (a total of 50 elements), TC and TN contents, and

their stable C and N isotope composition ($\delta^{13}C$ and $\delta^{15}N$). These results have been partially presented in Chapters 3 and 4.

e. A total of 18 PM_{10} samples (9 from each sampling sites), from the samples collected in the study shown in Chapter 2, were analyzed by scanning electron microscopy coupled with energy dispersive X-ray analyzer in order to better understand the characteristic and origin of the PM and support the results discussed in Chapter 2.

Annex II

Published papers

- Alonso Hernández, C.M., Díaz Asencio, M., Gómez Batista, M., Bolaños Alvares, Y., Muñoz Caravaca, A., Morera Gómez, Y., 2016. Radiocronología de sedimentos marinos y su aplicación en la comprensión de los procesos de contaminación ambiental en ecosistemas marinos cubanos. Nucleus 60, 35–40.
- Alonso-Hernández, C.M., Garcia-Moya, A., Tolosa, I., Diaz-Asencio, M., Corcho-Alvarado, J.A., Morera-Gomez, Y., Fanelli, E., 2017. Tracing organic matter sources in a tropical lagoon of the Caribbean Sea. Continental Shelf Research 148, 53–63. https://doi.org/10.1016/j.csr.2017.08.001
- Alonso-Hernández, C.M., Morera-Gomez, Y., Acosta-Melian, R., Sánchez-Llull, M., Cartas-Águila, H., Díaz-Asencio, M., Muñoz-Caravaca, A., 2016. Terrestrial gamma radiation dose rate in Cienfuegos, Cuba. Radioprotection 51, 245–248. https://doi.org/10.1051/radiopro/2016060
- Alonso-Hernández, C.M., Morera-Gómez, Y., Cartas-Águila, H., Guillén-Arruebarrena, A., 2014. Atmospheric deposition patterns of 210Pb and 7Be in Cienfuegos, Cuba. Journal of Environmental Radioactivity 138, 149–155. https://doi.org/10.1016/j.jenvrad.2014.08.023
- Morera-Gómez, Y., Cartas Águila, H.A., Alonso Hernández, C.M., Bernal Castillo, J.L., Guillén Arruebarrena, A., 2015. Monte Carlo simulation of the efficiency response of a well-type HPGe detector at 46.54 keV. Nucleus 57, 1–4.
- Morera-Gómez, Y., Cartas-Aguila, H.A., Alonso-Hernández, C.M., Bernal-Castillo, J.L., Guillén-Arruebarrena, A., 2015. Application of the Monte Carlo efficiency transfer method to an HPGe detector with the purpose of environmental samples measurement. Applied Radiation and Isotopes 97, 59–62. https://doi.org/10.1016/j.apradiso.2014.12.013
- Morera-Gómez, Y., Cartas-Aguila, H.A., Alonso-Hernández, C.M., Nuñez-Duartes, C., 2016. Validation of an efficiency calibration procedure for a coaxial n-type and a well-type HPGe detector used for the measurement of environmental radioactivity. Nuclear Instruments and Methods in Physics Research A 818, 51–56. https://doi.org/10.1016/j.nima.2016.02.039

- Morera-Gómez, Y., Santamaría, J.M., Elustondo, D., Alonso-Hernández, C.M., Widory, D., 2018. Carbon and nitrogen isotopes unravels sources of aerosol contamination at Caribbean rural and urban coastal sites. Science of the Total Environment 642, 723–732. https://doi.org/10.1016/j.scitotenv.2018.06.106